9TH INTERNATIONAL CONFERENCE ON COMPUTATIONAL MATHEMATICS AND ENGINEERING SCIENCES

17 – 19 May 2025,
Diyarbakır – Türkiye

BOOK OF FULL TEXT

ISBN-77733

Publish date: 02.10.2025

THE NINETH INTERNATIONAL CONFERENCE ON COMPUTATIONAL MATHEMATICS AND ENGINEERING SCIENCES (CMES-2025), DiYARBAKIR/TÜRKİYE, MAY 17-19, 2025

The **Nineth International Conference on Computational Mathematics and Engineering Sciences (CMES-2025)** will be held in Dicle University from **17- to 19 May 2025 in Dicle, Türkiye.** It provides an ideal academic platform for researchers and professionals to discuss recent developments in both theoretical, applied mathematics and engineering sciences. This event also aims to initiate interactions among researchers in the field of computational mathematics and their applications in science and engineering, to present recent developments in these areas, and to share the computational experiences of our invited speakers and participants.

The Organizing Committee

Committee Chairs

Hasan Bulut, Fırat University, Türkiye
Zakia Hammouch, Ecole Normale Superierue de Meknes, Moulay Ismail University, Morocco
Ercan Çelik, Kyrgyz-Turkish Manas University, Kyrgyzstan
Haci Mehmet Baskonus, Harran University, Türkiye

MESSAGE FROM THE GENERAL CHAIRS

Dear Conference Attendees,

We are honored to welcome you to the **Nineth International Conference on Computational Mathematics and Engineering Sciences (CMES-2025)** at Dicle University from 17 to 19 May 2025 in Diyarbakır City, Türkiye.

CMES, founded in 2016 at Faculty of Science and Techniques Errachidia Moulay Ismail University Morocco is an annual intarnational conference, which was very successful in the past years by providing opportunities to the participants in sharing their knowledge and informations and promoting excellent networking among different international universities. This year, the conference includes 200 extended abstracts, several submissions were received in response to the call for papers, selected by the Program Committee. The program features keynote talks by distinguished speakers such as:

Dumitru Baleanu from Lebanese American University, Beirut, Lebanon; **Baver Okutmustur** from Middle East Technical University, Türkiye; **Mehrdad Lakestani** from Tabriz University, Iran, **Ekrem Savas** from Usak University, Türkiye; **Ozlem Defterli** from Çankaya University, Türkiye; **Sedaghat Shahmorad** from Tabriz University, Iran. The conference also comprises contributed sessions, posters sessions and various research highlights.

We would like to thank the Program Committee members and external reviewers for volunteering their time to review and discuss submitted abstracts. We would like to extend special thanks to the Honorary, Scientific and Organizing Committees for their efforts in making CMES-2025 a successful event. We would like to thank all the authors for presenting their research studies during our conference. We are grateful to DUBAP(ZGEF.25.003) for research funds. We hope that you will find CMES-2025 interesting and intellectually stimulating, and that you will enjoy meeting and interacting with researchers around the world.

.

***Hasan Bulut**,*

Firat University, Elazig, Türkiye.

Zakia Hammouch,

ENS Meknes, Moulay Ismail University Morocco

Thu Dau Mot University, Binh Duong Province, Vietnam

China Medical University Hospital Taichung 40402, Taiwan.

TOPICS

Control Theory,
Game Theory,
Applied Mathematics,
Financial Mathematics,
Artificial Intelligence,
Education Sciences,
Engineering Sciences,
Computer Science,
Information Technology,
Geometry and Its Applications,
Analysis and Its Applications,
Statistics and Its Applications,
Algebra and Its Applications,
Topology and Its Application,
Chaos and Dynamical Systems,
Cryptography and its Applications,
Fractional Calculus and Applications,
Economics and Econometric Studies,
Electrical and Electronic Engineering,
Defense industry and applications,
Mathematical Biology,
Computational Epidemiology,
Mathematical Chemistry,
Mathematics Education and Its Applications,
Numerical Methods and Scientific Programming,
Linearand Nonlinear programming and Dynamics,
Modeling of Bio-systems for Optimization and Control,
Ordinary, Partial, Stochastic and Delay Differential Equations,
Computational Fluids mechanics. Heat and Mass Transfers,
Earth Sciences,
Applied Sciences

COMMITTEE CHAIRS

Prof.Dr.Hasan Bulut, Firat University, Elazığ, Türkiye
Prof.Dr.Zakia Hammouch, ENS Meknes, Moulay Ismail University, Morocco
Prof. Dr. Ercan Çelik, Kyrgyz-Turkish Manas University, Kyrgyzstan
Prof.Dr.Haci Mehmet Baskonus, Harran University, Türkiye

COMMITTEE CO-CHAIRS

Prof.Dr. Carlo Cattani, Tuscia University, Viterbo, Italy
Prof.Dr. Mohammed Ouazzani Jamil, University Privee of Fez, Morocco
Prof. Dr. Hassan Qjidaa, Sidi Mohammed Ben Abdellah University, Fes Morocco
Prof. Dr. El Mehdi El Khattabi, Moulay Ismail University Morocco

Assoc. Prof. Dr. Tolga Aktürk, Ordu University, Türkiye

HONORARY COMMITTEE

Prof. Dr. Alpaslan Ceylan, Rector of Kyrgyz-Turkish Manas University, Kyrgyzstan
Prof. Dr. Aytaç Coşkun, Vice Rector of Dicle University, Türkiye
Prof. Dr. Ahmed Mouchtachi, Rector of Moulay Ismail University, Meknes, Morocco
Prof. Dr. Abdelmjid Abourriche, Vice Rector of Moulay Ismail University, Meknes, Morocco
Prof. Dr. Bülent Çakmak, Rector of Erzurum Technical University, Erzurum, Türkiye
Prof. Dr. Ekrem Savaş, Rector of Uşak University, Türkiye
Prof. Dr. Etibar Penahh, Baku State University, Baku, Azerbaijan
Prof. Dr. Fahrettin Göktaş, Rector of Firat University, Elazığ, Türkiye
Prof. Dr Haddad Abderrahman, Vice Rector of Moulay Ismail University Morocco
Prof. Dr. Hamdullah Şevli, Rector of Van Yüzüncü Yıl University, Türkiye
İbrahim Taşel, Final International University, Gime, Cyprus
İzzettin Toraman, Chairman of the Board of Toraman Tekstil
Prof. Dr. Kamuran Eronat, Rector of Dicle University, Diyarbakır, Türkiye
Prof. Dr. Mahmut Ergüt, Namık Kemal University, Tekirdağ, Türkiye
Prof. Dr. Mehmet Siraç Özerdem, Vice Rector of Dicle University, Diyarbakır, Türkiye
Prof. Dr. Mehmet Tahir Güllüoğlu, Rector of Harran University, Sanliurfa, Türkiye
Prof. Dr. Mohammed Aziz Lahlou, President of Universite Privee of Fes, Morocco
Prof. Dr. Necdet Bildik, Retired Faculty Member, Celal Bayar University, Türkiye
Prof. Dr. Orhan Baş, Rector of Ordu University, Ordu, Turkey
Prof. Dr. Orhan Gemikonaklı, Rector of International Final University, Gime, Cyprus
Prof. Dr. Ouazzani Jamil Mohamed, Vice President of Universite Privee of Fez, Morocco
Prof. Dr. Rengin Ak, Rector of Kırklareli University, Kırklareli, Türkiye
Prof. Dr. Rıfat Çolak, Retired Faculty Member, Fırat University, Türkiye
Şahin Otu, Chairman of Final Schools Diyarbakır
Prof. Dr. Şengül Kocaman, Dean of Education Faculty, Diyarbakır, Türkiye
Şevket Ertem, Final International University, Gime, Cyprus
Prof. Dr. Sezai Asubay, Dean of Science Faculty, Diyarbakır, Türkiye
Prof. Dr. Subhan N. Namazov, Vice Rector, Azerbaijan Technical University, Baku, Azerbaijan
Prof. Dr. Velat Şen, Vice Rector of Dicle University, Türkiye
Prof. Dr. Vilayet M. Veliyev, Rector of Azerbaijan Technical University, Baku, Azerbaijan
Prof. Dr. Volkan Öngel, Rector of İstanbul Beykent Üniversity, İstanbul, Türkiye
Prof. Dr. Yusif Gasimov, Azerbaijan University, Baku, Azerbaijan

SCIENTIFIC COMMITTEE

Abdellah Rababah (University of Science and Technology Irbid, Jordan)
Abdellah Rezzouk (Sidi Mohamed Ben Abdellah University, Morocco)
Abdelmjid Bouazizi (ENS Moulay Ismail University Morocco)
Abdelaziz Sbai (EST Moulay Ismail University, Morocco)
Abdelouahed Alla Hamou (FS, Mohamed V University Rabat, Morocco)

Abdulhamit Subaşı (University of Turku, Finland)
Abdulkadir Karakaş (Siirt University, Türkiye)
Abdullah Çağman (Agrı İbrahim Cecen University, Türkiye)
Abdullah Kopuzlu (Ataturk University, Türkiye)
Abdullahi Yusuf (Biruni University, Istanbul, Türkiye)
Adnène Arbi (University of Carthage, Tunisia)
Agamirza Bashirov (Eastern Mediterranean University, Cyprus)
Ahmed Elngar (Beni Suef University, Egypt)
Ahmet Bedri Özer (Firat University, Elazığ, Türkiye)
Ahmet Dumlu (Erzurum Technical University, Türkiye)
Ahmet Ocak Akdemir (Agrı İbrahim Cecen University, Türkiye)
Ahmet Yıldız (İnönü University, Malatya, Türkiye)
Akbar Barati Chiyaneh (Yüzüncüyıl University, Bitlis, Van)
Ali Akgül (Siirt University, Türkiye)
Ali Çakmak (Bitlis Eren University, Bitlis, Türkiye)
Ali İhsan Mut (Dicle University, Türkiye)
Ali Karcı (İnönü University, Malatya)
Ali Rostami (University of Tabriz, Tabriz, Iran)
Ali Yousef (Kuwait College Of Science And Technology, Kuwait)
Alireza Khalili Golmankhaneh (IAU Urmia Branch, Iran)
Alla Belousova (Don State Technical University, Russian Federation)
Alev Dülger (Dicle University, Türkiye)
Alper Ekinci (Bandırma 17 Eylul University, Türkiye)
Alper Osman Öğrenmiş (Fırat University, Elazığ, Türkiye)
Alper Polat (Munzur University, Türkiye)
Aly Ramadan Seadawy (Taibah University, Saudi Arabia)
Anargül Urdaletova (Kyrgyz-Turkish Manas University, Kyrgyzstan)
Aneta Barakoska (Faculty of Philosophy, University St. Cyril, Macedonia)
Anna Sandulyak (Université de Moscow, Russia)
Arife Atay (Dicle University, Türkiye)
Armando Ciancio (University of Messina, Italy)
Arzu Akbulut (Eskisehir Osmangazi University, Türkiye)
Arzu Denk Oguz (Atılım University, Türkiye)
Asan Ömüraliyev (Kyrgyz-Turkish Manas University, Kyrgyzstan)
Atif A. Namazov (Azerbaijan Technical University, Baku, Azerbaijan)
Avıt Asanov (Kyrgyz-Turkish Manas University, Kyrgyzstan)
Ayhan Şerbetçi (Ankara University, Ankara)
Aynur Keskin Kaymakçı (Selcuk University, Konya)
Ayşe Dilek Maden (Selçuk University, Konya)
Ayşe Metin Karakaş (Bitlis Eren University, Bitlis, Türkiye)
Ayşegül Çetinkaya (Ahi Evran University, Türkiye)
Badr Abou E Majd (Mohammed V University in Rabat, Morocco)
Bashar A. Al-Talip (University of Mosul, Iraq)
Bayram Çekim (Gazi University, Türkiye)
Bayram Şahin (Ege University, İzmir, Türkiye)

Behçet Öznacar (Near East University, Cyprus)
Berivan Polat (Munzur University, Türkiye)
Beytullah Yağız (Yüzüncü Yıl University, Türkiye)
Bilal Alatas (Fırat University, Türkiye)
Bilal Şenol (İnönü University, Malatya)
Bilgehan Polatoğlu (Atatürk University, Türkiye)
Burcu Gürbüz (Johannes Gutenberg-University Mainz, Germany)
Burçin Doğan (Malatya Turgut Özal University, Türkiye)
Burhan Tiryakioğlu (Marmara University, Türkiye)
Bülent Tavlı (Tobb Economics And Technology University, Türkiye)
Cameron Browne (University of Louisiana at Lafayette, USA)
Carla M.A. Pinto (ISEP, Porto, Portugal)
Carlo Cattani (Tuscia University, Viterbo, Italy)
Cemil İnan (Mardin Artuklu University, Türkiye)
Ceren Kına (Malatya Turgut Özal University, Türkiye)
Cesim Temel (Yüzüncüyıl University, Türkiye)
Chérif Ziti (Moulay Ismail University, Morocco)
Christos Volos (Aristotle University, Greece)
Çağrı Karaman (Atatürk University, Erzurum, Türkiye)
Çiğdem İnan (Mersin University, Türkiye)
Damla Yılmaz (Erzurum Technical University, Türkiye)
Danyal Soybaş (Erciyes University, Türkiye)
Davut Hanbay (İnönü University, Malatya)
Derya Arslan (Bitlis Eren University, Türkiye)
Derya Avci (Balikesir University, Türkiye)
Dilek Okuyucu (Erzurum Technical University, Türkiye)
Dumitru Baleanu (Cankaya University, Türkiye)
Dursun Irk (Eskişehir Osmangazi University, Eskişehir)
Dyyak Ivan (Ivan Franko National University, Lviv, Ukraine)
Ebru Bozkurt (Ataturk University, Türkiye)
Ecem Acar (Harran University, Şanlıurfa, Türkiye)
El Abbassi Ahmed (FSTE, Moulay Ismail University, Morocco)
El Ayyadi Rachid (FST, Sidi Mohammed Benabdellah University, Morocco)
El Hassan Ben Ahmed (Ens Meknes, Moulay Ismail University, Morocco)
El Houcine Lafhim (Sidi Mohamed Ben Abdellah University, Morocco)
El Khomssi Mohamed (Sidi Mohamed Ben Abdellah University, Morocco)
El Mehdi El Khattabi (Ens Meknes, Moulay Ismail University, Morocco)
Ella Abilayeva (Kyrgyz-Turkish Manas University, Kyrgyzstan)
Elman Hazar (Igdır University, Türkiye)
Emel Biçer (Bingöl University, Türkiye)
Emrah Yılmaz (Fırat University, Elazığ)
Engin Özkan (Erzincan Binali Yıldırım University, Erzincan)
Ennahnahi Noureddine (Sidi Mohamed Ben Abdellah University, Morocco)
Erdal Baş (Fırat University, Elazığ, Türkiye)
Erdal Ekici (Çanakkale Onsekiz Mart University, Çanakkale)

Erdal Ulualan (Kutahya University, Türkiye)
Erdal Ünlüyol (Ordu University, Türkiye)
Erhan Deniz (Kafkas University, Türkiye)
Erhan Güler (Bartın University, Türkiye)
Erhan Pişkin (Dicle University, Diyarbakır, Türkiye)
Erhan Set (Ordu University, Türkiye)
Erol Yaşar (Mersin University, Türkiye)
Esin Ilhan (Kırşehir Ahi Evran University, Türkiye)
Esra Karataş Akgül (Siirt University, Türkiye)
Eva Kaslik (University of Timisoara, Romania)
Evrim Toklu (Agrı İbrahim Cecen University, Türkiye)
Ezgi Kaya (Iğdır University, Türkiye)
Fahd Jarad (Cankaya University, Türkiye)
Fahrettin Muhtarov (Bakü State University, Azerbaijan)
Fatma Ayaz (Gazi University, Türkiye)
Fatma Berna Benli (Erciyes University, Türkiye)
Fatma Bulut (Bitlis University, Türkiye)
Fatma Erdoğan (Firat University, Türkiye)
Fatma Sağsöz (Atatürk University, Türkiye)
Fatma Taşdelen Yeşildal (Ankara University, Türkiye)
Fethi Bin Muhammad Belgacem (Paaet, Shaamyia, Kuwait)
Fethiye Müge Sakar (Dicle University, Türkiye)
Feyza Esra Erdoğan (Ege University, İzmir, Türkiye)
Fikret Aliyev (Bakü State University, Azerbaijan)
Filiz Taşcan (Eskişehir Osmangazi University, Eskişehir)
Firat Evirgen (Balikesir University, Türkiye)
Francesco Villecco (University Salerno, Italy)
Fulya Şahin (Ege University, İzmir, Türkiye)
Gonca Onargan (Final International University, Girne, Cyprus)
Gökhan Gökdere (Fırat University, Elazığ)
Gülşat Muhametjanov (Kyrgyz-Turkish Manas University, Kyrgyzstan)
Gürhan İçöz (Gazi University, Türkiye)
Güven Kaya (Bingöl University, Türkiye)
Hacer Sengul (Harran University, Sanlı urfa, Türkiye)
Haldun Kucuk (Tarsus University, Mersin, Türkiye)
Hamit Akyüz (Gazi University, Ankara, Türkiye)
Hasan Can Kısakürek (İstanbul University, İstanbul, Türkiye)
Hasan Doğan (Karamanoğlu Mehmetbey University, Karaman)
Hasan Taş (Fırat University, Elazığ, Türkiye)
Hasan Yusuf (The University of Nigeria, Nsukka)
Hatice Taş (Bitlis Eren University, Bitlis, Türkiye)
Hazım Sürer (Ataturk University, Erzurum, Türkiye)
Hidayet Eski (Mersin University, Türkiye)
Hussain Benazza (ENSAM, Moulay Ismail University Morocco)
Hüseyin Kalaycı (Mersin University, Türkiye)

Hüseyin Kaya (İnönü University, Malatya, Türkiye)
Hüseyin Yılmaz (Ankara University, Ankara)
Ilyas Öztürk (Dicle University, Diyarbakır, Türkiye)
İbrahim Arslan (Fırat University, Türkiye)
İbrahim Korkmaz (Kırıkkale University, Türkiye)
İbrahim Okan Öztürk (Dicle University, Diyarbakır)
İsmail Yılmaz (Çanakkale Onsekiz Mart University, Türkiye)
İsmail Hakkı Keskin (Fırat University, Elazığ)
Ismail Küçük (Eskişehir Osmangazi University, Eskişehir)
Iván Reyes (Universidad Autónoma de Querétaro, México)
Jakub Tichy (Czech University of Life Sciences, Czech Republic)
Jean-Côme Toutain (University of Poitiers, France)
João Barbosa (University of Lisbon, Portugal)
João Luís (IST, University of Lisbon, Portugal)
John K. B. (University of York, UK)
Josep A. R. (University of Barcelona, Spain)
Joseph Asongu (University of Juba, Sudan)
Juan E. López (University of Chile, Chile)
Jürgen Noack (Brandenburg University of Technology, Germany)
Júlia Kovács (Technical University of Budapest, Hungary)
Kadir S. (University of Uludag, Türkiye)
Kamran E. (University of Tehran, Iran)
Kamran Yavuz (Ankara University, Ankara, Türkiye)
Kamil Kose (Gazi University, Türkiye)
Karim Jebli (University of Monastir, Tunisia)
Keith A. (University of Oxford, UK)
Kenan Kavasoğlu (Çankırı Karatekin University, Türkiye)
Khaled M. (King Fahd University of Petroleum and Minerals, Saudi Arabia)
Khoa T. (Vietnam National University)
Kohei T. (Kyoto University, Japan)
Kostas G. (University of Thessaloniki, Greece)
Krzysztof K. (Silesian University, Poland)
László Sz. (University of Szeged, Hungary)
Louay Al-Kharouf (University of Bahrain, Bahrain)
Maher Shoukry (Cairo University, Egypt)
Mohamed S. S. (Al-Mansoura University, Egypt)
Mohamed Tarek Hamza (Mansoura University, Egypt)
Mubariz Alvi (University of Sindh, Pakistan)
Murat Karakas (Bitlis University, Türkiye)
Mustafa Arslan (Gazi University, Türkiye)
Mustafa Tunc (Erzurum Technical University, Türkiye)
Nezih Gülkır (Akdeniz University, Türkiye)
Nima Mostafavi (Isfahan University of Technology, Iran)
Nural Özkaya (Dicle University, Diyarbakır, Türkiye)
Ouberka Hanane (ENS, Moulay Ismail University Morocco)

Oğuz Karabacak (İstanbul University, İstanbul, Türkiye)
Ömer Gökhan Kaya (Sakarya University, Türkiye)
Ömer Yılmaz (İnönü University, Malatya, Türkiye)
Ouarghi Khalid (ENS, Moulay Ismail University Morocco)
Rafik Ben Fadhel (University of Carthage, Tunisia)
Ramazan Alper (İnönü University, Malatya, Türkiye)
Rattan Kumar Sahu (IIT Bhubaneswar, India)
Samir Ben Lakhdar (University of Carthage, Tunisia)
Selma R. (University of Graz, Austria)
Sergiy R. (Ukrainian Academy of Science, Ukraine)
Sinan Deniz (Yüzüncü Yıl University, Türkiye)
Sipahi, D (Bilkent University, Türkiye)
Skouri Rachid (EST, Moulay Ismail University Morocco)
Soledad Torregrosa (University of Murcia, Spain)
Srikant Mishra (Biju Patnaik University of Technology, India)
Stephen T. (University of Maryland, USA)
Sulaiman Al-Harbi (King Saud University, Saudi Arabia)
Şakir İşleyen (Yüzüncü Yıl University, Türkiye)
Şule Kocabaş (Istanbul University, Istanbul, Türkiye)
Tamara T. (Kyiv National University, Ukraine)
Tantaoui Mouad (ENS, Moulay Ismail University Morocco)
Tial Mohammed (FSTE, Moulay Ismail University Morocco)
Tomasz Z. (Warsaw University, Poland)
Valter S. (University of Porto, Portugal)
Viktor Barbu (University of Oradea, Romania)
Yilmaz K. (Ege University, İzmir, Türkiye)
Yener Altun (Yüzüncü Yıl University, Türkiye)
Zafer E. (Tunceli University, Türkiye)
Zain Siham (ENS, Moulay Ismail University Morocco)
Zaki Mohammed (ENS, Moulay Ismail University Morocco)
Zekeriya H. (Malatya University, Türkiye)
Zekeriya M. (Atatürk University, Türkiye)
Zubair M. (Ministry of Higher Education, Pakistan)

ORGANIZING COMMITTEE

Prof. Dr. Hasan Bulut, (Chair), Fırat University, Türkiye
Prof. Dr. Zakia Hammouch, (Chair), ENS, Moulay Ismail University Morocco
Prof. Dr. Ercan Çelik, (Chair), Kyrgyz-Turkish Manas University, Kyrgyzstan
Prof. Dr. Haci Mehmet Baskonus, (Chair), Harran University, Türkiye
Prof. Dr. Hatun Özlem Güney, (Chair), Dicle University, Diyarbakır, Türkiye
Prof. Dr. Erhan Pişkin, (Chair), Dicle University, Diyarbakır, Türkiye
Prof. Dr. Ouazzani Jamil Mohammed, (Co-Chair), Universite Privee de Fes Morocco
Prof. Dr. Hassan Qjidaa, (Co-Chair), Sidi Mohammed Ben Abdellah University, Fes Morocco
Prof. Dr. El Mehdi El Khattabi, (Co-Chair), Moulay Ismail University Morocco

Assoc. Prof. Dr. Tolga Aktürk, (Co-Chair), Ordu University, Türkiye
Prof. Dr. Mikail Et, Fırat University, Türkiye
Prof. Dr. Vedat Asil, Fırat University, Türkiye
Prof. Dr. Alper Öğrenmiş, Fırat University, Türkiye
Prof. Dr. Muhittin Evren Aydın, Fırat University, Türkiye
Prof. Dr. Fevzi Erdoğan, Yüzüncüyıl University, Türkiye
Prof. Dr. Alaattin Esen, İnönü University, Türkiye
Prof. Dr. Yusuf Pandır, Bozok University, Türkiye
Prof. Dr. Yusuf Gürefe, Mersin University, Türkiye
Prof. Dr. Bahaddin Sinsoysal, Istanbul Beykent University
Assoc. Prof. Dr. Mahmut Modanlı, Harran University, Türkiye
Assoc. Prof. Dr. Gülnur Yel, Final International University, Girne, Cyprus
Assoc. Prof. Dr. Muhammed Yiğider, Erzurum Technic University, Türkiye
Dr. Nuray Eroğlu, Tekirdağ Namık Kemal University, Türkiye

LOCAL COMMITTEE

Sedat İlhan (Dicle University, Türkiye)
Zehra Yücedağ (Dicle University, Türkiye)
Kemal Özgen (Dicle University, Türkiye)
Mehmet Aydın (Dicle University, Türkiye)
Tuğba Örnek (Dicle University, Türkiye)
Seçil Yalaz (Dicle University, Türkiye)
Arife Atay (Dicle University, Türkiye)
Ömer Oruç (Dicle University, Türkiye)
Damla Barlak (Dicle University, Türkiye)
Alev Dülger (Dicle University, Türkiye)
Yasin Kaya (Dicle University, Türkiye)
Nebi Yılmaz (Dicle University, Türkiye)
Ayşe Fidan (Dicle University, Türkiye)
Gülistan Butakın (Dicle University, Türkiye)
Erkan Sancar (Dicle University, Türkiye)
Hasan Kandemir (Dicle University, Türkiye)
Muhteşem Demir (Dicle University, Türkiye)
Yunus Özişçi (Dicle University, Türkiye)
Ayşe Demirhan (Dicle University, Türkiye)
Özlem Orhan (Bandırma Onyedi Eylül Ün, Balıkesir)
Mehmet Karay (Final Int. University, Girne, Cyprus)
Münevver Tuz (Fırat University, Elazığ, Türkiye)
Ebru Cavlak Aslan (Fırat University, Elazığ, Türkiye)
Tüba Gülşen (Fırat University, Elazığ, Türkiye)
Bahar Acay (Fırat University, Türkiye)
Ahu Ercan (Fırat University, Elazığ, Türkiye)
Berat Karaagac (Adıyaman University, Türkiye)
Ezgi Kaya (Igdır University, Igdır, Türkiye)
Onur Saldır (Van Yüzüncü Yıl University, Van, Türkiye)
Zelal Temel (Van Yüzüncü Yıl University, Van, Türkiye)
İbrahim Enam İnan (Fırat University, Elazığ, Türkiye)
Meltem Öğrenmiş (Fırat University, Elazığ, Türkiye)
Hajar Farhan Ismael (University of Zakho, Iraq)
Karmina K. Ali (University of Zakho, Iraq)
Sibel Şehriban Ataş (Fırat University, Elazığ, Türkiye)
Aysenur Akkılıç (Assistant, Fırat University, Türkiye)
Aslı Alkan (Fırat University ,Elazığ, Türkiye)
Beyhan Kemaloğlu (Fırat University, Elazığ, Türkiye)
Mucahit Saydam (Fırat University, Elazığ, Türkiye)
Çağrı Yılmazer (Fırat University, Elazığ, Türkiye)
Merve Zeynep Gecmen (Ağrı Ibrahim Çeçen University, Ağrı, Türkiye)
Necati Erdoğan (Van Yüzüncü Yıl Üniversity,Van, Türkiye)

LANGUAGE EDITORIAL COMMITTEE

International Communications Consultant

PROCEEDINGS

Full version of submitted papers will be published in Special Volumes of reputed journals. Procedure, Guidelines and Checklist for the preparation and submission of papers to the Proceedings of CMES-2025 can be found in the journals websites. The journals in which selected and peer-reviewed full papers of CMES-2025 will be published are as follows:

1. **BOOK OF ABSTRACTS [Free of charge]**

If Authors submit ABSTRACT TEXTS, then, after getting referees evaluations for these abstracts, they will be published in ABSTRACT PROCEEDING BOOK of CMES-2025. For FULL TEXT PAPERS, Authors have to submit their FULL TEXT PAPERS online via submission system of CMES-2025. These FULL TEXT PAPERS will be published in FULL TEXT PROCEEDING BOOK of CMES-2025 after getting at least two positive reports.

2. **CONFERENCE PROCEEDINGS [Free of charge]**

At the beginning, if Authors submit FULL TEXT PAPERS, then, after getting at least two positive referee reports, FULL TEXT PAPERS will be published in FULL TEXT PROCEEDING BOOK of CMES-2025 with ISBN:77733 number. Therefore, Abstracts of these FULL TEXT PAPERS will **NOT** be published in ABSTRACT PROCEEDING BOOK of CMES-2025.

3. FRACTAL AND FRACTIONAL JOURNAL [SCI-E],
Selected papers from CMES-2025 will be published in a special issue dedicated to the Conference entitled "**Feature Papers for Mathematical Physics Section".**
https://www.mdpi.com/journal/fractalfract/special_issues/1TAP5BBZ45
This journal is indexed by SCI-E.

4. PROCEEDINGS OF THE INSTITUTE OF MATHEMATICS AND MECHANICS [E-SCI]
Selected papers from CMES-2025 will be published by https://proc.imm.az/special/

This journal is indexed by E-SCI.

5.TURKISH JOURNAL OF SCIENCE, [FREE]
Participants of CMES 2025 can submit their good quality papers to Turkish Journal of Science. After the peer review process, the papers will be published at TJOS. The authors must write "CMES 2025" as comments to the editor.
(Editor in Chief: Dr. Ahmet Ocak AKDEMİR) For on-line submission: https://dergipark.org.tr/tr/pub/tjos

6.TURKISH JOURNAL OF INEQUALITIES, [FREE]
"Participants of CMES 2025 can submit their good quality papers to Turkish Journal of Inequalities. Selected papers will be published at TJI after the

peer review process. The participants can send their papers to erhanset@tjinequality.com. The authors must write “CMES 2025” as the subject.
(Editor in Chief: Prof. Dr. Erhan SET)
http://tjinequality.com/

7. MATHEMATICS IN NATURAL SCIENCE (MNS)
Authors can submit their full text paper directly to the journal by using the following link
https://www.isr-publications.com/mns

8. MATHEMATICS IN ENGINEERING, SCIENCE AND AEROSPACE (MESA), [FREE, SCOPUS]
“Selected papers will be published after peer review in the Journal of Mathematics in Engineering, Science and Aerospace (MESA)”
(Editor in Chief: Prof. Seenith Sivasundaram)
http://nonlinearstudies.com/index.php/mesa

9. APPLIED MATHEMATICS AND NONLINEAR SCIENCES, [SCOPUS]
Participants of CMES 2025 can submit their high quality full text papers to Applied Mathematics and Nonlinear Sciences by selecting CMES-2025 under the Select Article Type Menu.
https://www.editorialmanager.com/amns/default.aspx

10. MATHEMATICAL MODELLING AND NUMERICAL SIMULATION WITH APPLICATIONS (MMNSA), [TR DİZİN]
The Special Issue on “Advanced Methods of Modelling and Numerical Computation in Science and Engineering”. Authors can submit their full text paper directly to the journal by using the information provided in the following link
https://mmnsa.org/index.php/mmnsa/special_issues/SI-CMES2023

11. SYMMETRY [SCI-E] ; SPECIAL ISSUE "ADVANCES IN MATRIX TRANSFORMATIONS, OPERATORS AND SYMMETRY"
Authors can submit their full text paper directly to the journal by using the following link
https://www.mdpi.com/journal/symmetry/special_issues/Advances_Matrix_Transformations_Operators_Symmetry

12. YUZUNCU YIL UNIVERSITY JOURNAL OF THE INSTITUTE OF NATURAL AND APPLIED SCIENCES (TR-Dizin)
Authors can submit their full text paper directly to the journal by using the following link
https://dergipark.org.tr/tr/pub/yyufbed

13. PEDAGOGICAL PERSPECTIVE (PEDPER)
Pedagogical Perspective **(PedPer)** is an international, double blind reviwing, non-profit, professional scientific journal. PedPer is a journal that accepts manuscripts related to pedagogy and education.
http://pedagogicalperspective.com/

PLENARY & INVITED TALKS

MODIFIED FRACTIONAL OPERATORS: THEORY AND APPLICATIONS

Dumitru Baleanu [1]

[1] Department of Computer Science and Mathematics,Lebanese American University, Beirut, Lebanon and Institute of Space Sciences-Subsidiary of INFLPR,

Magurele-Bucharest, Romania

dumitru.baleanu@lau.edu.lb,

Abstract

Fractional Calculus deals with the study of so-called fractional order integral and derivative operators over real or complex domains, and their applications. In this talk I will discuss the modified ABC operator and I will explain the related properties and its real world applications.

Keywords: Fractional calculus;General kernel; Modified ABC operator.

REFERENCES

1. Mohammed Al-Refai, Dumitru Baleanu,On an extension of the operator with Mittag-Leffler kernel, Fractals, 30(51), 2022, Article number 2240129.

.

A COMPARATIVE STUDY OF ADAPTIVE GRID METHODS FOR BURGERS MODELS

Baver Okutmustur [1]

[1] Department of Mathematics, Middle East Technical University (METU), Ankara, Turkey

baver@metu.edu.tr

Abstract

This work presents comparative numerical study of shock solutions in classical and relativistic a Burgers models using two finite volume-based adaptive mesh refinement (AMR) strategies: *h*-adaptivity (local grid refinement) and *r*-adaptivity (mesh redistribution). The *h*-method dynamically adjusts resolution by adding/removing cells in shock regions, while the *r*-method maintains a fixed cell count but optimally redistributes points to sharpen shock resolution. We compare both approaches in terms of accuracy and efficiency, demonstrating their effectiveness for handling shocks and nonlinear waves in both classical and relativistic cases. This work is based on the joint work [4].

Keywords: Adaptive grid; h-refinement; r-refinement; Monitor function; Finite volume method; Relativistic Burgers equation

REFERENCES

1. J.M. Stockie, J.A. Mackenzie, R.D. Russell, A moving mesh method for one-dimensional hyperbolic conservation laws, **SIAM** J. Sci. Comput. 22 (2001) 1791–1813.

2. H.Z. Tang, T. Tang, Adaptive mesh methods for one- and two-dimensional hyperbolic conservation laws, **SIAM** J. Numer. Anal. 41 (2003) 487–515.

3. A. van Dam, P.A. Zegeling, A robust moving mesh finite volume method applied to 1D hyperbolic conservation laws from magnetohydrodynamics, Journal of Computational Physics, Volume 216, Issue 2, 2006, 526-546.

4. B. Okutmustur, K. Vuik, K. Yigit, Adaptive Mesh Refinement Methods for Relativistic Burgers-Schwarzshild Model, in preparation.

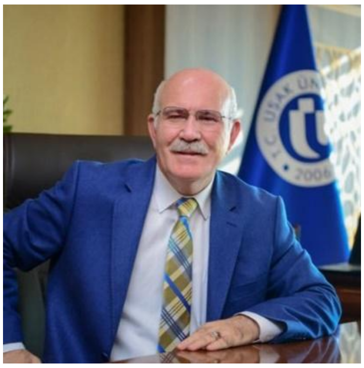

The development adventure of mathematics

Ekrem SAVAŞ

Uşak University, Uşak-Turkey

Email: ekremsavas@yahoo.com

Abstract:

Mathematics has always existed since the first steps of culturel history of the living creatures called human beings. It has always been a part of culture with numbers, figures, characteristics and with their applications according to the technical levels of the day. In this study, a general knowledge will be given concerning how math began and what phases it went through up to now. In getting the data, books and articles dealing with the issue have been studied. The findings we have show that it is not possible to say exactly where and when mathematics began. However, we can say, on the basis of findings, that math began in Epypt and Mesopotamia between 3000-2000 B.C. and then spread to other countries.

ADVANCED MATHEMATICAL MODELLING AND INFERENCE OF GENE REGULATORY NETWORKS WITH REAL DATA

Ozlem Defterli[1]

[1] Department of Mathematics, Faculty of Arts and Sciences,

Cankaya University, Ankara, Turkey

defterli@cankaya.edu.tr

Abstract

Systems biology addresses the challenge of understanding living systems in their entirety, as opposed to concentrating on individual biological elements.One approach to describing biological systems is through networks which are the graphical representations in which nodes denote entities of the system and edges signify the relationships between them.Given that the underlying structure of many networks remains partially or entirely unknown, a key objective of systems biology is to predict the complex and dynamic interactions among genes.This is called *network inference (NI) that* focuses on deducing network structures by leveraging high-throughput data in combination with reverse engineering methods. A fundamental challenge in network inference is the high dimensionality—often involving thousands of genes—contrasted with the relatively small number of available samples. Consequently, gene regulatory network (GRN) inference is inherently under-determined [1,2]. In this study, a time-series gene expression data-set derived from a micro-array chip experiment involving a model eukaryotic organism is used for illustrative purposes. The dataset's key characteristics are analyzed to gain insights into the structure and behavior of the underlying biological process. Subsequently, the temporal dynamics of the system are modeled in a discrete-time framework, employing advanced mathematical modeling techniques to capture the complexity and regulatory mechanisms of gene interactions [3,4].

Keywords: Network inference, Mathematical modelling, Data processing.

REFERENCES

1. Slonim K. Donna, From patterns to pathways: gene expression data analysis comes of age (Review), Nature Genetics, Vol:32(Suppl.), 502–508, 2002.

SOME EFFECTIVE NUMERICAL METHODS FOR FRACTIONAL DIFFERENTIAL EQUATIONS

S. Shahmorad[1]

shahmorad@tabrizu.ac.ir

[1]Department of Applied Mathematics, University of Tabriz, Tabriz,

East Azarbaijan, Iran

Abstract

Some efficient numerical methods such as block-by-block, fuzzy transform and interpolation based methods are studied for solving linear and nonlinear single term and multi-term frac- tional differential equations (MFDEs). The approaches involve converting the given linear and nonlinear MFDEs with some initial conditions into equivalent Volterra integral equa- tions (VIE), and applying the mentioned numerical approaches to the obtained VIES. Error bounds and convergence theorems are discussed for each case, separately. Finally, illustra- tive and comparative examples are provided to demonstrate the applications of the proposed methods and verify the theoretical results.

Keywords: Multi-term fractional initial value problem, Block-by-block method, Fuzzy tarnsform, Nonlinear Volterra integral equation, weak singularity.

NUMERICAL SOLUTION OF SINGULARLY PERTURBED INITIAL VALUE PROBLEMS WITH DELAY USING B-SPLINE WAVELETS

MEHRDAD LAKESTANI

Department of Applied Mathematics, University of Tabriz, Tabriz, Iran

mehrdadlakestani@yyu.edu.tr

ABSTRACT

In this paper, we solve a singularly perturbed initial value problem with delay by using c B-Spline wavelets. The properties of these functions are provided, and by employing the operational matrix of differentiation, a numerical method is genereted over some subintervals that reformulates the problem into a system of algebraic equations. This system can be solved to find the approximate solution. Numerical results demonstrate the efficiency of the method.

Keywords: Singularly perturbed problem; B-Spline wavelets; Delay differential equation.

REFERENCES

1. M. Lakestani, M. Dehghan, The solution of a second-order nonlinear differential equation with Neumann boundary conditions using semi-orthogonal B-spline wavelets, International Journal of Computer Mathematics, Vol: 83, No:8- 9, 685–694, 2006.

2. G.M. Amiraliyev, F. Erdogan, A finite difference scheme for a class of singularly perturbed initial value problems for delay differential equations, Numerical Algorithms, Vol: 52, 663- 675, 2009.

THE GAUSSIAN PELL NUMBERS VIA PERMANENTS AND DETERMINANT OF TRIDIAGONAL MATRICES

İnci Gültekin[1] Yasemin Taşyurdu[2] and Hiranur Karaca[3]

[1] Department of Mathematics, Atatürk University, Erzurum, Turkey

igultekin@atauni.edu.tr,

[2] Department of Mathematics, Erzincan University, Erzincan, Turkey

ytasyurdu@atauni.edu.tr,

[3] Graduate School of Natural and Applied Sciences, Atatürk University, Erzurum, Turkey

hiranur.karaca17@ogr.atauni.edu.tr

Abstract

Gaussian number means representation as Complex numbers. Our goal in this work is to give the Gaussian Pell numbers by using permanent and determinant of some tridiagonal matrices.

Keywords: Permanent, Gaussian pell number, Tridiagonal matrix.

Introduction

The Fibonacci, Lucas, Pell and Pell-Lucas numbers have received much interest in recent years and studied by a wide range of researchers in a variety of branches of mathematics, including linear algebra, applied mathematics, and calculus. The investigation of Gaussian numbers is a research topic of great interest. Gaussian numbers are complex numbers $z = a + ib,\ a, b \in \mathbb{Z}$ were investigated by Gauss in 1932 and the set of these numbers is denoted by $\mathbb{Z}[i]$. Furthermore, the study of Gaussian numbers is a very interesting academic field, and various research have been done in this area. In 1963, Horadam [1] introduced complex Fibonacci numbers and named them Gaussian Fibonacci numbers. In 1965, Jordan [2] considered two complex number sequences and extended some of the characteristics associated with usual Fibonacci sequences.

The Generalized Fibonacci sequences $U_n(p, q, a, b)$ are defined as follows

$$U_{n+1} = pU_n + qU_{n-1} \qquad U_0 = 0,\ U_1 = 1$$

where p and q are nonzero real numbers and $n \geq 1$. If $p = 2,\ q = 1$ is taken in the Generalized Fibonacci sequences $U_n(p, q, a, b)$, then the Pell sequences

$$\{ P_n \} = \{ 1, 2, 5, 12, \dots \}$$

is obtained [1] [3].

The Generalized Gaussian Fibonacci sequences $U_n(p, q, a, b)$ are defined as follows

$$GU_{n+1} = pGU_n + qGU_{n-1} \qquad GU_0 = a,\ GU_1 = b$$

Where a and b are initial values [4]..

Definition 1: The Gaussian Pell numbers $\{GP_n\}_{n\geq 0}$ are determined by:

$$GP_n = 2GP_{n-1} + GP_{n-2}$$

With initial conditions $GP_0 = i$, $GP_1 = 1$

If $p = 2,\ q = 1,\ a = i,\ b = 1$ is taken ın the generalized Gaussian Fibonacci sequences $U_n(p, q, a, b)$, then the Gaussian Pell sequences

$$\{ GP_n \} = \{i, 1, 2 + i, 5 + 2i, 12 + 5i, \dots\}$$

is obtained [4].

Let $A_n = [a_{ij}]$ be an nxn matrix and S_n is a symetric group of permutations over the set $\{1,2, \dots n\}$. The determinant of A matrix defined by

$$\det A = \sum_{\alpha \in S_n} sgn(\alpha) \prod_{i=1}^{n} a_{i\alpha(i)}$$

where the sum ranges over all the permutations of the integers $1, 2, \dots, n$. It can be denoted by $sgn(\alpha) = \pm 1$ the signature of α, equal to $+1$ if α is the product an even number of transposition and -1 otherwise. The permanent of A matrix is defined by

$$\operatorname{per} A = \sum_{\alpha \in S_n} \prod_{i=1}^{n} a_{i\alpha(i)}$$

where the summation extends over all permutations α of the symmetric group S_n [5].

Main Results

The general formula for the n-th Gaussian Pell numbers is given by the following theorem..

Theorem 1: For integer $n \geq 0$ where $GP_0 = i$

$$GP_{n+1} = \sum_{k=0}^{\left\lfloor \frac{n}{2} \right\rfloor} 2^{n-2k} \binom{n-k}{k} + i \sum_{k=0}^{\left\lfloor \frac{n-1}{2} \right\rfloor} 2^{n-1-2k} \binom{n-1-k}{k}$$

Proof: The proof can be completed using the inductive method. Let $n \geq 0$ be an integer. For $n < 2$ where $\left\lfloor \frac{n}{2} \right\rfloor = 0$

$$GP_1 = 1 \text{ ve } GP_2 = 2 + i$$

Let $n \geq 2$ and equality (2) be true for n. In this case it must be shown that it is true for $n+1$ From definition 1 and the inductive hypothesis

$$GP_{n+2} = 2GP_{n+1} + GP_n$$

$$= \sum_{k=0}^{\left\lfloor \frac{n}{2} \right\rfloor} 2^{n+1-2k} \binom{n-k}{k} + i \sum_{k=0}^{\left\lfloor \frac{n-1}{2} \right\rfloor} 2^{n-2k} \binom{n-1-k}{k}$$

$$+ \sum_{k=0}^{\left\lfloor \frac{n-1}{2} \right\rfloor} 2^{n-1-2k} \binom{n-1-k}{k} + i \sum_{k=0}^{\left\lfloor \frac{n-2}{2} \right\rfloor} 2^{n-2-2k} \binom{n-2-k}{k}$$

$$= 2^{n+1} \binom{n}{0} + \sum_{k=1}^{\left\lfloor \frac{n}{2} \right\rfloor} 2^{n+1-2k} \binom{n-k}{k} + \sum_{k=0}^{\left\lfloor \frac{n-1}{2} \right\rfloor} 2^{n-1-2k} \binom{n-1-k}{k}$$

$$+i \left(2^n \binom{n-1}{0} + \sum_{k=1}^{\left\lfloor \frac{n-1}{2} \right\rfloor} 2^{n-2k} \binom{n-1-k}{k} + \sum_{k=0}^{\left\lfloor \frac{n-2}{2} \right\rfloor} 2^{n-2-2k} \binom{n-2-k}{k} \right)$$

$$= 2^{n+1} + \sum_{k=0}^{\left\lfloor \frac{n}{2} \right\rfloor - 1} 2^{n+1-2(k+1)} \binom{n-(k+1)}{k+1} + \sum_{k=0}^{\left\lfloor \frac{n-1}{2} \right\rfloor} 2^{n-1-2k} \binom{n-(k+1)}{k}$$

$$+i \left(2^n + \sum_{k=0}^{\left\lfloor \frac{n-1}{2} \right\rfloor - 1} 2^{n-2(k+1)} \binom{n-1-(k+1)}{k+1} + \sum_{k=0}^{\left\lfloor \frac{n-2}{2} \right\rfloor} 2^{n-2-2k} \binom{n-2-k}{k} \right)$$

$$= 2^{n+1} + \sum_{k=0}^{\left\lfloor \frac{n}{2} \right\rfloor - 1} 2^{n-1-2k} \binom{n-(k+1)}{k+1} + \sum_{k=0}^{\left\lfloor \frac{n-1}{2} \right\rfloor} 2^{n-1-2k} \binom{n-(k+1)}{k}$$

$$+i\left(2^n+\sum_{k=0}^{\left\lfloor\frac{n-1}{2}\right\rfloor-1}2^{n-2-2k}\binom{n-2-k}{k+1}+\sum_{k=0}^{\left\lfloor\frac{n-2}{2}\right\rfloor}2^{n-2-2k}\binom{n-2-k}{k}\right)$$

$$=2^{n+1}+\sum_{k=0}^{\left\lfloor\frac{n-1}{2}\right\rfloor}2^{n-1-2k}\binom{n-(k+1)+1}{k+1}$$

$$+i\left(2^n+\sum_{k=0}^{\left\lfloor\frac{n-2}{2}\right\rfloor}2^{n-2-2k}\binom{n-1-k}{k+1}\right)$$

$$=2^{n+1}+\sum_{k=1}^{\left\lfloor\frac{n+1}{2}\right\rfloor}2^{n+1-2k}\binom{n+1-k}{k}$$

$$+i\left(2^n+\sum_{k=1}^{\left\lfloor\frac{n}{2}\right\rfloor}2^{n-2k}\binom{n-k}{k}\right)g$$

$$=\sum_{k=0}^{\left\lfloor\frac{n+1}{2}\right\rfloor}2^{n+1-2k}\binom{n+1-k}{k}+i\sum_{k=0}^{\left\lfloor\frac{n}{2}\right\rfloor}2^{n-2k}\binom{n-k}{k}$$

And the desired result is obtained. Thus, the proof is completed.

In the proof of Theorem is taken into consideration $x<y\Rightarrow\binom{x}{y}=0, x<0\Rightarrow\binom{x}{y}=0$ and $\binom{x}{0}=1$.

In this section, we define some tridiagonal matrix and than show that the permanent and determinant of this matrices equal to the Gaussian Pell numbers.

Definition 2: We define a nxn tridiagonal matrix $A=(a_{ij})$ with $a_{11}=2i-1$, $i\neq 1, a_{ii}=2i$ $a_{i+1,i}=a_{i,i+1}=1$ for $1\leq i\leq n$ and 0 otherwise. That is,

$$A=\begin{bmatrix} 2i-1 & 1 & 0 & 0 & \cdots & 0 & 0 \\ 1 & 2i & 1 & 0 & \cdots & 0 & 0 \\ 0 & 1 & 2i & 1 & \cdots & 0 & 0 \\ \vdots & \vdots & \vdots & & \ddots & \vdots & \vdots \\ 0 & 0 & 0 & & & 2i & 1 \\ 0 & 0 & 0 & & \cdots & 1 & 2i \end{bmatrix}_{nxn}$$

Then we give following Theorem.

Theorem 2: Let the matrix A be as in following.

$$A = \begin{bmatrix} 2i-1 & 1 & 0 & 0 & \cdots & 0 & 0 \\ 1 & 2i & 1 & 0 & \cdots & 0 & 0 \\ 0 & 1 & 2i & 1 & \cdots & 0 & 0 \\ \vdots & \vdots & \vdots & & \ddots & \vdots & \vdots \\ 0 & 0 & 0 & & & & \\ 0 & 0 & 0 & & \cdots & \begin{matrix} 2i \\ 1 \end{matrix} & \begin{matrix} 1 \\ 2i \end{matrix} \end{bmatrix}_{nxn}$$

Then for $n \geq 2$

$GP_0 = i$, $GP_1 = 1$ and $detA_0 = 1$

$$GP_n = (-i)^{n-1} detA_{(n-1)x(n-1)}$$

where GP_n is the nth-Gaussian Pell number

Proof: If the determinant is calculated according to the nth row

$$detA_{nxn} = (-1)^{n+n-1} det \begin{bmatrix} 2i-1 & 1 & 0 & 0 & \cdots & 0 & 0 \\ 1 & 2i & 1 & 0 & \cdots & 0 & 0 \\ 0 & 1 & 2i & 1 & \cdots & 0 & 0 \\ \vdots & \vdots & \vdots & & \ddots & \vdots & \vdots \\ 0 & 0 & 0 & & & & \\ 0 & 0 & 0 & & \cdots & \begin{matrix} 2i \\ 1 \end{matrix} & \begin{matrix} 0 \\ 1 \end{matrix} \end{bmatrix}_{(n-1)x(n-1)}$$

$$+2i(-1)^{n+n} detA_{(n-1)x(n-1)} \tag{1}$$

$$det \begin{bmatrix} 2i-1 & 1 & 0 & 0 & \cdots & 0 & 0 \\ 1 & 2i & 1 & 0 & \cdots & 0 & 0 \\ 0 & 1 & 2i & 1 & \cdots & 0 & 0 \\ \vdots & \vdots & \vdots & & \ddots & \vdots & \vdots \\ 0 & 0 & 0 & & & & \\ 0 & 0 & 0 & & \cdots & \begin{matrix} 2i \\ 1 \end{matrix} & \begin{matrix} 0 \\ 1 \end{matrix} \end{bmatrix}_{(n-1)x(n-1)}$$

If the determinant is calculated according to the last column,

$$det \begin{bmatrix} 2i-1 & 1 & 0 & 0 & \cdots & 0 & 0 \\ 1 & 2i & 1 & 0 & \cdots & 0 & 0 \\ 0 & 1 & 2i & 1 & \cdots & 0 & 0 \\ \vdots & \vdots & \vdots & & \ddots & \vdots & \vdots \\ 0 & 0 & 0 & & & & \\ 0 & 0 & 0 & & \cdots & \begin{matrix} 2i \\ 1 \end{matrix} & \begin{matrix} 0 \\ 1 \end{matrix} \end{bmatrix}_{(n-1)x(n-1)} = (-1)^{2n-2} detA_{(n-2)x(n-2)} \tag{2}$$

If (2) is written instead of (1);

$$detA_{nxn} = (-1)^{n+n-1}(-1)^{2n-2} detA_{(n-2)x(n-2)} + 2i(-1)^{n+n} detA_{(n-1)x(n-1)}$$

$$= -detA_{(n-2)x(n-2)} + 2idetA_{(n-1)x(n-1)} \tag{3}$$

If The inductive method is used to show that

$$GP_n = (-i)^{n-1}detA_{(n-1)x(n-1)}$$

For $n = 2$,

$$GP_2 = (-i)^{2-1}detA_{1x1} = (-i)det[2i - 1] = (-i)(2i - 1) = 2 + i$$

Let's assume that it is true for $n = k$. Accordingly,

$$GP_k = (-i)^{k-1}detA_{(k-1)x(k-1)}$$

For $n = k + 1$, Let's show that it is

$$GP_{k+1} = (-i)^k detA_{kxk}$$

From the relation

$$GP_{k+1} = 2GP_k + GP_{k-1}$$

$$\begin{aligned} GP_{k+1} &= 2(-i)^{k-1}detA_{(k-1)x(k-1)} + (-i)^{k-2}detA_{(k-2)x(k-2)} \\ &= (-i)^k[2(-i)^{-1}detA_{(k-1)x(k-1)} + (-i)^{-2}detA_{(k-2)x(k-2)}] \\ &= (-i)^k[2idetA_{(k-1)x(k-1)} - detA_{(k-2)x(k-2)}] \end{aligned}$$

From equation (3)

$$GP_{k+1} = (-i)^k detA_{kxk}$$

Definition 3: We define a nxn tridiagonal matrix B= (b_{ij}) with $b_{11} = 2i - 1$, $i \neq 1, b_{ii} = 2i$ $b_{i+1,i} = 1$ $b_{i,i+1} = -1$ for $1 \leq i \leq n$ and 0 otherwise. That is,

$$B = \begin{bmatrix} 2i-1 & -1 & 0 & 0 & \cdots & 0 & 0 \\ 1 & 2i & -1 & 0 & \cdots & 0 & 0 \\ 0 & 1 & 2i & -1 & \cdots & 0 & 0 \\ \vdots & \vdots & \vdots & & \ddots & \vdots & \vdots \\ 0 & 0 & 0 & & & 2i & -1 \\ 0 & 0 & 0 & & \cdots & 1 & 2i \end{bmatrix}_{nxn}$$

Then we give following Theorem.

Theorem 3:

$$B = \begin{bmatrix} 2i-1 & -1 & 0 & 0 & \cdots & 0 & 0 \\ 1 & 2i & -1 & 0 & \cdots & 0 & 0 \\ 0 & 1 & 2i & -1 & \cdots & 0 & 0 \\ \vdots & \vdots & \vdots & & \ddots & \vdots & \vdots \\ 0 & 0 & 0 & & & 2i & -1 \\ 0 & 0 & 0 & & \cdots & 1 & 2i \end{bmatrix}_{nxn}$$

Then for $n \geq 2$

$GP_0 = i$, $GP_1 = 1$ and $PerB_0 = 1$

$$GP_n = (-i)^{n-1} PerB_{(n-1)x(n-1)}$$

where GP_n is the nth-Gaussian Pell number

Proof : We prove this by induction on n.

$$GP_n = (-i)^{n-1} PerB_{(n-1)x(n-1)}$$

It s true for $n = 2$,

$$PerB_{1X1} = a_{11} = (2i - 1)$$

$$GP_2 = (-i)^1 (2i - 1) = 2 + i.$$

Let's assume that it is true for $n = k$. Accordingly,

$$GP_k = (-i)^{k-1} PerB_{(k-1)x(k-1)}.$$

For $n = k + 1$, Let's show that it is

$$GP_{k+1} = (-i)^k PerB_{kxk}$$

From the relation

$$GP_{k+1} = 2GP_k + GP_{k-1}$$

$$\begin{aligned} GP_{k+1} &= 2(-i)^{k-1} PerB_{(k-1)x(k-1)} + (-i)^{k-2} PerB_{(k-2)x(k-2)} \\ &= (-i)^k [2(-i)^{-1} PerB_{(k-1)x(k-1)} + (-i)^{-2} PerB_{(k-2)x(k-2)}] \\ &= (-i)^k [2iPerB_{(k-1)x(k-1)} - PerB_{(k-2)x(k-2)}] \qquad (4) \end{aligned}$$

If we expand the $PerB_{kxk}$ by the Laplace expansion of a permanent with respect to the last row

$$PerB_{kxk} = 1.Per\begin{bmatrix} 2i-1 & -1 & 0 & 0 & \cdots & 0 & 0 \\ 1 & 2i & -1 & 0 & \cdots & 0 & 0 \\ 0 & 1 & 2i & -1 & \cdots & 0 & 0 \\ \vdots & \vdots & \vdots & & \ddots & \vdots & \vdots \\ 0 & 0 & 0 & & & 2i & 0 \\ 0 & 0 & 0 & & \cdots & 1 & -1 \end{bmatrix}_{(n-1)x(n-1)}$$

$$+ 2i.Per\begin{bmatrix} 2i-1 & -1 & 0 & 0 & \cdots & 0 & 0 \\ 1 & 2i & -1 & 0 & \cdots & 0 & 0 \\ 0 & 1 & 2i & -1 & \cdots & 0 & 0 \\ \vdots & \vdots & \vdots & & \ddots & \vdots & \vdots \\ 0 & 0 & 0 & & & 2i & 0 \\ 0 & 0 & 0 & & \cdots & 1 & 2i \end{bmatrix}_{(n-1)x(n-1)}$$

$$Per\begin{bmatrix} 2i-1 & -1 & 0 & 0 & \cdots & 0 & 0 \\ 1 & 2i & -1 & 0 & \cdots & 0 & 0 \\ 0 & 1 & 2i & -1 & \cdots & 0 & 0 \\ \vdots & \vdots & \vdots & & \ddots & \vdots & \vdots \\ 0 & 0 & 0 & & & 2i & 0 \\ 0 & 0 & 0 & & \cdots & 1 & -1 \end{bmatrix}_{(n-1)x(n-1)}$$

by the Laplace expansion of a permanent with respect to the last coloumn

$$PerB_{kxk} = 1.(-1)Per\begin{bmatrix} 2i-1 & -1 & 0 & 0 & \cdots & 0 & 0 \\ 1 & 2i & -1 & 0 & \cdots & 0 & 0 \\ 0 & 1 & 2i & -1 & \cdots & 0 & 0 \\ \vdots & \vdots & \vdots & & \ddots & \vdots & \vdots \\ 0 & 0 & 0 & & & 2i & -1 \\ 0 & 0 & 0 & & \cdots & 1 & 2i \end{bmatrix}_{(n-2)x(n-2)}$$

$$+ 2i.Per\begin{bmatrix} 2i-1 & -1 & 0 & 0 & \cdots & 0 & 0 \\ 1 & 2i & -1 & 0 & \cdots & 0 & 0 \\ 0 & 1 & 2i & -1 & \cdots & 0 & 0 \\ \vdots & \vdots & \vdots & & \ddots & \vdots & \vdots \\ 0 & 0 & 0 & & & 2i & 0 \\ 0 & 0 & 0 & & \cdots & 1 & 2i \end{bmatrix}_{(n-1)x(n-1)}$$

And then

$$PerB_{kxk} = 1.(-1)PerB_{(k-2)x(k-2)} + 2iPerB_{(k-1)x(k-1)} \tag{5}$$

If (5) is used to (4);

$$GP_{k+1} = (-i)^k\left[2iPerB_{(k-1)x(k-1)} - PerB_{(k-2)x(k-2)}\right] = (-i)^k PerB_{kxk}$$

REFERENCES

1. Horadam, A.F. Complex Fibonacci numbers and Fibonacci quaternions. The American Mathematical Monthly, Vol:70, No:3, 289-291, 1963.

2. Jordan, J.H. Gaussian Fibonacci and Lucas numbers. The Fibonacci Quarterly, Vol:3, No:4,315-318, 1965.
3. Horadam, A.F. Generalized Fibonacci Sequence, The American Mathematical Monthly, Vol:68, No:5, 455-459, 1961.
4. Halıcı, S., Öz, S. On Some Gaussian Pell and Pell –Lucas numbers. Ordu University journal of sciences and technology,Vol: 6 , No:1,8-18, 2016.
5. Minc, H., Marcus, M. Permanents, Encyclopedia Math. Appl., Addison–Wesley Publishing Company, London, Vol: 6, 1978.

A NOTE ON DEMI WEAK ALMOST LIMITED OPERATORS

Gül Sinem Keleş [1], Birol Altın [2]

Department of Mathematics, University of Gazi, Ankara, Turkey

gsinemkeles@gmail.com,

birola@gazi.edu.tr

Abstract

In this study, we introduce the class of demi-weak almost limited operators on a Banach lattice as a generalization of weak almost limited operators defined by Elbour A., Machrafi N., and Moussa M. in 2015. Let E be a Banach lattice, an operator $T: E \to E$ is called a demi-weak almost limited operator if for every sequence $(x_n) \subset E$ and every pairwise disjoint sequence $(f_n) \subset E'$ whenever $x_n \xrightarrow{w} 0$, $f_n \xrightarrow{w^*} 0$ and $(f_n(x_n) - f_n(T(x_n))) \to 0$ implies $f_n(x_n) \to 0$. We examine the relationship between weak almost limited operators and demi-weak almost limited operators. In addition, we establish a characterization of demi-weak almost limited operators. Finally, we obtain some properties of the class of demi-weak almost limited operators.

Keywords: Weak almost limited operators; Demi-weak almost limited operators; Limited operators; Banach lattice.

1.INTRODUCTION

The demi notation was first used by Petryshyn in 1966 [11]. Krichen and Regan studied the class of weakly demicompact operators in 2019 [3]. After that, the class of demi Dunford-Pettis operators was introduced by Benkhaled, Hajji and Jeribi [8]. The class of order weakly demicompact operators was studied by Benkhaled, Elluech and Jeribi in 2020 [9]. Recently, further studies on the demi class were introduced by Keles and Altın [6,7].

Elbour, Machrafi, and Moussa introduced the class of weak almost limited operators in 2015. Recall from [1] let E be a Banach space and F be a Banach lattice. An operator $T: E \to F$ is called a weak almost limited operator if $f_n(T(x_n)) \to 0$ for every weakly null sequence $(x_n) \subset E$ and every weak* null sequence $(f_n) \subset F'$ with pairwise disjoint terms. The class of all weak almost limited operators from E into F is denoted by $L_{wal}(E, F)$.

In this study, we introduce the class of demi-weak almost limited operators on a Banach lattice as a generalization of weak almost limited operators.

In this study, the identity operator is denoted by *I*. For all other undefined terms and notations, we will adhere to the conventions in [4,5,10].

2.MAIN RESULTS

Definition 2.1. Let E be a Banach lattice, an operator $T: E \to E$ is called a demi-weak almost limited operator if for every sequence $(x_n) \subset E$ and every pairwise disjoint sequence $(f_n) \subset E'$ whenever $x_n \overset{w}{\to} 0$, $f_n \overset{w^*}{\to} 0$ and $(f_n(x_n) - f_n(T(x_n))) \to 0$ implies $f_n(x_n) \to 0$. The class of all demi-weak almost limited operators on E is denoted by $DL_{wal}(E)$.

Example 2.1 Let E be a Banach lattice. Then, αI is a demi-weak almost limited operator on E for all $\alpha \neq 1$.

Indeed; assume that for every sequence $(x_n) \subset E$ and every pairwise disjoint sequence $(f_n) \subset E'$ such that $x_n \overset{w}{\to} 0$, $f_n \overset{w^*}{\to} 0$ and $(f_n(x_n) - \alpha f_n(x_n)) \to 0$. Thus, it follows that $f_n(x_n)(1-\alpha) \to 0$, and hence $f_n(x_n) \to 0$. This shows that αI is a demi-weak almost limited operator for all $\alpha \neq 1$.

Example 2.2 Let $E = c_0$. Consider the sequence $(e_n) \subset E$ whose the n-th term is one, and all other terms are zero. It is well known that $e_n \overset{w}{\to} 0$ in E and $(f_n) \subset E'$ defined $f_n: l_1 \to \mathbb{R}$ by $f_n(\alpha) = \alpha_n$ for all $\alpha = (\alpha_n) \in l_1$. Then, each the sequence (f_n) is pairwise disjoint, $f_n \overset{w^*}{\to} 0$ and $(f_n(e_n) - f_n(I(e_n)) = (0) \to 0$ holds. On the other hand; since $f_n(e_n) = 1$ for all $n \in \mathbb{N}$, the identity operator on c_0 is not a demi- weak almost limited operator.

Example 2.3 Let $n \in \mathbb{N}$, and define the operator $T_n: c_0 \to c_0$ by $T_n(x) = \sum_{i=1}^{n} x_i e_i$. The operator T_n is a demi-weak almost limited operator. Now, define $R_n = I + T_n$ for each $n \in \mathbb{N}$. It is clear that R_n is not a demi-weak almost limited operator for each $n \in \mathbb{N}$.

Theorem 2.1 Let E be a Banach lattice. Then, every weak almost limited operator on E is demi-weak almost limited.

Proof Let $T: E \to E$ be a weak almost limited operator. Assume that for every sequence $(x_n) \subset E$ and every pairwise disjoint sequence $(f_n) \subset E'$ such that $x_n \overset{w}{\to} 0$, $f_n \overset{w^*}{\to} 0$ and $(f_n(x_n) - f_n(T(x_n))) \to 0$. It can be written as

$$f_n(x_n) = [f_n(x_n) - f_n(T(x_n))] + [f_n(T(x_n))].$$

From the assumption, the equality and $T \in L_{wal}(E)$, it is obtained that $f_n(x_n) \to 0$. As a result, T is a demi-weak almost limited operator.

It is given in Theorem 2.1 that every weak almost limited operator is a demi-weak almost limited; however, the converse is not true in general.

Example 2.4 Let $T: c_0 \to c_0$ be an operator and $T = \frac{1}{2}I$. Since I is not demi-weak almost limited from Example 2.2, I is not a weak almost limited operator. As a result, it is easily seen that $\frac{1}{2}I$ is not weak almost limited but T is a demi-weak almost limited operator from Example 2.1.

Example 2.5 Let $T, S: c_0 \to c_0$ be operators defined by $T = S = \frac{1}{2}I$. By Example 2.1 T and S are demi-weak almost limited operators. However, $T + S = I$ is not a demi-weak almost limited operator from Example 2.2.

As a result, Example 2.5 shows that the class of demi-weak almost limited operators is not a vector space.

Theorem 2.2 Let E be a Banach lattice, $T: E \to E$ be a weak almost limited operator and $S: E \to E$ be a demi-weak almost limited operator. Then, $T + S$ is demi-weak almost limited.

Proof Let $(x_n) \subset E$ be a sequence and $(f_n) \subset E'$ be a pairwise disjoint sequence such that $x_n \xrightarrow{w} 0$, $f_n \xrightarrow{w^*} 0$ and $(f_n(x_n) - f_n((T+S)(x_n))) \to 0$. Since T is a weak almost limited operator, it is obtained that $f_n(T(x_n)) \to 0$. It can be written as

$$f_n(x_n) - f_n(S(x_n)) = f_n(x_n) - f_n(T(x_n)) + f_n(T(x_n)) - f_n(S(x_n))$$

$$= f_n(x_n) - f_n((T+S)(x_n)) + f_n(T(x_n)).$$

From the hypothesis, the equality and $T \in L_{wal}(E)$, it is obtained that $f_n(x_n) - f_n(S(x_n)) \to 0$. Since $S \in DL_{wal}(E)$, it is seen that $f_n(x_n) \to 0$. Thus, $T + S$ is a demi-weak almost limited operator.

Definition 2.2 Let E be a Banach lattice. E has the weak almost limited-property (wal-property) if for every weakly null sequence $(x_n) \subset E$ and every weak* null sequence $(f_n) \subset E'$ with pairwise disjoint terms, then $f_n(x_n) \to 0$.

Example 2.6 Let $E = l_1$. E has the wal-propery. Indeed; assume that sequence $(x_n) \subset E$, disjoint sequence $(f_n) \subset E'$ such that $x_n \overset{w}{\rightarrow} 0$ and $f_n \overset{w^*}{\rightarrow} 0$. Since E has the Schur property, $x_n \overset{\|.\|}{\rightarrow} 0$ [4], and from Banach Steinhaus Theorem [2], it is obtained that $sup\{ \|f_n\| : n \in \mathbb{N} \} = M < \infty$. On the other hand, $0 \leq |f_n(x_n)| \leq \|f_n\|\|x_n\| \leq M\|x_n\| \xrightarrow{n\to\infty} 0$. Hence, $f_n(x_n) \to 0$.

Example 2.7 All finite-dimensional spaces have the wal-property.

For the next theorem, we need some notations.

$$L_{cwal}(E) \coloneqq \{T |\; T: E \longrightarrow E \text{ continuous weak almost limited operator}\}$$
$$DL_{cwal}(E) \coloneqq \{T |\; T: E \longrightarrow E \text{ continuous demi} - \text{ weak almost limited operator}\}$$

Theorem 2.3 Let E be a Banach lattice. Then, the following statements are equivalent.

i) E has the wal-property.

ii) $L_{cwal}(E)$= $DL_{cwal}(E)$.

Proof $(i) \Longrightarrow (ii)$ It is known that $L_{cwal}(E) \subset DL_{cwal}(E)$ from Theorem 2.1. Let $(x_n) \subset E$ be a sequence, $(f_n) \subset E'$ be a disjoint sequence such that $x_n \overset{w}{\rightarrow} 0$ and $f_n \overset{w^*}{\rightarrow} 0$ and let T be a continuous demi-weak almost limited operator. Given that T is a continuous operator, it is obtained that $T(x_n) \overset{w}{\rightarrow} 0$. Since E has the wal-property, it follows that $f_n(T(x_n)) \rightarrow 0$. Thus, T is demi-weak almost limited.

$(ii) \Longrightarrow (i)$ Let $L_{cwal}(E) = DL_{cwal}(E)$. Since $\frac{I}{2} \in \mathfrak{D}L_{cwal}(E)$ from Example 2.1, then $\frac{I}{2} \in L_{cwal}(E)$. Thus, $I \in L_{cwal}(E)$. Hence, E has wal-property from Definition 2.2.

Conclusion 2.1 Let E be a Banach lattice. Then, the following statements are equivalent:

i) All continuous operators on E are demi-weak almost limited operator.

(ii) $I: E \rightarrow E$ is a demi-weak almost limited operator.

(iii) E has the wal-property.

3.CONCLUSIONS

In this study, the class of demi-weak almost limited operators on a Banach lattice is introduced as a generalization of the weak almost limited operators defined by Elbour A., Machrafi N., and Moussa M. in 2015. It is shown that the class of demi- weak almost limited operators is not generally a vector space. In addition, the relationship between weak almost limited operators and demi- weak almost limited operators is studied. Moreover, it is concluded that the class of demi-weak almost limited operators includes the class of weak almost limited operators. Finally, the wal-property is defined on Banach lattice E, and a characterization of the wal-property is examined in terms of continuous demi-weak almost limited operators.

REFERENCES

[1] A. Elbour, N. Machrafi, M. Moussa, On the class of weak almost limited operators, Quaestiones Mathematicae, Vol:38, No:6, 817–827, 2015.

[2] A.P. Robertson, W. Robertson, Topologıcal Vector Spaces, Cambridge at the University Press, 1973.

[3] B. Krichen, D. O'Regan, Weakly demicompact linear operators and axiomatic measures of weak noncompactness, Mathematica Slovaca, Vol: 69, No:6, 2019.

[4] C.D. Aliprantis, O. Burkinshaw, Positive Operators, Berlin, Springer, 2006.

[5] C.D. Aliprantis, O. Burkinshaw, Locally Solid Riesz Spaces, New York, Academic Press, 1978.

[6] G.S. Keles, B. Altın, The Class of Demi-Order Norm Continuous Operators, Gazi University Journal of Science, Vol:36, No:4, 1693 - 1698, 2023.

[7] G.S. Keles, B. Altın, The Class of Demi-Strongly Order Bounded Operators, Sakarya University Journal of Science, Vol:28, No:2, 364 - 370, 2024.

[8] H. Benkhaled, M. Hajji, A. Jeribi. On the class of demi Dunford-Pettis operators Rendiconti del Circolo Matematico di Palermo Series2, 1-11, 2022.

[9] H. Benkhaled, A. Elluech, A. Jeribi. The class of order weakly demicompact operators, Revista de la Real Academia de Ciencias Exactas, Físicas y Naturales. Serie A Matemáticas, Vol:114, No:2, 2020.

[10] P. Meyer-Nieberg, Banach Lattices, Berlin, Springer, 1991.

[11] W.V. Petryshyn, Construction of fixed points of demicompact mappings in Hilbert space, Journal of Mathematical Analysis and Applications, Vol:14, No:2, 276-284,1966.

A STUDY ON WARDOWSKI CONTRACTION IN *A*-METRIC SPACES

SÜHEYLA ELMAS [1] AND ALEYNA KAMBER ÖZEL[2]

Abstract

In this writing, we explore Wardowski's contraction principle for F -contraction mappings and demonstrate the existence and uniqueness o fixed points in A -Metric Spaces.

Introduction and preliminaries

The Banach contraction principle (BCP) [1] is widely regarded as one of the most signi cant results in metric xed point theory, largely in view of its simplicity and the practicality with which it can be applied across various mathematical disciplines. The theory of xed points combines ideas from topology, analysis, and geometry to investigate the existence and uniqueness of fixed points of a map. Over time, the BCP hasundergone a variety of generalizations in diferent directions. For example, Wardowski (2012) [2] extended the BCP and formulated the F -contraction , which inspired a range of subsequent studies on F -contractions more, [3], [4], [5]and [6]

Definition: [2]Let (H, A) be a metric space. A map $H: w \to w$ is called to be a F – contractions if there $\tau > 0$ such that for any $w, \varpi \in \mathrm{H}$

$$\left[d(H_w, H_\varpi) > 0 \Rightarrow \tau + F\left(d(H_w, H_\varpi) \leq F\big(d(w, \varpi)\big)\right)\right]$$

Here $F: R_+ \to R$ is a map fulfilling the following criterias:

$(F1)$ F is strictly increasing, via, for every $w, \varpi \in R_+$such that $w < \varpi$, $H_w < H_\varpi$

$(F2)$ For all sequence $\{\chi_n\}_{n=1}^{\infty} \subseteq R_+ \lim\limits_{n\to\infty} \chi_n = 0$ iff $\lim\limits_{n\to\infty} F(\chi_n) = -\infty$

$(F3)$ There is $k \in (0,1)$ such that $\lim\limits_{\chi \to 0^+} \chi^k F(\chi) = 0$

The set F is defined as the collection of whole maps fulfilling states $(\mathrm{F1}) - (\mathrm{F3})$. Gähler (1963) [8] presented the concept of a 2- metrict space and argued that this space is a generalization of an ordinary metric space. For valuable investigations on fixed point results, Dhage (1992) [9] recommended refining the basic framework of the 2-metric space. In (1984) [10] introduced the concept of a D-metric space. Naidu et al. (2004) [11] demonstrated that the notions of convergent sequences and sequential continuity are not clearly de ned in D - metric spaces. In (2005) [12], they highlighted certain limitations in the notion of open balls in D -metric spaces. The authors (2006) [13] developed the notion of G-metric space and examined its topological characteristics. Unlike the theory of G-metric spaces, here states

$(D1)$ $D(w, \varpi, \psi) \geq 0$, $\forall\, w, \varpi, \psi \in \mathrm{H}$ and equality is valid if $w = \varpi = \psi$ where $D: \mathrm{H}^3 \to \mathbb{R}$ is the function;

was replaced by the following three separate axioms, here $G: \mathrm{H}^3$ is the function $G: \mathrm{H}^3 \to \mathbb{R}$ is the function

$(G1)$ $G(w, \varpi, \psi) = 0$ if $w = \varpi = \psi$, $\forall\, w, \varpi, \psi \in \mathrm{H}$

$(G2)$ $G(w, \varpi, \varpi) \geq 0, \forall\, w, \varpi, \in \mathrm{H}$

$(G2)$ $G(w, w, \varpi) \leq G(\, w, \varpi, \psi), \forall\, w, \varpi, \psi \in \mathrm{H}$ via $\varpi \neq \psi$

Sedghi et al. (2007) [14] pointed out that condition (D1) could be substituted by just two axioms and thereby proposed the concept of a D^* - metric space.

Remark 1. Each G -metric space is a D^* metric space as well.

The authors (2012) [15] highlighted that condition (G3) is a distinct limitation of the G metric space, whereas the symmetry condition was identifed as a shared weakness in both D^* and G -metric spaces. To tackle these problems, these authors developed a new generalized metric space referred to as a S metric space.

Remark 2.[7] Each D^* -metric space is also a S -metric space.

Remark 3. [7]The S -metric space serves as a broader concept that includes both the G -metric space and the D^*metric space.

Abbas, et al. (2015) [7] present the notion of an A-metric space as outlined:

Definition 2. [7] Let be H a nonvoid set. A map $A: \mathrm{H}^n \to [0, \infty)$ is said an A-metric space is said on if for any w_i , $i = 1,2,3, \dots, n$ the following terms apply:

1) $A(w_1, w_{2,} w_3, \dots, w_{n-1}, w_n) \geq 0$

2) $A\left(w_1, w_{2,} w_3, \dots, w_{n-1}, w_n\right) = 0 \Leftrightarrow w_1 = w_2 = w_3 = \cdots = w_{n-1} = w_n$

3)$\mathrm{A}\left(w_1, w_{2,} w_3, \dots, w_{n-1}, w_n\right) \leq A\left(w_1, w_1, w_1, \dots, w_{1_{(n-1)}}, \gamma\right)$

$$+A\left(w_2, w_2, w_2, \dots, w_{2_{(n-1)}}, \gamma\right)$$

$$.$$

$$.$$

$$.$$

$$+A(w_{(n-1),} w_{(n-1),} w_{(n-1),} \dots, w_{(n-1)_{(n-1)}}, \gamma)$$

$$A(w_n, w_n, w_n, \dots, w_{n_{(n-1)}}, \gamma)$$

The dual (H, A) is said an A-metric space. From here it can be seen that the A-metric space is actually the n -dimensional S -metric space.

Example 1. Let $\mathrm{H} = \mathbb{R}$. Describe a map $A: \mathrm{H}^n \to [0, \infty)$ as

$$A(w_1, w_{2,}w_3, \dots, w_{n-1}, w_n) = |w_{(n)} + w_{(n-1)} + \dots + w_2 - (n-1)w_1|$$

$$+|w_{(n)} + w_{(n-1)} + \dots + w_3 - (n-2)w_2|$$

.

.

.

$$+|w_{(n)} + w_{(n-1)} + w_{(n-2)} - 3w_{(n-3)}|$$

$$+|w_{(n)} + w_{(n-1)} - 2w_{(n-2)}|$$

$$+|w_{(n)} + w_{(n-1)}|$$

Then (H, A) is an A-metric space.

Encouraged by these points, we first introduce and examine F-contraction in A-metric space as indicated below:

Definition 3. Let (H, A) be an A-metric space. A map $H: \mathrm{H} \to \mathrm{H}$ is called to be F-contraction if there is $\tau > 0$ such that for any $w, \varpi \in \mathrm{H}$,

$$A(\mathrm{H_w}, \mathrm{H_w}, \mathrm{H_w}, \dots, \mathrm{H_w}, \mathrm{H_\varpi}) > 0 \Rightarrow$$

$$\tau + F(\mathrm{H_w}, \mathrm{H_w}, \mathrm{H_w}, \dots, \mathrm{H_w}, \mathrm{H_\varpi}) \leq \mathrm{F}(\mathrm{A}(\mathrm{w}, \mathrm{w}, \mathrm{w}, \dots, \mathrm{w}, \omega))$$

Here $F: R_+ \to R$ is a satisfying the following states:

$(F1)$ F is strictly increasing,via, for every $w, \varpi \in R_+$ such that $w < \varpi$, $F(w) < F(\varpi)$

$(F1)$ For all sequence $\{\chi_n\}_{n=1}^{\infty} \subseteq R_+$ $\lim_{n\to\infty} \chi_n = 0$ iff $\lim_{n\to\infty} F(\chi_n) = -\infty$

$(F3)$ There is $k \in (0,1)$ such that $\lim_{\chi\to 0^+} \chi^k F(\chi) = 0$

Lemma 1. Let $F: R_+ \to R$ be an increasing map and $\{\chi_n\}_{n=1}^{\infty} \subseteq R_+$. Then the following terms apply:

(a) If $\lim_{n\to\infty} F(\chi_n) = -\infty$, then $\lim_{n\to\infty} \chi_n = 0$

(b)If $infF = -\infty$ and $\lim_{n\to\infty} \chi_n = 0$,then $\lim_{n\to\infty} F(\chi_n) = -\infty$

By proving Lemma 1. , Secelan [17] verified that the condition $(F2)$ in Definition 1. can be substituted with an equivalent, simpler condition,

$(F2^{'})$ $infF = -\infty$

as an alternative, additionally, with

$(F2^{''})$ there exist a sequence $\{\chi_n\}_{n=1}^{\infty} \subseteq R_+$ such that $\lim_{n\to\infty} F(\chi_n) = -\infty$

In the current paper, we use F-contraction maps in A-metric spaces and aim to extend Wardowski's theorem to A-metric spaces. There has been a rising interest in the generalization of classical metric spaces in the past few years. In this framework, 2-metric, D-metric, and G-metric spaces are viewed as generalized forms of usual metric spaces. The most crucial of these generalizations is A-metric spaces, since this space was developed to measure the distance between $n$points at the same time.

Theorem 1.Let (H, A) be a complete A-metric space and let a map $H\colon \mathrm{H} \to \mathrm{H}$ be a F contraction. Suppose $F \in \mathscr{F}$ and $\tau > 0$ such that for any $w, \varpi \in \mathrm{H}$

$$A(\mathrm{H_w}, \mathrm{H_w}, \mathrm{H_w}, \dots, \mathrm{H_w}, \mathrm{H_\varpi}) > 0 \Rightarrow$$

$$\tau + F(\mathrm{H_w}, \mathrm{H_w}, \mathrm{H_w}, \dots, \mathrm{H_w}, \mathrm{H_\varpi}) \leq \mathrm{F(A(w, w, w, \dots, w, \omega))}$$

Then H has a unique fixed point $w^* \in \mathrm{H}$ and for every $w_0 \in \mathrm{H}$ the sequence $\{H_{w_0}^n\}$ converges to w^*.

Proof. Select $w_0 \in \mathrm{H}$ express a sequence $\{w_n\}_{n=1}^{\infty}$ by

$w_1 = H_{w_0}$, $w_2 = H_{w_1}$=$H_{w_0}^2$, … , $w_{n+1} = H_n = H_{w_0}^{n+1}$ for each $n \in N$.

If there is $n \in N$ such that $A(w_n, w_n, w_n, \dots, w_n, H_{w_n}) = 0$ the proof is concluded. Thus,we presume that for every $n \in N$.

$0< A(w_n, w_n, w_n, \dots, w_n, H_{w_n}) = A(H_{w_{n-1}}, H_{w_{n-1}}, H_{w_{n-1}}, \dots, H_{w_{n-1}}, H_{w_n})$

For all $n \in N$, we attain

$\tau + F(A(H_{w_{n-1}}, H_{w_{n-1}}, H_{w_{n-1}}, \dots, H_{w_{n-1}}, H_{w_n})) \leq F(A(w_{n-1}, w_{n-1}, w_{n-1}, \dots, w_{n-1}, w_n)$,

i.e.,

$F(A(H_{w_{n-1}}, H_{w_{n-1}}, H_{w_{n-1}}, \dots, H_{w_{n-1}}, H_{w_n}))) \leq F(A(w_{n-1}, w_{n-1}, w_{n-1}, \dots, w_{n-1}, w_n) - \tau$

Reapplying this method,we arrive at

$$F(A(H_{w_{n-1}}, H_{w_{n-1}}, H_{w_{n-1}}, \dots, H_{w_{n-1}}, H_{w_n}))) \tag{2.3}$$

$\leq F(A(w_{n-1}, w_{n-1}, w_{n-1}, \dots, w_{n-1}, w_n) - \tau$

$\leq F\left(A\left(H_{w_{n-2}}, H_{w_{n-2}}, H_{w_{n-2}}, \dots, H_{w_{n-2}}, H_{w_{n-1}}\right)\right) - \tau$

$\leq \; F\left(A\left((w_{n-2}, w_{n-2}, w_{n-2}, \dots, w_{n-2}, w_{n-1})\right)\right) - 2\tau$

$\leq F\left(A\left(H_{w_{n-3}}, H_{w_{n-3}}, H_{w_{n-3}}, \dots, H_{w_{n-3}}, H_{w_{n-2}}\right)\right) - 2\tau$

$\leq \; F\left(A\left((w_{n-3}, w_{n-3}, w_{n-3}, \dots, w_{n-3}, w_{n-2})\right)\right) - 3\tau$

$\leq F\left(A\left(H_{w_{n-4}}, H_{w_{n-4}}, H_{w_{n-4}}, \dots, H_{w_{n-4}}, H_{w_{n-3}}\right)\right) - 3\tau$

.

.

.

$\leq \; F\left(A\left((w_0, w_0, w_0, \dots, w_0, w_1)\right)\right) - \; n\tau$

Due to (2.3),we acquire $\lim_{n\to\infty} F(A\left(H_{w_{n-1}}, H_{w_{n-1}}, H_{w_{n-1}}, \dots, H_{w_{n-1}}, H_{w_n}\right))) = -\infty$ which together with $(F2)'$ and Lemma1 gives

$$\lim_{n\to\infty} A\left(H_{w_{n-1}}, H_{w_{n-1}}, H_{w_{n-1}}, \dots, H_{w_{n-1}}, H_{w_n}\right) = 0$$

i.e.,

$$\lim_{n\to\infty} A\left(w_n, w_n, w_n, \dots, w_n, H_{w_n}\right) = 0 \qquad (2.4)$$

Next, we maintain that $\{w_n\}_{n=1}^{\infty}$ is a Cauchy sequence .Reasoning by contradiction, we presume that there exist $\varepsilon > 0$ and sequences $\{\chi_n\}_{n=1}^{\infty}, \{\vartheta_n\}_{n=1}^{\infty} \subset N$ such that

$\chi_n > \vartheta_n > n$ for every $n \in N$.

$$A(w_{\chi_n}, w_{\chi_n}, w_{\chi_n}, \dots, w_{\chi_n}, w_{\vartheta_n}) \geq \in \qquad (2.5)$$

$$(w_{\chi_{n-1}}, w_{\chi_{n-1}}, w_{\chi_{n-1}}, \dots, w_{\chi_{n-1}}, w_{\vartheta_n}) < \in \qquad (2.6)$$

So we have

$\in \leq A\left(w_{\chi_n}, w_{\chi_n}, w_{\chi_n}, \dots, w_{\chi_n}, w_{\vartheta_n}\right)$

$\leq (n-1)A\left(w_{\chi_n}, w_{\chi_n}, w_{\chi_n}, \dots, w_{\chi_n}, w_{\chi_{n-1}}\right) + A(w_{\vartheta_n}, w_{\vartheta_n}, w_{\vartheta_n}, \dots, w_{\vartheta_n}, w_{\chi_{n-1}})$

$= (n-1)A\left(w_{\chi_n}, w_{\chi_n}, w_{\chi_n}, \dots, w_{\chi_n}, w_{\chi_{n-1}}\right) + A(w_{\chi_{n-1}}, w_{\chi_{n-1}}, w_{\chi_{n-1}}, \dots, w_{\chi_{n-1}}, w_{\vartheta_n})$

$\leq (n-1)A\left(w_{\chi_n}, w_{\chi_n}, w_{\chi_n}, \dots, w_{\chi_n}, w_{\chi_{n-1}}\right) + \in$

$$\leq (n-1)A\left(w_{\chi_{n-1}}, w_{\chi_{n-1}}, w_{\chi_{n-1}}, \dots, w_{\chi_{n-1}}, H_{w_{\chi_{n-1}}}\right) + \in$$

It follow from (2.4) and last sentences

$$\lim_{n\to\infty} A(w_{\chi_n}, w_{\chi_n}, w_{\chi_n}, \dots, w_{\chi_n}, w_{\vartheta_n}) = \varepsilon \qquad (2.7)$$

On the other hand from (2.4) there is $N \in \mathbb{N}$ such that

$$A(w_{\chi_n}, w_{\chi_n}, w_{\chi_n}, \dots, w_{\chi_n}, H_{w_{\chi_n}}) < \frac{\varepsilon}{4(n-1)} \qquad (2.8)$$

$$A(w_{\vartheta_n}, w_{\vartheta_n}, w_{\vartheta_n}, \dots, w_{\vartheta_n}, H_{w_{\vartheta_n}}) < \frac{\varepsilon}{4}, \qquad (2.9)$$

$\forall \chi > \vartheta.$

Next we affirm that for any $\forall \chi > \vartheta$

$$A\left(H_{w_{\chi_n}}, H_{w_{\chi_n}} H_{w_{\chi_n}}, \dots, H_{w_{\chi_n}}, H_{w_{\vartheta_n}}\right) = A(w_{\chi_{n+1}}, w_{\chi_{n+1}}, w_{\chi_{n+1}}, \dots, w_{\chi_{n+1}}, w_{\vartheta_{n+1}}) > 0 \quad \forall n \geq N \qquad (2.10)$$

Arguing by contradiction there exist $\mathscr{M} \geq N$ such that

$$A\left(w_{\chi_{\mathscr{M}+1}}, w_{\chi_{\mathscr{M}+1}}, w_{\chi_{\mathscr{M}+1}}, \dots, w_{\chi_{\mathscr{M}+1}}, w_{\vartheta_{\mathscr{M}+1}}\right) = 0 \qquad (2.11)$$

It follows from (2.5), (2.6), (2.8), (2.9) and (2.11) that

$$\varepsilon \leq A\left(w_{\chi_n}, w_{\chi_n}, w_{\chi_n}, \dots, w_{\chi_n}, w_{\vartheta_n}\right)$$

$$\leq (n-1)A\left(w_{\chi_n}, w_{\chi_n}, w_{\chi_n}, \dots, w_{\chi_n}, w_{\chi_{n+1}}\right) + A(w_{\vartheta_n}, w_{\vartheta_n}, w_{\vartheta_n}, \dots, w_{\vartheta_n}, w_{\chi_{n+1}})$$

$$\leq (n-1)A\left(w_{\chi_n}, w_{\chi_n}, w_{\chi_n}, \dots, w_{\chi_n}, w_{\chi_{n+1}}\right) + A(w_{\chi_{n+1}}, w_{\chi_{n+1}} w_{\chi_{n+1}}, \dots, w_{\chi_{n+1}}, w_{\vartheta_n})$$

$$\leq (n-1)A\left(w_{\chi_n}, w_{\chi_n}, w_{\chi_n}, \dots, w_{\chi_n}, w_{\chi_{n+1}}\right) + (n-1)\, A(w_{\chi_{n+1}}, w_{\chi_{n+1}} w_{\chi_{n+1}}, \dots, w_{\chi_{n+1}}, w_{\vartheta_{n+1}}) \quad + A(w_{\vartheta_n}, w_{\vartheta_n}, w_{\vartheta_n}, \dots, w_{\vartheta_n}, w_{\vartheta_{n+1}})$$

$$\leq (n-1)A\left(w_{\chi_n}, w_{\chi_n}, w_{\chi_n}, \dots, w_{\chi_n}, w_{\chi_{n+1}}\right) + (n-1)\, A(w_{\chi_{n+1}}, w_{\chi_{n+1}} w_{\chi_{n+1}}, \dots, w_{\chi_{n+1}}, w_{\vartheta_{n+1}}) \quad + A(w_{\vartheta_{n+1}}, w_{\vartheta_{n+1}}, w_{\vartheta_{n+1}}, \dots, w_{\vartheta_{n+1}}, w_{\vartheta_n})$$

$$\leq \frac{\varepsilon}{4} + 0 + \frac{\varepsilon}{4}$$

This contradiction established the relation (2.10).Consequently, it can be inferred from (2.10) and the hypothesis of the theorem that

$$\tau + A\left(H_{w_{\chi_n}}, H_{w_{\chi_n}} H_{w_{\chi_n}}, \dots, H_{w_{\chi_n}}, H_{w_{\vartheta_n}}\right) \leq A\left(w_{\chi_n}, w_{\chi_n}, w_{\chi_n}, \dots, w_{\chi_n}, w_{\vartheta_n}\right) \quad \forall n \in N$$

From $(F3'$, (2.7) and (2.12) we gather $\tau + F(\varepsilon) \leq F(\varepsilon)$. This contradiction shows that $\{w_n\}_{n=1}^{\infty}$ is a Cauchy sequence. Owing to completeness of (H, A) , $\{w_n\}_{n=1}^{\infty}$ converges the some point w in H. Finally, the continuity of H yields.

$$A(H_w, H_w, H_w, \dots, H_w, w) = \lim_{n\to\infty}(H_{\chi_n}, H_{\chi_n}, H_{\chi_n}, \dots, H_{\chi_n}, \chi_n)$$

$$= \lim_{n\to\infty}(\chi_{n+1}, \chi_{n+1}, \chi_{n+1}, \cdots, \chi_{n+1}, \chi_n)$$

$$=A(w^*, w^*, w^*, \dots, w^*, w^*)$$

At this point, let us illustrate that H possesses at most one xed point. In fact, if $w, \varpi \in \mathrm{H}$ be to distinctive xed points of H, namely, $H_w = w \neq \varpi = H_\varpi$

Therefore

$$A(H_w, H_w, H_w, \dots, H_w, H_\varpi) = A(w, w, w, \dots, w, \varpi) > 0$$

then we get

$$F\big(A(w, w, w, \dots, w, \varpi)\big) = \mathrm{F}(A(H_w, H_w, H_w, \dots, H_w, H_\varpi))$$

$$< \tau + \mathrm{F}(A(H_w, H_w, H_w, \dots, H_w, H_\varpi))$$

$$\leq F\big(A(w, w, w, \dots, w, \varpi)\big)$$

which is a contradiction. Thereof, the xed point is a unique.

References

[1] Banach, B: Sur les opérations dons les ensembles abstraits et leur application aux équations intégrales. Fundam. Math. 3, 133-181 (1922)

[2] D. Wardowski, Fixed Points of a New Type of Contractive Mappings in Complete Metric Spaces, Fixed Point Theory Appl. 2012 (2012), 94

[3] E. Karap¬nar, A. Fulga, R.P. Agarwal, A Survey: F-Contractions With Related Fixed Point Results, J. Fixed Point Theory Appl. 22 (2020), 69. https://doi.org/10.1007/s11784-020 00803-7.

[4] Fabiano, Nicola, et al. "On F-contractions: A survey." Contemporary Mathematics (2022): 327-342.

[5] Acar, Özlem, Aybala Sevde Özkapu, and Mahpeyker Öztürk. "Some xed point results on ultrametric spaces endowed with a graph." Demonstratio Mathematica 57.1 (2024): 20230132.

[6] Bajovi´c, Du an, et al. "Remarks on Some Results of Extended Interpolative Hardy-Rogers Geraghty-Wardowski Contractions and ´Ciri´c-Reich-Rus Type F-Contractions." Sahand Com munications in Mathematical Analysis 22.1 (2025): 25-38.

[7] Abbas, Mujahid, Bashir Ali, and Yusuf I. Suleiman. "Generalized coupled common xed point results in partially ordered A-metric spaces." Fixed point theory and applications 2015 (2015): 1-24.

[8] Gähler, S: 2-metriche raume und ihre topologische strukture. Math. Nachr. 26, 115-148 (1963)

[9] Dhage, BC: Generalized metric spaces mappings with xed point. Bull. Calcutta Math. Soc. 84, 329-336 (1992)

[10] Dhage, BC: A study of some xed point theorem. Ph.D. thesis, Marathwada University, Aurangabad, India (1984)

[11] Naidu, SVR, Rao, KPR, Srinivasa, N: On the topology of D-metric spaces and the generation of D-metric spaces from metric spaces. Int. J. Math. Math. Sci. 51, 2719-2740 (2004)

[12] Naidu, SVR, Rao, KPR, Srinivasa, N: On the concepts of balls in a D-metric space. Int. J. Math. Math. Sci. 1, 133-141 (2005)

[13] Mustafa, Z, Sims, B: A new approach to generalized metric spaces. J. Nonlinear Convex Anal. 7(2), 289-297 (2006)

[14] Sedghi, S, Shobe, N, Zhou, H: A common xed point theorem in D metric spaces. Fixed Point Theory Appl. 2007, Article ID 027906 (2007)

[15] Sedghi, S, Shobe, N, Aliouche, A: A generalization of xed point theorems in S-metric spaces. Mat. Vesn. 64(3), 258-266 (2012)

[16] Piri, Hossein, and Poom Kumam. "Some xed point theorems concerning F-contraction in complete metric spaces." Fixed point theory and applications 2014 (2014): 1-11

[17] Secelean, NA: Iterated function systems coinsisting of F-contractions. Fixed point theory and applications. 2013. Article ID 277(2013)

[1] Ataturk University,Faculty of Education,Department of Mathematics and Sci ences,Erzurum−Türkiye,https://orcid.org/0000−0002−2639−9027

[2] Ataturk University,Graduate School of Natural and Applied Sciences,Erzurum−Türkiye,https://orcid.org/0009 0009−3168−8331

[1] suheylaelmas@atauni.edu.tr

[2] aleyna.kamber16@ogr.atauni.edu.tr

A BRIEF NOTE REGARDING F −CONTRACTIONS IN COMPLETE S −METRIC SPACES

Department of Mathematics, University of Atatürk, Erzurum, Turkey

ferdi.cinar18@ogr.atauni.edu.tr

Süheyla ELMAS[1] Ferdi ÇINAR[2]

may 17, 2025

Abstract

In this writing, we investigate fixed points of F −contraction in an abstract space. Additionally, the effectiveness of our work is confirmed through appropriate examples.

Keywords: S −metric space; Fixed point; F −contraction.

1.INTRODUCTION

The Banach contraction principle (BCP) [1] is widely regarded as one of the most significant results in metric fixed point theory, largely due to its simplicity and the practicality with which it can be applied across various mathematical disciplines. Over time, the BCP has undergone a variety of generalizations in different directions. Recently, Sedghi et al [13] introduced the concept of S −metric space which is different from other space and proved fixed point theorems in S −metric space. They also gives some examples of S − metric spaces which shows that S −metric space is different form other spaces. In this article, we will denote by $\mathbb{N}$ the set of all natural numbers, by $\mathbb{R}$ the set of all real numbers, and by $\mathbb{R}^+$ the set of all positive real numbers. The famous European mathematician Stefan Banach proved a theorem in 1922, which was a great first. Since the day he proved his theorem, scientists have been publishing studies on contraction mappings and metric spaces. Important works on S −metric spaces are the papers of S. Sedghi. [13]

2.GENERAL PROPERTIES OF METHOD

Theorem 1: Let $(\mathrm{M}, \mathrm{d_s})$ be a complete S −metric space and consider a mapping $\theta: \mathrm{M} \to \mathrm{M}$. Assume that for all $\eta, \mu \in \mathrm{M}$ with $\eta \neq \mu$, the condition

$$\mathrm{d_s}(\theta_\eta, \theta_\eta, \theta_\eta) < \mathrm{d_s}(\eta, \eta, \mu)$$

holds. Then, the mapping θ possesses a unique fixed point in M.

In 2008, Suzuki [2] provided generalized versions of Edelstein's results in the context of complete S −metric spaces.

Theorem 2: Let $(\mathrm{M}, \mathrm{d_s})$ be a complete S−metric space, and let $\theta: \mathrm{M} \to \mathrm{M}$ be a self−mapping. Suppose that for all $\eta, \mu \in \mathrm{M}$ with $\eta \neq \mu$,

$$\frac{1}{2_2}\mathrm{d_s}(\eta, \eta, \theta_\eta) < \mathrm{d_s}(\eta, \eta, \mu) \Rightarrow \mathrm{d_s}(\theta_\eta, \theta_\eta, \theta_\mu) < \mathrm{d_s}(\eta, \eta, \mu)$$ then θ has a unique fixed point in M.

In 2012, Wardowski [11] introduced a novel class of contraction mappings, known as F-contractions, and established a new fixed point theorem related to them. Through this contribution, Wardowski [11] offered a new perspective on the Banach contraction principle, distinct from the classical formulations found in the literature. The concept of F-contraction proposed by Wardowski is defined the as follows.

Definition 1. Let X be a non-empty set and let $\mathrm{d_s}: X^3 \to [0, \infty)$ For all $\forall \eta, \mu, \xi, t \in X$ let S be a function satisfying the following conditions:
1−) $\mathrm{d_s}(\eta, \mu, \xi) \geq 0$,
2−) $\mathrm{d_s}(\eta, \mu, \xi) = 0 \Leftrightarrow \eta = \mu = \xi$
3−) $\mathrm{d_s}(\eta, \mu, \xi) \leq S(\eta, \eta, t) + S(\mu, \mu, t) + S(\xi, \xi, t)$.
In this case, $\mathrm{d_s}$ is called an S −metric on X, and the pair $(X, \mathrm{d_s})$ is called an S −metric space.

Definition 2: Let $(\mathrm{M}, \mathrm{d_s})$ be a S-metric space. A mapping $\theta: \mathrm{M} \to \mathrm{M}$ is said to be an F −contraction if there exists $\lambda > 0$ such that $\forall \eta, \mu \in \mathrm{M}$,

$$\mathrm{d_s}(\theta_\eta, \theta_\eta, \theta_\mu) > 0 \Rightarrow \lambda + \mathrm{F}\left(\mathrm{d_s}(\theta_\eta, \theta_\eta, \theta_\mu)\right) \leq \mathrm{F}\left(\mathrm{d_s}(\eta, \eta, \mu)\right) \qquad (\mathbf{1})$$

where $\mathrm{F}: \mathbb{R}^+ \to \mathbb{R}$ is a mapping satisfying the following conditions:

(F1) F is strictly increasing, i.e. for all $\eta, \mu \in \mathbb{R}^+$ such that $\eta < \mu$, $\mathrm{F}(\eta) < \mathrm{F}(\mu)$;

(F2) For each sequence $\{\eta_n\}_{n=1}^{\infty}$ of positive numbers, $\lim_{n\to\infty}(\eta_n) = 0$ if and only if

$\lim_{n\to\infty} F(\eta_n) = -\infty$;

(F3) There exist $k \in (0,1)$ such that $\lim_{\eta\to\infty} \eta^k . F(\eta) = 0$

We denote by $\mathcal{F}$, the set of all functions satisfying the conditions (F1)-(F3). For examples of the function F the reader is referred to [12] and [11].

Remark 1: Based on conditions (F1) and (1), it is straightforward to deduce that every F −contraction is necessarily a continuous function.

Theorem 3: Let (M, d_s) be a complete S−metric space and suppose let $\theta: M \to M$ is an F −contraction. Then θ possesses a unique fixed point $\eta^* \in M$, and for any point $\eta \in M$ the sequence $\{\eta_n\}_{n\in\mathbb{N}}^{\infty}$ converges to η^*. Recently, Secelean [12] presented the following results:

Lemma 1: Let $F: \mathbb{R}^+ \to \mathbb{R}$ be an increasing function, and let $\{\eta_n\}_{n=1}^{\infty}$ be a sequence of positive real numbers.

Then the following statements are true:

(a) if $\lim_{n\to\infty} F(\eta_n) = -\infty$, then $\lim_{n\to\infty} \eta_n = 0$

(b) if $\inf F = -\infty$, and $\lim_{n\to\infty} \eta_n = 0$ then $\lim_{n\to\infty} F(\eta_n) = -\infty$.

Using Lemma 1, Secelean demonstrated that the condition (F2) from Definition 2 can be equivalently replaced with a simpler condition:

(F2′) $inf F = -\infty$

or also,by

(F2′′) There exist a sequence $\{\eta_n\}_{n=1}^{\infty}$ positive real numbers such that

Remark 2: Define $F: \mathbb{R}^+ \to \mathbb{R}$ by $F_\mu(\eta) = \ln \eta$. In this setting, F_μ belongs to the class $\mathcal{F}$. Notice that whan $F = F_\mu$, the corresponding F -contraction coincides with the classical Banach contraction. Consequently, every Banach contraction is a particular case of an F -contractions. Nevertheless, there are also F -contractions that lie outside the Banach framework (see [11],[12]).

Rather than imposing condition (F3) from Definition 2, we replace it here with the following simpler requirement:

(F3′) F is continuous on $(0,\infty)$.

We let $\mathfrak{I}$ denote the family of all functions satisfying (F1), (F2′), and (F3′).

Example 1: Consider the functions $F_1(\eta) = (-1)/\eta$, $F_2(\eta) = (-1)/\eta + \eta$, $F_3(\eta) = (1/1 - e^{\eta})$, $F_4(\eta) = (1/e^{\eta} - e^{-\eta})$. Then it follows that $F_1, F_2, F_3, F_4 \in \mathcal{F}$.

Remark 3: It should be noted that the condition (F3) and (F3′) are not dependent on one another.
For istance, for $p \geq 1$, the function $F(\eta) = -1/\eta^p$ satisfies the conditions (F1) and (F2), yet does not satisfy (F3); thus, $\mathfrak{I} \not\subseteq \mathcal{F}$. Alternatively $F(\eta) = -1/(\eta + [\eta])^t$, where $[\eta]$ denotes the greatest integer less than or equal to η, and $t \in (0,1/n)$. For $\eta > 1$, this function meets the criteria (F1) and (F2) but fails to meet (F3); nonetheless, it satisfies (F3′), while it satisfies the condition (F3) for any $k \in (1/\eta, 1)$. Therefore, $\mathcal{F} \not\subseteq \mathfrak{I}$. Also, if we take $F(\eta) = \ln\eta$, then $F \in \mathcal{F}$ and $F \in \mathfrak{I}$. Therefore, $\mathcal{F} \cap \mathfrak{I} \neq \emptyset$.

Motivated by Remark 3, we reformulate Wardowski's result [11] by allowing the contraction to involve functions F from the class $\mathfrak{I}$ reather than $F \in \mathcal{F}$. We then introduce the notion of an F-Suzuki contraction and state a corresponding variant of Theorem 3.

Definition 3: Let (M, d_s) be an S-metric space. A mapping $\theta: M \to M$ is called an F-Suzuki contraction if there exists a constant $\lambda > 0$ such that for all $\eta, \mu \in M$ with $\theta\eta \neq \theta\mu$ implication

$$1/2.\, d_s(\eta,\eta,\theta\eta) < d_s(\eta,\eta,\mu) \Rightarrow \lambda + F(d_s(\theta\eta,\theta\eta,\theta\mu)) \leq F(d_s(\eta,\eta,\mu)),$$

holds, where $F \in \mathfrak{I}$.

3.APPLICATIONS

Example 2 : Given $M = (0, \infty)$ let

$$d_s(\eta, \mu, \zeta) = |\eta - \mu| + |\mu - \zeta| + |\zeta - \eta|, \qquad \forall\, \eta, \mu, \zeta \in M$$

and

$$\theta(\eta) = \ln(\eta + 2)$$

be the metric and function, respectively, with the function,

$$F(t) = \frac{t}{5}$$

We aim to show that for ,

$$d_s(\theta\eta, \theta\eta, \theta\mu) > 0 \Rightarrow \lambda + F\big(d_s(\theta\eta, \theta\eta, \theta\mu)\big) \le F\big(d_s(\eta, \eta, \mu)\big), \qquad \lambda > 0$$

We have

$$\theta(\eta) = \ln(\eta + 2)$$

and

$$\theta(\mu) = \ln(\mu + 2) \qquad \eta, \mu \in M.$$

$$d_s(\theta\eta, \theta\eta, \theta\mu) = |\ln(\eta + 2) - \ln(\mu + 2)| + |\ln(\mu + 2) - \ln(\eta + 2)|$$

$$= 2.\, |\ln(\eta + 2) - \ln(\mu + 2)|$$

$$d_s(\eta, \eta, \mu) = |\eta - \mu| + |\mu - \eta|$$

$$= 2.\, |\eta - \mu|$$

$$F\left(d_s(\eta,\eta,\mu)\right)=\frac{2}{5}|\eta-\mu|$$

$$F\left(d_s(\theta\eta,\theta\eta,\theta\mu)\right)=\frac{2}{5}|\ln(\eta+2)-\ln(\mu+2)|$$

from the condition of the theorem ,

$$\lambda+\frac{2}{5}|\ln(\eta+2)-\ln(\mu+2)|\leq\frac{2}{5}|\eta-\mu|$$

Therefore, $\lambda>0$ is found to satisfy the inequality.

Let η^* be the fixed point of the

$$\theta(\eta)=\ln(\eta+2)$$

transformation and there exist η^* such that

$\ln(\eta^*+2)=\eta^*\Rightarrow(\eta^*+2)=e^{\eta^*}$

be

$$\eta^*=1{,}146.$$

Let's define an array with initial value $\eta_0>0$;

$$\begin{aligned}\eta_{n+1}&=\theta(\eta_n)\\&=\ln(\eta_n+2).\end{aligned}$$

$$\eta_1=\ln(\eta_0+2)$$

$$\eta_2 = \ln(\eta_1 + 2) = \ln(\ln(\eta_0 + 2) + 2)$$

$$\eta_3 = \ln(\eta_2 + 2) = \ln(\ln(\ln(\eta_0 + 2)) + 2)$$

$$\vdots$$

$$\ln(\eta + 2) = \eta$$

That is, for $\eta > 0$ the series converges decreasingly to η^*.

4.CONCLUSIONS

Theorem 3: Let M be a complete S −metric space. Suppose $\theta: M \to M$ is a F −contraction assume $F \in \mathcal{F}$ and there exist $\lambda > 0$ such that for,

$$\forall \eta, \mu \in M, [d_s(\theta\eta, \theta\eta, \theta\mu) > 0 \Rightarrow \lambda + F(d_s(\theta\eta, \theta\eta, \theta\mu)) \leq F(d_s(\eta, \eta, \mu))]$$

Then θ has a unique fixed point $\eta^* \in M$ and for every $\eta_0 \in M$ the sequence $\{\theta^n \eta_0\}_{n=0}^{\infty}$ convers to η^*.

Proof: Choose $\eta_0 \in M$ and define a sequence

$$\eta_1 = \theta\eta_0,\ \eta_2 = \theta\eta_1 = \theta^2\eta_0, \ldots$$

$$\eta_{n+1} = \theta\eta_n = \theta^{n+1}\eta_0 \qquad \forall n \in \mathbb{N} \qquad \textbf{(2)}$$

In the context of the S-metric space when $d_s(\eta_n, \eta_n, \eta_{n+1}) > 0$ the given condition

$$\lambda + F(d_s(\eta_n, \eta_n, \eta_{n+1})) \leq F((d_s(\eta_n, \eta_n, \eta_{n+1}))$$

holds for a chosen $\lambda > 0$.

This satisfies the definition of an S −metric space, implying that there exist a uniqe fixed point $\eta^* \in M$ for the mapping θ, and for every $\eta_0 \in M$ the sequence $\{\theta\eta_0\}_{n=0}^{\infty}$ converges to η^*.

If there exist $n \in \mathbb{N}$ such that $d_s(\eta_n, \eta_n, \theta\eta_n) = 0$ the proof is complete so we assume that

$$0 < \mathrm{d_s}(\eta_n, \eta_n, \theta\eta_n) = \mathrm{d_s}\left(\theta\eta_{n-1}, \theta\eta_{n-1}, \theta\eta_n\right)\ \forall n \in \mathbb{N} \qquad \textbf{(3)}$$

for any $n \in \mathbb{N}$ we have

$$\lambda + F\big(\mathrm{d_s}(\theta\eta_{n-1}, \theta\eta_{n-1}, \theta\eta_n)\big) \le \mathrm{d_s}(\eta_{n-1}, \eta_{n-1}, \eta_n)$$

i.e

$$F\big(\mathrm{d_s}(\theta\eta_{n-1}, \theta\eta_{n-1}, \theta\eta_n)\big) \le \mathrm{d_s}(\eta_{n-1}, \eta_{n-1}, \eta_n) - \lambda$$

Repeating this process we get ;

$$\begin{aligned}
F\big(\mathrm{d_s}(\theta\eta_{n-1}, \theta\eta_{n-1}, \theta\eta_n)\big) &\le F(\mathrm{d_s}(\eta_{n-1}, \eta_{n-1}, \eta_n)) - \lambda \\
&= F\big(\mathrm{d_s}(\theta\eta_{n-2}, \theta\eta_{n-2}, \theta\eta_{n-1})\big) - \lambda \\
&\le F\big(\mathrm{d_s}(\eta_{n-2}, \eta_{n-2}, \eta_{n-1})\big) - 2\lambda \\
&= F\big(\mathrm{d_s}(\theta\eta_{n-3}, \theta\eta_{n-3}, \theta\eta_{n-2})\big) - 2\lambda \\
&\le F\big(\mathrm{d_s}(\eta_{n-3}, \eta_{n-3}, \eta_{n-2})\big) - 3\lambda \\
&\quad . \\
&\quad . \\
&\quad . \\
&\quad F(\mathrm{d_s}(\eta_0, \eta_0, \eta_1)) - n\lambda. \qquad \textbf{(4)}
\end{aligned}$$

from (4) we obtain $\lim_{n\to\infty} F\big(\mathrm{d_s}(\theta\eta_{n-1}, \theta\eta_{n-1}, \theta\eta_n)\big) = -\infty$, which together with (F2′) and lemma 1 gives,

$$\lim_{n\to\infty} F\big(\mathrm{d_s}(\theta\eta_{n-1}, \theta\eta_{n-1}, \theta\eta_n)\big) \neq 0$$

i.e

$$\lim_{n\to\infty}\big(\mathrm{d_s}(\eta_n, \eta_n, \theta\eta_n)\big) = 0.$$

Now we claim that $\{\eta_n\}_{n=0}^{\infty}$ is a cauchy sequence. Arguing by contradiction,

we assume that there exist $\varepsilon > 0$ and sequences $\{\rho(n)\}_{n=1}^{\infty}$ and $\{\omega(n)\}_{n=1}^{\infty}$ of natural numbers such that

$$\rho(n) > \omega(n) > n, \mathrm{d_s}(\eta_{\rho(n)}, \eta_{\rho(n)}, \eta_{\omega(n)}) \ge 0, \mathrm{d_s}(\eta_{\rho(n)-1}, \eta_{\rho(n)-1}, \eta_{\omega(n)}) < \varepsilon$$

(6)

so, we have

$$\varepsilon \leq \mathrm{d_s}\left(\eta_{\rho(\mathrm{n})}, \eta_{\rho(\mathrm{n})}, \eta_{\omega(\mathrm{n})}\right)$$
$$\leq \mathrm{d_s}\left(\eta_{\rho(\mathrm{n})}, \eta_{\rho(\mathrm{n})}, \eta_{\rho(\mathrm{n})-1}\right) + \mathrm{d_s}\left(\eta_{\rho(\mathrm{n})-1}, \eta_{\rho(\mathrm{n})-1}, \eta_{\omega(\mathrm{n})}\right)$$

$$\leq \mathrm{d_s}\left(\eta_{\rho(\mathrm{n})}, \eta_{\rho(\mathrm{n})}, \eta_{\rho(\mathrm{n})-1}\right) + \varepsilon$$
$$= \mathrm{d_s}\left(\eta_{\rho(\mathrm{n})-1}, \eta_{\rho(\mathrm{n})-1}, \theta\eta_{\rho(\mathrm{n})-1}\right) + \varepsilon$$

It follows from (5) and the above inequality that,

$$\lim_{n\to\infty} \mathrm{d_s}\left(\eta_{\rho(\mathrm{n})}, \eta_{\rho(\mathrm{n})}, \eta_{\omega(\mathrm{n})}\right) = \varepsilon \qquad \textbf{(7)}$$

On the other hand, from (5) there exists $N \in \mathbb{N}$, such that

$$\mathrm{d_s}\left(\eta_{\rho(\mathrm{n})}, \eta_{\rho(\mathrm{n})}, \theta\eta_{\rho(\mathrm{n})}\right) < \frac{\varepsilon}{4}$$

and

$$\mathrm{d_s}\left(\eta_{\omega(\mathrm{n})}, \eta_{\omega(\mathrm{n})}, \theta\eta_{\omega(\mathrm{n})}\right) < \frac{\varepsilon}{4} \quad \forall \mathrm{n} \geq N. \qquad (\mathbf{8})$$

Next, we claim that

$$\mathrm{d_s}\left(\theta\eta_{\rho(\mathrm{n})}, \theta\eta_{\rho(\mathrm{n})}, \theta\eta_{\rho(\mathrm{n})}\right) = \mathrm{d_s}\left(\eta_{\bar{\rho}(\mathrm{n})+1}, \eta_{\rho(\mathrm{n})+1}, \eta_{\omega(\mathrm{n})+1}\right) > 0 \quad \forall \mathrm{n} \in N. \qquad (\mathbf{9})$$

Arguing by contradiction, there exists $\mathrm{m} \geq N$ such that

$$\mathrm{d_s}\left(\eta_{\rho(\mathrm{m})+1}, \eta_{\rho(\mathrm{m})+1}, \eta_{\omega(\mathrm{m})+1}\right) = 0 \qquad (\mathbf{10})$$

It follows from (6), (8), and (10) that,

$$\varepsilon \leq \mathrm{d_s}\left(\eta_{\rho(\mathrm{m})}, \eta_{\rho(\mathrm{m})}, \eta_{\omega(\mathrm{m})}\right)$$

$$
\begin{aligned}
&\leq d_s\big(\eta_{\rho(m)}, \eta_{\rho(m)}, \eta_{\rho(m)+1}\big) + d_s\big(\eta_{\rho(m)+1}, \eta_{\rho(m)+1}, \eta_{\omega(m)}\big) \\
&\leq d_s\big(\eta_{\rho(m)}, \eta_{\rho(m)}, \eta_{\rho(m)+1}\big) + d_s\big(\eta_{\rho(m)+1}, \eta_{\rho(m)+1}, \eta_{\omega(m)+1}\big) \\
&+ d_s\big(\eta_{\omega(m)+1}, \eta_{\omega(m)+1}, \eta_{\omega(m)}\big) \\
&= d_s\big(\eta_{\rho(m)}, \eta_{\rho(m)}, \theta\eta_{\rho(m)}\big) + d_s\big(\eta_{\rho(m)+1}, \eta_{\rho(m)+1}, \eta_{\omega(m)+1}\big) \\
&+ d_s\big(\eta_{\omega(m)}, \eta_{\omega(m)}, \theta\eta_{\omega(m)}\big) \\
&< \frac{\varepsilon}{4} + 0 + \frac{\varepsilon}{4} \\
&= \frac{\varepsilon}{2}
\end{aligned}
$$

This contradiction establishes the realition (9). Therefore, it follows from (9) and the assumption of the theorem that

$$\lambda + F(d_s\big(\theta\eta_{\rho(n)}, \theta\eta_{\rho(n)}, \theta\eta_{\omega(n)}\big)) \leq F(d_s\big(\eta_{\rho(n)}, \eta_{\rho(n)}, \eta_{\omega(n)}\big)) \quad \forall n \in N \qquad \mathbf{(11)}$$

From condition (F3´), equation (7), and relation (11), it follows that

$$\lambda + F(\varepsilon) \leq F(\varepsilon).$$

Which leads to a contradiction.

This result confirms that the sequence $\{\eta_n\}_{n=1}^{\infty}$ is a Cauchy sequence. Due to the completeness of the space (M, d_s), the sequence $\{\eta_n\}_{n=1}^{\infty}$ converges to a point $\eta \in M$. By the continuity of the mapping θ, we obtain the following:

$$
\begin{aligned}
d_s(\theta\eta, \theta\eta, \eta) &= \lim_{n\to\infty} d_s(\theta\eta_n, \theta\eta_n, \eta_n) \\
&= \lim_{n\to\infty} d_s(\eta_{n+1}, \eta_{n+1}, \eta_n) = d_s(\eta^*, \eta^*, \eta^*) = 0
\end{aligned}
$$

Now we demonstrate that the mapping θ admits at most one fixed point. Suppose for the sake of contradiction, that there exist $\eta, \mu \in M$ such that they are two distinct fixed points of θ, meaning, , $\theta\eta = \eta \neq \mu = \theta\mu$. Therefore,

$$d_s(\theta\eta, \theta\eta, \theta\mu) \ = d_s(\eta, \eta, \mu) > 0,$$

then we get, which is a contradiction

$$\begin{aligned} F\big(d_s(\eta, \eta, \mu)\big) &= F\big(d_s(\theta\eta, \theta\eta, \theta\mu)\big) \\ &< \lambda + F\left(d_s(\theta\eta, \theta\eta, \theta\mu)\right) \\ &\leq F\left(d_s(\eta, \eta, \mu)\right), \end{aligned}$$

which is a contradiction. Therefore, the fixed point is unique.

REFERENCES

[1] Banach, B: Sur les opérations dons les ensembles abstraits et leur applica- tion aux équations intégrales. Fundam. Math. 3, 133-181 (1922)

[2] Suzuki, T: A new type of fixed point theorem in metric spaces. Nonlinear Anal. 71, 5313-5317 (2009)

[3] Suzuki, T: Generalized distance and existence theorems in complete metric spaces. J. Math. Anal. Appl. 253, 440-458 (2001)

[4] Suzuki, T: Several fixed point theorems concerning τ-distance. Fixed Point Theory Appl. 2004, 195-209 (2004)

[5] Tataru, D: Viscosity solutions of Hamilton-Jacobi equations with un- bounded nonlinear terms. J. Math. Anal. Appl. 163, 345-392 (1992)

[6] Vályi, I: A general maximality principle and a fixed point theorem in uni- form space. Period. Math. Hung. 16, 127-134 (1985)

[7] Włodarczyk, K, Plebaniak, R: Quasigauge spaces with generalized quasi- pseudodistances and periodic points of dissipative set-valued dynamic sys- tems. Fixed Point Theory Appl. 2011, Article ID 712706 (2011)

[8] Włodarczyk, K, Plebaniak, P: Kannan-type contractions and fixed points in uniform spaces. Fixed Point Theory Appl. 2011, Article ID 90 (2011)

[9] Włodarczyk, K, Plebaniak, R: Contractivity of Leader type and fixed points in uniform spaces with generalized pseudodistances. J. Math. Anal. Appl. 387, 533-541 (2012)

[10] Edelstein, M: On fixed and periodic points under contractive mappings. J. Lond. Math. Soc. 37, 74-79 (1962)

[11] Wardowski, D: Fixed point theory of a new type of contractive mappings in complete metric spaces. Fixed Point Theory Appl. 2012, Article ID 94 (2012)

[12] Secelean, NA: Iterated function systems consisting of F-contractions. Fixed Point Theory Appl. 2013, Article ID 277 (2013). doi:10.1186/1687-1812-2013-277.

ON GENERALIZED PROPORTIONAL FRACTIONAL INTEGRAL

Yasin Kaya[1]

[1] Department of Mathematics, University of Dicle, Turkey

ykaya@dicle.edu.tr

Abstract

Fractional calculus operators deal with investigatin and applications of integrals and derivatives of arbitrary (real or complex) order. There are many definitions of fractional integral and fractional derivatives of different types. Object of this talk is to present an introductory overview of the theory of an integral operator of fractional calculus known as generalized proportional fractional integral. We also show a fractional integral inequality whose proof based on techniques to the existing literature.

Keywords: Generalized proportional fractional integral; Inequality; Operator.

1.INTRODUCTION

Fractional calculus was developed as a generalization (extension) of the classical calculus, in which both integrals and derivatives order can take real or complex number. Fractional integrals and derivatives are important since they have many application in science and technology. In particularly, fractional operators are excellent tools to use in modeling long-memory processes and many phenomena that appear in physics, chemistry, electricity, mechanics and many other disciplines. Since there are several reasons which lead to the fractional-order models, in the literature, there are many fractional operators. A very important form of fractional integral is given by the Riemann - Liouville integral. For a integrable function $g: [a, b] \to \mathbb{R}$, of order $\delta \in (0, \infty)$, left Riemann – Liouville fractional integral is given as

$$I_{a^+}^{\delta} g(x) = \frac{1}{\Gamma(\delta)} \int_a^x (x-t)^{\delta-1} g(t)dt \quad x \in [a,b]$$

and right Riemann – Liouville fractional integral is given as

$$I_{b^-}^{\delta} g(x) = \frac{1}{\Gamma(\delta)} \int_x^b (t-x)^{\delta-1} g(t)dt \quad x \in [a,b].$$

Here $\Gamma(\delta)$ is the well-known gamma function given by

$$\Gamma(\delta) = \int_0^\infty \tau^{\delta-1} e^{-\tau} d\tau.$$

2.GENERAL PROPERTIES OF METHOD

Let $\delta \in (0, \infty)$ be the order, $p \in (0,1]$ be proportion. For a integrable function $g: [a, b] \to \mathbb{R}$, the left generalized proportional fractional integral is given as

$$I_{a^+}^{\delta,p} g(x) = \frac{1}{p^\delta \Gamma(\delta)} \int_a^x e^{\frac{p-1}{p}(x-t)} (x-t)^{\delta-1} g(t) dt \ \ x \in [a, b]$$

and right generalized proportional fractional integral is given as

$$I_{b^-}^{\delta,p} g(x) = \frac{1}{p^\delta \Gamma(\delta)} \int_x^b e^{\frac{p-1}{p}(t-x)} (t-x)^{\delta-1} g(t) dt \ \ x \in [a, b].$$

The left and right generalized proportional fractional integral is introduced by Jarad et al. in [3]. Given the function $g: [3,7] \to \mathbb{R}$, $g(x) = \ln(x)$ the generalized proportional fractional integral of order $\sqrt{5}$ is given as

$$I_{3^+}^{\sqrt{5},p} \ln(x) = \frac{1}{p^{\sqrt{5}} \Gamma(\sqrt{5})} \int_a^x e^{\frac{p-1}{p}(x-t)} (x-t)^{\sqrt{5}-1} \ln(t)\, dt \ \ x \in [a, b].$$

More discussion on generalized proportional fractional calculus can be found in [1,2,4]

Teorem 2.1. ([5]) Let a function $g: [a, b] \to \mathbb{R}$ be decreasing, positive and continuous. Let $a < x \le b, \theta > 0, 0 < k \le \beta, p \in (0,1]$ and $\delta, s \in (0, \infty)$. Then the left generalized proportional fractional integral satisfy

$$\frac{I_{a^+}^{\delta,p}[g^\beta(x)] I_{a^+}^{\delta,p}[(x-a)^\theta g^k(x)] + I_{a^+}^{s,p}[g^\beta(x)] I_{a^+}^{\delta,p}[(x-a)^\theta g^k(x)]}{I_{a^+}^{\delta,p}[(x-a)^\theta g^\beta(x)] I_{a^+}^{\delta,p}[g^k(x)] + I_{a^+}^{s,p}[(x-a)^\theta g^\beta(x)] I_{a^+}^{\delta,p}[g^k(x)]} \ge 1.$$

3.APPLICATIONS

Proof of the next theorem follows exactly the same line of reasoning as the proof of [5]. The next lemma is actually implicit in [5].

Theorem 3.1. Let a function $g: [a, b] \to \mathbb{R}$ be increasing, positive and continuous. Let $a < x \le b, \theta > 0, 0 < k \le \beta, p \in (0,1]$ and $\delta, s \in (0, \infty)$. Then the left generalized proportional fractional integral satisfy

$$\frac{I_{a^+}^{\delta,p}\left[g^{\beta}(x)\right]I_{a^+}^{\delta,p}\left[(x-a)^{\theta}g^{k}(x)\right]+I_{a^+}^{s,p}\left[g^{\beta}(x)\right]I_{a^+}^{\delta,p}\left[(x-a)^{\theta}g^{k}(x)\right]}{I_{a^+}^{\delta,p}\left[(x-a)^{\theta}g^{\beta}(x)\right]I_{a^+}^{\delta,p}\left[g^{k}(x)\right]+I_{a^+}^{s,p}\left[(x-a)^{\theta}g^{\beta}(x)\right]I_{a^+}^{\delta,p}\left[g^{k}(x)\right]}\leq -1$$

Proof It's obvious that for $t,y\in[a,x]$ we have

$$\left((y-a)^{\theta}-(t-a)^{\theta}\right)\left(g^{\beta-k}(t)-g^{\beta-k}(y)\right)\leq 0 \tag{3.1}$$

From (3.1) , we have

$$(y-a)^{\theta}g^{\beta-k}(t)+(t-a)^{\theta}g^{\beta-k}(y)-(y-a)^{\theta}g^{\beta-k}(y)-(t-a)^{\theta}g^{\beta-k}(t)\leq 0 \quad (3,2)$$

Define a function F such that

$$F(x,t)=\frac{1}{p^{\delta}\Gamma(\delta)}e^{\frac{p-1}{p}(x-t)}(x-t)^{\delta-1}.$$

It's obvious that for each $t\in(a,x), x\in(a,b]$ then $F(x,t)>0$. Now if we multiply (3.1) by

$$F(x,t)g^{k}(t)=\frac{1}{p^{\delta}\Gamma(\delta)}e^{\frac{p-1}{p}(x-t)}(x-t)^{\delta-1}g^{k}(t)$$

we obtain

$$\begin{aligned}F(x,t)\big[&(y-a)^{\theta}g^{\beta-k}(t)+(t-a)^{\theta}g^{\beta-k}(y)-(y-a)^{\theta}g^{\beta-k}(y)\\&-(t-a)^{\theta}g^{\beta-k}(t)\big]g^{k}(t)\end{aligned}$$

$$=(y-a)^{\theta}\frac{1}{p^{\delta}\Gamma(\delta)}e^{\frac{p-1}{p}(x-t)}(x-t)^{\delta-1}g^{k}(t)g^{\beta-k}(t)$$

$$+(t-a)^{\theta}\frac{1}{p^{\delta}\Gamma(\delta)}e^{\frac{p-1}{p}(x-t)}(x-t)^{\delta-1}g^{k}(t)g^{\beta-k}(y)$$

$$-(y-a)^{\theta}\frac{1}{p^{\delta}\Gamma(\delta)}e^{\frac{p-1}{p}(x-t)}(x-t)^{\delta-1}g^{k}(t)g^{\beta-k}(y)$$

$$-(t-a)^{\theta}\frac{1}{p^{\delta}\Gamma(\delta)}e^{\frac{p-1}{p}(x-t)}(x-t)^{\delta-1}g^{k}(t)g^{\beta-k}(t)\leq 0$$

Now, integrating over (a,x) with respect to t we obtain

$$(y-a)^{\theta}\frac{1}{p^{\delta}\Gamma(\delta)}\int_{a}^{x}e^{\frac{p-1}{p}(x-t)}(x-t)^{\delta-1}g^{\beta}(t)\,dt$$

$$+g^{\beta-k}(y)\frac{1}{p^{\delta}\Gamma(\delta)}\int_{a}^{x} e^{\frac{p-1}{p}(x-t)}(x-t)^{\delta-1}(t-a)^{\theta}g^{k}(t)dt$$

$$-(y-a)^{\theta}g^{\beta-k}(y)\frac{1}{p^{\delta}\Gamma(\delta)}\int_{a}^{x} e^{\frac{p-1}{p}(x-t)}(x-t)^{\delta-1}g^{k}(t)d\,t$$

$$-\frac{1}{p^{\delta}\Gamma(\delta)}\int_{a}^{x} e^{\frac{p-1}{p}(x-t)}(x-t)^{\delta-1}(t-a)^{\theta}g^{\beta}(t)dt \leq 0$$

It follows from this

$$(y-a)^{\theta}I_{a^{+}}^{\delta,p}\left[g^{\beta}(x)\right]+g^{\beta-k}(y)I_{a^{+}}^{\delta,p}\left[(x-a)^{\theta}g^{k}(x)\right]$$

$$-(y-a)^{\theta}g^{\beta-k}(y)I_{a^{+}}^{\delta,p}[g^{k}(x)]-I_{a^{+}}^{\delta,p}\left[(x-a)^{\theta}g^{\beta}(x)\right]. \qquad (3.3)$$

By multiplying both sides of (3.3) by

$$F(x,y)g^{k}(y)=\frac{1}{p^{s}\Gamma(\delta)}e^{\frac{p-1}{p}(x-y)}(x-y)^{s-1}g^{k}(y)$$

where $y\in(a,x), x\in(a,b]$. Then integrating this resultant over (a,x) with respect to y we obtain

$$I_{a^{+}}^{\delta,p}\left[g^{\beta}(x)\right]I_{a^{+}}^{s,p}\left[(x-a)^{\theta}g^{k}(x)\right]+I_{a^{+}}^{s,p}\left[g^{\beta}(x)\right]I_{a^{+}}^{\delta,p}\left[(x-a)^{\theta}g^{k}(x)\right]$$

$$-I_{a^{+}}^{\delta,p}\left[(x-a)^{\theta}g^{\beta}(x)\right]I_{a^{+}}^{\delta,p}[g^{k}(x)]-I_{a^{+}}^{s,p}\left[(x-a)^{\theta}g^{\beta}(x)\right]I_{a^{+}}^{\delta,p}[g^{k}(x)]\leq 0. \quad (3.4)$$

Now, we achieve the desired inequality by dividing (3.4) by

$$I_{a^{+}}^{\delta,p}\left[(x-a)^{\theta}g^{\beta}(x)\right]I_{a^{+}}^{s,p}[g^{k}(x)]+I_{a^{+}}^{s,p}\left[(x-a)^{\theta}g^{\beta}(x)\right]I_{a^{+}}^{\delta,p}[g^{k}(x)].$$

4.CONCLUSIONS

In this talk, we presented a inequality whose proof method based on paper of Rahman et al. [5]. Our constraint the functions must be increasing. It will be a good idea to investigate validation of the inequality for more general class of constraints.

REFERENCES

1. Aljaaidi, T. A., Pachpatte, D. B., Abdeljawad, T., Abdo, M. S., Almalahi, M. A., & Redhwan, S. S. (2021). Generalized proportional fractional integral Hermite–Hadamard's inequalities. *Advances in Difference Equations*, *2021*(1), 493.

2. Alzabut, J., Sudsutad, W., Kayar, Z., & Baghani, H. (2019). A new Gronwall–Bellman inequality in frame of generalized proportional fractional derivative. *Mathematics*, *7*(8), 747.

3. Jarad, F., Abdeljawad, T., & Alzabut, J. (2017). Generalized fractional derivatives generated by a class of local proportional derivatives. *The European Physical Journal Special Topics*, *226*, 3457-3471.

4. Neamah, M. K., & Ibrahim, A. (2021). Generalized proportional fractional integral inequalities for convex functions. *AIMS Mathematics*, *6*(10), 10765-10777.

5. Rahman, G., Abdeljawad, T., Khan, A., & Nisar, K. S. (2019). Some fractional proportional integral inequalities. *Journal of Inequalities and Applications*, *2019*, 1-13.

Analytical Solution of a Caputo Fractional-Order Computer Virus Propagation Model

Erkan Günerhan[1], **Ercan Çelik** [2,3]

[1]Department of Computer engineering, Kafkas University, Kars, Turkey

erkan.gunerhan@gmail.com

[2] Department of Applied Mathematics and Informatics, Kyrgyz-Turkish Manas University, Bishkek, Kyrgyzstan

[3]Department of Mathematics, Atatürk University, Erzurum, Turkey

ercan.celik@manas.edu.kg

Abstract

In this study, a proposed model describing the propagation of a computer virus in the network with antidote in a vulnerable system is analyzed. Using the Laplace Adomian Decomposition Method (LADM), the model's analytical and approximate-analytical solutions are determined. These solutions are found in the form of fast converging series that portray the system dynamics accurately. The efficiency of the method was tested and the validity of the introduced fractional-order model was proved through the numerical simulations.

Keywords: Caputo fractional derivative; Computer Virus Propagation; Laplace Adomian decomposition; Nonlinear system.

1.Introduction

A computer virus is a type of malicious software program that spreads between systems by replicating itself, often disrupting operations or compromising data security. To understand and control the spread of such viruses in a network, researchers use mathematical models that simulate infection dynamics among computers. These models often draw inspiration from epidemiological models used in biology, such as the SIR or SAIR models, where each computer (or node) can transition between states like susceptible, infected, and recovered. By analyzing these models, it becomes possible to predict outbreak patterns, evaluate the impact of security measures, and optimize virus containment strategies.

Many dynamical models describing propagation of computer viruses have been established by scholars at home and abroad. Particularly the classic epidemic models, such as computer virus propagation model [1] model, SIRS [2–4] model, SEIRS model [5], and SEIQRS model [6, 7], are used to investigate the spreading law of computer viruses due to the common feature between the computer virus and the biological virus. Some computer virus models with infectivity in both seizing and latent computers have been also proposed by Yang et al. [8–12].

In this research, we are also exploring the potential of using the Laplace Adomian decomposition method (LADM) to solve the fractionalomputer virus propagation model. This method is a powerful yet straightforward approach to tackling epidemic models and has been successfully applied in biology, engineering, and applied mathematics. It combines the Laplace transform and the Adomian decomposition method, offering several advantages for solving complex problems. One of the advantages of this method is its accuracy, as by employing the Laplace transform, it transforms the differential equations into algebraic equations, which are often easier to solve. This transformation reduces the complexity of the problem and enables the use of powerful algebraic techniques to obtain accurate solutions. Additionally, the Adomian decomposition method provides a systematic and robust approach to handling nonlinear terms, allowing for accurate approximation of the solution even in the presence of nonlinearity. This method does not require any perturbation or linearization, nor does it need a defined size of the step like the Rung-Kutta of order 4 technique. Various models have already been solved using this particular technique, such as HIV infection of CD4+ T cells model [13], fractional-order smoking model [14], epidemic childhood diseases [15], Radhakrishnan–Kundu–Lakshmanan equation [16], Asian option pricing model [17], Burger's equation [18], Chen-Lee-Liu equation [19], prey-predator model [20], nonlinear fractional smoking mathematical model [21], COVID-19 model [22], HIV model [23], Smoking epidemic model [24], fractional-order co-infection SEIR model [24].

2.Model formulation

In this article, we propose a computer virus propagation model that incorporates varying antidote rates for invulnerable nodes, taking into account both immunization methods and operating system vulnerabilities [1].

$$S'(t) = B - \lambda S(t)A(t) + \omega I(t) - \varepsilon R(t) - \mu S(t),$$

$$A'(t) = \lambda S(t)A(t) - \delta A(t) - \gamma A(t) - \mu A(t),$$
$$I'(t) = \gamma A(t) - \propto I(t) - \mu I(t) - \omega I(t),$$

$$R'(t) = \delta A(t) + \propto I(t) - \mu R(t) + \varepsilon R(t). \qquad (2.1)$$

The model considers a computer network in which each node exists in one of four possible states: susceptible (S), latent (A), infectious (I), or recovered (R). Susceptible nodes are healthy but vulnerable to infection. Latent nodes are infected, though the virus remains inactive. Infectious nodes carry active viruses, capable of spreading the infection. Recovered nodes have acquired immunity. The total number of nodes at time $\boldsymbol{t}$ is given by $N(t) = S(t) + A(t) + I(t) + R(t)$.

B is the constant recruitment of the susceptible nodes;μ is the same rate at which every node in the states $S(t)$, A(t),$I(t)$, and $R(t)$ disconnects from the network; ε is the constantrate at which every susceptible node acquires temporaryimmunity due to antidote and Khanh and Huy [1] assume that $\varepsilon < \mu$ taking system vulnerability into account; α, λ , δ,and ω are the other state transition rates of system (2.1).

By applying the fractional derivative operator ${}_0^cD_t^\alpha$ of order $\alpha,\ 0 < \alpha \leq 1$ in the system (2.1), we have

$${}_{0}^{c}D_{t}^{\alpha}S(t) = B - \lambda S(t)A(t) + \omega I(t) - \varepsilon R(t) - \mu S(t),$$

$${}_{0}^{c}D_{t}^{\alpha}A(t) = \lambda S(t)A(t) - \delta A(t) - \gamma A(t) - \mu A(t),$$
$${}_{0}^{c}D_{t}^{\alpha}I(t) = \gamma A(t) - \propto I(t) - \mu I(t) - \omega I(t),$$

$${}_{0}^{c}D_{t}^{\alpha}R(t) = \delta A(t) + \propto I(t) - \mu R(t) + \varepsilon R(t). \tag{2.2}$$

With the initial condition

$$S(0) = k_1, A(0) = k_2, I(0) = k_3, R(0) = k_4. \tag{2.3}$$

3.Basic Definitions

In this section, we will introduce some basic definitions and properties of the theory of fractional calculus that will be later.

Definition 3.1 A real function $f(x),\ x > 0$ is said to be in the space $C_\mu,\ \mu \epsilon R$ if there exists a real number $P > \mu$ such that $f(x) = x^p f_1(x)$ where $f_1(x) \epsilon C[0,\infty)$. Clearly $C_\mu < C_\beta$ if $\mu < \beta$.

Definition 3.2 A function $f(x),\ x > 0$ is said to be in the spaceC_μ^m, $m \epsilon N \cup \{0\}$ if $f^{(m)} \in C_\mu$.

Definition 3.3 [25] The Riemann-Liouville fractional integral operator of the order $\alpha > 0$ of a function, $f \in C_\mu, \mu \geq -1$ is defined as

$$(J_a^\alpha f)(x) = \frac{1}{\Gamma(\alpha)} \int_a^x (x-\tau)^{\alpha-1} f(\tau) d\tau, x \ > a, \tag{3.1}$$

$$(J_a^0 f)(x) = f(x). \tag{3.2}$$

All the properties of the operator J^α can be found in [19] which we mention only the following, for $f \in C_\mu,\ \mu \geq -1, \alpha, \beta \geq 0$, rand $\gamma > -1$ we have

$$(J_a^\alpha J_a^\beta f)(x) = (J_a^{\alpha+\beta} f)(x), \tag{3.3}$$

$$(J_a^\alpha J_a^\beta f)(x) = (J_a^\beta J_a^\alpha f)(x) \tag{3.4}$$

$$J_a^\alpha x^\gamma = \frac{\Gamma(\gamma+1)}{\Gamma(\alpha+\gamma+1)} x^{\alpha+\gamma}. \tag{3.5}$$

The basic definition of the Riemann–Louville fractional derivative possesses some advantages over other definitions when used to simulate real-world phenomena in the form of a fractional-type differential equation.

Definition 3.4 [26] The fractional derivative of the function $f(x)$ in Caputo's sense is defined as

$$\left(D^{\alpha}_{a} f\right)(x) = \left(J^{m-\alpha}_{a} D^{m} f\right)(x) = \frac{1}{\Gamma(m-\alpha)} \int_{a}^{x} (x-t)^{m-\alpha-1} f^{(m)}(t)dt, \text{ for } m-1 < \alpha < m, m \in N, x > 0. \quad (3.6)$$

Lemma 3.1 If $-1 < \alpha < m$, $m \in$ N and $\mu \geq -1$, then

$$(J^{\alpha}_{a} D^{\alpha}_{a} f)(x) = f(x) - \sum_{k=0}^{m-1} f^{k}(a) \left(\frac{(x-a)^{k}}{k!}\right), a \geq 0 \quad (3.7)$$

$$(D^{\alpha}_{a} J^{\alpha}_{a} f)(x) = f(x) \quad (3.8)$$

4.Laplace Adomian Decomposition Method

This section will illustrate the basic steps for the Laplace Adomian decomposition method (LADM). We first need the following definitions.

Definition 4.1 [27] A function f on $0 \leq t < \infty$ is exponentially bounded of order $\sigma \in R$ if satisfies $\| f(t) \| \leq Me^{\sigma t}$, for some real constant $M > 0$.

Definition 3.2 The Caputo fractional derivative is defined as follows:

$$L\{D^{\sigma} f(t)\} = s^{\sigma} L\{f(t)\} - \sum_{k=0}^{m} s^{\sigma-k-1} f^{(k)}(0), \quad (4.a)$$

where $m = \sigma + 1$, and $[\alpha]$ represents the integer part of σ. As a result, the following useful formula is obtained:

$$L(t^{\sigma}) = \frac{\Gamma(\sigma+1)}{s^{(\sigma+1)}}, \quad \sigma \in R^{+}. \quad (4.b)$$

The last-mentioned definitions can be used in this section to discuss the general procedures for solving the proposed mathematical model (2.2). First of all, the Laplace transform is applied to both lift-hand and right-hand sides of Eq. (2.2) in the following form:

$$L\left({}_{0}^{c}D_{t}^{\alpha} S(t)\right) = L\left(B - \lambda S(t)A(t) + \omega I(t) - \varepsilon R(t) - \mu S(t)\right),$$

$$L\left({}_{0}^{c}D_{t}^{\alpha} A(t)\right) = L = \left(\lambda S(t)A(t) - \delta A(t) - \gamma A(t) - \mu A(t)\right),$$

$$L({}_{0}^{c}D_{t}^{\alpha} I(t)) = L\left(\gamma A(t) - \propto I(t) - \mu I(t) - \omega I(t)\right),$$

$$L({}_{0}^{c}D_{t}^{\alpha} R(t)) = L(\delta A(t) + \propto I(t) - \mu R(t) + \varepsilon R(t)). \quad (4.1)$$

Then, by applying the formula (4.a) to Eq. (4.1), we get

$$s^{\alpha}L(S)-s^{\alpha-1}S(0)=\frac{B}{s}-\lambda L(SA)+\omega\, L(I)-\varepsilon L(R)-\mu L(S),$$

$$s^{\alpha}L(A)-s^{\alpha-1}A(0)=\lambda L(SA)-\ \delta L(A)-\gamma L(A)-\mu L(A),$$

$$s^{\alpha}L(\mathrm{I})-s^{\alpha-1}I(0)=\gamma L(A)-\propto L(I)-\mu L(I)-\omega L(I),$$

$$s^{\alpha}L(R)-s^{\alpha-1}R(0)=\delta L(A)+\propto L(I)-\mu L(R)+\varepsilon L(R). \tag{4.2}$$

Next, by substituting the initial conditions in Eq.(2.3) into the model (4.2), we get

$$L(S)=\frac{k_1}{s}+\frac{B}{s^{\alpha+1}}-\frac{\lambda}{s^{\alpha}}L(SA)+\frac{\omega}{s^{\alpha}}\,L(I)-\frac{\varepsilon}{s^{\alpha}}L(R)-\ \frac{\mu}{s^{\alpha}}L(S),$$

$$L(\mathrm{A})=\frac{k_2}{s}+\frac{\lambda}{s^{\alpha}}L(SA)-\ \frac{\delta}{s^{\alpha}}L(A)-\frac{\gamma}{s^{\alpha}}L(A)-\frac{\mu}{s^{\alpha}}L(A),$$

$$L(\mathrm{I})=\frac{k_3}{s}+\frac{\gamma}{s^{\alpha}}L(A)-\frac{\propto}{s^{\alpha}}\,L(I)-\frac{\mu}{s^{\alpha}}L(I)-\frac{\omega}{s^{\alpha}}L(I),$$

$$L(R)=\frac{k_4}{s}+\frac{\delta}{s^{\alpha}}L(A)+\frac{\propto}{s^{\alpha}}\,L(I)-\frac{\mu}{s^{\alpha}}L(R)+\frac{\varepsilon}{s^{\alpha}}L(R). \tag{4.3}$$

The proposed method gives the solution as an infinite series. Let the value of $C=SA$ to be able to apply the Adomian decomposition method. We consider the solution as an infinite series in the form

$$S(t)=\sum_{n=0}^{\infty}S_n(t),\ \mathrm{A}(t)=\sum_{n=0}^{\infty}A_n(t),\ I(t)=\sum_{n=0}^{\infty}I_n(t),\ R(t)=\sum_{n=0}^{\infty}R_n(t). \tag{4.4}$$

Then, by decomposing the nonlinear part named C in the following form

$$C=\sum_{n=0}^{\infty}C_n, \tag{4.5}$$

Here, C_n can be computed using the convolution operation as

$$C_n=\frac{1}{\Gamma(n+1)}\frac{d^n}{d\varepsilon^n}\left[\sum_{i=0}^{n}\varepsilon^i S_i\sum_{i=0}^{n}\varepsilon^i A_i\right]_{\varepsilon=0},$$

(4.6)

By substituting Eq. (4.4- 4.6) into Eq. (4.3) we have resulted in the form.

$$L\left(\sum_{n=0}^{\infty} S_n(t)\right) = \frac{k_1}{s} + \frac{B}{s^{\alpha+1}} - \frac{\lambda}{s^\alpha} L\left(\sum_{n=0}^{\infty} C_n\right) + \frac{\omega}{s^\alpha} L(I) - \frac{\varepsilon}{s^\alpha} L\left(\sum_{n=0}^{\infty} R_n(t)\right) - \frac{\mu}{s^\alpha} L\left(\sum_{n=0}^{\infty} S_n(t)\right),$$

$$L\left(\sum_{n=0}^{\infty} A_n(t)\right) = \frac{k_2}{s} + \frac{\lambda}{s^\alpha} L\left(\sum_{n=0}^{\infty} C_n\right) - \frac{\delta}{s^\alpha} L\left(\sum_{n=0}^{\infty} A_n(t)\right) - \frac{\gamma}{s^\alpha} L\left(\sum_{n=0}^{\infty} A_n(t)\right) - \frac{\mu}{s^\alpha} L\left(\sum_{n=0}^{\infty} A_n(t)\right),$$

$$L(\mathrm{I}) = \frac{k_3}{s} + \frac{\gamma}{s^\alpha} L\left(\sum_{n=0}^{\infty} A_n(t)\right) - \frac{\propto}{s^\alpha} L\left(\sum_{n=0}^{\infty} I_n(t)\right) - \frac{\mu}{s^\alpha} L\left(\sum_{n=0}^{\infty} I_n(t)\right) - \frac{\omega}{s^\alpha} L\left(\sum_{n=0}^{\infty} I_n(t)\right),$$

$$L(R) = \frac{k_4}{s} + \frac{\delta}{s^\alpha} L\left(\sum_{n=0}^{\infty} A_n(t)\right) + \frac{\propto}{s^\alpha} L\left(\sum_{n=0}^{\infty} I_n(t)\right) - \frac{\mu}{s^\alpha} L\left(\sum_{n=0}^{\infty} R_n(t)\right) + \frac{\varepsilon}{s^\alpha} L\left(\sum_{n=0}^{\infty} R_n(t)\right).$$

(4.7)

Then, matching the two sides of Eq. (4.7) yields the following iterative algorithm

$$S_0 = \frac{k_1}{s}, \qquad A_0 = \frac{k_2}{s}, \qquad I_0 = \frac{k_3}{s}, \qquad R_0 = \frac{k_4}{s},$$

$$L(S_1) = \frac{B}{s^{\alpha+1}} - \frac{\lambda}{s^\alpha} L(C_0) + \frac{\omega}{s^\alpha} L(I_0) - \frac{\varepsilon}{s^\alpha} L(R_0) - \frac{\mu}{s^\alpha} L(S_0),$$

$$L(A_1) = \frac{\lambda}{s^\alpha} L(C_0) - \frac{\delta}{s^\alpha} L(A_0) - \frac{\gamma}{s^\alpha} L(A_0) - \frac{\mu}{s^\alpha} L(A_0),$$

$$L(\mathrm{I}_1) = \frac{\gamma}{s^\alpha} L(A_0) - \frac{\propto}{s^\alpha} L(I_0) - \frac{\mu}{s^\alpha} L(I_0) - \frac{\omega}{s^\alpha} L(I_0),$$

$$L(R_1) = \frac{\delta}{s^\alpha} L(A_0) + \frac{\propto}{s^\alpha} L(I_0) - \frac{\mu}{s^\alpha} L(R_0) + \frac{\varepsilon}{s^\alpha} L(R_0), \ldots,$$

$$L(S_n) = -\frac{\lambda}{s^\alpha} L(C_{n-1}) + \frac{\omega}{s^\alpha} L(I_{n-1}) - \frac{\varepsilon}{s^\alpha} L(R_{n-1}) - \frac{\mu}{s^\alpha} L(S_{n-1}),$$

$$L(A_n) = \frac{\lambda}{s^\alpha} L(C_{n-1}) - \frac{\delta}{s^\alpha} L(A_{n-1}) - \frac{\gamma}{s^\alpha} L(A_{n-1}) - \frac{\mu}{s^\alpha} L(A_{n-1}),$$

$$L(\mathrm{I}_n) = \frac{\gamma}{s^\alpha} L(A_{n-1}) - \frac{\propto}{s^\alpha} L(I_{n-1}) - \frac{\mu}{s^\alpha} L(I_{n-1}) - \frac{\omega}{s^\alpha} L(I_{n-1}),$$

$$L(R_n) = \frac{\delta}{s^\alpha} L(A_{n-1}) + \frac{\propto}{s^\alpha} L(I_{n-1}) - \frac{\mu}{s^\alpha} L(R_{n-1}) + \frac{\varepsilon}{s^\alpha} L(R_{n-1}). \qquad (4.8)$$

Finally, by taking the inverse transform of Eq. (4.8), we have the following equation

$$S_0 = k_1, \qquad A_0 = k_2, \qquad I_0 = k_3, \quad R_0 = k_4,$$

$$S_1 = [B - \lambda C_0 + \omega I_0 - \mu S_0] \frac{t^\alpha}{\Gamma(\alpha+1)},$$

$$\mathrm{A}_1 = [\lambda C_0 - \delta A_0 - \gamma A_0 - \mu A_0] \frac{t^\alpha}{\Gamma(\alpha+1)},$$

$$I_1 = [\gamma A_0 - \propto I_0 - \mu I_0 - \omega I_0] \frac{t^\alpha}{\Gamma(\alpha+1)},$$

$$R_1 = [\delta A_0 + \propto I_0 - \mu R_0 + \varepsilon R_0] \frac{t^\alpha}{\Gamma(\alpha+1)}, \ldots,$$

$$S_n = [-\lambda C_{n-1} + \omega I_{n-1} - \mu S_{n-1}] \frac{t^\alpha}{\Gamma(\alpha+1)},$$

$$\mathrm{A}_n = [\lambda C_{n-1} - \delta A_{n-1} - \gamma A_{n-1} - \mu A_{n-1}] \frac{t^\alpha}{\Gamma(\alpha+1)},$$

$$I_n = [\gamma A_{n-1} - \propto I_{n-1} - \mu I_{n-1} - \omega I_{n-1}] \frac{t^\alpha}{\Gamma(\alpha+1)},$$

$$R_n = [\delta A_{n-1} + \propto I_{n-1} - \mu R_{n-1} + \varepsilon I_{n-1}] \frac{t^\alpha}{\Gamma(\alpha+1)}, \ldots, \qquad (4.9)$$

Similarly, at the final step, we get the rest of the terms as infinite series as,

$$S(t) = \sum_{n=0}^{\infty} S_n(t) = k_1 + [\lambda C_0 - \delta A_0 - \gamma A_0 - \mu A_0] \frac{t^\alpha}{\Gamma(\alpha+1)} + \cdots,$$

$$A(t) = \sum_{n=0}^{\infty} A_n(t) = k_2 + [\lambda C_0 - \delta A_0 - \gamma A_0 - \mu A_0] \frac{t^\alpha}{\Gamma(\alpha+1)} + \cdots,$$

$$I(t) = \sum_{n=0}^{\infty} I_n(t) = k_3 + [\gamma A_0 - \propto I_0 - \mu I_0 - \omega I_0] \frac{t^\alpha}{\Gamma(\alpha+1)} + \cdots,$$

$$R(t) = \sum_{n=0}^{\infty} R_n(t) = k_4 + [\delta A_0 + \propto I_0 - \mu R_0 + \varepsilon R_0]\frac{t^{\alpha}}{\Gamma(\alpha+1)} + \cdots. \tag{4.10}$$

Equation (4.10) solves the main SAIR model of Eq. (2.1) which will be illustrated in the next section.

5.Numerical Simulations

In this section, we test the effectiveness of the proposed technique by examining the acquired results for model (2.1) for different α. The numerical simulations are presented by taking partial parameters from numerical simulations in [1]. In this section, the values of various parameters are presented for two different cases.

The results obtained by LADM match the exact solutions when $\alpha = 1$. Figure 1-13 presents a comparison between the results obtained using LADM and those generated by MATLAB's ODE45 (a Runge-Kutta 4th order method) across various model categories.It is evident from this figure that the proposed technique is efcient and accurate, as it perfectly agrees with the MATLAB code results.

Case 1: Consider $B = 5$, $\propto = 0.1, \delta = 0.35, \varepsilon = 0.1, \gamma = 0.45, \lambda = 0.7, \mu = 0.35$ and $\omega = 0.1$. With the initial condition $\big(S(0), L(0), I(0), R(0)\big) = (0.5, 3.5, 5, 5.5)$.

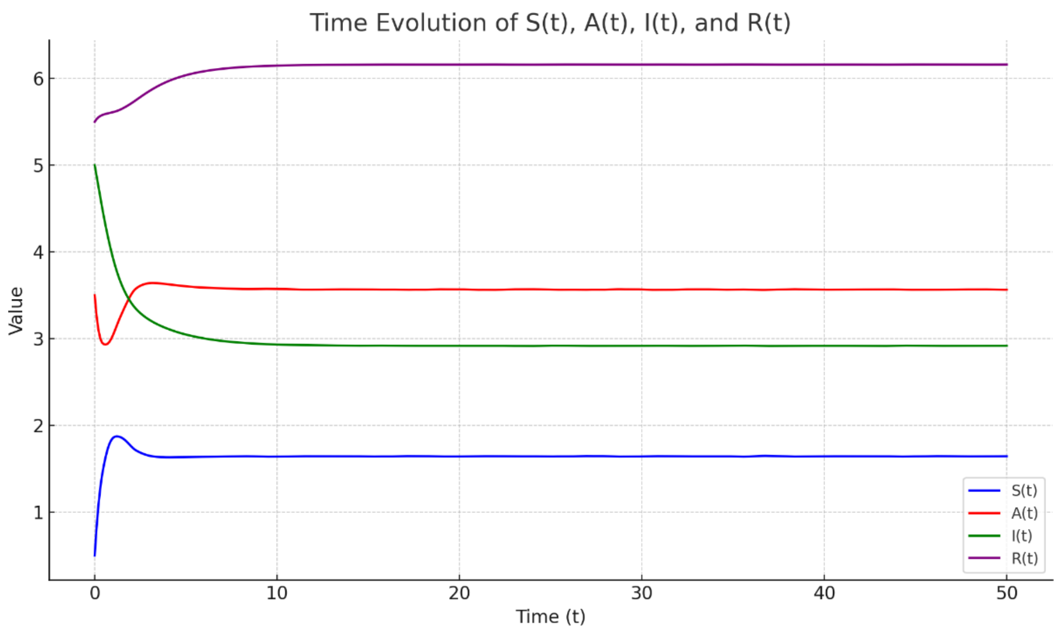

Fig. 1 The solution of $S(t), A(t), I(t)$ and $R(t)$ obtained by Rung-Kutta of order 4 technique (ODE 45) for $\alpha = 1$, and $0 < t < 50$.

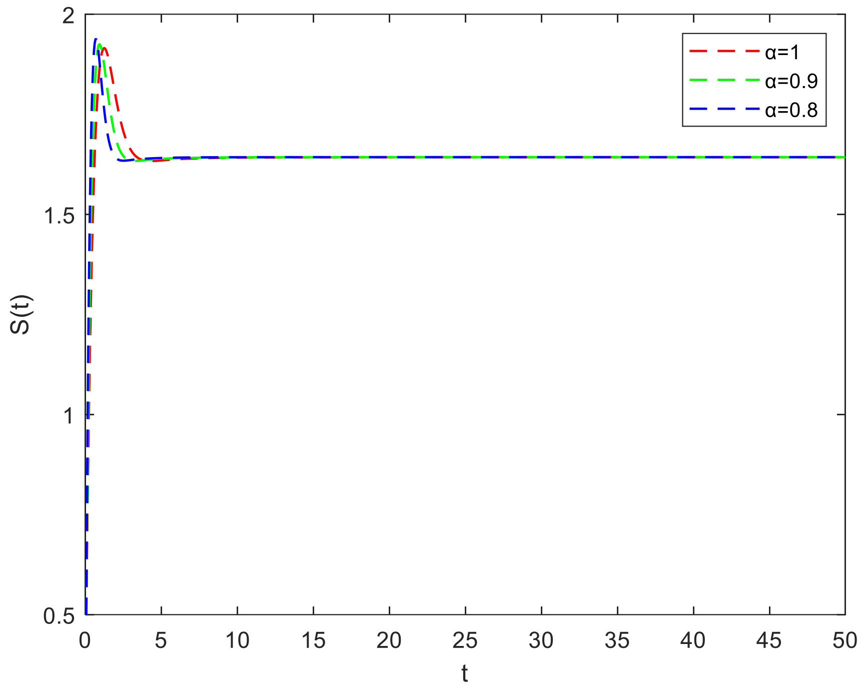

Fig. 2 The solution of $S(t)$ obtained by LADM for different values of α, (a) of $\alpha = 1$, (b) of $\alpha = 0.9$, (c) of $\alpha = 0.8$. and $0 \leq t \leq 50$.

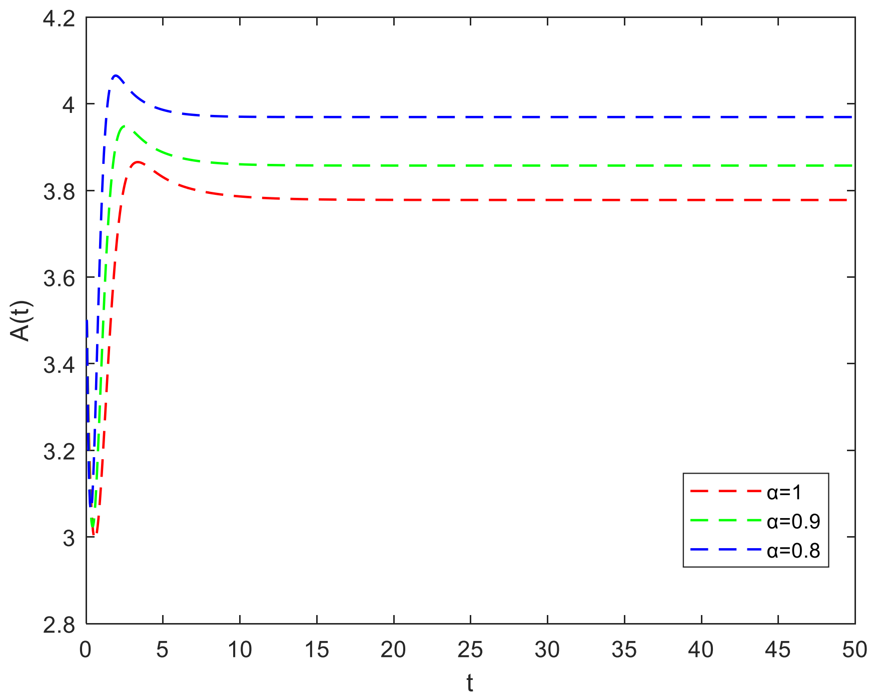

Fig. 3 The solution of $A(t)$ obtained by LADM for different values of α, (a) of $\alpha = 1$, (b) of $\alpha = 0.9$, (c) of $\alpha = 0.8$. and $0 \leq t \leq 50$.

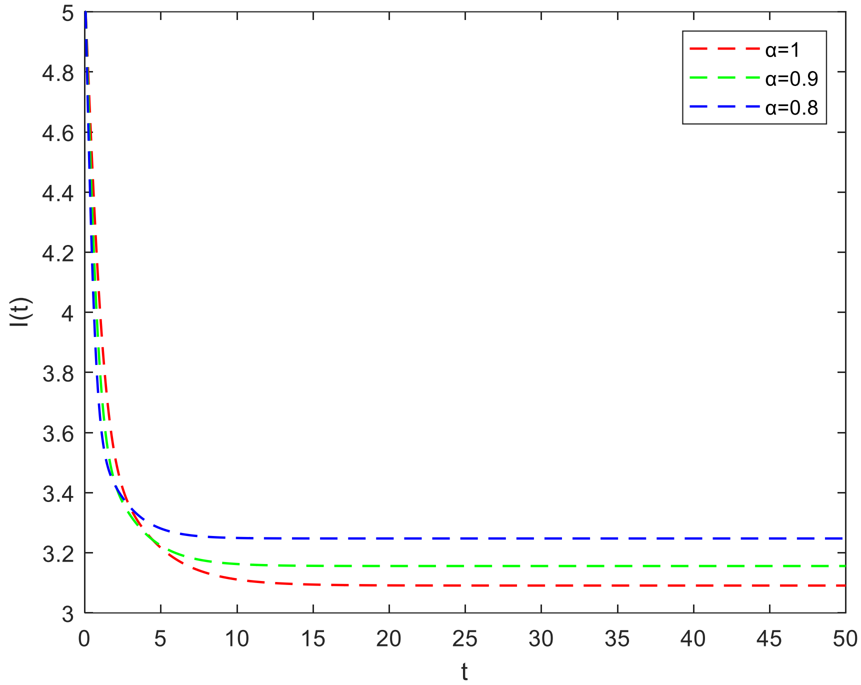

Fig. 4 The solution of $I(t)$ obtained by LADM for different values of α, (a) of $\alpha = 1$, (b) of $\alpha = 0.9$, (c) of $\alpha = 0.8$. and $0 \leq t \leq 50$.

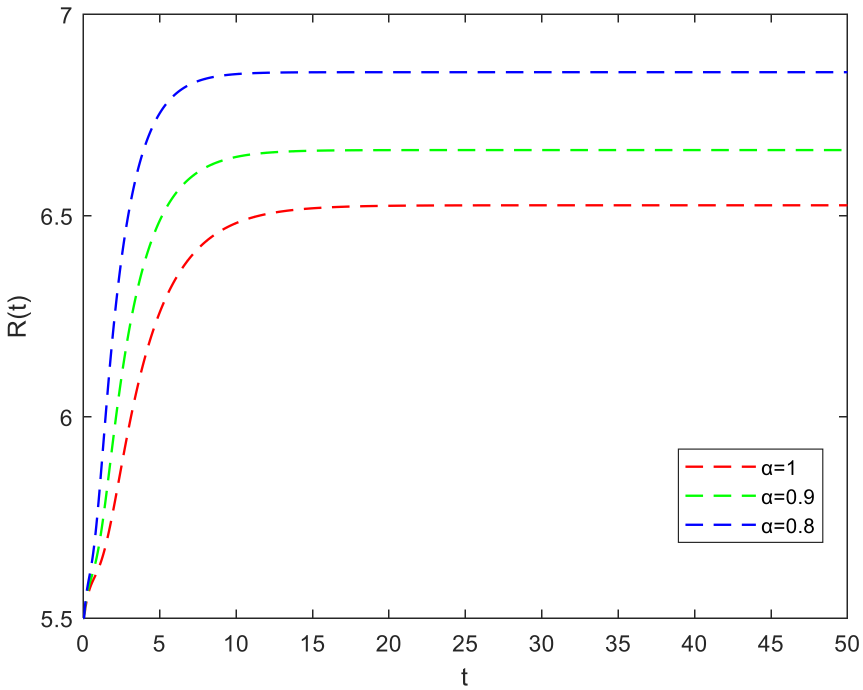

Fig. 5 The solution of $R(t)$ obtained by LADM for different values of α, (a) of $\alpha = 1$, (b) of $\alpha = 0.9$, (c) of $\alpha = 0.8$. and $0 \leq t \leq 50$.

Case 2: Consider $B = 3$, $\propto = 0.05, \delta = 0.25, \varepsilon = 0.02, \gamma = 0.001, \lambda = 0.25, \mu = 0.35$ and $\omega = 0.01$. With the initial condition $\left(S(0), L(0), I(0), R(0)\right) = (1.5, 0.01, 0.02, 0.001)$.

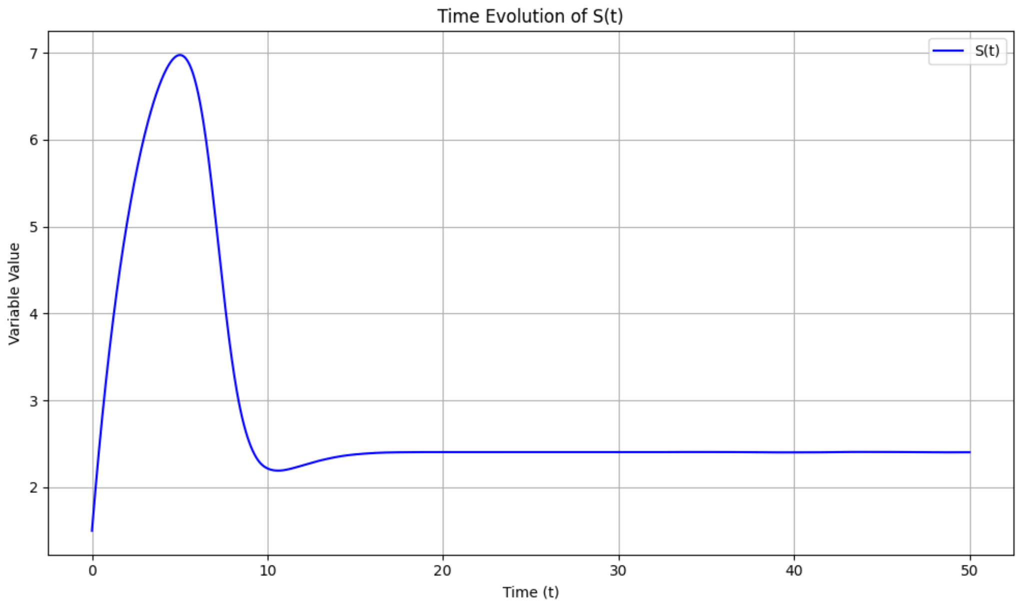

Fig. 6 The solution of $S(t)$ obtained by ODE 45 for $\alpha = 1$, and $0 < t < 50$.

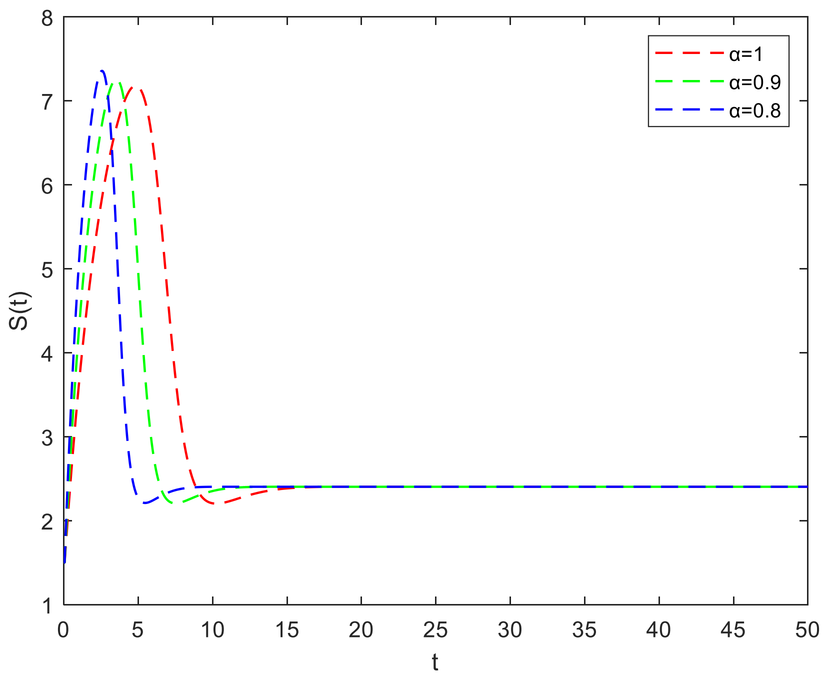

Fig. 7 The solution of $S(t)$ obtained by LADM for different values of α, (a) of $\alpha = 1$, (b) of $\alpha = 0.9$, (c) of $\alpha = 0.8$. and $0 \leq t \leq 50$.

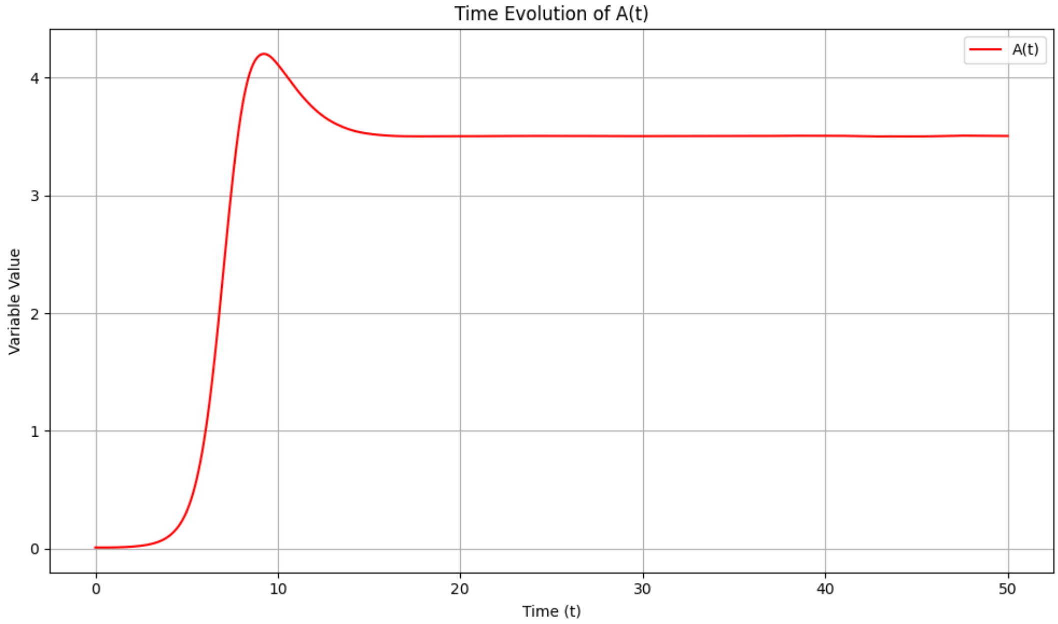

Fig. 8 The solution of $A(t)$ obtained by ODE 45 for $\alpha = 1$, and $0 < t < 50$.

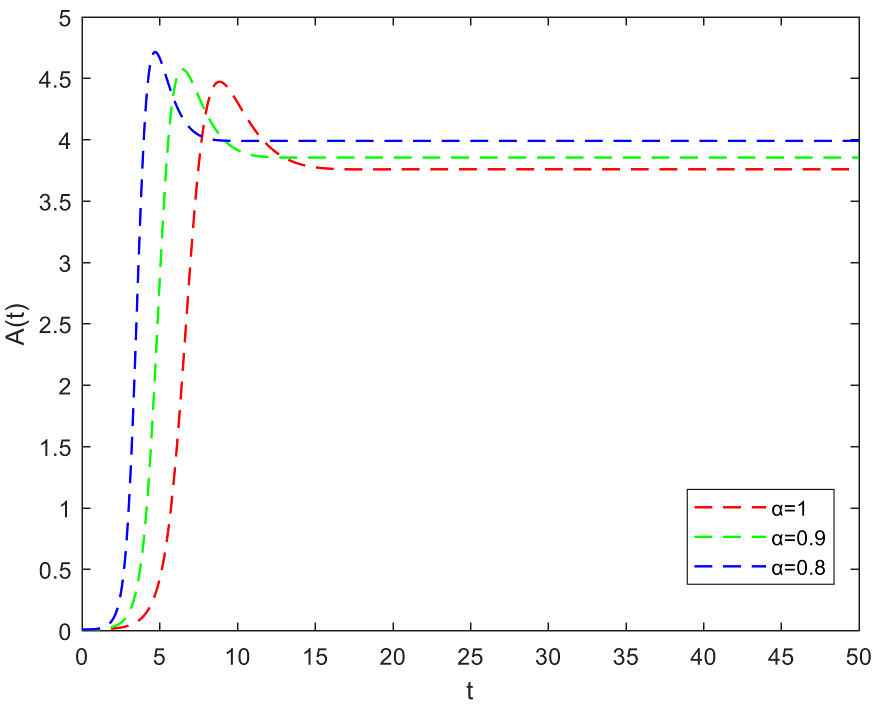

Fig. 9 The solution of $A(t)$ obtained by LADM for different values of α, (a) of $\alpha = 1$, (b) of $\alpha = 0.9$, (c) of $\alpha = 0.8$. and $0 \leq t \leq 50$.

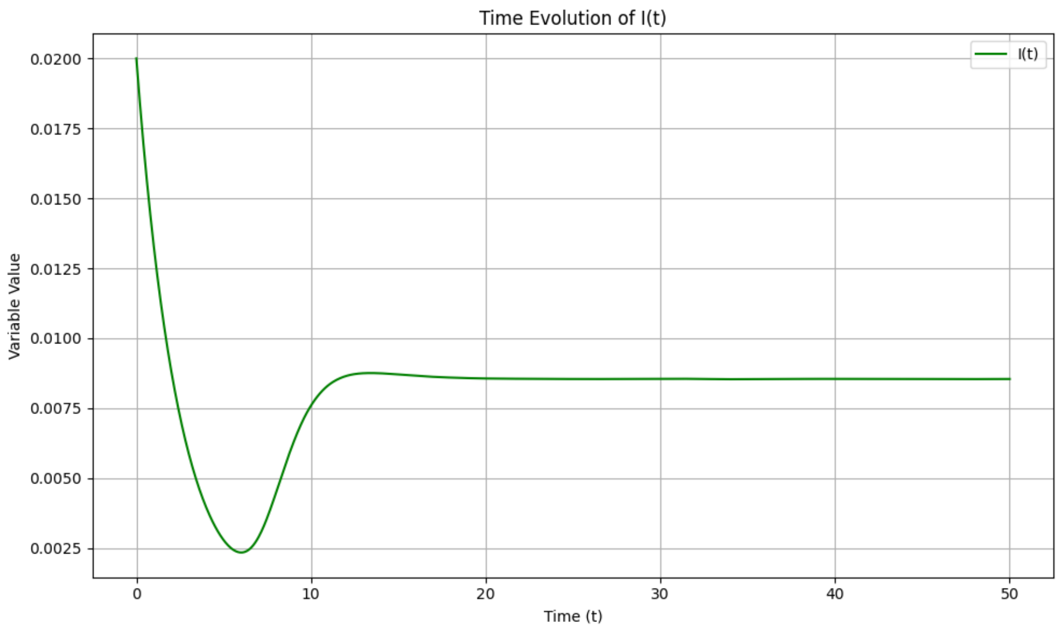

Fig. 10 The solution of $I(t)$ obtained by ODE 45 for $\alpha = 1$, and $0 < t < 50$.

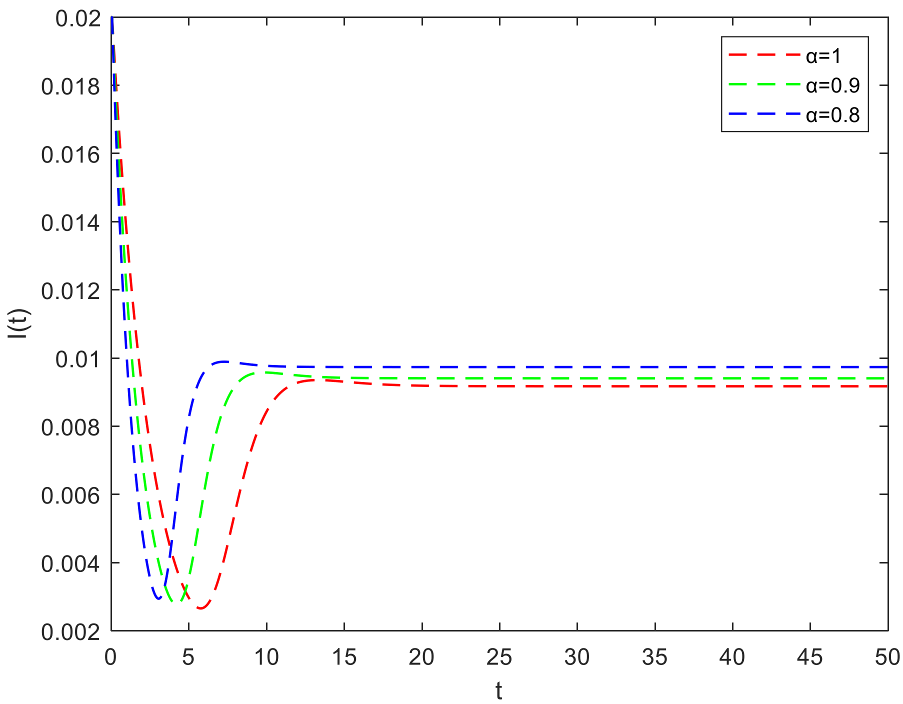

Fig. 11 The solution of $I(t)$ obtained by LADM for different values of α, (a) of $\alpha = 1$, (b) of $\alpha = 0.9$, (c) of $\alpha = 0.8$. and $0 \leq t \leq 50$.

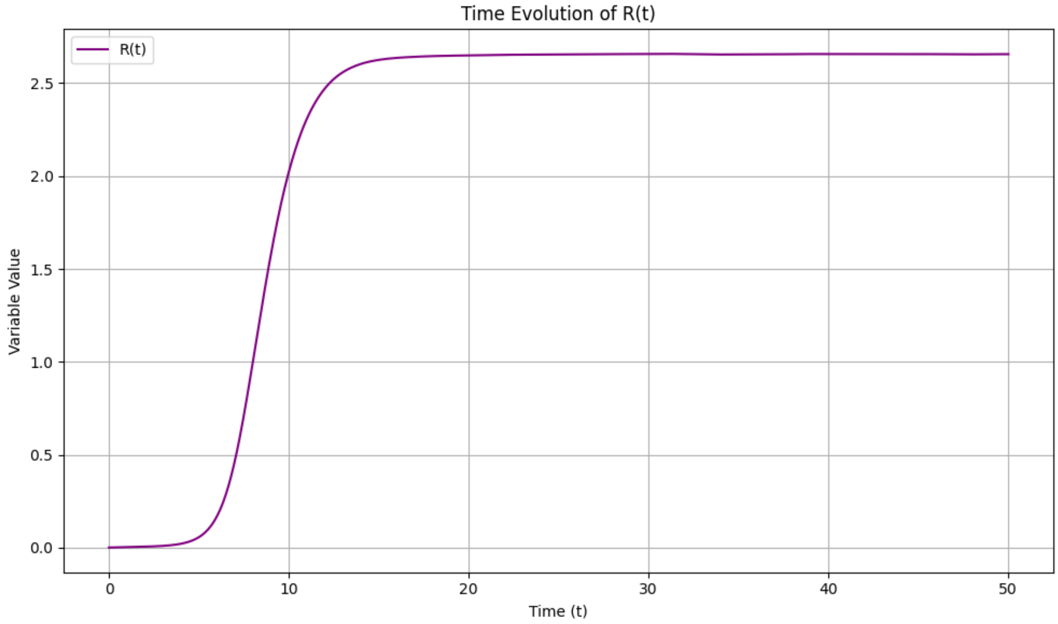

Fig. 12 The solution of $R(t)$ obtained by ODE 45 for $\alpha = 1$, and $0 < t < 50$.

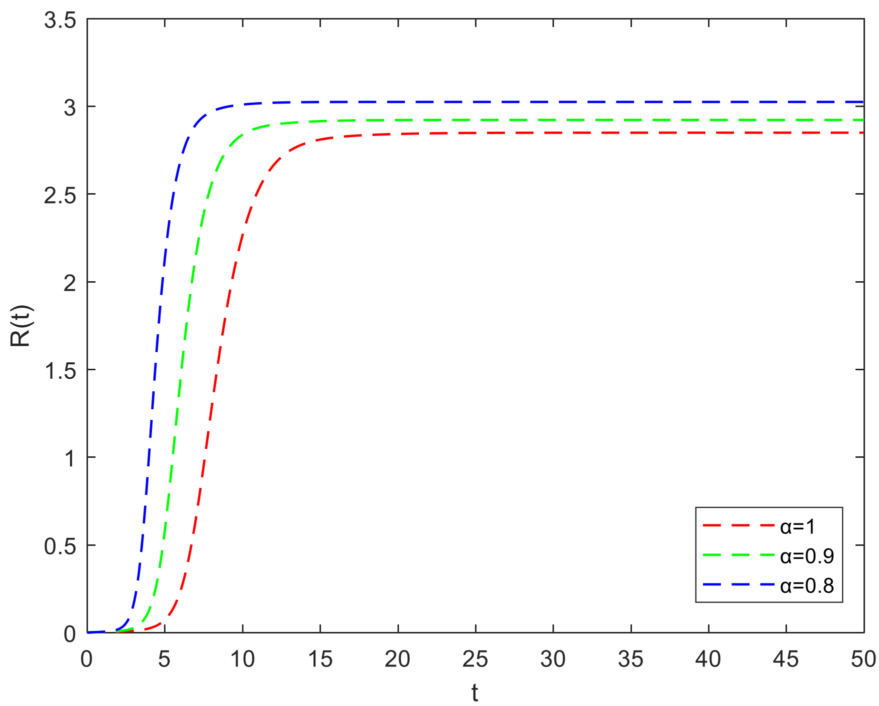

Fig. 13 The solution of $R(t)$ obtained by LADM for different values of α, (a) of $\alpha = 1$, (b) of $\alpha = 0.9$, (c) of $\alpha = 0.8$. and $0 \leq t \leq 50$.

6.Conclusions

In this paper, an improved fractional model for propagation of computer virus in the network, that containing the latent, antidotal computers and susceptible computers with low cure rate, is introduced and studied. the model has been successfully solved using two different approaches: the Rung-Kutta of order 4 and Laplace Adomian decomposition method.The acquired results ensure accurate solutions and are investigated for different values of the fractional-order α and transmission rates.All obtained results have been analyzed and compared for various cases. Our results and methods in this work can be further extended or generalized in solving other interesting nonlinear models arising from some phenomena in physics and engineering. In addition, our results can also be applied for models formulated using other fractional derivatives.

References:

1. Khanh N. H., Huy N. B., Stability analysis of a computer virus propagation model with antidote in vulnerable system, *Acta Mathematica Scientia. Series B. English Edition*, Vol:36, No:1, 49–61, 2016.
2. Feng L., Liao X., Li H., Han Q., Hopf bifurcation analysis of a delayed viral infection model in computer networks, *Mathematical and Computer Modelling*, Vol:56, No:7–8, 167–179, 2012.
3. Han X., Tan Q., Dynamical behavior of computer virus on Internet, *Applied Mathematics and Computation*, Vol:217, No:6, 2520–2526, 2010.
4. Yuan H., Chen G., Network virus-epidemic model with the point-to-group information propagation, *Applied Mathematics and Computation*, Vol:206, 357–367, 2008.
5. Mishra B. K., Saini D. K., SEIRS epidemic model with delay for transmission of malicious objects in computer network, *Applied Mathematics and Computation*, Vol:188, No:2, 1476–1482, 2007.
6. Mishra B. K., Jha N., SEIQRS model for the transmission of malicious objects in computer network, *Applied Mathematics and Computation*, Vol:34, No:3, 710–715, 2010.
7. Liu J., Hopf bifurcation in a delayed SEIQRS model for the transmission of malicious objects in computer network, *Journal of Applied Mathematics*, Vol:2014, Article ID: 492198, 8 pages, 2014.
8. Yang L.-X., Yang X. F., A new epidemic model of computer viruses, *Communications in Nonlinear Science and Numerical Simulation*, Vol:19, No:6, 1935–1944, 2014.
9. Yang L.-X., Yang X. F., Zhu Q., Wen L., A computer virus model with graded cure rates, *Nonlinear Analysis: Real World Applications*, Vol:14, No:1, 414–422, 2013.

10. Yang L.-X., Yang X. F., Propagation behavior of virus codes in the situation that infected computers are connected to the internet with positive probability, *Discrete Dynamics in Nature and Society*, Vol:2012, Article ID: 693695, 13 pages, 2012.

11. Muroya Y., Kuniya T., Global stability of nonresident computer virus models, *Mathematical Methods in the Applied Sciences*, Vol:38, No:2, 281–295, 2015.

12. Muroya Y., Li H., Kuniya T., On global stability of a nonresident computer virus model, *Acta Mathematica Scientia. Series B. English Edition*, Vol:34, No:5, 1427–1445, 2014.

13. Ongun M. Y., The Laplace Adomian decomposition method for solving a model for HIV infection of CD4+ T cells, *Mathematical and Computer Modelling*, Vol:53, No:5–6, 597–603, 2011.

14. Haq F., Shah K., Rahman G. U., Shahzad M., Numerical solution of fractional order smoking model via Laplace Adomian decomposition method, *Alexandria Engineering Journal*, Vol:57, No:2, 1061–1069, 2018.

15. Baleanu D., Aydogn S. M., Mohammadi H., Rezapour S., On modelling of epidemic childhood diseases with the Caputo-Fabrizio derivative by using the Laplace Adomian decomposition method, *Alexandria Engineering Journal*, Vol:59, No:5, 3029–3039, 2020.

16. González-Gaxiola O., Biswas A., Optical solitons with Radhakrishnan–Kundu–Lakshmanan equation by Laplace–Adomian decomposition method, *Optik*, Vol:179, 434–442, 2019.

17. Edeki S. O., Motsepa T., Khalique C. M., Akinlabi G. O., The Greek parameters of a continuous arithmetic Asian option pricing model via Laplace Adomian decomposition method, *Open Physics*, Vol:16, No:1, 780–785, 2018.

18. Naghipour A., Manafian J., Application of the Laplace Adomian decomposition and implicit methods for solving Burgers' equation, *TWMS Journal of Pure and Applied Mathematics*, Vol:6, No:1, 68–77, 2015.

19. González-Gaxiola O., Biswas A., W-shaped optical solitons of Chen–Lee–Liu equation by Laplace–Adomian decomposition method, *Optical and Quantum Electronics*, Vol:50, No:8, 1–11, 2018.

20. Paul S., Mondal S. P., Bhattacharya P., Numerical solution of Lotka Volterra prey-predator model by using Runge–Kutta–Fehlberg method and Laplace Adomian decomposition method, *Alexandria Engineering Journal*, Vol:55, No:1, 613–617, 2016.

21. Günerhan H., Kaabar M. K. A., Çelik E., Novel analytical and approximate-analytical methods for solving the nonlinear fractional smoking mathematical model, *Sigma Journal of Engineering and Natural Sciences*, Vol:41, 331–343, 2023.

22. Adel W., Günerhan H., Nisar K. S., et al., Designing a novel fractional order mathematical model for COVID-19 incorporating lockdown measures, *Scientific Reports*, Vol:14, 2926, 2024.

23. Günerhan H., Dutta H., Dokuyucu M. A., Adel W., Analysis of a fractional HIV model with Caputo and constant proportional Caputo operators, *Chaos, Solitons & Fractals*, Vol:139, 110053, 2020.

24. Günerhan H., Rezazadeh H., Adel W., et al., Analytical approximate solution of fractional order smoking epidemic model, *Advances in Mechanical Engineering*, Vol:14, No:9, 2022.

25. Meenakshi A., Renuga E., Čep R., Karthik K., Analysis of Caputo Fractional-Order Co-Infection COVID-19 and Influenza SEIR Epidemiology by Laplace Adomian Decomposition Method, *Mathematics*, Vol:12, No:12, 1876, 2024.

26. Herrmann R., Fractional calculus: an introduction for physicists, Wiley-VCH, 2011.

27. Caputo M., Linear models of dissipation whose Q is almost frequency independent—II, *Geophysical Journal International*, Vol:13, No:5, 529–539, 1967.

28. Zhang Y., Yu X., Sun H., et al., Applicability of time fractional derivative models for simulating the dynamics and mitigation scenarios of COVID-19, *Chaos, Solitons & Fractals*, Vol:138, 109959, 2020.

Exact solutions and modulation instability analysis of the $(3+1)-$dimensional Gross-Pitaevskii equation with periodic potential

Esra Ünal Yılmaz,[1] Yeşim Sağlam Özkan[2]
[1] Department of Mathematics, Bolu Abant Izzet Baysal University, 16059, Bolu, Turkey
[2] Department of Mathematics, Bursa Uludag University, 16059, Bursa, Turkey
esraunal@ibu.edu.tr, ysaglam@uludag.edu.tr

Abstract

In this paper we examine the $(3+1)-$dimensional Gross-Pitaevskii equation, which describes phenomena such as wave propagation. The solitonic wave solutions of the underlying problem are examined using two efficient techniques: the modified auxiliary equation method and the $exp(-w(\xi))$ method. This approach yields solutions that are stated as exponential, rational, trigonometric, and hyperbolic functions. To have a better understanding of their dynamic behavior, several of the distinct types of solitons, including dark waves, have also been shown using 3D visuals for varying parameter values. The stability of the obtained results is confirmed by investigating the modulation instability for the governing model.

Keywords: The modified auxiliary equation method; $exp(-w(\xi))$ method; Gross-Pitaevskii equation.

1 Introduction

Numerous disciplines, such as ocean engineering, solitary wave theory, hydrodynamics, optical fibers, chaos theory, and turbulent theory, utilize nonlinear evolution equations (NLEEs). Many nonlinear mathematical and physical processes depend on the search for accessible properties and the building of accurate solutions for nonlinear dynamical models. Since the end of the 1970s, numerous approaches have been put forth in this context to methodically find answers for such models. The reference list [1]-[22] contains some of these techniques. One classical example of a nonlinear evolution equation is the Gross–Pitaevskii equation. It is an alternative form of the well-known nonlinear Schrödinger equation (NLSE), a general model controlling complex field envelope evolution in nonlinear dispersive media. Generally speaking, the Gross–Pitaevskii equation , which is essentially a mean-field approximation for the interparticle interactions, describes the dynamics of the condensate at zero temperature. Formal analytical results of the Gross–Pitaevskii equation are given in [23]. In [24] Bao, Jaksch and Markowich investigate the numerical solution of the time-dependent Gross–Pitaevskii equation at very low or zero temperature, which describes a Bose–Einstein condensate (BEC). In [25] with the help of numerical approaches, the Bose-Einstein condensate of trapped interacting neutral atoms at zero temperature is described by the time-independent nonlinear Gross-Pitaevskii equation in two dimensions. The (3+1)-dimensional periodic potential has certain modernistic soliton solutions, which are investigated by researchers in [26]. To obtain a range of novel solutions for the governing model, three methods are used: the extended G/G'-expansion approach, the Sardar sub-equation method, and the function method. In this work, we focus Manjun's $(3+1)-$dimensional Gross–Pitaevskii equation in [27] given as

$$i\frac{\partial}{\partial t}h(s,t) = -\nabla h(s,t) + U(x)h(s,t) + g(s,t)|h|^2 h, \tag{1}$$
$$\nabla = \frac{\partial^2}{\partial x^2} + \frac{\partial^2}{\partial y^2} + \frac{\partial^2}{\partial z^2},$$

where $s \in \Re^3; t > 0$. ∇ stands for the Laplacian operator. The function $U(x)$ describes the potential of the trap to confine the condensate and $s = (x, y, z)$ is the propagation variable and t is the transverse variable. The nonlinear coefficient $g(s,t)$ is the real-valued functions of time and spatial coordinates. We apply the $exp(-w(xi))$-expansion approach and modified auxiliary equation method to obtain soliton solutions. By displaying the 2D, 3D, and contour plots, more thorough information regarding the dynamical representation of some of the solutions is shown.

This paper is organized as follows: we give the presentation of methodologies in Section 2. In the next section, the mathematical analysis and an application of the mentioned methods are given. In section 4, we discuss the modulation instability analysis. In Section 5, we give some conclusions and discussions about the obtained solutions. Finally, the study is concluded with the Conclusion section.

2 Presentation of methodologies

In this part, the $exp(-w(\xi))$ method and the modified auxiliary equation method have been explained in detail.

2.1 The $exp(-w(\xi))$-expansion method

Consider the following nonlinear evolution equation [28, 29]

$$Q(u, u_t, u_x, u_{tt}, u_{tt}, ...) = 0, \tag{2}$$

where Q is a polynomial in $u(x,t)$ and its derivatives in which higher order derivatives and nonlinear terms are involved. In virtue of the traveling wave transformation

$$u = u(\xi),\ \xi = x - ct, \tag{3}$$

where c is a constant to be determined later, Eq. (2) can be reduced to an ordinary differential equation (ODE)

$$P(u, u', u'', ...) = 0, \tag{4}$$

where prime denotes the derivative with respect to ξ. The, the traveling wave solutions of Eq. (4) can be expressed as follows

$$u = a_0 + a_1 \exp(-w(\xi)) + ... + a_n(\exp(-w(\xi)))^n \tag{5}$$

where n is determined by balancing the highest order nonlinear terms with the highest order derivatives of $u(\xi)$ in Eq. (4) and $w = w(\xi)$ satisfies the following ODE

$$w'(\xi) = \exp(-w(\xi)) + a\exp(w(\xi)) + b. \tag{6}$$

Eq. (6) has the following analytical solutions:
Case 1: $a \neq 0, b^2 - 4a > 0,$

$$w_1(\xi) = \ln\left(\frac{-b - \sqrt{b^2 - 4\,a}\tanh\left(\frac{\sqrt{b^2-4\,a}}{2}\xi\right)}{2a}\right). \tag{7}$$

Case 2: $a \neq 0, b^2 - 4a < 0,$

$$w_2(\xi) = \ln\left(\frac{-b + \sqrt{-b^2 + 4a}\tan\left(\frac{\sqrt{-b^2+4a}}{2}\xi\right)}{2a}\right). \tag{8}$$

Case 3: $a \neq 0,\ b^2 - 4a = 0,$

$$w_3(\xi) = \ln\left(-\frac{2\,b\,\xi + 4}{b^2\xi}\right). \tag{9}$$

Case 4: $b \neq 0,\ a = 0,$

$$w_4(\xi) = -\ln\left(\frac{b}{\exp(b\xi) - 1}\right). \tag{10}$$

Case 5: $a = 0, b = 0.$

$$w_5\,(\xi) = \ln(\xi). \tag{11}$$

Here, for simplicity, in $w_i(\xi), 1 \leq i \leq 5$, have been replaced all of $\xi + \xi_0$ with ξ, since Eq. (6) is an autonomous ODE. Next, substituting Eq. (5) along with Eq. (6) into Eq. (4) yields a polynomial in $\exp(-w(\xi))$. Setting each coefficient of this polynomial to zero, a set of algebraic equations in terms of $a_0, a_1, ..., a_n, c, b, a$ is obtained. Lastly solving the system of algebraic equations and later substituting these results and analytical solutions $w_1(\xi), ..., w_5(\xi)$ into Eq. (5) give traveling wave solutions of Eq. (4).

2.2 The modified auxiliary equation method

To summarize the basic steps of this method let us consider the following PDE

$$Q(u, u_t, u_x, u_{tt}, u_{tt}, ...) = 0, \tag{12}$$

where Q is a polynomial in dependent function and its partial derivatives. With the help of the traveling wave transformation $u = u(\xi),\ \xi = x - ct$, where c is arbitrary constants, Eq. (12) can be transformed to an following ODE

$$P(u, u', u'', ...) = 0. \tag{13}$$

Here $(.)' = \frac{d}{d\zeta}(.)$. To obtain the solution of Eq. (13) via the modified auxiliary equation method, the general solution has the form

$$u = a_0 + \sum_{i=1}^{n} a_i K^{if(\xi)} + \sum_{i=1}^{n} b_i K^{-if(\xi)}, \tag{14}$$

where a_i, b_i $(0 \le i \le n)$ and K are constants to be determined and $f(\xi)$ satisfy the following auxiliary equation

$$f'(\xi) = \frac{b + aK^{-f(\xi)} + cK^{f(\xi)}}{In(K)}, \tag{15}$$

where a, b and c are parameters to be determined and $K > 0$, $K \neq 1$. The integer n can be determined by balancing procedure. Putting Eq. (14) with Eq. (15) into Eq. (13) and collecting coefficients of $K^{if(\xi)}$ $(i = -n, ..., n)$ by equating them to zero, a system of algebraic equations is obtained. Then, solving this system, the values of constants a_i, b_i, a, b, c are obtained. By putting all the values of constants into Eq. (14), the required solutions of considered equation have been obtained. Substituting these values and the solutions of Eq. (14) into Eq. (13), the exact solutions of Eq. (12) can be derived. The solution of Eq. (15) subject to the couple of cases is given as:
If $b^2 - 4ac < 0$ and $c \neq 0$, then

$$\begin{aligned} K^{f(\xi)} &= \frac{-b + \sqrt{4ac - b^2}\tan(\frac{1}{2}\sqrt{4ac - b^2}\xi)}{2c}, \\ \text{or} &- \frac{-b + \sqrt{4ac - b^2}\cot(\frac{1}{2}\sqrt{4ac - b^2}\xi)}{2c}. \end{aligned} \tag{16}$$

If $b^2 - 4ac > 0$ and $c \neq 0$, then

$$\begin{aligned} K^{f(\xi)} &= \frac{-b + \sqrt{4ac - b^2}\tanh(\frac{1}{2}\sqrt{4ac - b^2}\xi)}{2c}, \\ \text{or} &- \frac{-b + \sqrt{4ac - b^2}\coth(\frac{1}{2}\sqrt{4ac - b^2}\xi)}{2c}. \end{aligned} \tag{17}$$

If $b^2 - 4ac = 0$ and $c \neq 0$, then

$$K^{f(\xi)} = -\frac{2 + b\xi}{2c\xi}. \tag{18}$$

3 Mathematical analysis

In this section, the exact solutions of Eq. (1) are established by means of $exp(-w(\xi))$-expansion method and the modified auxiliary equation method.

To seek exact analytical wave solutions of Eq. (1) we take the similarity transformation [30] by Malfliet,

$$h(x, y, z, t) = \Psi(\xi)e^{ik(\alpha x + \gamma y + \lambda z + \beta t)}, \ \xi = x + y + z - \varsigma t. \tag{19}$$

Applying Eq.(19) into Eq. (1), we have the real and imaginary parts given as follows:
The real part:

$$3\Psi^{''} - \Psi[k^2(\alpha^2 + \gamma^2 + \lambda^2) + k\beta + U] - g\Psi^3 = 0. \tag{20}$$

The imaginary part:

$$\Psi[2k(\alpha + \gamma + \lambda) - \varsigma] = 0. \tag{21}$$

From Eq. (21), we obtain the velocity of solitons, given as:

$$\varsigma = \Psi[2k(\alpha + \gamma + \lambda)]. \tag{22}$$

By utilizing the homogenous balance approach in Eq. (20), we achieve $n = 1$. Now we will find the soliton solutions to the above Eq. (20) by using the described approaches.

3.1 Implementation of $exp(-w(\xi))$-expansion method

For $n = 1$, Eq. (5) reduces into

$$\Psi(\xi) = a_0 + a_1\exp(w(\xi)), \tag{23}$$

where $a_1 \neq 0$, a_0 is a constant. Firstly, we substitute the expressions of Ψ in Eq. (23) into Eq. (20) and collect all terms with the same order of together. Then by equating the coefficient of each polynomial to zero and by solving the gained system with the use of the Maple tool, we achieve the below solution set:

$$\text{Set 2}: \left\{ a_0 = \frac{\sqrt{6}\sqrt{\frac{1}{g}}\,b}{2}, a_1 = \sqrt{6}\sqrt{\frac{1}{g}}, \beta = -\frac{2\alpha^2k^2 + 2\gamma^2k^2 + 2k^2\lambda^2 + 3b^2 + 2U - 12a}{2k}, k = k \right\} \tag{24}$$

The respective solutions are as following:
Case 1: If $b^2 - 4a > 0$

$$\Psi_1 = \left(\frac{\sqrt{6}\sqrt{\frac{1}{g}}\,b}{2} - \frac{2\sqrt{6}\sqrt{\frac{1}{g}}\,a}{\sqrt{b^2-4a}\,\tanh\left(\frac{\sqrt{b^2-4a}\,(-2k(\alpha+\gamma+\lambda)t+x+y+z)}{2}\right)+b} \right) \mathrm{e}^{\mathrm{I}k\left(\alpha x - \frac{\left(2\alpha^2k^2+2\gamma^2k^2+2k^2\lambda^2+3b^2+2U-12a\right)t}{2k}+\gamma y+bz\right)}. \quad (25)$$

Case 2: If $b^2 - 4a < 0$

$$\Psi_2 = \left(\frac{\sqrt{6}\sqrt{\frac{1}{g}}\,b}{2} - \frac{2\sqrt{6}\sqrt{\frac{1}{g}}\,a}{b-\sqrt{-b^2+4a}\,\tan\left(\frac{\sqrt{-b^2+4a}\,(-2k(\alpha+\gamma+\lambda)t+x+y+z)}{2}\right)} \right) \mathrm{e}^{\mathrm{I}k\left(\alpha x - \frac{\left(2\alpha^2k^2+2\gamma^2k^2+2k^2\lambda^2+3b^2+2U-12a\right)t}{2k}+\gamma y+bz\right)}. \quad (26)$$

Case 3: If $a = b^2/4$

$$\Psi_3 = \frac{2\sqrt{6}\sqrt{\frac{1}{g}}\,b\,\mathrm{e}^{\mathrm{I}k\left(\alpha x - \frac{\left(2k^2\alpha^2+2k^2\gamma^2+2k^2\lambda^2+3b^2+2U-12a\right)t}{2k}+\gamma y+bz\right)}}{2b\,(-2k\,(\alpha+\gamma+\lambda)\,t+x+y+z)+4}. \quad (27)$$

Case 4: If $a = 0$

$$\Psi_4 = \frac{\left(\frac{\sqrt{6}\sqrt{\frac{1}{g}}\,b\,\mathrm{e}^{b(-2k(\alpha+\gamma+\lambda)t+x+y+z)}}{2} + \frac{\sqrt{6}\sqrt{\frac{1}{g}}\,b}{2} \right) \mathrm{e}^{\mathrm{I}k\left(\alpha x - \frac{\left(2\alpha^2k^2+2\gamma^2k^2+2k^2\lambda^2+3b^2+2U-12a\right)t}{2k}+\gamma y+bz\right)}}{\mathrm{e}^{b(-2k(\alpha+\gamma+\lambda)t+x+y+z)}-1}. \quad (28)$$

Case 5: If $a = 0,\ b = 0$

$$\Psi_5 = \frac{\sqrt{6}\sqrt{\frac{1}{g}}\,\mathrm{e}^{\mathrm{I}k\left(\alpha x - \frac{\left(2k^2\alpha^2+2k^2\gamma^2+2k^2\lambda^2+2U\right)t}{2k}+\gamma y\right)}}{-2k\,(\alpha+\gamma+\lambda)\,t+x+y+z}. \quad (29)$$

3.2 Implementation of modified auxiliary equation method

Considering the homogeneous balance $n = 1$, we suppose that the solution of Eq. (20) can be expressed by

$$\Psi = a_0 + a_1 K^{f(\xi)} + b_1 K^{-f(\xi)}, \quad (30)$$

where a_0, a_1, b_1 are constants to be determined later. Putting Eq. (30) with Eq. (15) into Eq. (20), and by collecting all coefficients of $K^{if((\xi)}) \, (i = 0, 1)$, and setting them equal to zero, yields an algebraic system. At this stage, Maple can be used to solve this equation system. Therefore, the following set of values of constants are obtained. Substituing this set into Eq. (30) with the help of Eq. (19) the exact solutions of Eq. (1) are obtained.

$$\text{Set 3}: \left\{ a_0 = \frac{\sqrt{6}\sqrt{\frac{1}{g}}\,b}{2}, a_1 = 0, b_1 = a\sqrt{6}\sqrt{\frac{1}{g}}, k = \frac{-\beta+\sqrt{(-4\,U+24\,ac-6\,b^2)\,(\gamma^2+\lambda^2+\alpha^2)+\beta^2}}{2\alpha^2+2\gamma^2+2\lambda^2} \right\} \quad (31)$$

$$\text{Set 4}: \left\{ a_0 = \frac{\sqrt{6}\sqrt{\frac{1}{g}}\,b}{2}, a_1 = 0, b_1 = a\sqrt{6}\sqrt{\frac{1}{g}}, k = \frac{-\beta\sqrt{(-4\,U+24\,ac-6\,b^2)\,(\gamma^2+\lambda^2+\alpha^2)+\beta^2}}{2\alpha^2+2\gamma^2+2\lambda^2} \right\} \quad (32)$$

According to Set 3 in (31), the solitary wave solutions of Eq. (1) can be obtained as
If $b^2 - 4ac < 0$ then

$$\Psi_6(x,y,z,t) = \left(\frac{b\sqrt{6}}{2g\sqrt{\frac{1}{g}}} + \frac{\left(-b+\sqrt{4ac-b^2}\,\tan\left(\frac{(x+y+z-\varsigma t)\sqrt{4ac-b^2}}{2}\right)\right)\sqrt{6}\sqrt{\frac{1}{g}}}{2} \right) \mathrm{e}^{\mathrm{I}k(\alpha x+\beta t+\gamma y+\lambda z)} \quad (33)$$

or

$$\Psi_7(x,y,z,t) = -\left(\frac{b\sqrt{6}}{2g\sqrt{\frac{1}{g}}} + \frac{\left(-b+\sqrt{4ac-b^2}\,\cot\left(\frac{(x+y+z-\varsigma t)\sqrt{4ac-b^2}}{2}\right)\right)\sqrt{6}\sqrt{\frac{1}{g}}}{2} \right) \mathrm{e}^{\mathrm{I}k(\alpha x+\beta t+\gamma y+\lambda z)}, \quad (34)$$

where $\varsigma = 2k(\alpha+\gamma+\lambda)$.
If $b^2-4ac>0$ then

$$\Psi_8(x,y,z,t) = \left(\frac{b\sqrt{6}}{2g\sqrt{\frac{1}{g}}} + \frac{\left(-b+\sqrt{-4ac+b^2}\,\tanh\left(\frac{(x+y+z-\varsigma t)\sqrt{-4ac+b^2}}{2}\right)\right)\sqrt{6}\,\sqrt{\frac{1}{g}}}{2}\right)\mathrm{e}^{\mathrm{I}k(\alpha x+\beta t+\gamma y+\lambda z)} \tag{35}$$

or

$$\Psi_9(x,y,z,t) = -\left(\frac{b\sqrt{6}}{2g\sqrt{\frac{1}{g}}} + \frac{\left(-b+\sqrt{-4ac+b^2}\,\coth\left(\frac{(x+y+z-\varsigma t)\sqrt{-4ac+b^2}}{2}\right)\right)\sqrt{6}\,\sqrt{\frac{1}{g}}}{2}\right)\mathrm{e}^{\mathrm{I}k(\alpha x+\beta t+\gamma y+\lambda z)}, \tag{36}$$

where $\varsigma = 2k(\alpha+\gamma+\lambda)$.
If $b^2-4ac=0$

$$\Psi_{10}(x,y,z,t) = \frac{\sqrt{6}\,\mathrm{e}^{\mathrm{I}k(\alpha x+\beta t+\gamma y+\lambda z)}}{2\sqrt{\frac{1}{g}}\,g\left(\frac{\varsigma t}{2}-\frac{x}{2}-\frac{y}{2}-\frac{z}{2}\right)}, \tag{37}$$

where $\varsigma = 2k(\alpha+\gamma+\lambda)$.
According to Set 4 in (32), the solitary wave solutions of Eq. (1) can be obtained as
If $b^2-4ac<0$ then

$$\Psi_{11}(x,y,z,t) = \left(\frac{\sqrt{6}\,\sqrt{\frac{1}{g}}\,b}{2} + \frac{2ca\sqrt{6}\,\sqrt{\frac{1}{g}}}{-b+\sqrt{4ac-b^2}\,\tan\left(\frac{(x+y+z-\varsigma t)\sqrt{4ac-b^2}}{2}\right)}\right)\mathrm{e}^{\mathrm{I}k(\alpha x+\beta t+\gamma y+\lambda z)} \tag{38}$$

or

$$\Psi_{12}(x,y,z,t) = -\left(\frac{\sqrt{6}\,\sqrt{\frac{1}{g}}\,b}{2} + \frac{2ca\sqrt{6}\,\sqrt{\frac{1}{g}}}{-b+\sqrt{4ac-b^2}\,\cot\left(\frac{(x+y+z-\varsigma t)\sqrt{4ac-b^2}}{2}\right)}\right)\mathrm{e}^{\mathrm{I}k(\alpha x+\beta t+\gamma y+\lambda z)}, \tag{39}$$

where $\varsigma = 2k(\alpha+\gamma+\lambda)$.
If $b^2-4ac>0$ then

$$\Psi_{13}(x,y,z,t) = \left(\frac{\sqrt{6}\,\sqrt{\frac{1}{g}}\,b}{2} + \frac{2ca\sqrt{6}\,\sqrt{\frac{1}{g}}}{-b+\sqrt{-4ac+b^2}\,\tanh\left(\frac{(x+y+z-\varsigma t)\sqrt{-4ac+b^2}}{2}\right)}\right)\mathrm{e}^{\mathrm{I}k(\alpha x+\beta t+\gamma y+\lambda z)} \tag{40}$$

or

$$\Psi_{14}(x,y,z,t) = -\left(\frac{\sqrt{6}\,\sqrt{\frac{1}{g}}\,b}{2} + \frac{2ca\sqrt{6}\,\sqrt{\frac{1}{g}}}{-b+\sqrt{-4ac+b^2}\,\coth\left(\frac{(x+y+z-\varsigma t)\sqrt{-4ac+b^2}}{2}\right)}\right)\mathrm{e}^{\mathrm{I}k(\alpha x+\beta t+\gamma y+\lambda z)}, \tag{41}$$

where $\varsigma = 2k(\alpha+\gamma+\lambda)$.
If $b^2-4ac=0$ then

$$\Psi_{15}(x,y,z,t) = -\frac{8\,\mathrm{e}^{\mathrm{I}k(\alpha x+\beta t+\gamma y+\lambda z)}\sqrt{6}\,\sqrt{\frac{1}{g}}\,\left(\left(-\frac{\varsigma t}{8}+\frac{x}{8}+\frac{y}{8}+\frac{z}{8}\right)b^2+\frac{b}{4}+\left(\frac{\varsigma t}{2}-\frac{x}{2}-\frac{y}{2}-\frac{z}{2}\right)ac\right)}{-4+(2\varsigma t-2x-2y-2z)\,b}, \tag{42}$$

where $\varsigma = 2k(\alpha+\gamma+\lambda)$.

4 Graphical Illustration

In this section, graphical representation will be given for some of the solutions obtained.

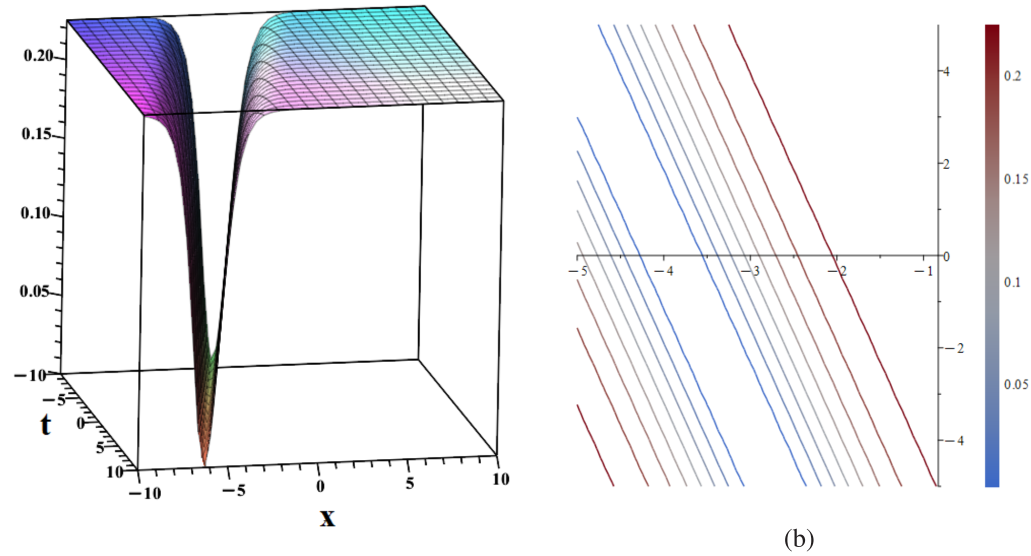

(b)

(a)

Figure 1: Dark soliton solution 3D-profile and contour plot of $|\Psi_1|^2$ for $b = 2, a = 0.1, \alpha = -0.1, \gamma = 0.5, \lambda = -0.1, \beta = 5, g = 24, k = -0.4, y = 1, z = 1$ within $-5 \leq t \leq 5,\ -5 \leq x \leq 5$.

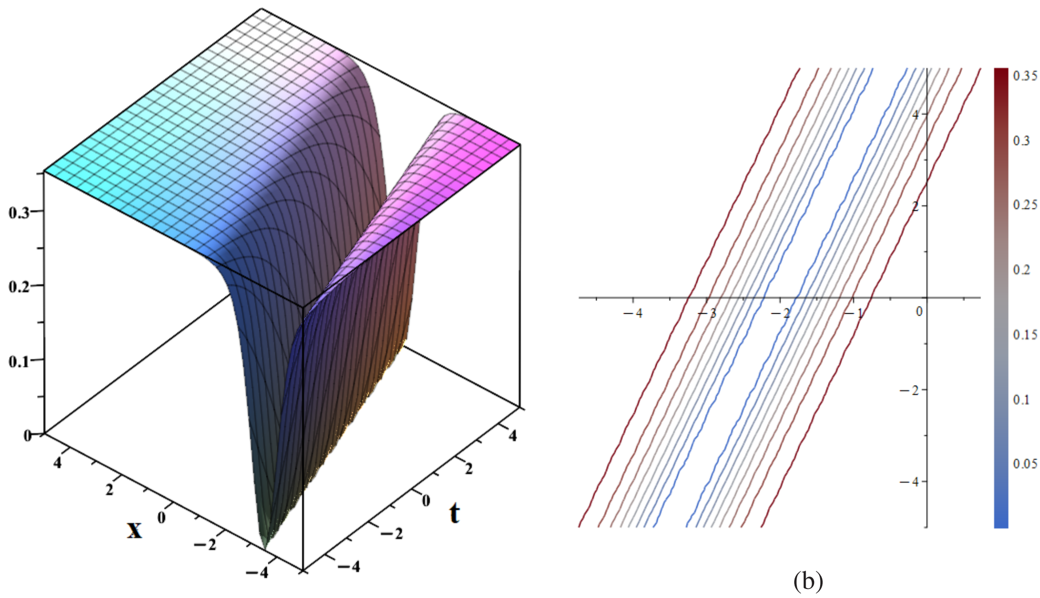

(b)

(a)

Figure 2: Dark soliton solution 3D-profile and contour plot of $|\Psi_7|^2$ for $a = -2, b = 0.5, c = 1, g = 35, k = -0.1, y = 1, z = 1, \alpha = 0.5, \beta = 0.3, \gamma = 0.5, \lambda = -2.5, y = 1, z = 1$ within $-5 \leq t \leq 5,\ -5 \leq x \leq 5$.

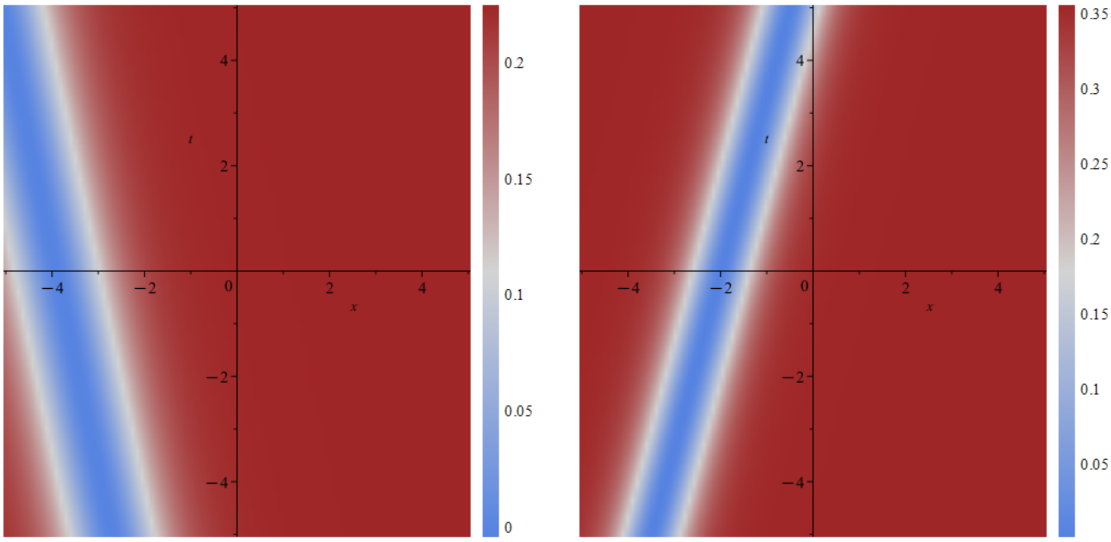

(a) (b)

Figure 3: Density plots of the solution $|\Psi_1|^2$ **(a)** and $|\Psi_7|^2$ **(b)**.

In Figure 1 (a) the 3D surface plot shows a characteristic dip, which is a typical of a dark soliton. In (b) the contour plot displays the same solution from a top-down perspective, with color coding indicating intensity levels.

In Figure 2 the 3D plot shows a deeper and wider soliton structure, reflecting the parameter changes.

In Figure 3 (a) and (b) provide clearer visualization of the spatial and temporal evolution of the soliton profiles, with intensity gradients distinctly highlighting propagation characteristics.

5 Modulation instability analysis

In this part of the study, modulation instability analysis (MI) for the stationary solutions of Eq. (1) is studied by supposing that Eq. (1) have the following stationary solution

$$h(x,y,z,t) = \left(\sqrt{P} + \phi(x,y,z,t)\right) e^{iP\eta t}, \tag{43}$$

where the optical power P is normalized and η is a constant. We investigate the evolution of the perturbation $\phi(x,y,z,t)$ using the concept of linear stability analysis. Substituting Eq. (43) into Eq. (1) and linearizing, we obtain

$$i\frac{d\phi}{dt} + \frac{d^2\phi}{dx^2} + \frac{d^2\phi}{dy^2} + \frac{d^2\phi}{dz^2} - U\phi - P\eta\phi + -Pg(\phi^* + 2\phi) = 0 \tag{44}$$

where ϕ^* is the conjugate function. Supposing solutions of Eq. (44) are in the following form:

$$\phi(x,y,z,t) = \alpha_1\, e^{i(k_1x+k_2y+k_3z-\omega t)} + \alpha_2\, e^{-i(k_1x+k_2y+k_3z-\omega t)}, \tag{45}$$

where ω is the frequency of perturbation and k_1, k_2, k_3 are normalized wave numbers. Putting Eq. (45) into Eq. (44) gives a set of two homogenous equations as follows

$$\begin{gathered}\left(-P\eta - 2Pg - {k_1}^2 - {k_2}^2 - {k_3}^2 - U - \omega\right)\alpha_2 - g\alpha_1 P = 0,\\[2ex] \left(-P\eta - 2Pg - {k_1}^2 - {k_2}^2 - {k_3}^2 - U + \omega\right)\alpha_1 - g\alpha_2 P = 0.\end{gathered} \tag{46}$$

From Eq. (46), one can easily obtain the following coefficient matrix of α_1 and α_2

$$\begin{pmatrix} -Pg & -P\eta - 2Pg - {k_1}^2 - {k_2}^2 - {k_3}^2 - U - \omega \\ -P\eta - 2Pg - {k_1}^2 - {k_2}^2 - {k_3}^2 - U + \omega & -Pg \end{pmatrix} \begin{pmatrix} \alpha_1 \\ \alpha_2 \end{pmatrix} = \begin{pmatrix} 0 \\ 0 \end{pmatrix}. \tag{47}$$

The coefficient matrix in Eq. (47) has a nontrivial solution if the determinant equal to zero. By expanding the determinant, we obtain the following

$$\left(-\eta^2 - 4\eta g - 3g^2\right)P^2 - 4\left({k_1}^2 + {k_2}^2 + {k_3}^2 + U\right)\left(g + \frac{\eta}{2}\right)P - \left({k_1}^2 + {k_2}^2 + {k_3}^2 + U - \omega\right)\left({k_1}^2 + {k_2}^2 + {k_3}^2 + U + \omega\right) = 0. \tag{48}$$

Eq. (48) has the following solutions for ω :

$$\omega = \pm\sqrt{\left(P\eta + 3Pg + {k_1}^2 + {k_2}^2 + {k_3}^2 + U\right)\left(P\eta + Pg + {k_1}^2 + {k_2}^2 + {k_3}^2 + U\right)}. \tag{49}$$

It is clear that the steady state is stable if $\left(P\eta + 3Pg + {k_1}^2 + {k_2}^2 + {k_3}^2 + U\right)\left(P\eta + Pg + {k_1}^2 + {k_2}^2 + {k_3}^2 + U\right) > 0$. Furthermore, the steady state becomes unstable if $\left(P\eta + 3Pg + {k_1}^2 + {k_2}^2 + {k_3}^2 + U\right)\left(P\eta + Pg + {k_1}^2 + {k_2}^2 + {k_3}^2 + U\right) < 0$. The MI gain spectrum is finally determined as:

$$G(k_1) = 2Im(\omega) = \pm 2\sqrt{\left(P\eta + 3Pg + {k_1}^2 + {k_2}^2 + {k_3}^2 + U\right)\left(P\eta + Pg + {k_1}^2 + {k_2}^2 + {k_3}^2 + U\right)}. \tag{50}$$

From Fig. 4, it can be easily observed that, the modulation stability gain spectrum increases with the increase of the incidence power P.

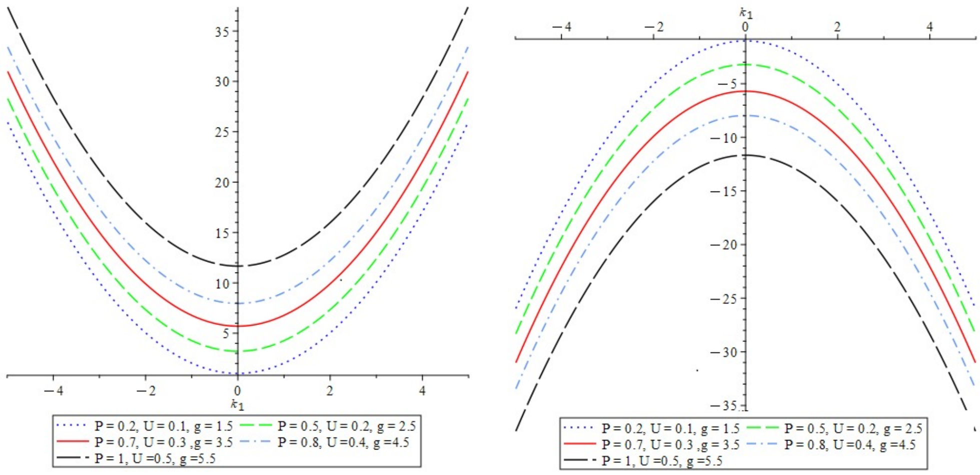

Figure 4: The modulation instability graphs for $k_2 = .1, k_3 = .3, \eta = 1.3$ in Eq. (49)

6 Conclusion

In this work we considered $(3+1)$-dimensional Gross-Pitaevskii equation (1). We first discussed the exact travelling wave solutions with the exp function method and modified auxiliary equation approach. We have systematically get dark wave type solution forms for $(3+1)-$ dimensional Gross-Pitaevskii equation Eq.(1). Fig. 1 displays the stability analysis solutions. The MI analysis is used to examine the stability analysis of the obtained solutions and the movement role of the waves. In order to examine how the model looks physically, we have set up 3D, contour and density graphs for various value sets. We think the research's findings are innovative and will help to improve the dynamic behavior of NLEEs that are seen in nonlinear sciences. The goal is to look into greater interaction in the future.

References

[1] Mirzazadeh M, Yıldırım Y, Yaşar E, Triki H, Zhou Q, Moshokoa SP, et al. Optical solitons and conservation law of Kundu-Eckhaus equation. Optik - Int J Light Electron Opt 2018;154:551–7.

[2] Sağlam Özkan Y, Yaşar E, Seadawy A. A third-order nonlinear Schrödinger equation: the exact solutions, group-invariant solutions and conservation laws. J Taibah Univ Sci 2020;14(1):585–97.

[3] Wazwaz AM. A new (2+ 1)-dimensional Korteweg–de Vries equation and its extension to a new (3+1)-dimensional Kadomtsev–Petviashvili equation. Physics Scr 2011;84(3):035010.

[4] Ahmed I, Seadawy AR, Lu D. M-Shaped rational solitons and their interaction with kink waves in the Fokas–Lenells equation. Physics Scr 2019;94(5):055205.

[5] Seadawy AR. Travelling-wave solutions of a weakly nonlinear two-dimensional higher-order Kadomtsev-Petviashvili dynamical equation for dispersive shallow-water waves. Eur Phys J Plus 2017;132(1):29.

[6] Seadawy AR. Modulation instability analysis for the generalized derivative higher order nonlinear Schrödinger equation and its the bright and dark soliton solutions. J Electromagn Waves Appl 2017;31(14):1353–62.

[7] Seadawy AR. Solitary wave solutions of two-dimensional nonlinear Kadomtsev–Petviashvili dynamic equation in dust-acoustic plasmas. Pramana 2017;89(3):49.

[8] Seadawy AR. Ion acoustic solitary wave solutions of two-dimensional nonlinear Kadomtsev–Petviashvili–Burgers equation in quantum plasma. Math Methods Appl Sci 2017;40(5):1598–607.

[9] Kumar D, Seadawy AR, Joardar AK. Modified Kudryashov method via new exact solutions for some conformable fractional differential equations arising in mathematical biology. Chin J Phys 2018;56(1):75–85.

[10] Ghanbari B, Akgül A. Abundant new analytical and approximate solutions to the generalized Schamel equation. Phys Scr 2020;95(7):075201.

[11] Seadawy AR. Two-dimensional interaction of a shear flow with a free surface in a stratified fluid and its solitary-wave solutions via mathematical methods. Eur Phys J Plus 2017;132(12):518.

[12] He JH. Application of homotopy perturbation method to nonlinear wave equations. Chaos Solitons Fractals 2005;26(3):695–700.

[13] Olver PJ. Application of lie groups to differential equations. New York: Springer- Verlag; 1993.

[14] Ahmad H, Seadawy AR, Khan TA. Numerical solution of Korteweg-de Vries-Burgers equation by the modified variational iteration algorithm-II arising in shallow water waves. Phys Scr 2020;95(4):045210.

[15] Muatjetjeja B, Adem AR. Rosenau-KdV equation coupling with the Rosenau-RLW equation: conservation laws and exact solutions. Int J Nonlinear SciNumer Simul 2017;18(6):451–6.

[16] Yaşar E, Yıldırım Y, Yaşar E. New optical solitons of space-time conformable fractional perturbed Gerdjikov-Ivanov equation by sine-Gordon equation method. Results Phys 2018;9:1666–72.

[17] Yaşar E, Yaşar E. Optical solitons of conformable space-time fractional NLSE with spatio-temporal dispersion. New Trends Math Sci 2018;6(3): 116–127.

[18] Yıldırım Y, Yaşar E, Adem AR, A novel scheme for nonlinear evolution equations using symbolic computations. J Appl Nonlinear Dyn 2019;8(3):463–73.

[19] Yaşar E, Ozer T. Invariant solutions and conservation laws to nonconservative FP equation. Comput Math Appl 2010;59:3203–10.

[20] Saglam Özkan Y, Yaşar E, Seadawy A. On the multi-waves, interaction and Peregrine-like rational solutions of perturbed Radhakrishnan–Kundu–Lakshmanan equation. Phys Scr 2020;95(8):085205.

[21] Liu CS. Trial equation method to nonlinear evolution equations with rank inhomogeneous: mathematical discussions and its applications. Commun Theor Phys 2006;45:219–23

[22] Aly R. Seadawy, Dianchen Lu, Mostafa M.A. Khater, Solitary wave solutions for the generalized Zakharov–Kuznetsov–Benjamin–Bona–Mahony nonlinear evolution equation, Journal of Ocean Engineering and Science,Volume 2, Issue 2, 2017,Pages 137-142, ISSN 2468-0133.

[23] C. Trallero-Giner, Julio C. Drake-Perez, V. López-Richard, Joseph L. Birman, Formal analytical solutions for the Gross–Pitaevskii equation, Physica D: Nonlinear Phenomena, Volume 237, Issue 18, 2008, Pages 2342-2352, ISSN 0167-2789.

[24] Weizhu Bao, Dieter Jaksch, Peter A. Markowich, Numerical solution of the Gross–Pitaevskii equation for Bose–Einstein condensation, Journal of Computational Physics, Volume 187, Issue 1, 2003, Pages 318-342, ISSN 0021-9991.

[25] Sadhan K. Adhikari, Numerical solution of the two-dimensional Gross–Pitaevskii equation for trapped interacting atoms, Physics Letters A, Volume 265, Issues 1–2, 2000, Pages 91-96, ISSN 0375-9601.

[26] Qawaqneh H., Altalbe A., Bekir A., Tariq K., Investigation of soliton solutions to the truncated M-fractional (3+1)-dimensional Gross-Pitaevskii equation with periodic potential, AIMS Mathematics 2024, Volume 9, Issue 9: 23410-23433.

[27] Ma. Manjun, Zhe Huang, Bright soliton solution of a Gross– Pitaevskii equation, Appl. Math. Lett. 26 (2013) 718–724.

[28] Abdelrahman, M. A., Zahran, E. H., Khater, M. M. Exact Traveling Wave Solutions for Power law and Kerr law non Linearity Using the $exp(-\phi(\xi))$-expansion Method. Global Journal of Science Frontier Research, 2014, 14(4).

[29] Hosseini, K., Bekir, A., Ansari, R. Exact solutions of nonlinear conformable time-fractional Boussinesq equations using the $\exp\left(-\phi\left(\varepsilon\right)\right)$-expansion method. Optical and Quantum Electronics, 2017 49(4), 131.

[30] W. Malfliet, Solitary wave solutions of nonlinear wave equations, Am. J. Phys. 60 (7) 1992, 650–654.

An Analytical Study of a Fractional Differential Model for COVID-19

Hatıra Günerhan [1]

[1] Department of Mathematics, Faculty of Education, Kafkas University, Kars, Turkey

gunerhanhatira@gmail.com

Abstract

This study investigates a nonlinear SITR system that models the dynamics of COVID-19 by incorporating fractional-order derivatives in the sense of the Caputo definition. The model categorizes the population into four compartments: susceptible (S), infected (I), under treatment (T), and recovered (R). To analyze the fractional-order SITR system, the Laplace Adomian Decomposition Method (LADM) is employed. Approximate analytical solutions are obtained, demonstrating rapid convergence and effectively capturing the system's behavior. The accuracy and applicability of the method are assessed, confirming the validity of the proposed fractional-order model.

Keywords: Caputo fractional derivative; Laplace Adomian decomposition; Covid-19; Nonlinear system.

1. INTRODUCTION

The COVID-19 pandemic, which emerged in late 2019, rapidly evolved into a global health crisis, highlighting the critical role of mathematical modeling in understanding and controlling infectious diseases. Epidemic models have been widely used to analyze transmission dynamics, forecast disease spread, and assess the effectiveness of intervention strategies [1–3]. Common models for COVID-19 build upon classical frameworks such as the Susceptible-Infected-Recovered (SIR) and Susceptible-Exposed-Infected-Recovered (SEIR) models. However, due to the unique characteristics of COVID-19, including asymptomatic cases, varying infectious periods, and treatment processes, these models have been extended to include additional compartments such as treatment classes, quarantine, and age or comorbidity-based risk factors [4–7].

Recently, fractional-order models and stochastic approaches have gained popularity, offering greater flexibility to capture memory effects, heterogeneity, and randomness in transmission dynamics [8–11]. Moreover, network-based models have been developed to simulate complex social contact structures and better predict the spread under different intervention scenarios [12,13]. Agent-based and data-driven models have also been used to incorporate detailed individual behavior and mobility patterns, improving prediction accuracy and aiding in targeted intervention strategies [14,15].

These mathematical models not only help monitor the current state of the pandemic but also provide critical insights for healthcare capacity planning and public health decision-making. This is especially important for evaluating the impact of emerging variants and vaccination campaigns on the course of the epidemic [3]. n this research, we are also exploring the potential of using the Laplace Adomian decomposition method (LADM) to solve the fractionalomputer virus propagation model. This method is a powerful yet straightforward approach to tackling epidemic models and has been successfully applied in biology, engineering, and applied mathematics. It combines the Laplace transform and the Adomian decomposition method, offering several advantages for solving complex problems. One of the advantages of this method is its accuracy, as by employing the Laplace transform, it transforms the differential equations into algebraic equations, which are often easier to solve. This transformation reduces the complexity of the problem and enables the use of powerful algebraic techniques to obtain accurate solutions. Additionally, the Adomian decomposition method provides a systematic and robust approach to handling nonlinear terms, allowing for accurate approximation of the solution even in the presence of nonlinearity. This method does not require any perturbation or linearization, nor does it need a defined size of the step like the Rung-Kutta of order 4 technique. Various models have already been solved using this particular technique, such as HIV infection of CD4+ T cells model [16], fractional-order smoking model [17], epidemic childhood diseases [18], Radhakrishnan–Kundu–Lakshmanan equation [19], Asian option pricing model [20], Burger's equation [21], Chen-Lee-Liu equation [22], prey-predator model [23], nonlinear fractional smoking mathematical model [24], HIV model [25], Smoking epidemic model [26], fractional-order co-infection SEIR model [27].

2.Model formulation

Mathematical models are crucial for understanding and predicting the spread of infectious diseases. These models typically use differential equations to describe how infections evolve over time. They consider population groups such as susceptible, asymptomatic, infected, and recovered individuals, along with disease characteristics and intervention strategies. Parameters quantify transmission and recovery rates, while equations capture the dynamics of these groups. Through mathematical analysis and computer simulations, such models reveal the core mechanisms driving epidemics and support public health officials in designing effective control measures.

The proposed fractional SITR model can be expressed as follows:

The SITR model for COVID-19 dynamics categorizes the population into four classes: susceptible (S), infected (I), treatment (T), and recovered (R). The susceptible class is further divided into two subgroups: $S_1(t)$, representing individuals not affected by COVID-19, and $S_2(t)$, representing individuals not infected but with pre-existing conditions or advanced age. The infected class $I(t)$ includes those currently infected with COVID-19. The treatment class T(t) represents individuals undergoing medical care, and the recovered class $R(t)$ includes those who have recovered from the disease. The mathematical model describing the dynamics of these classes is presented as follows [10]:

$$S_1{}'(t) = B - \beta I(t)S_1(t) - \delta B\, T(t) - \propto S_1(t),$$

$$S_2{}'(t) = B - \beta I(t)S_2(t) - \delta B\, T(t) - \alpha\, S_2(t),$$

$$I'(t) = -\mu I(t) + \beta I(t)\big(S_1(t) + S_2(t)\big) - \propto I(t) + \beta\delta T(t) + \sigma I(t),$$

$$T'(t) = \mu I(t) - \rho T(t) - \propto T(t) + \psi T(t) + \varepsilon T(t),$$

$$R'(t) = -\propto R(t) + \rho T(t). \tag{2.1}$$

Table 1. State variables for the dynamics of the SITR model.

Variable	Description
$S_1(t)$ $S_2(t)$	Non-infected individuals Non-infected older or major diseased people
$I(t)$	Rate of infected from COVID-19
$R(t)$	Recovery rate from COVID-19
$T(t)$	Treatment

Table 2. Descriptions of the state variables based on the nonlinear SITR model.

Parameter	Description	Assigned Value
β	Contact rate	0.1
B	Rate of natural birth	0.3
δ	Reduce infection from treatment	0.3
σ	Fever, tiredness and dry cough rate	0.005
μ	Recovery rate	0.1
∝	Death rate	0.25
ρ	Rate of infection from treatment	0.3
ψ	Healthy food rate	0.2
ε	Sleep rate	0.1
$Aj, j = 1, \ldots, 5$	Initial conditions	$(0.65, 0.15, 0.75, 0.35, 0.1)$

By applying the fractional derivative operator ${}_0^cD_t^\alpha$ of order $\alpha,\ 0<\alpha\leq 1$ in the system (2.1), we have

$$
\begin{aligned}
&{}_0^cD_t^\alpha S_1(t) = B - \beta I(t)S_1(t) - \delta B\, T(t) - \propto S_1(t),\\
&{}_0^cD_t^\alpha S_2(t) = B - \beta I(t)S_2(t) - \delta B\, T(t) - \alpha\, S_2(t),\\
&{}_0^cD_t^\alpha I(t) = -\mu I(t) + \beta I(t)\big(S_1(t) + S_2(t)\big) - \propto I(t) + \beta\delta T(t) + \sigma I(t),\\
&{}_0^cD_t^\alpha T(t) = \mu I(t) - \rho T(t) - \propto T(t) + \psi T(t) + \varepsilon T(t),\\
&{}_0^cD_t^\alpha R(t) = -\propto R(t) + \rho T(t).
\end{aligned}
\tag{2.2}
$$

İntial condition

$$S_1(0) = A_1, S_2(0) = A_2, I(0) = A_3, T(0) = A_4, R(0) = A_5. \tag{2.3}$$

3.Basic Definitions

In this section, we will introduce some basic definitions and properties of the theory of fractional calculus that will be later.

Definition 3.1 A real function $f(x),\ x>0$ is said to be in the space $C_\mu,\ \mu \epsilon R$ if there exists a real number $P>\mu$ such that $f(x) = x^p f_1(x)$ where $f_1(x)\epsilon C[0,\infty)$. Clearly $C_\mu < C_\beta$ if $\mu < \beta$.

Definition 3.2 A function $f(x),\ x>0$ is said to be in the spaceC_μ^m, $m\epsilon N \cup \{0\}$ if $f^{(m)} \in C_\mu$.

Definition 3.3 [25] The Riemann-Liouville fractional integral operator of the order $\alpha>0$ of a function, $f \in C_\mu, \mu \geq -1$ is defined as

$$(J_a^\alpha f)(x) = \frac{1}{\Gamma(\alpha)}\int_a^x (x-\tau)^{\alpha-1} f(\tau)d\tau, x > a, \tag{3.1}$$

$$(J_a^0 f)(x) = f(x). \tag{3.2}$$

All the properties of the operator J^α can be found in [19] which we mention only the following, for $f \in C_\mu,\ \mu \geq -1, \alpha, \beta \geq 0,$ rand $\gamma > -1$ we have

$$(J_a^\alpha J_a^\beta f)(x) = (J_a^{\alpha+\beta} f)(x), \tag{3.3}$$

$$(J_a^\alpha J_a^\beta f)(x) = (J_a^\beta J_a^\alpha f)(x) \tag{3.4}$$

$$J_a^\alpha x^\gamma = \frac{\Gamma(\gamma+1)}{\Gamma(\alpha+\gamma+1)} x^{\alpha+\gamma}. \tag{3.5}$$

The basic definition of the Riemann–Louville fractional derivative possesses some advantages over other definitions when used to simulate real-world phenomena in the form of a fractional-type differential equation.

Definition 3.4 [26] The fractional derivative of the function $f(x)$ in Caputo's sense is defined as

$\left(D_{a}^{\alpha}f\right)(x) = \left(J^{m-\alpha}_{a} D^{m}f\right)(x) = \frac{1}{\Gamma(m-\alpha)}\int_{a}^{x}(x-t)^{m-\alpha-1}f^{(m)}(t)dt$, for $m-1<\alpha<m, m \in N, x>0.$ (3.6)

Lemma 3.1 If $-1<\alpha<m$, $m \in$ N and $\mu \geq -1$, then

$$(J_{a}^{\alpha}D_{a}^{\alpha}f)(x) = f(x) - \sum_{k=0}^{m-1} f^{k}(a)\left(\frac{(x-a)^{k}}{k!}\right), a \geq 0 \tag{3.7}$$

$$(D_{a}^{\alpha}J_{a}^{\alpha}f)(x) = f(x) \tag{3.8}$$

4.Laplace Adomian Decomposition Method

This section will illustrate the basic steps for the Laplace Adomian decomposition method (LADM). We first need the following definitions.

Definition 4.1 [27] A function f on $0 \leq t < \infty$ is exponentially bounded of order $\sigma \in R$ if satisfies $\parallel f(t) \parallel \leq Me^{\sigma t}$, for some real constant $M>0$.

Definition 3.2 The Caputo fractional derivative is defined as follows:

$$L\{D^{\sigma}f(t)\} = s^{\sigma}L\{f(t)\} - \sum_{k=0}^{m} s^{\sigma-k-1}f^{(k)}(0), \tag{4.a}$$

where $m=\sigma+1$, and $[\alpha]$ represents the integer part of σ. As a result, the following useful formula is obtained:

$$L(t^{\sigma}) = \frac{\Gamma(\sigma+1)}{s^{(\sigma+1)}}, \quad \sigma \in R^{+}. \tag{4.b}$$

The last-mentioned definitions can be used in this section to discuss the general procedures for solving the proposed mathematical model (2.2). First of all, the Laplace transform is applied to both lift-hand and right-hand sides of Eq. (2.2) in the following form:

$$L({}_{0}^{c}D_{t}^{\alpha}S_{1}(t)) = L\left(B - \beta I(t)S_{1}(t) - \delta B\, T(t) - \propto S_{1}(t)\right),$$

$${}_{0}^{C}D_{t}^{\alpha}S_2(t) = L\big(B - \beta I(t)S_2(t) - \delta B\, T(t) - \alpha\, S_2(t)\big),$$
$${}_{0}^{C}D_{t}^{\alpha}I(t) = L(-\mu I(t) + \beta I(t)\big(S_1(t) + S_2(t)\big) - \propto I(t) + \beta\delta T(t) + \sigma I(t)),$$

$${}_{0}^{C}D_{t}^{\alpha}T(t) = L(\mu I - \rho T - \propto T + \psi T + \varepsilon T),$$

$${}_{0}^{C}D_{t}^{\alpha}R(t) = L(-\propto R(t) + \rho T(t)). \tag{4.1}$$

By applying the formula (4.a) to Eq. (4.1), we get

$$s^{\alpha}L(S_1) - s^{\alpha-1}S_1(0) = \frac{B}{s} - \beta L(IS_1) - \delta B\, L(T) - \propto L(S_1),$$

$$s^{\alpha}L(S_2) - s^{\alpha-1}S_2(0) = \frac{B}{s} - \beta L(IS_2) - \delta B L(T) - \alpha L(S_2),$$

$$s^{\alpha}L(\mathrm{I}) - s^{\alpha-1}I(0) = -\mu L(I) + \beta L(IS_1) + \beta L(IS_2) - \propto L(I) + \beta\delta L(T) + \sigma L(I),$$

$$s^{\alpha}L(T) - s^{\alpha-1}T(0) = \mu \mathrm{L}(I) - \rho \mathrm{L}(T) - \propto \mathrm{L}(T) + \psi \mathrm{L}(T) + \varepsilon \mathrm{L}(T),$$

$$s^{\alpha}L(R) - s^{\alpha-1}R(0) = -\propto L(R) + \rho L(T). \tag{4.2}$$

Next, by substituting the initial conditions in Eq.(2.3) into the model (4.2), we get

$$L(S_1) = \frac{A_1}{s} + \frac{B}{s^{\alpha+1}} - \frac{\beta}{s^{\alpha}}L(IS_1) - \frac{\delta B}{s^{\alpha}}\, L(T) - \frac{\propto}{s^{\alpha}}L(S_1),$$

$$L(S_2) = \frac{A_2}{s} + \frac{B}{s^{\alpha+1}} - \frac{\beta}{s^{\alpha}}L(IS_2) - \frac{\delta B}{s^{\alpha}}L(T) - \frac{\alpha}{s^{\alpha}}L(S_2),$$

$$L(\mathrm{I}) = \frac{A_3}{s} + \frac{-\mu}{s^{\alpha}}L(I) + \frac{\beta}{s^{\alpha}}L(IS_1) + \frac{\beta}{s^{\alpha}}L(IS_2) - \frac{\propto}{s^{\alpha}}L(I) + \frac{\beta}{s^{\alpha}}\delta L(T) + \frac{\sigma}{s^{\alpha}}L(I),$$

$$L(T) = \frac{A_4}{s} + \frac{\mu}{s^{\alpha}}\mathrm{L}(I) - \frac{\rho}{s^{\alpha}}\mathrm{L}(T) - \frac{\propto}{s^{\alpha}}\mathrm{L}(T) + \frac{\psi}{s^{\alpha}}\mathrm{L}(T) + \frac{\varepsilon}{s^{\alpha}}\mathrm{L}(T),$$

$$L(R) = \frac{A_5}{s} - \frac{\propto}{s^{\alpha}}L(R) + \frac{\rho}{s^{\alpha}}L(T). \tag{4.3}$$

The proposed method gives the solution as an infinite series. Let the values of $C = Is_1$ and $D = Is_2$ to be able to apply the Adomian decomposition method. We consider the solution as an infinite series in the form

$$S_1(t) = \sum_{n=0}^{\infty} S_{1,n}(t), \qquad S_2(t) = \sum_{n=0}^{\infty} S_{2,n}(t), \qquad I(t) = \sum_{n=0}^{\infty} I_n(t), \qquad T(t) = \sum_{n=0}^{\infty} T_n(t),$$

$$R(t) = \sum_{n=0}^{\infty} R_n(t).$$

$$\tag{4.4}$$

Then, by decomposing the nonlinear part named C in the following form

$$C = \sum_{n=0}^{\infty} C_n, \quad D = \sum_{n=0}^{\infty} D_n.$$

(4.5)

Here, C_n and D_n can be computed using the convolution operation as

$$C_n = \frac{1}{\Gamma(n+1)} \frac{d^n}{d\varepsilon^n} \left[\sum_{i=0}^{n} \varepsilon^i I_i \sum_{i=0}^{n} \varepsilon^i S_{1,i} \right]_{\varepsilon=0},$$
$$D_n = \frac{1}{\Gamma(n+1)} \frac{d^n}{d\varepsilon^n} \left[\sum_{i=0}^{n} \varepsilon^i I_i \sum_{i=0}^{n} \varepsilon^i S_{2,i} \right]_{\varepsilon=0},$$

(4.6)

By substituting Eq. (4.4- 4.6) into Eq. (4.3) we have resulted in the form.

$$L\left(\sum_{n=0}^{\infty} S_{1,n}(t)\right) = \frac{A_1}{s} + \frac{B}{s^{\alpha+1}} - \frac{\beta}{s^{\alpha}} L\left(\sum_{n=0}^{\infty} C_n\right) - \frac{\delta B}{s^{\alpha}} L\left(\sum_{n=0}^{\infty} T_n(t)\right) - \frac{\propto}{s^{\alpha}} L\left(\sum_{n=0}^{\infty} S_{1,n}(t)\right),$$

$$L\left(\sum_{n=0}^{\infty} S_{2,n}(t)\right) = \frac{A_2}{s} + \frac{B}{s^{\alpha+1}} - \frac{\beta}{s^{\alpha}} L\left(\sum_{n=0}^{\infty} D_n\right) - \frac{\delta B}{s^{\alpha}} L\left(\sum_{n=0}^{\infty} T_n(t)\right) - \frac{\alpha}{s^{\alpha}} L\left(\sum_{n=0}^{\infty} S_{2,n}(t)\right),$$

$$L\left(\sum_{n=0}^{\infty} I_n(t)\right) = \frac{A_3}{s} + \frac{-\mu}{s^{\alpha}} L\left(\sum_{n=0}^{\infty} I_n(t)\right) + \frac{\beta}{s^{\alpha}} L\left(\sum_{n=0}^{\infty} C_n\right) + \frac{\beta}{s^{\alpha}} L\left(\sum_{n=0}^{\infty} D_n\right) - \frac{\propto}{s^{\alpha}} L\left(\sum_{n=0}^{\infty} I_n(t)\right)$$
$$+ \frac{\beta}{s^{\alpha}} \delta L\left(\sum_{n=0}^{\infty} T_n(t)\right) + \frac{\sigma}{s^{\alpha}} L\left(\sum_{n=0}^{\infty} I_n(t)\right),$$

$$L\left(\sum_{n=0}^{\infty} T_n(t)\right) = \frac{A_4}{s} + \frac{\mu}{s^{\alpha}} \mathrm{L}\left(\sum_{n=0}^{\infty} I_n(t)\right) - \frac{\rho}{s^{\alpha}} \mathrm{L}\left(\sum_{n=0}^{\infty} T_n(t)\right) - \frac{\propto}{s^{\alpha}} \mathrm{L}\left(\sum_{n=0}^{\infty} T_n(t)\right)$$
$$+ \frac{\psi}{s^{\alpha}} \mathrm{L}\left(\sum_{n=0}^{\infty} T_n(t)\right) + \frac{\varepsilon}{s^{\alpha}} \mathrm{L}\left(\sum_{n=0}^{\infty} T_n(t)\right),$$

$$L\left(\sum_{n=0}^{\infty} R_n(t)\right) = \frac{A_5}{s} - \frac{\propto}{s^{\alpha}} L\left(\sum_{n=0}^{\infty} R_n(t)\right) + \frac{\rho}{s^{\alpha}} L\left(\sum_{n=0}^{\infty} T_n(t)\right).$$

(4.7)

Then, matching the two sides of Eq. (4.7) yields the following iterative algorithm

$$S_{1,0} = \frac{A_1}{s}, \qquad S_{2,0} = \frac{A_2}{s}, \qquad I_0 = \frac{A_3}{s}, \qquad T_0 = \frac{A_4}{s}, \qquad R_0 = \frac{A_5}{s},$$

$$L(S_{1,1}) = \frac{B}{s^{\alpha+1}} - \frac{\beta}{s^{\alpha}} L(C_0) - \frac{\delta B}{s^{\alpha}}\ L(T_0) - \frac{\propto}{s^{\alpha}} L(S_{1,0}),$$

$$L(S_{2,1}) = \frac{B}{s^{\alpha+1}} - \frac{\beta}{s^{\alpha}} L(D_0) - \frac{\delta B}{s^{\alpha}} L(T_0) - \frac{\alpha}{s^{\alpha}} L(S_{2,0}),$$

$$L(\mathrm{I}_1) = \frac{-\mu}{s^{\alpha}} L(I_0) + \frac{\beta}{s^{\alpha}} L(C_0) + \frac{\beta}{s^{\alpha}} L(D_0) - \frac{\propto}{s^{\alpha}} L(I_0) + \frac{\beta}{s^{\alpha}} \delta L(T_0) + \frac{\sigma}{s^{\alpha}} L(I_0),$$

$$L(T_1) = \frac{\mu}{s^{\alpha}} \mathrm{L}(I_0) - \frac{\rho}{s^{\alpha}} \mathrm{L}(T_0) - \frac{\propto}{s^{\alpha}} \mathrm{L}(T_0) + \frac{\psi}{s^{\alpha}} \mathrm{L}(T_0) + \frac{\varepsilon}{s^{\alpha}} \mathrm{L}(T_0),$$

$$L(R_1) = -\frac{\propto}{s^{\alpha}} L(R_0) + \frac{\rho}{s^{\alpha}} L(T_0), \ldots,$$

$$L(S_{1,n}) = -\frac{\beta}{s^{\alpha}} L(C_{n-1}) - \frac{\delta B}{s^{\alpha}}\ L(T_{n-1}) - \frac{\propto}{s^{\alpha}} L(S_{1,n-1}),$$

$$L(S_{2,n}) = -\frac{\beta}{s^{\alpha}} L(D_{n-1}) - \frac{\delta B}{s^{\alpha}} L(T_{n-1}) - \frac{\alpha}{s^{\alpha}} L(S_{2,n-1}),$$

$$L(\mathrm{I}_n) = \frac{-\mu}{s^{\alpha}} L(I_{n-1}) + \frac{\beta}{s^{\alpha}} L(C_{n-1}) + \frac{\beta}{s^{\alpha}} L(D_{n-1}) - \frac{\propto}{s^{\alpha}} L(I_{n-1}) + \frac{\beta}{s^{\alpha}} \delta L(T_{n-1}) + \frac{\sigma}{s^{\alpha}} L(I_{n-1}),$$

$$L(T_n) = \frac{\mu}{s^{\alpha}} \mathrm{L}(I_{n-1}) - \frac{\rho}{s^{\alpha}} \mathrm{L}(T_{n-1}) - \frac{\propto}{s^{\alpha}} \mathrm{L}(T_{n-1}) + \frac{\psi}{s^{\alpha}} \mathrm{L}(T_{n-1}) + \frac{\varepsilon}{s^{\alpha}} \mathrm{L}(T_{n-1}),$$

$$L(R_n) = -\frac{\propto}{s^{\alpha}} L(R_{n-1}) + \frac{\rho}{s^{\alpha}} L(T_{n-1}). \tag{4.8}$$

Finally, by taking the inverse transform of Eq. (4.8), we have the following equation

$$S_{1,0} = A_1, \qquad S_{2,0} = A_2, \qquad I_0 = A_3, \qquad T_0 = A_4, \qquad R_0 = A_5,$$

$$S_{1,1} = \left[B - \beta C_0 - \delta B\ T_0 - \propto S_{1,0}\right] \frac{t^{\alpha}}{\Gamma(\alpha+1)},$$

$$S_{2,1} = \left[B - \beta D_0 - \delta B T_0 - \alpha S_{2,0}\right] \frac{t^{\alpha}}{\Gamma(\alpha+1)},$$

$$\mathrm{I}_1 = [-\mu I_0 + \beta C_0 + \beta D_0 - \propto I_0 + \beta\delta T_0 + \sigma I_0] \frac{t^{\alpha}}{\Gamma(\alpha+1)},$$

$$T_1 = [\ \mu I_0 - \rho T_0 - \propto T_0 + \psi T_0 + \varepsilon T_0] \frac{t^{\alpha}}{\Gamma(\alpha+1)},$$

$$R_1 = [-\propto R_0 + \rho T_0] \frac{t^{\alpha}}{\Gamma(\alpha+1)}, \ldots,$$

$$S_{1,n} = \left[-\beta C_{n-1} - \delta B T_{n-1} - \propto S_{1,n-1}\right] \frac{t^{\alpha}}{\Gamma(\alpha+1)},$$

$$S_{2,n} = \left[-\frac{\beta}{s^\alpha} D_{n-1} - \frac{\delta B}{s^\alpha} T_{n-1} - \frac{\alpha}{s^\alpha} S_{2,n-1}\right] \frac{t^\alpha}{\Gamma(\alpha+1)},$$

$$\mathrm{I}_n = \left[\frac{-\mu}{s^\alpha} I_{n-1} + \frac{\beta}{s^\alpha} C_{n-1} + \frac{\beta}{s^\alpha} D_{n-1} - \frac{\propto}{s^\alpha} I_{n-1} + \frac{\beta}{s^\alpha} \delta T_{n-1} + \frac{\sigma}{s^\alpha} I_{n-1}\right] \frac{t^\alpha}{\Gamma(\alpha+1)},$$

$$T_n = \left[\frac{\mu}{s^\alpha} I_{n-1} - \frac{\rho}{s^\alpha} T_{n-1} - \frac{\propto}{s^\alpha} T_{n-1} + \frac{\psi}{s^\alpha} T_{n-1} + \frac{\varepsilon}{s^\alpha} T_{n-1}\right] \frac{t^\alpha}{\Gamma(\alpha+1)},$$

$$R_n = \left[-\frac{\propto}{s^\alpha} R_{n-1} + \frac{\rho}{s^\alpha} T_{n-1}\right] \frac{t^\alpha}{\Gamma(\alpha+1)}.$$

(4.9)

Similarly, at the final step, we get the rest of the terms as infinite series as,

$$S_1(t) = \sum_{n=0}^{\infty} S_{1,n}(t) = A_1 + \left[B - \beta C_0 - \delta B\, T_0 - \propto S_{1,0}\right] \frac{t^\alpha}{\Gamma(\alpha+1)} + \cdots,$$

$$S_2(t) = \sum_{n=0}^{\infty} S_{2,n}(t) = A_2 + \left[B - \beta D_0 - \delta B T_0 - \alpha S_{2,0}\right] \frac{t^\alpha}{\Gamma(\alpha+1)} + \cdots,$$

$$I(t) = \sum_{n=0}^{\infty} I_n(t) = A_3 + \left[-\mu I_0 + \beta C_0 + \beta D_0 - \propto I_0 + \beta\delta T_0 + \sigma I_0\right] \frac{t^\alpha}{\Gamma(\alpha+1)} + \cdots,$$

$$T(t) = \sum_{n=0}^{\infty} T_n(t) = A_4 + \left[\mu I_0 - \rho T_0 - \propto T_0 + \psi T_0 + \varepsilon T_0\right] \frac{t^\alpha}{\Gamma(\alpha+1)} + \cdots,$$

$$R(t) = \sum_{n=0}^{\infty} R_n(t) = A_5 + \left[-\propto R_0 + \rho T_0\right] \frac{t^\alpha}{\Gamma(\alpha+1)} + \cdots.$$

(4.10)

Equation (4.10) solves the main SITR model of Eq. (2.1) which will be illustrated in the next section.

5.Numerical Simulations

In this section, we test the effectiveness of the proposed technique by examining the acquired results for model (2.1) for different α. The numerical simulations are presented by taking partial parameters from numerical simulations in [10]. The results obtained by LADM match the exact solutions when $\alpha = 1$. Figure 2-11 provides a comparison of the results acquired by the LADM and the MATLAB code ODE45 (Rung-Kutta of order 4 technique) for the different model categories. It is evident from this figure that the proposed technique is efcient and accurate, as it perfectly agrees with the MATLAB code results.

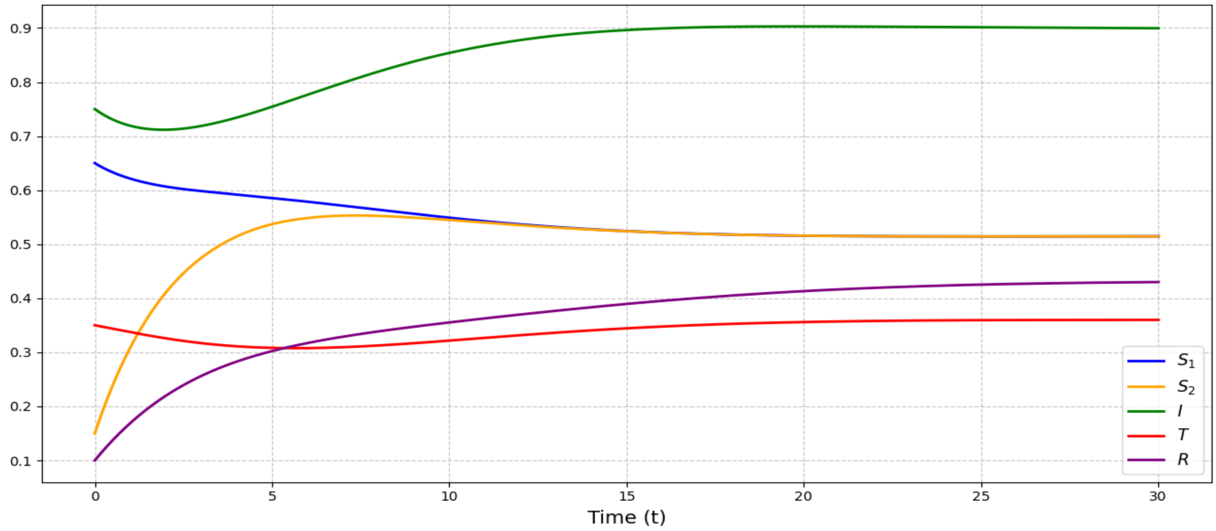

Fig. 1 The solution of $S_1(t), S_2(t), I(t), T(t)$ and $R(t)$ obtained by Rung-Kutta of order 4 technique (ODE 45) for $\alpha = 1$, and $0 < t < 30$.

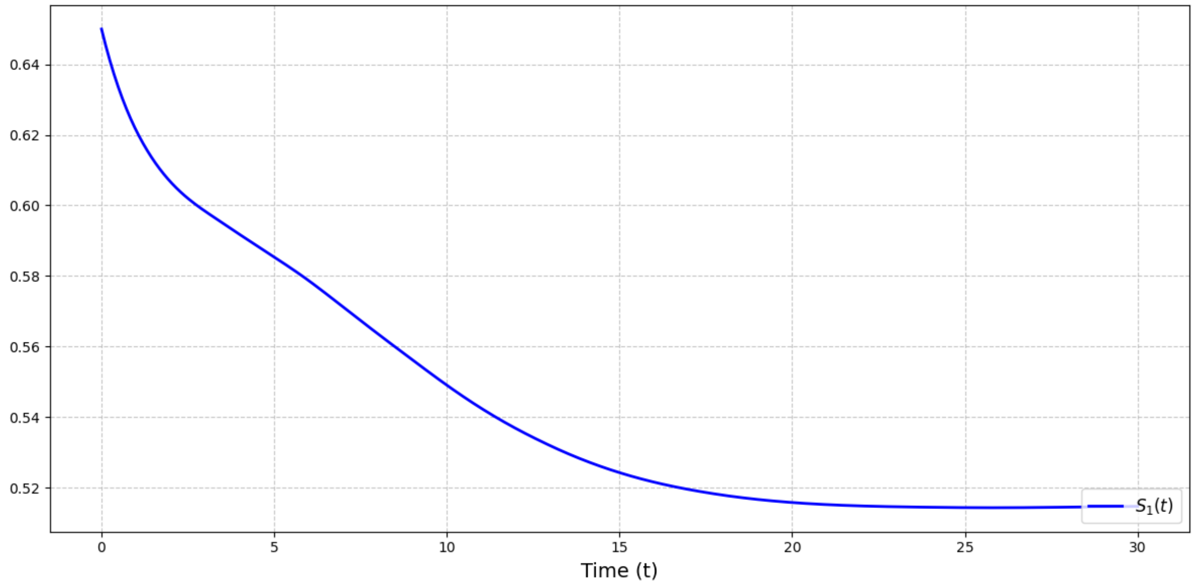

Fig. 2 The solution of $S_1(t)$ obtained by Rung-Kutta of order 4 technique (ODE 45) 45 for $\alpha = 1$, and $0 < t < 30$.

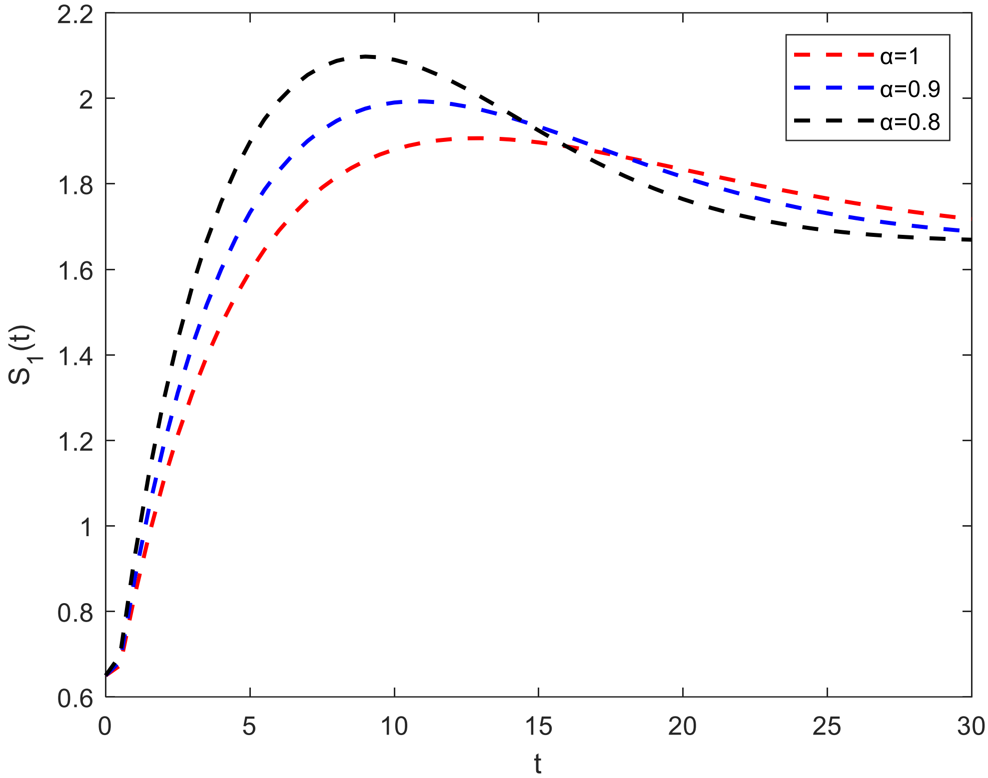

Fig. 3 The solution of $S_1(t)$ obtained by LADM for different values of α, (a) of $\alpha = 1$, (b) of $\alpha = 0.9$, (c) of $\alpha = 0.8$. and $0 \leq t \leq 30$.

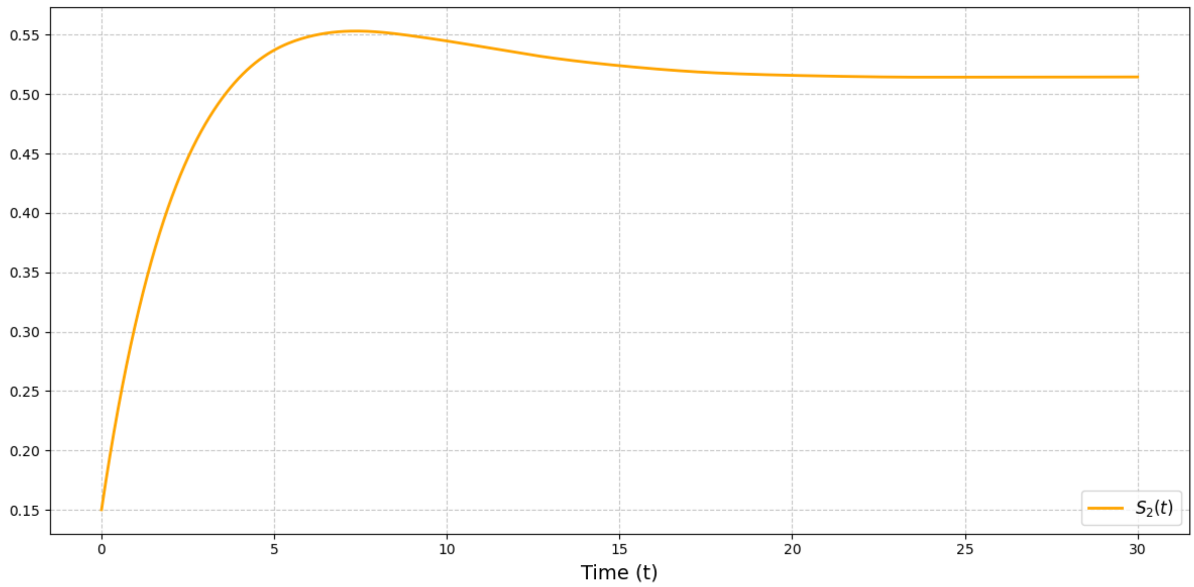

Fig. 4 The solution of $S_2(t)$ obtained by Rung-Kutta of order 4 technique (ODE 45) 45 for $\alpha = 1$, and $0 < t < 30$.

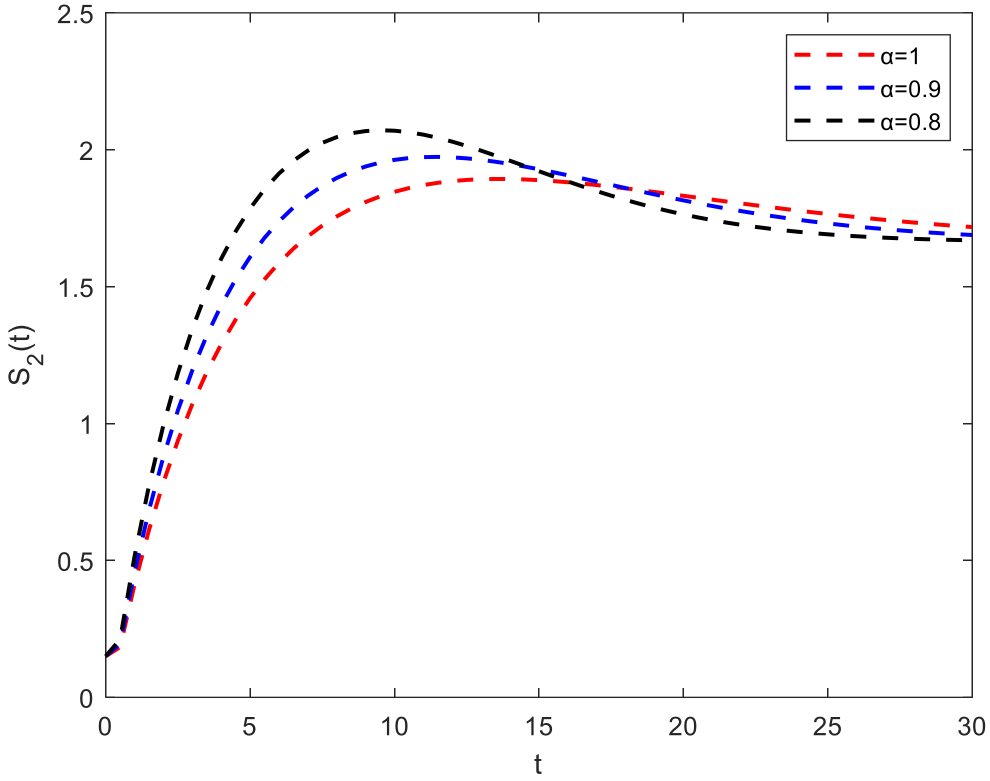

Fig. 5 The solution of $S_2(t)$ obtained by LADM for different values of α, (a) of $\alpha = 1$, (b) of $\alpha = 0.9$, (c) of $\alpha = 0.8$. and $0 \leq t \leq 30$.

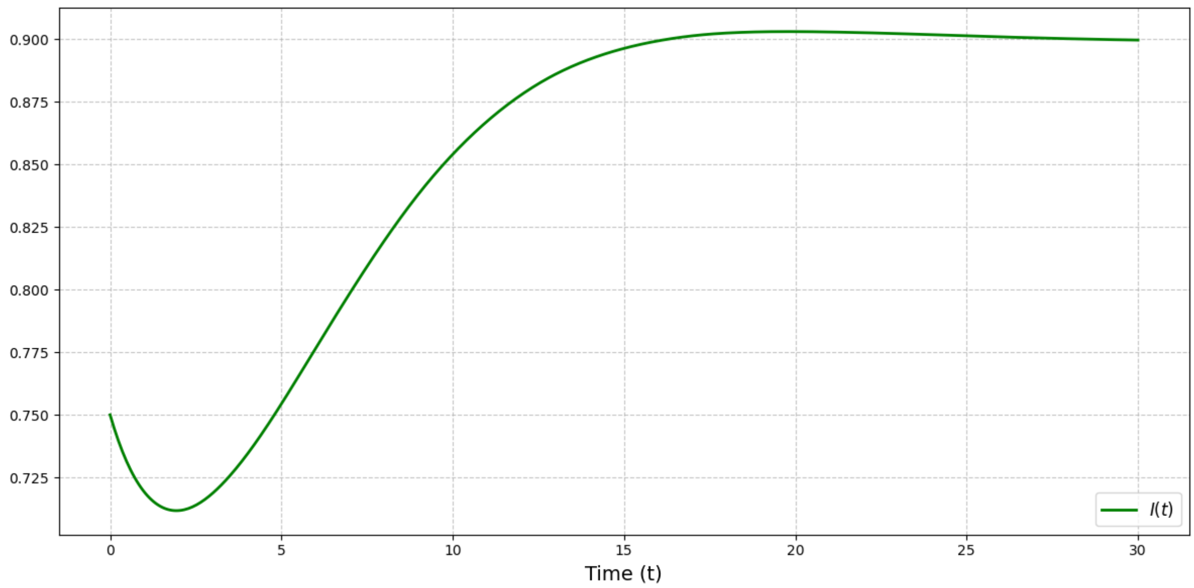

Fig. 6 The solution of $I(t)$ obtained by Rung-Kutta of order 4 technique (ODE 45) 45 for $\alpha = 1$, and $0 < t < 30$.

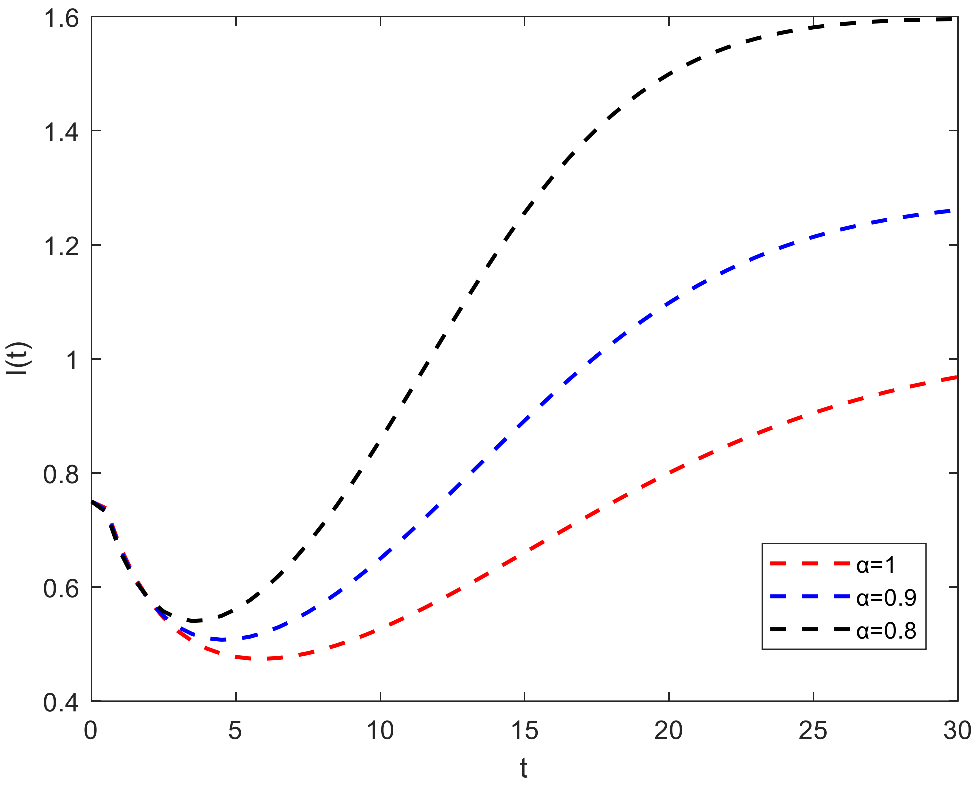

Fig. 7 The solution of $I(t)$ obtained by LADM for different values of α, (a) of $\alpha = 1$, (b) of $\alpha = 0.9$, (c) of $\alpha = 0.8$. and $0 \leq t \leq 30$.

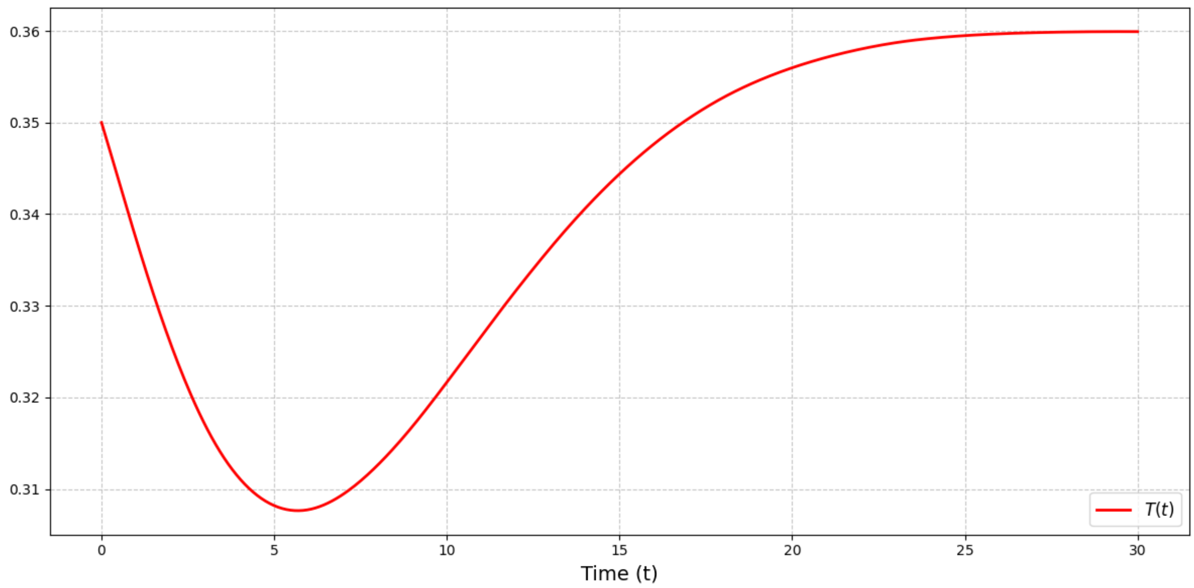

Fig. 8 The solution of $T(t)$ obtained by Rung-Kutta of order 4 technique (ODE 45) 45 for $\alpha = 1$, and $0 < t < 30$.

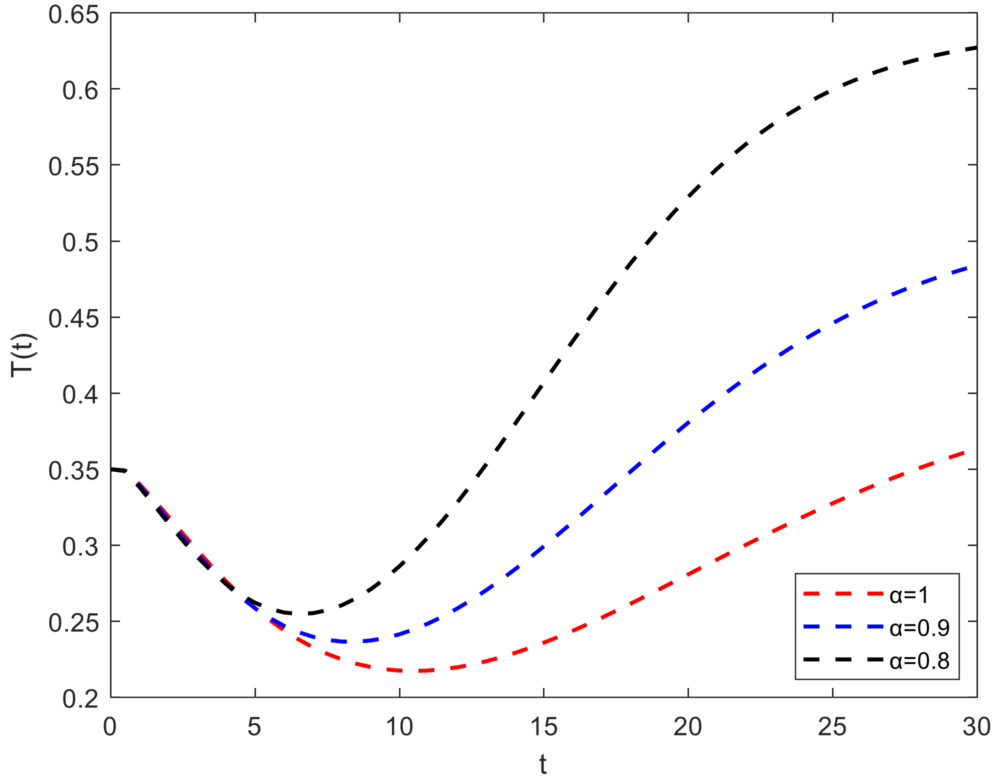

Fig. 9 The solution of $T(t)$ obtained by LADM for different values of α, (a) of $\alpha = 1$, (b) of $\alpha = 0.9$, (c) of $\alpha = 0.8$. and $0 \leq t \leq 30$.

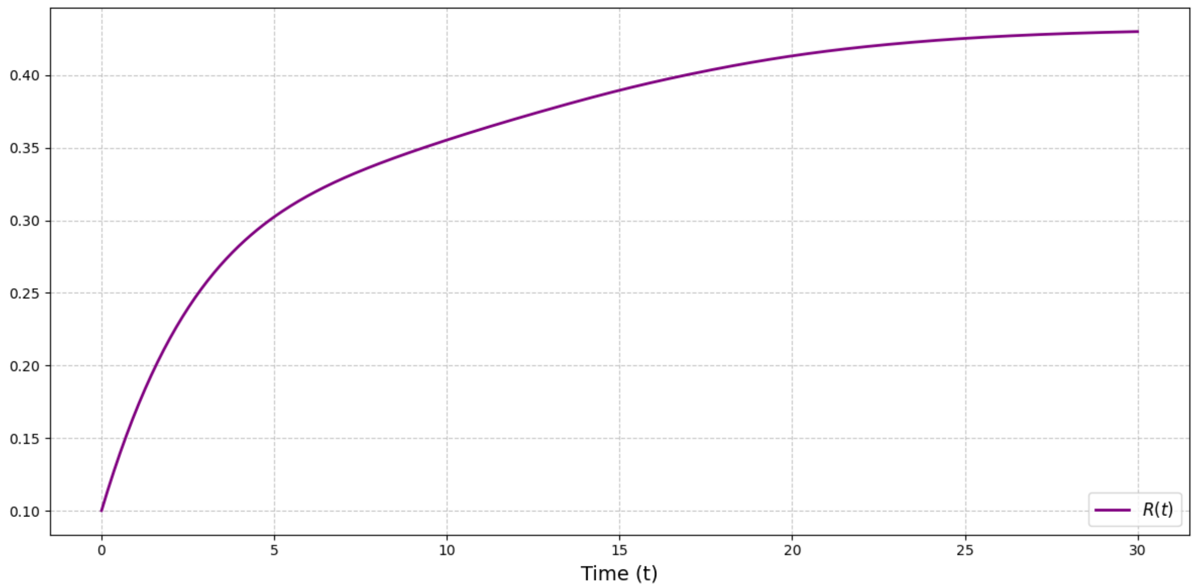

Fig. 10 The solution of $R(t)$ obtained by Rung-Kutta of order 4 technique (ODE 45) 45 for $\alpha = 1$, and $0 < t < 30$.

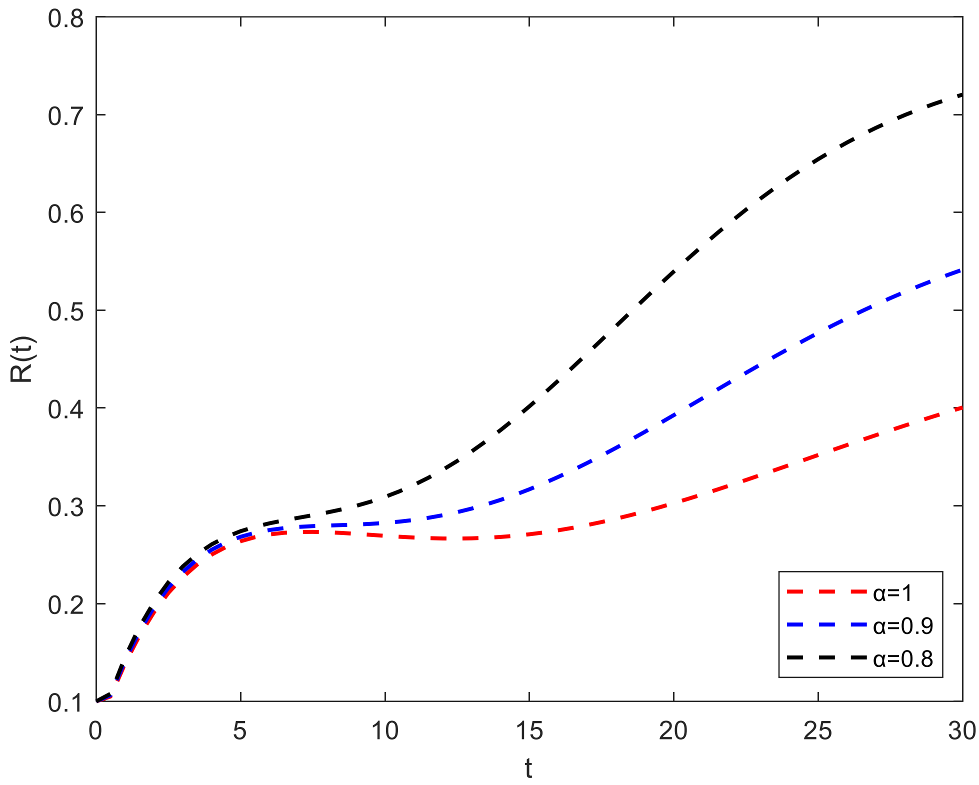

Fig. 11 The solution of $R(t)$ obtained by LADM for different values of α, (a) of $\alpha = 1$, (b) of $\alpha = 0.9$, (c) of $\alpha = 0.8$. and $0 \leq t \leq 30$.

6.Conclusions

we have presented an enhanced order of a nonlinear SITR system with COVID-19. The model has been effectively solved employing two different methods, namely, the Rung-Kutta of order 4 and the Adomian decomposition in the Laplace domain. The obtained results guarantee accurate solutions and are examined for varied fractional-order values of α and a transmission rate. All obtained findings have been compared and examined for different cases. Our findings and procedures in this research can be extended or generalized further in the resolution of other interesting nonlinear models emerging in certain phenomena in physics and engineering. Besides, our findings can be extended for models developed with other fractional derivatives.

REFERENCES

1. Kermack, W. O., McKendrick, A. G., A contribution to the mathematical theory of epidemics, Proceedings of the Royal Society of London. Series A, Vol:115, No:772, 700–721, 1927.
2. Kucharski, A. J., Russell, T. W., Diamond, C., et al., Early dynamics of transmission and control of COVID-19: a mathematical modelling study, The Lancet Infectious Diseases, Vol:20, No:5, 553–558, 2020.
3. Institute for Health Metrics and Evaluation (IHME), COVID-19 projections, 2023.
4. Ferguson, N. M., Laydon, D., Nedjati-Gilani, G., et al., Impact of non-pharmaceutical interventions (NPIs) to reduce COVID-19 mortality and healthcare demand, Imperial College COVID-19 Response Team, 2020.
5. Prem, K., Liu, Y., Russell, T. W., et al., The effect of control strategies to reduce social mixing on outcomes of the COVID-19 epidemic in Wuhan, China: a modelling study, The Lancet Public Health, Vol:5, No:5, e261–e270, 2020.
6. Giordano, G., Blanchini, F., Bruno, R., et al., Modelling the COVID-19 epidemic and implementation of population-wide interventions in Italy, Nature Medicine, Vol:26, No:6, 855–860, 2020.
7. Khairulbahri, M., The SEIR model incorporating asymptomatic cases, behavioral measures, and lockdowns: Lesson learned from the COVID-19 flow in Sweden, Biomedical Signal Processing and Control, Vol:81, 104416, 2023.
8. Ahmed, N., Elsonbaty, A., Raza, A., et al., Numerical simulation and stability analysis of a novel reaction–diffusion COVID-19 model, Nonlinear Dynamics, Vol:106, 1293–1310, 2021.
9. Adel, W., Günerhan, H., Nisar, K. S., et al., Designing a novel fractional order mathematical model for COVID-19 incorporating lockdown measures, Scientific Reports, Vol:14, 2926, 2024.
10. Umar, M., Sabir, Z., Raja, M. A. Z., et al., A stochastic intelligent computing with neuro-evolution heuristics for nonlinear SITR system of novel COVID-19 dynamics, Symmetry, Vol:12, No:10, 1628, 2020.
11. Zhuang, Z., Chen, Y., Wang, J., Fractional order SEIR model for COVID-19 with memory effect, Nonlinear Dynamics, Vol:106, 267–279, 2021.

12. Funk, S., Salathé, M., Jansen, V. A. A., Modelling the influence of human behaviour on the spread of infectious diseases: a review, Journal of the Royal Society Interface, Vol:7, No:50, 1247–1256, 2020.
13. Bubar, K. M., Reinholt, K., Kissler, S. M., et al., Model-informed COVID-19 vaccine prioritization strategies by age and serostatus, Science, Vol:371, No:6532, 916–921, 2021.
14. Chang, S., Pierson, E., Koh, P. W., et al., Mobility network models of COVID-19 explain inequities and inform reopening, Nature, Vol:589, No:7840, 82–87, 2021.
15. Chinazzi, M., Davis, J. T., Ajelli, M., et al., The effect of travel restrictions on the spread of the 2019 novel coronavirus (COVID-19) outbreak, Science, Vol:368, No:6489, 395–400, 2020.
16. Ongun, M. Y., The Laplace Adomian decomposition method for solving a model for HIV infection of CD4+ T cells, Mathematical and Computer Modelling, Vol:53, No:5–6, 597–603, 2011.
17. Haq, F., Shah, K., Rahman, G. U., et al., Numerical solution of fractional order smoking model via Laplace Adomian decomposition method, Alexandria Engineering Journal, Vol:57, No:2, 1061–1069, 2018.
18. Baleanu, D., Aydogn, S. M., Mohammadi, H., et al., On modelling of epidemic childhood diseases with the Caputo-Fabrizio derivative by using the Laplace Adomian decomposition method, Alexandria Engineering Journal, Vol:59, No:5, 3029–3039, 2020.
19. González-Gaxiola, O., Biswas, A., Optical solitons with Radhakrishnan–Kundu–Lakshmanan equation by Laplace–Adomian decomposition method, Optik, Vol:179, 434–442, 2019.
20. Edeki, S. O., Motsepa, T., Khalique, C. M., et al., The Greek parameters of a continuous arithmetic Asian option pricing model via Laplace Adomian decomposition method, Open Physics, Vol:16, No:1, 780–785, 2018.
21. Naghipour, A., Manafian, J., Application of the Laplace Adomian decomposition and implicit methods for solving Burgers' equation, TWMS Journal of Pure and Applied Mathematics, Vol:6, No:1, 68–77, 2015.
22. González-Gaxiola, O., Biswas, A., W-shaped optical solitons of Chen–Lee–Liu equation by Laplace–Adomian decomposition method, Optical and Quantum Electronics, Vol:50, No:8, 1–11, 2018.

23. Paul, S., Mondal, S. P., Bhattacharya, P., Numerical solution of Lotka Volterra prey-predator model by using Runge–Kutta–Fehlberg method and Laplace Adomian decomposition method, Alexandria Engineering Journal, Vol:55, No:1, 613–617, 2016.
24. Günerhan, H., Kaabar, M. K. A., Çelik, E., Novel analytical and approximate-analytical methods for solving the nonlinear fractional smoking mathematical model, Sigma Journal of Engineering and Natural Sciences, Vol:41, 331–343, 2023.
25. Günerhan, H., Dutta, H., Dokuyucu, M. A., et al., Analysis of a fractional HIV model with Caputo and constant proportional Caputo operators, Chaos, Solitons & Fractals, Vol:139, 110053, 2020.
26. Günerhan, H., Rezazadeh, H., Adel, W., et al., Analytical approximate solution of fractional order smoking epidemic model, Advances in Mechanical Engineering, Vol:14, No:9, 2022.
27. Meenakshi, A., Renuga, E., Čep, R., Karthik, K., Analysis of Caputo Fractional-Order Co-Infection COVID-19 and Influenza SEIR Epidemiology by Laplace Adomian Decomposition Method, Mathematics, Vol:12, No:12, 1876, 2024.

Analytical Solution of a Mathematical Model for the Spread of the Zika Virus

Hatıra Günerhan [1]

[1] Department of Mathematics, Faculty of Education, Kafkas University, Kars, Turkey

gunerhanhatira@gmail.com,

Abstract

In this study, a nonlinear SEIR system is analyzed to model the spread of the Zika virus, using a modified form of the Caputo fractional derivative. Analytical and approximate-analytical solutions of the proposed model are derived using the Laplace Adomian Decomposition Method (LADM). The solutions are presented as rapidly converging series. Approximate analytical solutions are obtained, demonstrating rapid convergence and accurately capturing the system's dynamics. The reliability of the method is verified, and the validity of the proposed fractional-order model is substantiated.

Keywords: Caputo fractional derivative; Laplace Adomian decomposition; Zika virus; Nonlinear system.

1.INTRODUCTION

Zika virus is an RNA virus belonging to the Flaviviridae family, first identified in 1947 in the Zika Forest of Uganda. Although initially thought to cause only mild and self-limiting illnesses in humans, it became a significant global public health threat during large outbreaks in Latin America and the Caribbean between 2015 and 2016. These outbreaks revealed the virus's association with severe neurological complications, including microcephaly in newborns and Guillain-Barré syndrome in adults. This led to a rapid increase in scientific research and the implementation of control measures [1,5]. The primary transmission vector of Zika virus is the Aedes aegypti mosquito; however, alternative transmission routes such as sexual contact and blood transfusions have also been documented, complicating the dynamics of disease spread [6,7].

To better understand the transmission dynamics of Zika virus and develop effective control strategies, extensive research using mathematical modeling methods has been conducted. Compartmental models that reflect the interactions between human and vector populations are commonly used to simulate the spread of the disease. For instance, Lee et al. [8] developed dynamic compartmental models that account for changes in both human and mosquito populations, allowing for a more realistic tracking of the epidemic. Rezapour and colleagues [9] introduced a novel mathematical framework incorporating additional transmission parameters to better capture the complexity of Zika spread. Additionally, Suantai et al. [10] used the classical SEIR (Susceptible-Exposed-Infectious-Recovered) model to perform numerical simulations, providing important insights into the temporal progression of the epidemic.

Beyond these basic models, more complex frameworks have been developed that include real-world factors such as seasonality, spatial heterogeneity, and social network structures [3,4]. These advanced models play a crucial role in evaluating the effectiveness of targeted interventions such as vector control, public awareness campaigns, and vaccination efforts, thereby guiding public health responses. In this research, we are also exploring the potential of using the Laplace Adomian decomposition method (LADM) to solve the fractionalomputer virus propagation model. This method is a powerful yet straightforward approach to tackling epidemic models and has been successfully applied in biology, engineering, and applied mathematics. It combines the Laplace transform and the Adomian decomposition method, offering several advantages for solving complex problems. One of the advantages of this method is its accuracy, as by employing the Laplace transform, it transforms the differential equations into algebraic equations, which are often easier to solve. This transformation reduces the complexity of the problem and enables the use of powerful algebraic techniques to obtain accurate solutions. Additionally, the Adomian decomposition method provides a systematic and robust approach to handling nonlinear terms, allowing for accurate approximation of the solution even in the presence of nonlinearity. This method does not require any perturbation or linearization, nor does it need a defined size of the step like the Rung-Kutta of order 4 technique. Various models have already been solved using this particular technique, such as HIV infection of CD4+ T cells model [11], fractional-order smoking model [12], epidemic childhood diseases [13], Radhakrishnan–Kundu–Lakshmanan equation [14], Asian option pricing model [15], Burger's equation [16], Chen-Lee-Liu equation [17], prey-predator model [18], nonlinear fractional smoking mathematical model [19], COVID-19 model [20], HIV model [21], Smoking epidemic model [22], fractional-order co-infection SEIR model [23].

2.Model formulation

This section presents a comprehensive mathematical model that incorporates both primary transmission routes of the Zika virus: vector-to-human and human-to-human. The model is structured according to compartmental population dynamics, dividing the total human population, denoted as $N_H(y)$, into four subgroups: susceptible humans $S_H(y)$, exposed humans $E_H(y)$, infected humans $I_H(y)$, and recovered humans $R_H(y)$, such that: $N_H(y) = S_H(y) + E_H(y) + I_H(y) + R_H(y)$. Similarly, the mosquito (vector) population, represented as$N_V(y)$, is classified into three compartments: susceptible vectors $S_V(y)$, exposed vectors$E_V(y)$, and infected vectors$I_N(y)$, satisfying the relation: $N_V(y) = S_V(y) + E_V(y) + I_V(y) + R_V(y)$. The resulting nonlinear SEIR-based model captures the dynamics of Zika virus transmission between and within species, and the governing differential equations are formally presented in Equation (2.1). A detailed representation of the compartmental interactions and transmission mechanisms is outlined in Table 1, following the structure described in [10].

$$S_H{}'(t) = A_H - S_H(t)\beta_H\big(I_V(t) + \rho I_H(t)\big) - \mu S_H(t),$$

$E_H{}'(t) = \beta_H\big(\rho I_H(t) + I_V(t)\big)S_H(t) - (\chi_H + \mu_H)E_H(t),$

$I_H{}'(t) = \chi_H E_H(t) - (\eta + \mu_H + \gamma)I_H(t),$

$R_H{}'(t) = -\mu_H R_H(t) + \gamma \mathrm{I}_H(t),$

$S_V{}'(t) = A_V - \beta_V I_H(t)S_V(t) - \mu_H S_V(t),$

$E_V{}'(t) = \beta_V I_H(t)S_V(t) - (\mu_V + \delta_H)E_V(t),$

$$I_V{}'(t) = E_V(t)\delta_V - \mu_V I_V(t). \tag{2.1}$$

By applying the fractional derivative operator ${}_0^cD_t^\alpha$ of order $\alpha,\ 0 < \alpha \le 1$ in the system (2.1), we have

${}_0^cD_t^\alpha S_H(t) = A_H - S_H(t)\beta_H\big(I_V(t) + \rho I_H(t)\big) - \mu S_H(t),$

${}_0^cD_t^\alpha E_H(t) = \beta_H\big(\rho I_H(t) + I_V(t)\big)S_H(t) - (\chi_H + \mu_H)E_H(t),$

${}_0^cD_t^\alpha I_H(t) = \chi_H E_H(t) - (\eta + \mu_H + \gamma)I_H(t),$

${}_0^cD_t^\alpha R_H(t) = -\mu_H R_H(t) + \gamma \mathrm{I}_H(t),$

${}_0^cD_t^\alpha S_V(t) = A_V - \beta_V I_H(t)S_V(t) - \mu_H S_V(t),$

${}_0^cD_t^\alpha E_V(t) = \beta_V I_H(t)S_V(t) - (\mu_V + \delta_H)E_V(t),$

$${}_0^cD_t^\alpha I_V(t) = E_V(t)\delta_V - \mu_V I_V(t). \tag{2.2}$$

İntial condition

$$(S_H)_0 = k_{1,}\,,\ (E_H)_0 = k_{2,}\ (I_H)_0 = k_{3,}\ (R_H)_o = k_4,\ (S_V)_0 = k_5,\ (E_V)_0 = k_{6,}\ (I_V)_0 = k_7. \tag{2.3}$$

Tablo1: Parameter descriptions of the SEIR nonlinear system based on the Zika virus

Parameters	Details
$S_H(t)$	Susceptible humans
$S_V(t)$	Susceptible vector
$E_H(t)$	Exposed humans
$E_V(t)$	Exposed vector
$I_H(t)$	Infected humans
$I_V(t)$	Infected vector
$R_H(t)$	Recovered humans

A_H	Susceptible: Humans recruiting
ρ	Susceptible: Humans to infection
B_H	Susceptible humans to infected mosquitoes
μ_H	Humans: Mortality rate
χ_H	Infected human ratio to susceptible mosquitoes
η	Treatment
γ	Natural rate
B_V	Transmission ratio of the Infected humans to susceptible vector
δ_H	Morality rate persuaded in people
μ_V	Natural rate of morality using the vector compartment
δ_V	Susceptible mosquitos' recruitment
$k_{i,} i = 1,\ 2,\ \ldots\ ,\ 7$	Initial conditions
t	Time

3.Basic Definitions

In this section, we will introduce some basic definitions and properties of the theory of fractional calculus that will be later.

Definition 3.1 A real function $f(x),\ x > 0$ is said to be in the space $C_\mu,\ \mu \epsilon R$ if there exists a real number $P > \mu$ such that $f(x) = x^p f_1(x)$ where $f_1(x) \epsilon C[0, \infty)$. Clearly $C_\mu < C_\beta$ if $\mu < \beta$.

Definition 3.2 A function $f(x),\ x > 0$ is said to be in the spaceC_μ^m, $m \epsilon N \cup \{0\}$ if $f^{(m)} \in C_\mu$.

Definition 3.3 [26] The Riemann-Liouville fractional integral operator of the order $\alpha > 0$ of a function, $f \in C_\mu, \mu \geq -1$ is defined as

$$(J_a^\alpha f)(x) = \frac{1}{\Gamma(\alpha)} \int_a^x (x-\tau)^{\alpha-1} f(\tau) d\tau, x \ \ > a, \tag{3.1}$$

$$(J_a^0 f)(x) = f(x). \tag{3.2}$$

All the properties of the operator J^α can be found in [19] which we mention only the following, for $f \in C_\mu,\ \mu \geq -1, \alpha, \beta \geq 0,$ rand $\gamma > -1$ we have

$$(J_a^\alpha J_a^\beta f)(x) = (J_a^{\alpha+\beta} f)(x), \tag{3.3}$$

$$(J_a^{\alpha} J_a^{\beta} f)(x) = (J_a^{\beta} J_a^{\alpha} f)(x) \tag{3.4}$$

$$J_a^{\alpha} x^{\gamma} = \frac{\Gamma(\gamma+1)}{\Gamma(\alpha+\gamma+1)} x^{\alpha+\gamma}. \tag{3.5}$$

The basic definition of the Riemann–Louville fractional derivative possesses some advantages over other definitions when used to simulate real-world phenomena in the form of a fractional-type differential equation.

Definition 3.4 [25] The fractional derivative of the function $f(x)$ in Caputo's sense is defined as

$$\left(D_a^{\alpha} f\right)(x) = \left(J_a^{m-\alpha} D^m f\right)(x) = \frac{1}{\Gamma(m-a)} \int_a^x (x-t)^{m-\alpha-1} f^{(m)}(t)dt, \quad \text{for } m-1 < \alpha < m, m \in N, x > 0. \tag{3.6}$$

Lemma 3.1 If$-1 < \alpha < m$, $m \in$ N and $\mu \geq -1$, then

$$(J_a^{\alpha} D_a^{\alpha} f)(x) = f(x) - \sum_{k=0}^{m-1} f^k(a) \left(\frac{(x-a)^k}{k!}\right), a \geq 0 \tag{3.7}$$

$$(D_a^{\alpha} J_a^{\alpha} f)(x) = f(x) \tag{3.8}$$

4.Laplace Adomian Decomposition Method

In this section, we will illustrate the basic steps for LADM. We discuss the following important definitions or our research study:

Definition 4.1 [24] A function f on $0 \leq t < \infty$ is exponentially bounded of order $\sigma \in R$ if satisfies $\| f(t) \| \leq Me^{\sigma t}$, for some real constant $M > 0$.

Definition 3.2 The Caputo fractional derivative is defined as follows:

$$L\{D^{\sigma} f(t)\} = s^{\sigma} L\{f(t)\} - \sum_{k=0}^{m} s^{\sigma-k-1} f^{(k)}(0), \tag{4.a}$$

where $m = \sigma + 1$, and $[\alpha]$ represents the integer part of σ. As a result, the following useful formula is obtained:

$$L(t^{\sigma}) = \frac{\Gamma(\sigma+1)}{s^{(\sigma+1)}}, \quad \sigma \in R^+. \tag{4.b}$$

The last-mentioned definitions can be used in this section to discuss the general procedures for solving the proposed mathematical model (2.2). First of all, the Laplace transform is applied to both lift-hand and right-hand sides of Eq. (2.2) in the following form:

$$L({}_0^cD_t^\alpha S_H(t)) = L\left(A_H - S_H(t)\beta_H\big(I_V(t) + \rho I_H(t)\big) - \mu_H S_H(t)\right),$$

$$L({}_0^cD_t^\alpha E_H(t)) = L(\beta_H\big(\rho I_H(t) + I_V(t)\big)S_H(t) - (\chi_H + \mu_H)E_H(t)),$$

$$L({}_0^cD_t^\alpha I_H(t)) = L(\chi_H E_H(t) - (\eta + \mu_H + \gamma)I_H(t)),$$

$$L({}_0^cD_t^\alpha R_H(t)) = L(-\mu_H R_H(t) + \gamma \mathrm{I}_H(t)),$$

$$L({}_0^cD_t^\alpha S_V(t)) = L(A_V - \beta_V I_H(t)S_V(t) - \mu_H S_V(t)),$$

$$L({}_0^cD_t^\alpha E_V(t)) = L(\beta_V I_H(t)S_V(t) - (\mu_V + \delta_H)E_V(t)),$$

$$L({}_0^cD_t^\alpha I_V(t)) = L(E_V(t)\delta_V - \mu_V I_V(t)), \tag{4.1}$$

Then, by applying the formula (4.a) to Eq. (4.1), we get

$$s^\alpha L(S_H) - s^{\alpha-1}S_H(0) = \frac{A_H}{s} - \beta_H L(I_V S_H) - \beta_H \rho L(I_H S_H) - \mu_H L(S_H),$$

$$s^\alpha L(E_H) - s^{\alpha-1}E_H(0) = \beta_H P L(I_H S_H) + \beta_H L(I_V S_H) - \chi_H L(E_H) - \mu_H L(E_H),$$

$$s^\alpha L(I_H) - s^{\alpha-1}I_H(0) = \chi_H L(E_H) - \eta L(I_H) - \mu_H L(I_H) - \gamma L(I_H),$$

$$s^\alpha L(R_H) - s^{\alpha-1}R_H(0) = -\mu_H L(R_H) + \gamma L(I_H),$$

$$s^\alpha L(S_V) - s^{\alpha-1}S_V(0) = \frac{A_V}{s} - \beta_V L(I_H S_V) - \mu_H L(S_V),$$

$$s^\alpha L(E_V) - s^{\alpha-1}E(0) = \beta_V L(I_H S_V) - \mu_V L(E_V) - \delta_H L(E_V),$$

$$s^\alpha L(I_V) - s^{\alpha-1}I_V(0) = \delta_V L(E_V) - \mu_V L(I_V),$$

(4.2)

Next, by substituting the initial conditions in Eq.(2.3) into the model (4.2), we get

$$L(S_H) = \frac{k_1}{s} + \frac{A_H}{s^{\alpha+1}} - \frac{\beta_H}{s^\alpha}L(I_V S_H) - \frac{\beta_H \rho}{s^\alpha}L(I_H S_H) - \frac{\mu_H}{s^\alpha}L(S_H),$$

$$L(E_H) = \frac{k_2}{s} + \frac{\beta_H \rho}{s^\alpha}L(I_H S_H) + \frac{\beta_H}{s^\alpha}L(I_V S_H) - \frac{\chi_H}{s^\alpha}L(E_H) - \frac{\mu_H}{s^\alpha}L(E_H),$$

$$L(I_H) = \frac{k_3}{s} + \frac{\chi_H}{s^\alpha}L(E_H) - \frac{\eta}{s^\alpha}L(I_H) - \frac{\mu_H}{s^\alpha}L(I_H) - \frac{\gamma}{s^\alpha}L(I_H),$$

$$L(R_H) = \frac{k_4}{s} + \frac{\mu_H}{s^\alpha}L(R_H) + \frac{\gamma}{s^\alpha}L(I_H),$$

$$L(S_V) = \frac{k_5}{s} + \frac{A_V}{s^{\alpha+1}} - \frac{\beta_V}{s^\alpha}L(I_H S_V) - \frac{\mu_H}{s^\alpha}L(S_V),$$

$$L(E_V) = \frac{k_6}{s} + \frac{\beta_V}{s^\alpha}L(I_H S_V) - \frac{\mu_H}{s^\alpha}L(E_V) - \frac{S_H}{s^\alpha}L(E_V),$$

$$L(I_V)=\frac{k_7}{s}+\frac{\delta_V}{s^{\alpha}}L(E_V)-\frac{\mu_V}{s^{\alpha}}L(I_V),$$

(4.3)

The proposed method gives the solution as an infinite series. Let the value of $A = I_H S_H, B = I_V S_H$ and $C = I_H S_V$ to be able to apply the Adomian decomposition method. We consider the solution as an infinite series in the form

$$S_H(t)=\sum_{n=0}^{\infty} S_{H,n}(t), \quad E_H(t)=\sum_{n=0}^{\infty} E_{H,n}(t), \quad I_H(t)=\sum_{n=0}^{\infty} I_{H,n}(t).$$

$$R_H(t)=\sum_{n=0}^{\infty} R_{H,n}(t), \quad S_V(t)=\sum_{n=0}^{\infty} S_{V,n}(t), \quad E_V(t)=\sum_{n=0}^{\infty} E_{V,n}(t), \quad I_V(t)=\sum_{n=0}^{\infty} I_{V,n}(t).$$

(4.4)

Then, by decomposing the nonlinear part named A, B, C in the following form

$$A=\sum_{n=0}^{\infty} A_n, \quad B=\sum_{n=0}^{\infty} B_n, \quad C=\sum_{n=0}^{\infty} C_n$$

(4.5)

Here, A_n, B_n, C_n can be computed using the convolution operation as

$$A_n=\frac{1}{\Gamma(n+1)}\frac{d^n}{d\varepsilon^n}\left[\sum_{i=0}^{n}\varepsilon^i I_{H,i}\sum_{i=0}^{n}\varepsilon^i S_{H,i}\right]_{\varepsilon=0},$$

$$B_n=\frac{1}{\Gamma(n+1)}\frac{d^n}{d\varepsilon^n}\left[\sum_{i=0}^{n}\varepsilon^i I_{V,i}\sum_{i=0}^{n}\varepsilon^i S_{H,i}\right]_{\varepsilon=0},$$

$$C_n=\frac{1}{\Gamma(n+1)}\frac{d^n}{d\varepsilon^n}\left[\sum_{i=0}^{n}\varepsilon^i I_{H,i}\sum_{i=0}^{n}\varepsilon^i S_{V,i}\right]_{\varepsilon=0},$$

(4.6)

By substituting Eq. (4.4- 4.6) into Eq. (4.3) and by matching the two sides of the equation yields the following iterative algorithm we have resulted in the form.

$$S_{H,0}=\frac{k_1}{s}, \quad E_{H,0}=\frac{k_2}{s}, \quad I_{H,0}=\frac{k_3}{s}, \quad R_{H,0}=\frac{k_4}{s}, \quad S_{V,0}=\frac{k_5}{s},$$

$E_{V,0} = \frac{k_6}{s}, \quad I_{V,0} = \frac{k_7}{s}.$

$$L(S_{H,1}) = \frac{A_H}{s^{\alpha+1}} - \frac{\beta_H}{s^\alpha} L(\mathrm{B}_0) - \frac{\beta_H \rho}{s^\alpha} L(A_0) - \frac{\mu_H}{s^\alpha} L(S_{H,0}),$$

$$L(E_{H,1}) = \frac{\beta_H \rho}{s^\alpha} L(A_0) + \frac{\beta_H}{s^\alpha} L(B_0) - \frac{\chi_H}{s^\alpha} L(E_{H,0}) - \frac{\mu_H}{s^\alpha} L(E_{H,0}),$$

$$L(I_{H,1}) = \frac{\chi_H}{s^\alpha} L(E_{H,0}) - \frac{\eta}{s^\alpha} L(I_{H,0}) - \frac{\mu_H}{s^\alpha} L(I_{H,0}) - \frac{\gamma}{s^\alpha} L(I_{H,0}),$$

$$L(R_{H,1}) = \frac{\mu_H}{s^\alpha} L(R_{H,0}) + \frac{\gamma}{s^\alpha} L(I_{H,0}),$$

$$L(S_{V,1}) = \frac{A_V}{s^{\alpha+1}} - \frac{\beta_V}{s^\alpha} L(C_0) - \frac{\mu_H}{s^\alpha} L(S_{V,0}),$$

$$L(E_{V,1}) = \frac{\beta_V}{s^\alpha} L(C_0) - \frac{\mu_H}{s^\alpha} L(E_{V,0}) - \frac{S_H}{s^\alpha} L(E_{V,0}),$$

$$L(I_{V,1}) = \frac{\delta_V}{s^\alpha} L(E_{V,0}) - \frac{\mu_V}{s^\alpha} L(I_{V,0}), \ldots,$$

$$L(S_{H,n}) = -\frac{\beta_H}{s^\alpha} L(\mathrm{B}_{n-1}) - \frac{\beta_H \rho}{s^\alpha} L(A_{n-1}) - \frac{\mu_H}{s^\alpha} L(S_{H,n-1}),$$

$$L(E_{H,n}) = \frac{\beta_H \rho}{s^\alpha} L(A_{n-1}) + \frac{\beta_H}{s^\alpha} L(B_{n-1}) - \frac{\chi_H}{s^\alpha} L(E_{H,n-1}) - \frac{\mu_H}{s^\alpha} L(E_{H,n-1}),$$

$$L(I_{H,n}) = \frac{\chi_H}{s^\alpha} L(E_{H,n-1}) - \frac{\eta}{s^\alpha} L(I_{H,n-1}) - \frac{\mu_H}{s^\alpha} L(I_{H,n-1}) - \frac{\gamma}{s^\alpha} L(I_{H,n-1}),$$

$$L(R_{H,n}) = \frac{\mu_H}{s^\alpha} L(R_{H,n-1}) + \frac{\gamma}{s^\alpha} L(I_{H,n-1}),$$

$$L(S_{V,n}) = -\frac{\beta_V}{s^\alpha} L(C_{n-1}) - \frac{\mu_H}{s^\alpha} L(S_{V,n-1}),$$

$$L(E_{V,n}) = \frac{\beta_V}{s^\alpha} L(C_{n-1}) - \frac{\mu_H}{s^\alpha} L(E_{V,n-1}) - \frac{S_H}{s^\alpha} L(E_{V,n-1}),$$

$$L(I_{V,n}) = \frac{\delta_V}{s^\alpha} L(E_{V,n-1}) - \frac{\mu_V}{s^\alpha} L(I_{V,n-1}),$$

(4.7)

Finally, by taking the inverse transform of Eq. (4.7), we have the following equation

$S_{H,0} = k_1, \quad E_{H,0} = k_2, \quad I_{H,0} = k_3, \quad R_{H,0} = k_4, \quad S_{V,0} = k_5,$

$E_{V,0} = k_6, \quad I_{V,0} = k_7 .$

$$S_{H,1} = [A_H - \beta_H \mathrm{B}_0 - \beta_H \rho A_0 - \mu_H S_{H,0}] \frac{t^\alpha}{\Gamma(\alpha+1)},$$

$$E_{H,1} = [\beta_H \rho A_0 + \beta_H \mathrm{B}_0 - \chi_H E_{H,0} - \mu_H E_{H,0}] \frac{t^\alpha}{\Gamma(\alpha+1)},$$

$$I_{H,1} = [\chi_H E_{H,0} - \eta I_{H,0} - \mu_H I_{H,0} - \gamma I_{H,0}] \frac{t^\alpha}{\Gamma(\alpha+1)},$$

$$R_{H,1} = [\mu_H R_{H,0} + \gamma I_{H,0}] \frac{t^\alpha}{\Gamma(\alpha+1)},$$

$$S_{V,1} = [A_V - \beta_V C_0 - \mu_H S_{V,0}] \frac{t^\alpha}{\Gamma(\alpha+1)},$$

$$E_{V,1} = [\beta_V C_0 - \mu_H E_{V,0} - S_H E_{V,0}] \frac{t^\alpha}{\Gamma(\alpha+1)},$$

$$L(I_{V,1}) = [\delta_V E_{V,0} - \mu_V I_{V,0}] \frac{t^\alpha}{\Gamma(\alpha+1)},$$

(4.8)

Similarly, at the final step, we get the rest of the terms as infinite series as,

$$S_H(t) = \sum_{n=0}^{\infty} S_{H,n}(t) = k_1 + [-\beta_H \mathrm{B}_0 - \beta_H \rho A_0 - \mu_H S_{H,0}] \frac{t^\alpha}{\Gamma(\alpha+1)} + \cdots,$$

$$E_H(t) = \sum_{n=0}^{\infty} E_{H,n}(t) = k_2 + [\beta_H \rho A_0 + \beta_H \mathrm{B}_0 - \chi_H E_{H,0} - \mu_H E_{H,0}] \frac{t^\alpha}{\Gamma(\alpha+1)} + \cdots,$$

$$I_H(t) = \sum_{n=0}^{\infty} I_{H,n}(t) = k_3 + [\chi_H E_{H,0} - \eta I_{H,0} - \mu_H I_{H,0} - \gamma I_{H,0}] \frac{t^\alpha}{\Gamma(\alpha+1)} + \cdots,$$

$$R_H(t) = \sum_{n=0}^{\infty} R_{H,n}(t) = k_4 + [\mu_H R_{H,0} + \gamma I_{H,0}] \frac{t^\alpha}{\Gamma(\alpha+1)} + \cdots,$$

$$S_V(t) = \sum_{n=0}^{\infty} S_{V,n}(t) = k_5 + [-\beta_V C_0 - \mu_H S_{V,0}] \frac{t^\alpha}{\Gamma(\alpha+1)} + \cdots,$$

$$E_V(t) = \sum_{n=0}^{\infty} E_{V,n}(t) = k_6 + [\beta_V C_0 - \mu_H E_{V,0} - S_H E_{V,0}] \frac{t^\alpha}{\Gamma(\alpha+1)} + \cdots,$$

$$I_V(t) = \sum_{n=0}^{\infty} I_{V,n}(t) = k_7 + [\delta_V E_{V,0} - \mu_V I_{V,0}] \frac{t^\alpha}{\Gamma(\alpha+1)} + \cdots.$$

(4.9)

Equation (4.9) solves the main SAIR model of Eq. (2.2) which will be illustrated in the next section.

5.Numerical Simulations

In this section, we test the effectiveness of the proposed technique by examining the acquired results for model (2.2) for different α. The numerical simulations are presented by taking partial parameters from numerical simulations in [10]. In this section, the values of various parameters are presented for two different cases.

The results obtained by LADM match the exact solutions when $\alpha = 1$. Figure 1-13 presents a comparison between the results obtained using LADM and those generated by MATLAB's ODE45 (a Runge-Kutta 4th order method) across various model categories.It is evident from this figure that the proposed technique is efcient and accurate, as it perfectly agrees with the MATLAB code results.

Consider the SEIR nonlinear system based on the Zika virus with $\beta_H = 0.12$, $A_H = 0.1$, $\mu_H = 0.1$, $\chi_H = 0.13$, $\rho = 0.14$, $\eta = 0.15$, $\beta_V = 0.2$, $\gamma = 0.17$, $\delta_H = 0.22$, $\delta_V = 0.3$, $\mu_V = 0.25$, $k_1 = 0.1$, $k_2 = 0.12$, $k_3 = 0.14$, $k_4 = 0.16$, $k_5 = 0.18$, $k_6 = 0.2$ and $k_7 = 0.22$ is presented as:

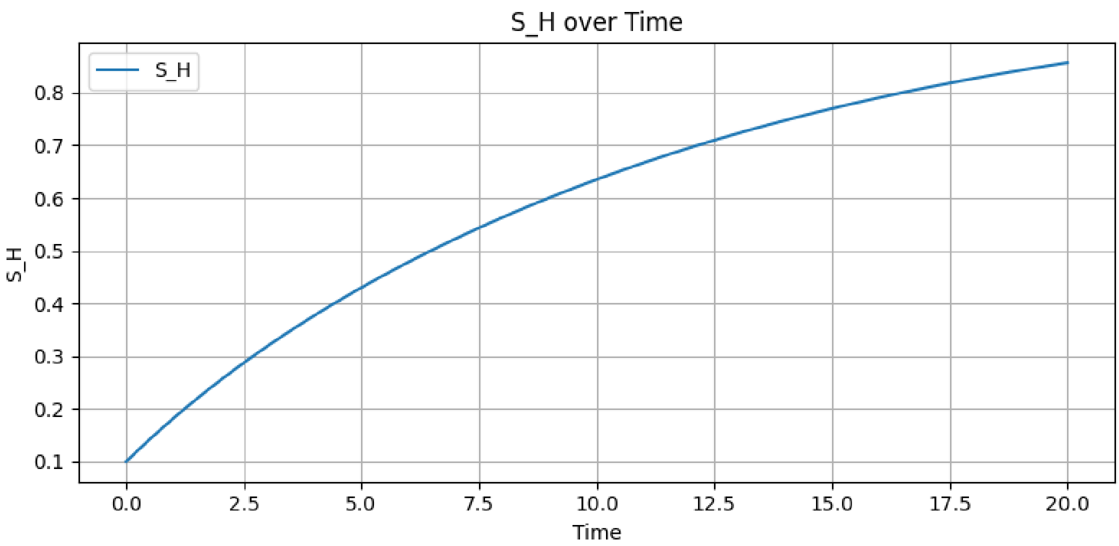

Fig. 1 The solution of $S_H(t)$ obtained by ODE 45 for $\alpha = 1$, and $0 < t < 20$.

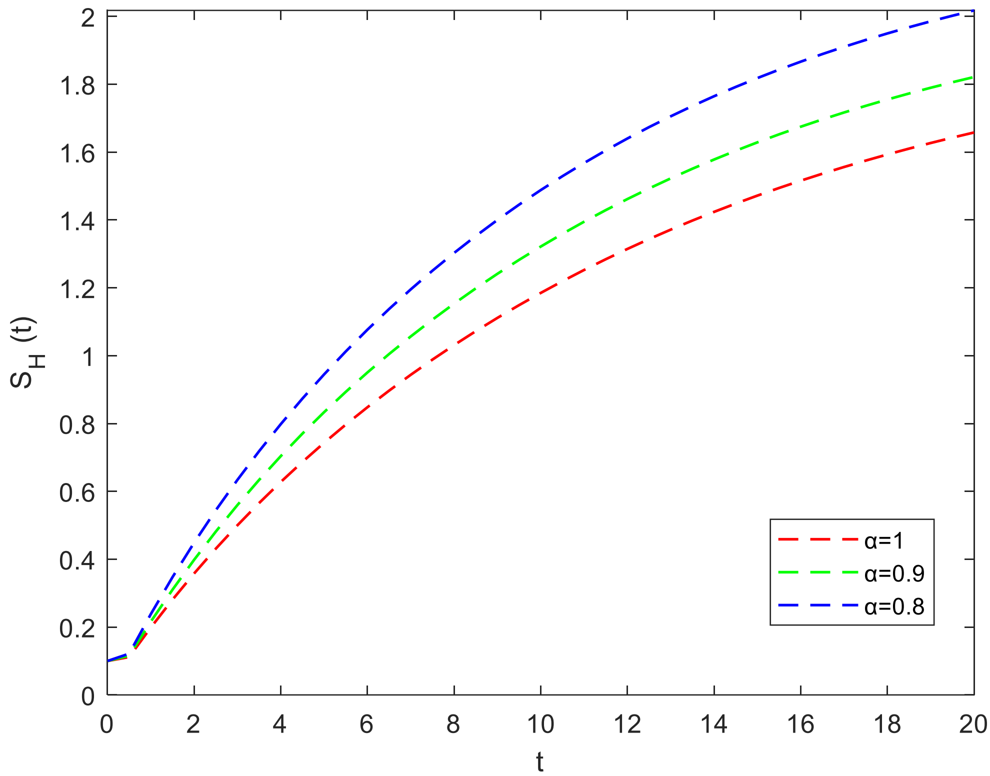

Fig. 2 The solution of $S_H(t)$ obtained by LADM for different values of α, (a) of $\alpha = 1$, (b) of $\alpha = 0.9$, (c) of $\alpha = 0.8$ and $0 \leq t \leq 20$.

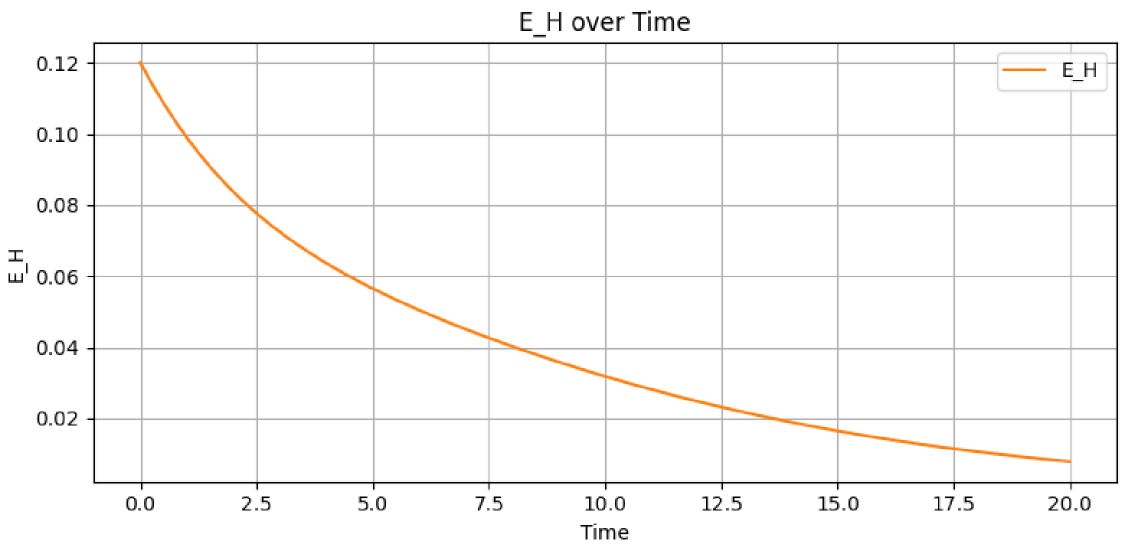

Fig. 3 The solution of $E_H(t)$ obtained by ODE 45 for $\alpha = 1$, and $0 < t < 20$.

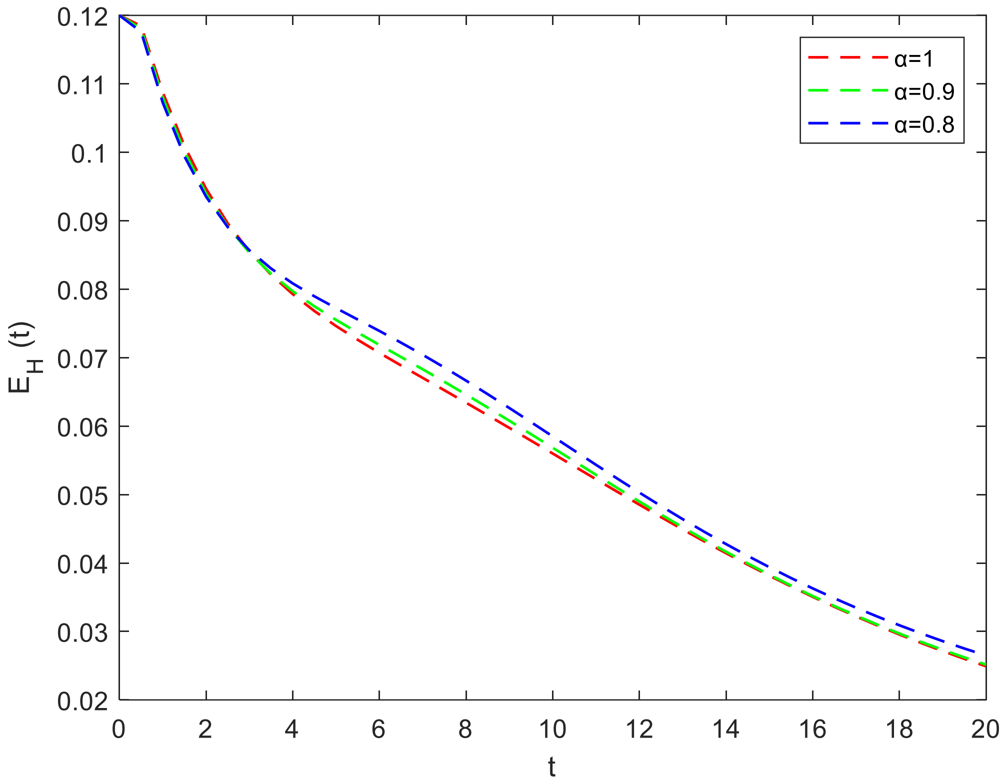

Fig. 4 The solution of $E_H(t)$ obtained by LADM for different values of α, (a) of $\alpha = 1$, (b) of $\alpha = 0.9$, (c) of $\alpha = 0.8$ and $0 \leq t \leq 20$.

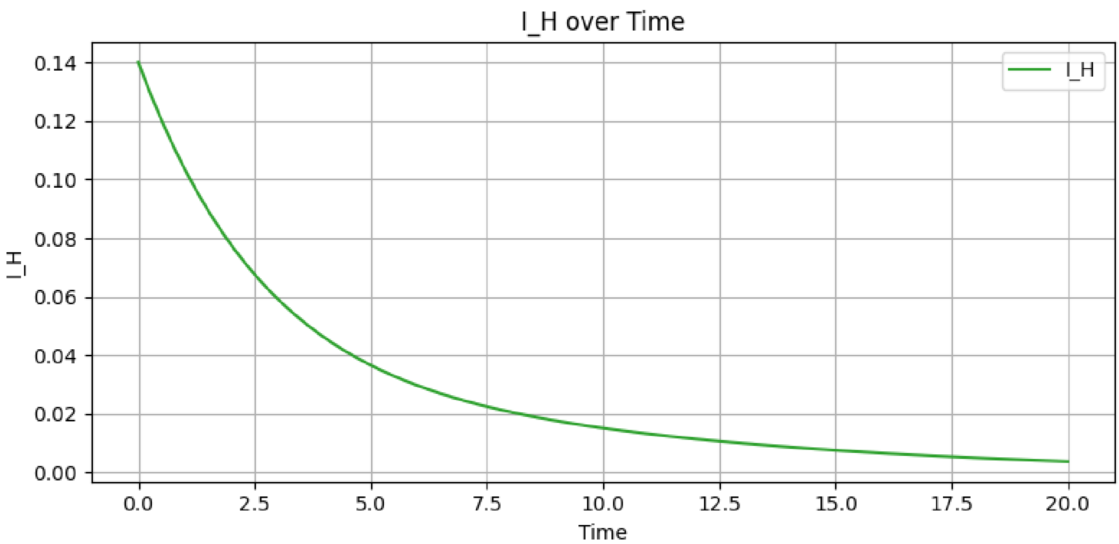

Fig. 5 The solution of $I_H(t)$ obtained by ODE 45 for $\alpha = 1$, and $0 < t < 20$.

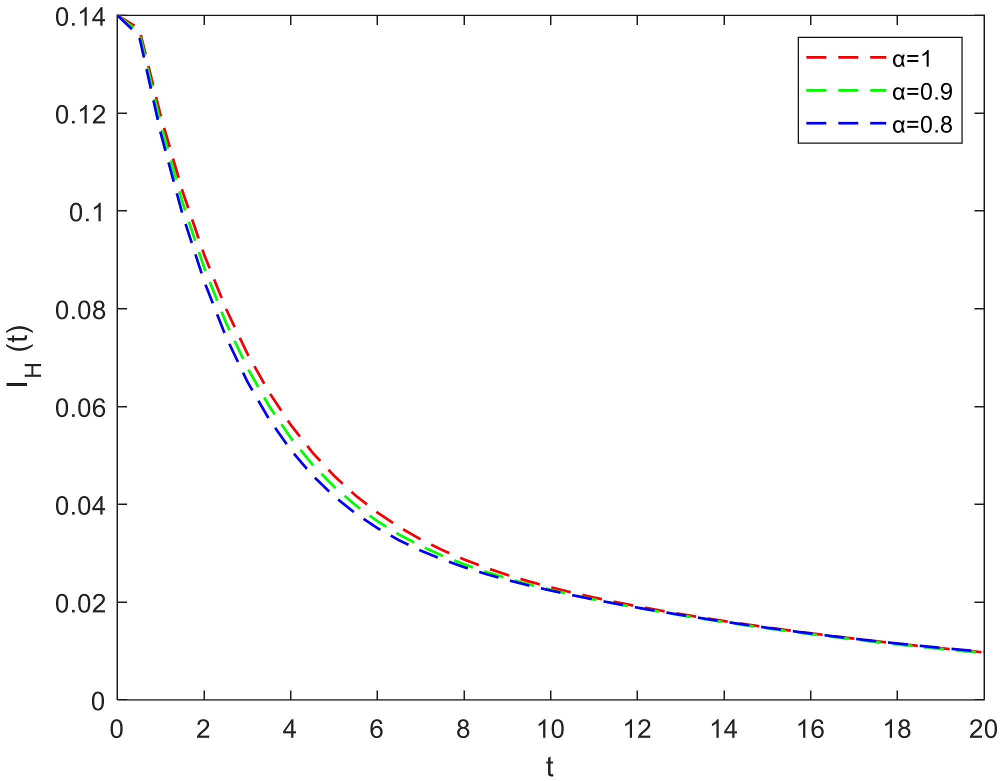

Fig. 6 The solution of $I_H(t)$ obtained by LADM for different values of α, (a) of $\alpha = 1$, (b) of $\alpha = 0.9$, (c) of $\alpha = 0.8$ and $0 \leq t \leq 20$.

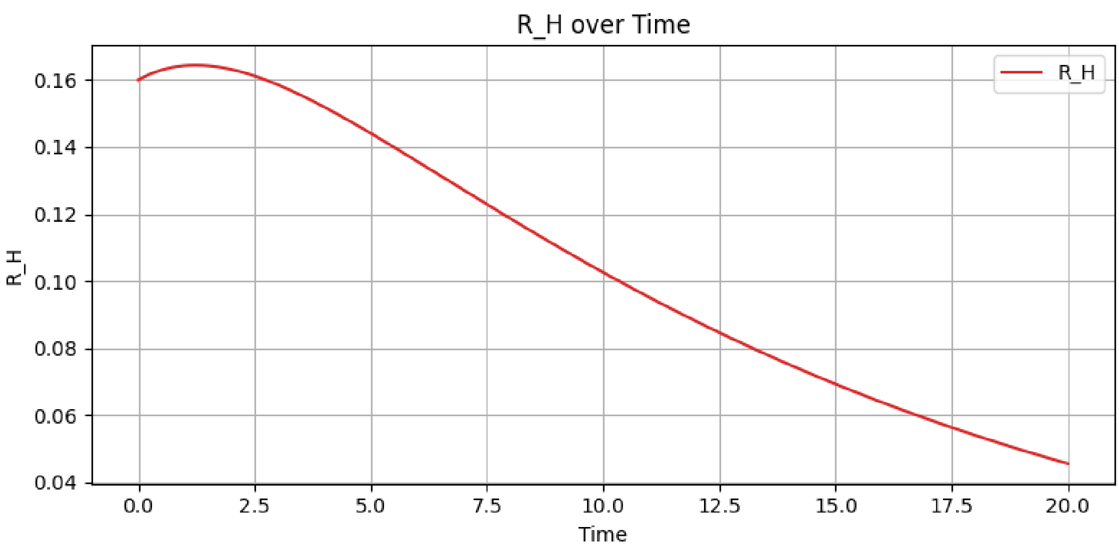

Fig. 7 The solution of $R_H(t)$ obtained by ODE 45 for $\alpha = 1$, and $0 < t < 20$.

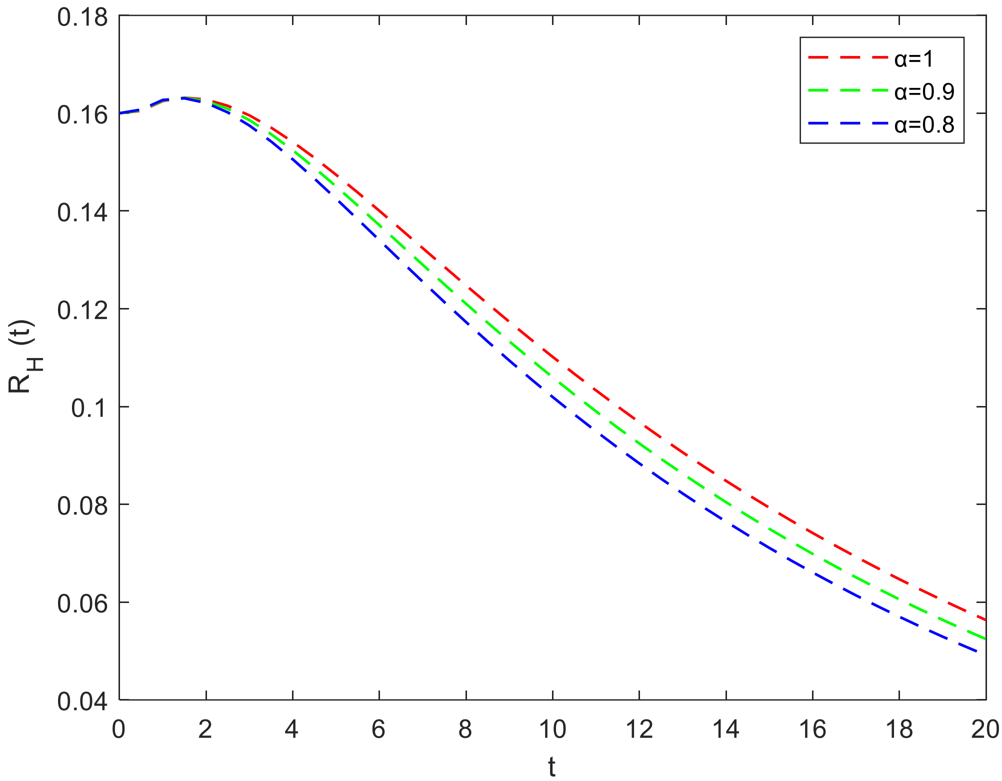

Fig. 8 The solution of $R_H(t)$ obtained by LADM for different values of α, (a) of $\alpha = 1$, (b) of $\alpha = 0.9$, (c) of $\alpha = 0.8$ and $0 \leq t \leq 20$.

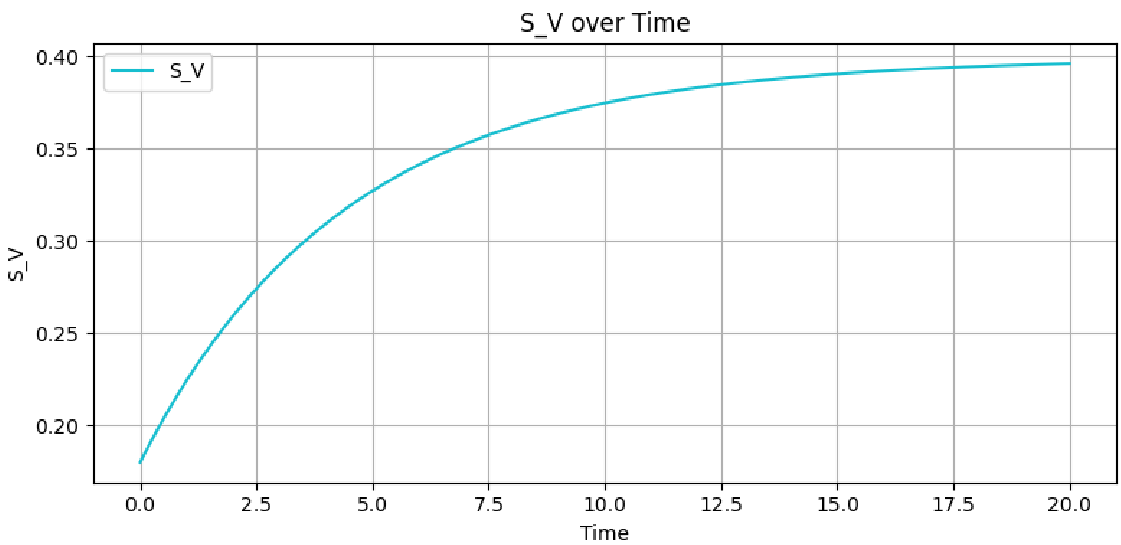

Fig. 9 The solution of $S_V(t)$ obtained by ODE 45 for $\alpha = 1$, and $0 < t < 20$.

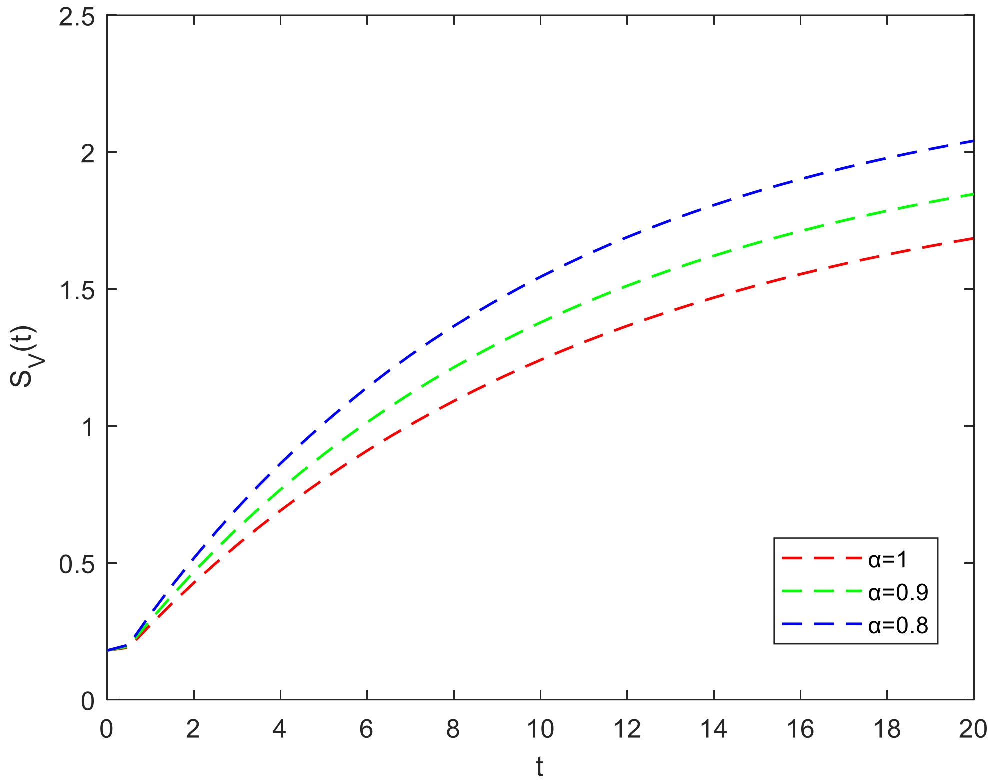

Fig. 10 The solution of $S_V(t)$ obtained by LADM for different values of α, (a) of $\alpha = 1$, (b) of $\alpha = 0.9$, (c) of $\alpha = 0.8$ and $0 \leq t \leq 20$.

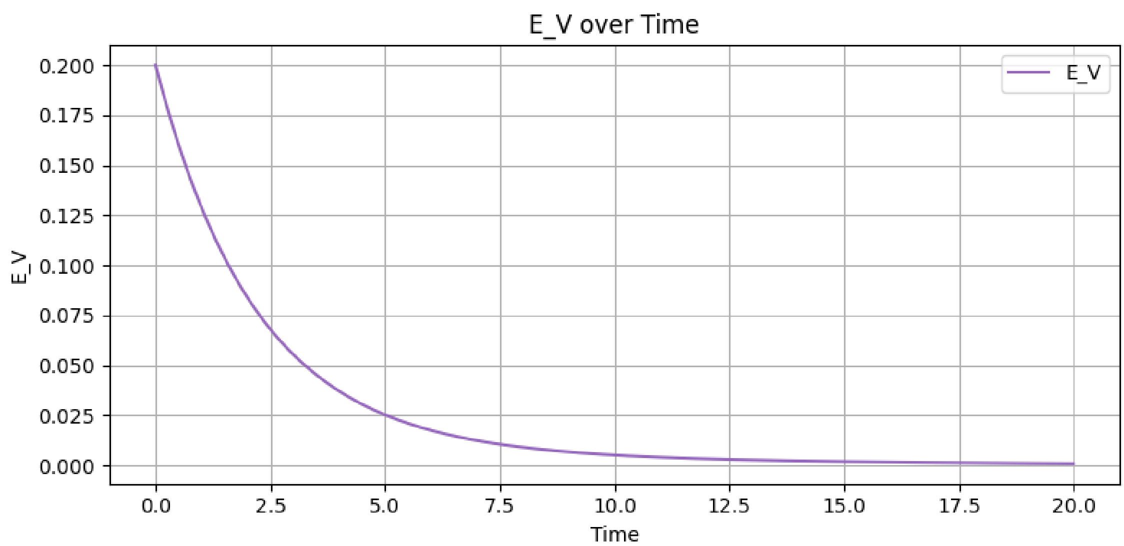

Fig. 13 The solution of $E_V(t)$ obtained by ODE 45 for $\alpha = 1$, and $0 < t < 20$.

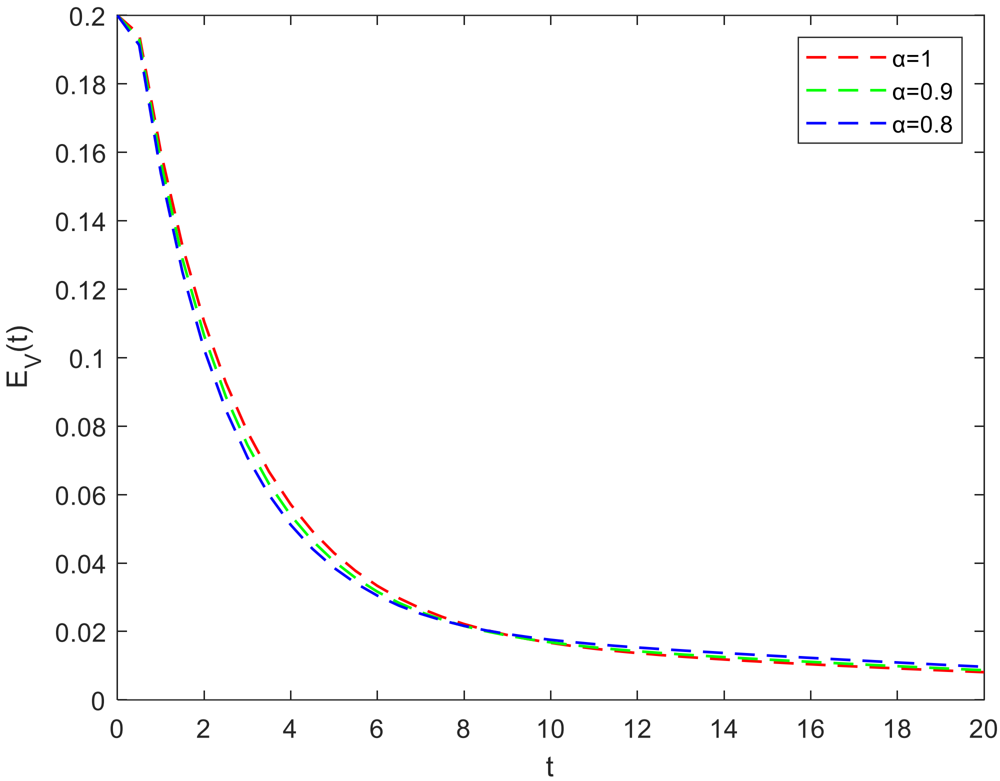

Fig. 14 The solution of $E_V(t)$ obtained by LADM for different values of α, (a) of $\alpha = 1$, (b) of $\alpha = 0.9$, (c) of $\alpha = 0.8$ and $0 \leq t \leq 20$.

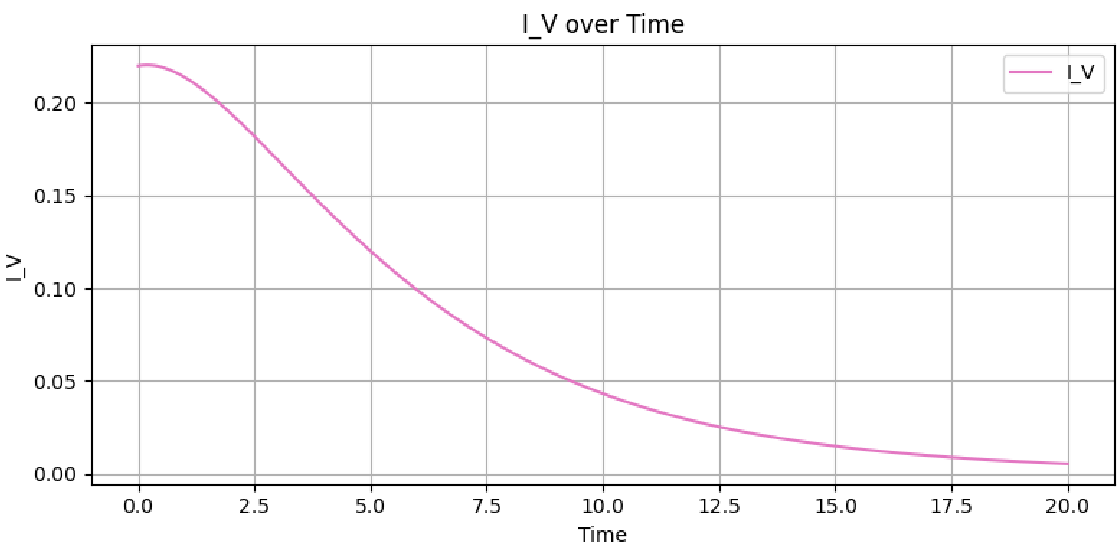

Fig. 13 The solution of $I_V(t)$ obtained by ODE 45 for $\alpha = 1$, and $0 < t < 20$.

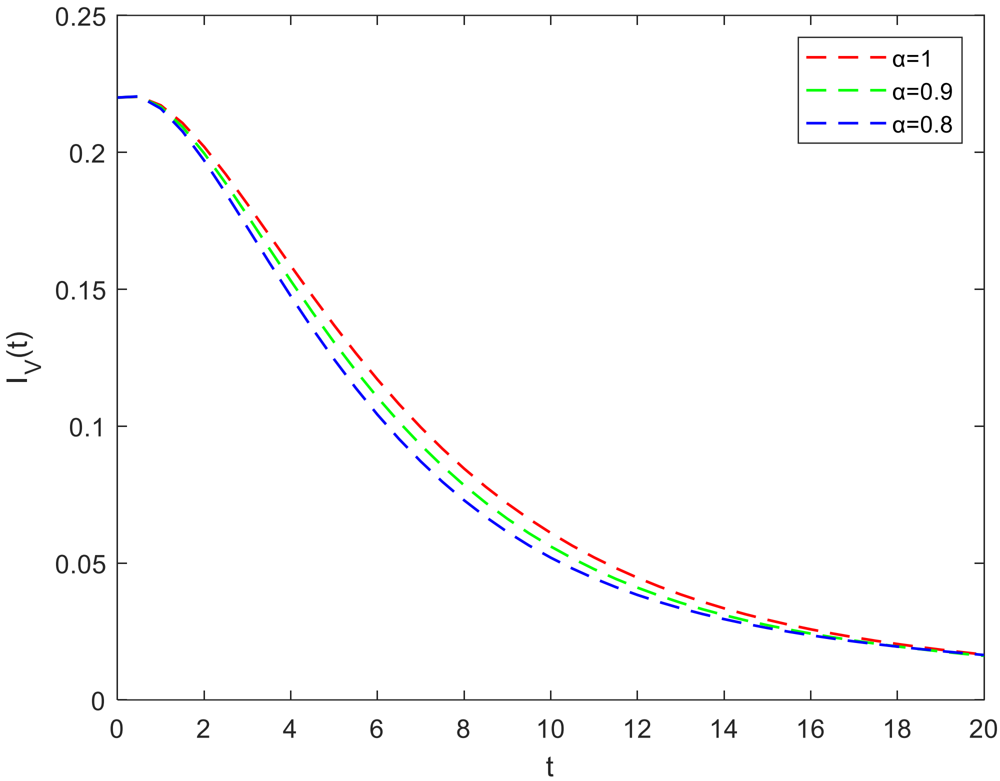

Fig. 14 The solution of $I_V(t)$ obtained by LADM for different values of α, (a) of $\alpha = 1$, (b) of $\alpha = 0.9$, (c) of $\alpha = 0.8$ and $0 \leq t \leq 20$.

6.Conclusions

In this study, a nonlinear SEIR model incorporating a modified Caputo fractional derivative was developed to analyze the transmission dynamics of the Zika virus. The model has been successfully solved using two different approaches: the Rung-Kutta of order 4 and Laplace Adomian decomposition method. The acquired results ensure accurate solutions and are investigated for different values of the fractional-order α and transmission rates.All obtained results have been analyzed and compared for various cases. The obtained results demonstrate high accuracy and stability across various values of the fractional-order parameter α and different transmission rates. Our results and methods in this work can be further extended or generalized in solving other interesting nonlinear models arising from some phenomena in physics and engineering. In addition, our results can also be applied for models formulated using other fractional derivatives.

REFERENCES

1. Musso, D., Gubler, D. J., Zika Virus, *Clinical Microbiology Reviews*, Vol:29, No:3, 487–524, 2016.
2. Ferguson, N. M., et al., Modeling the spread of Zika virus in the Americas, *PLoS Neglected Tropical Diseases*, Vol:10, No:12, e0005173, 2016.

3. Zhang, Q., et al., Spread of Zika virus in the Americas, *Proceedings of the National Academy of Sciences*, Vol:114, No:22, E4334–E4343, 2017.
4. Agusto, F. B., et al., Mathematical Model of Zika Virus with Sexual Transmission, *Computational and Mathematical Methods in Medicine*, Vol:2017, No:1, 1–10, 2017.
5. Marbán-Castro, E., et al., Zika virus infection in pregnant women and their children: A review, *European Journal of Obstetrics & Gynecology and Reproductive Biology*, Vol:265, No:3, 162–168, 2021.
6. Ferraris, P., Yssel, H., Missé, D., Zika virus infection: An update, *Microbes and Infection*, Vol:21, No:8–9, 353–360, 2019.
7. Musso, D., et al., Potential for Zika virus transmission through blood transfusion during an outbreak in French Polynesia, *Eurosurveillance*, Vol:19, No:14, 20761, 2014.
8. Lee, E. K., Liu, Y., Pietz, F. H., A compartmental model for Zika virus with dynamic human and vector populations, *AMIA Annual Symposium Proceedings*, Vol:2016, No:1, 743–752, 2016.
9. Rezapour, S., Mohammadi, H., Jajarmi, A., A new mathematical model for Zika virus transmission, *Advances in Difference Equations*, Vol:2020, No:1, 1–15, 2020.
10. Suantai, S., et al., Numerical computation of SEIR model for the Zika virus spreading, *Computers, Materials & Continua*, Vol:75, No:1, 2155–2170, 2023.
11. Ongun, M. Y., The Laplace Adomian decomposition method for solving a model for HIV infection of CD4+ T cells, *Mathematical and Computer Modelling*, Vol:53, No:5–6, 597–603, 2011.
12. Haq, F., et al., Numerical solution of fractional order smoking model via Laplace Adomian decomposition method, *Alexandria Engineering Journal*, Vol:57, No:2, 1061–1069, 2018.
13. Baleanu, D., et al., On modelling of epidemic childhood diseases with Caputo-Fabrizio derivative by Laplace Adomian decomposition method, *Alexandria Engineering Journal*, Vol:59, No:5, 3029–3039, 2020.
14. González-Gaxiola, O., Biswas, A., Optical solitons with Radhakrishnan–Kundu–Lakshmanan equation by Laplace–Adomian decomposition method, *Optik*, Vol:179, No:1, 434–442, 2019.
15. Edeki, S. O., et al., The Greek parameters of a continuous arithmetic Asian option pricing model via Laplace Adomian decomposition method, *Open Physics*, Vol:16, No:1, 780–785, 2018.
16. Naghipour, A., Manafian, J., Application of the Laplace Adomian decomposition and implicit methods for solving Burgers' equation, *TWMS Journal of Pure and Applied Mathematics*, Vol:6, No:1, 68–77, 2015.
17. González-Gaxiola, O., Biswas, A., W-shaped optical solitons of Chen–Lee–Liu equation by Laplace–Adomian decomposition method, *Optical and Quantum Electronics*, Vol:50, No:8, 1–11, 2018.
18. Paul, S., et al., Numerical solution of Lotka–Volterra prey–predator model by using Runge–Kutta–Fehlberg method and Laplace Adomian decomposition method, *Alexandria Engineering Journal*, Vol:55, No:1, 613–617, 2016.
19. Günerhan, H., et al., Novel analytical and approximate-analytical methods for solving the nonlinear fractional smoking mathematical model, *Sigma Journal of Engineering and Natural Sciences*, Vol:41, No:1, 331–343, 2023.
20. Adel, W., et al., Designing a novel fractional order mathematical model for COVID-19 incorporating lockdown measures, *Scientific Reports*, Vol:14, No:1, 2926, 2024.

21. Günerhan, H., et al., Analysis of a fractional HIV model with Caputo and constant proportional Caputo operators, *Chaos, Solitons & Fractals*, Vol:139, No:1, 110053, 2020.
22. Meenakshi, A., et al., Analysis of Caputo fractional-order co-infection COVID-19 and influenza SEIR epidemiology by Laplace Adomian decomposition method, *Mathematics*, Vol:12, No:12, 1876, 2024.
23. Zhang, Y., et al., Applicability of time fractional derivative models for simulating the dynamics and mitigation scenarios of COVID-19, *Chaos, Solitons & Fractals*, Vol:138, No:1, 109959, 2020.
24. Caputo, M., Linear models of dissipation whose Q is almost frequency independent—II, *Geophysical Journal International*, Vol:13, No:5, 529–539, 1967.

On the reducibility of weighted composition operators

Teubé Cyrille Mbainaissem[a] and Déthié Dione[b]
[a]University of N'Djaména, Chad
[b]University of Gaston Berger, Senegal

Abstract

In this paper the main result is a lower estimation for the norm of a resolvent operator, the spectrum of which is a unit circle. It is shown that for arbitrary function $\phi(\lambda)$ analytic on a unit circle, there exist an operator which resolvent norm is greater than $|\phi(\lambda)|$.

2010 *Mathematics Subject Classification 57N20*

Key Words: Displacement operator with weight, reducibility, homological equation

1 Introduction

A bounded linear operator B, acting in a Banach space $\mathcal{F}(X)$ of functions on a set X is called a weighted displacement operator (WDO) if it can be put into the form:

$$(Bu)(x) = a(x)u[\alpha(x)], \quad x \in X \tag{1.1}$$

where $\alpha : X \to X$ is a certain application and $a(\cdot)$ is a function defined on X.
Operators of the form:

$$(T_\alpha u)(x) = u(\alpha(x)), \quad x \in X \tag{1.2}$$

are called composition operators or displacement operators

Such operators, the algebras of operators they generate and the functional equations linked to them, have been studied by several authors in various function spaces as independent objects and in connection with various applications [[1] -[4]], [[6] - [11]]. The study of a concrete class of operators is closely linked to the study of a Banach algebra generated by such operators. In this case, commutative algebras are simpler to construct and this simplifies the study of the corresponding operators. These operators examined (with α fixed) give rise to a non-commutative Banach algebra. But if we restrict ourselves to examining operators whose coefficients are constant or invariant with respect to the displacement $(a(\alpha(x)) = a(x))$, then the corresponding algebra of operators is commutative.

This is why it is useful to reduce the study of the given operator to the examination of another operator with a better, constant or invariant coefficient. Similar problems have been examined for other forms of operator. For example, one of the problems analogous to the one examined is the problem of reducing a partial derivative (differential) operator to a canonical form. Another analogous approach is found in the theory of linear systems of differential equations of the form:

$$\dot{U}(t) = A(t)u(t) \tag{1.3}$$

Let $D(t)$ be a matrix of bounded, invertible functions with the inverse $D^{-1}(t)$ also bounded. The change in the system (1.3) of the unknown function $Z(t) = D(t)u(t)$ is called the Liapounov transformation of the system. The linear system (1.3) is said to be reducible if there is a Lyapounov transformation, reducing this system to a system with a constant coefficient.

By analogy with the theory of differential equations, we will call the invertible operator D of multiplication by a continuous function the Lyapounov transformation $d(\cdot) \in \mathcal{C}(X)$:

$$DU(x) = d(x).u(x).$$

The weighted displacement operator (WDO) B will be said to be reducible to a constant coefficient operator, if there exists a Lyapunov transformation such that:

$$DBD^{-1} = a_0 T_\alpha, \quad a_0 \in \mathbb{C} \tag{1.4}$$

$$DBD^{-1} = a_0 T_\alpha, \quad \text{où} \quad a_0(\alpha(x)) = a_0(x) \tag{1.5}$$

From the point of view of operator theory, these definitions mean that the operator $B = aT_\alpha$ is similar to the constant or invariant coefficient operator $a_0 T_\alpha$. As already noted, the Banach algebra generated by such weighted shift operators is commutative, but in the case of examining these operators in the space $L^2(X, \mu)$, it is a C^*-algebra. This makes it possible, for example, to apply the spectral theorem to reducible weighted shift operators.

In this work, we examine the reducibility of weighted shift operators with continuous coefficients, generated by periodic, continuous applications of a compact, separable topological space X. Such operators operate in classical Banach spaces of functions on X, such as the spaces $\mathcal{L}_p(X, \mu)$ and $\mathcal{C}(X)$. For any α applications, the spectrum of the weighted displacement operator depends on the space of functions considered, but in the case of a α periodic application, the spectrum of the weighted displacement operator is the same in the classical spaces indicated. The results obtained in the article also remain true if we examine these operators in any Banach space of functions on X where these operators are bounded.

2 Factorisation with displacement and homological equation

First of all, let us note that by virtue of the compactness of X, the condition of invertibility of the operator of multiplication by a continuous function, existing in the definition of the Lyapounov transformation, is written as the condition: $d(x) \neq 0$ for all x.

Any Lyapounov transformation transforms a weighted displacement operator (1.1) with a continuous coefficient into a weighted displacement operator (with a different continuous coefficient):

$$DBD^{-1} = DaT_\alpha D^{-1} = a(x)\frac{d(x)}{d(\alpha(x))}T_\alpha$$

. This is why the question about the reducibility of the operator is equivalent to the question about the representation of the coefficient a in form:

$$a(x) = a_0(x)\frac{d(\alpha(x))}{dx} \tag{2.1}$$

with a_0-constant or invariant. Such a representation is called a factorisation with displacement of the function a. Note that if the function d is invariant, then during the Lyapounov transformation the operator reduces to itself. This is why the function d is defined to within one multiplicative invariant factor.

The method, based on factorisation with coefficient shift, is generally used to examine weighted shift operators on a contour [3, 4]. This research is related to singular integro-functional equations on a Γ contour, containing a singular Cauchy integral operator:

$$SU(z) = \frac{1}{\pi i}\int_\Gamma \frac{U(\xi)}{\xi - z}d\xi$$

.

Note that the operator $SD - DS$ is compact in the case of a continuous function d and is non-compact in the case of a piecewise continuous function. This is why the continuity condition of the d-function is essential in the theory of singular integro-functional equations.

The question relating to the existence of a factorisation with displacement for a given function is closely linked to the solvability of the homological equation, corresponding to the application considered. [2, 6, 7, 11] call these equations, the functional equations of form:

$$(T_\alpha - I)\varphi(x) \equiv \varphi(\alpha(x)) - \varphi(x) = f(x) \tag{2.2}$$

In reality, let's assume $a(x) > 0$ for all x. Denoting by

$$varphi(x) = \ln S(x), \quad g(x) = \ln a(x), \quad \xi(x) = \ln a_0(x)$$

and passing to the logarithm in the equality 2.1, we obtain for the function *varphi* the homological equation

$$\varphi(\alpha(x)) - \varphi(x) = g(x) - \xi(x)$$

In general, the image of the operator $T_\alpha - I$ is not closed and, consequently, there are no explicit necessary and sufficient conditions for the solvability of the homological equation. A classic example of a homological equation with bad "properties" is the equation, related to an irrational rotation of the circle [6, 7]. If we realise the circle as a unit circle on the complex plane.

$$S^1 = \{z \in \mathbb{C}, \quad |z| = 1\}$$

then, such an application acts according to the formula $\alpha(z) = \mathrm{e}^{i2\pi h}$ where h irrational.

The pathological properties of the corresponding homological equation are well known. For example, in [7] it was proved that for any function other than a polynomial of z, there exists h such that the solution is a non-measurable function. This is why the existence of a continuous or bounded solution (and consequently, the reducibility of the operator generated by an irrational rotation, into an operator with a constant coefficient) is an exceptional case, the set of coefficients a, for which a factorisation with displacement is possible, is a certain non-closed subset of $\mathcal{C}(X)$, which cannot be described explicitly and depends essentially on the arithmetic properties of the irrational number h.

The case of a periodic application here is singular. In this case the image of the operator $T_\alpha - I$ is closed, and the normally solvable homological equation is affordable enough for the study. In [11], it has been proved that this case is unique. If the application is invertible, then the homological equation is normally solvable in the space $\mathcal{C}(X)$ of continuous functions on the compact space X if and only if α is periodic.

Let's remind ourselves of certain notions linked to the property of a periodic application. Let be $\alpha_0(x) \equiv x, \quad \alpha_k(x) = \alpha(\alpha_{k-1}(x)), \quad k = 1, 2, \ldots$. The application α is said to be periodic with period m, if $\alpha_m = \alpha_0$ and $\alpha_k \neq \alpha_0$ for $1 \leq k < m$. The weight x is periodic with period $p(x)$ if $\alpha_{p(x)} = x$ and $\alpha_k(x) \neq x$ for $1 \leq k < p(x)$. If the application α is periodic with period m, then each point x is periodic and the number $p(x)$ is a divisor of m, note that in this case, it is possible for $p(x) < m$ for all x.

Example 2.1 *Consider the space :*

$$X = \{z = r\mathrm{e}^{i2\pi t} : 0 \leq r \leq 1; t_k = \frac{k}{12}, \quad k \in \{0, 1, \cdots, 11\}\}$$

As a set in the complex plane, this space is made up of six segments of length 2 whose midpoints are the points O. The application $\alpha : X \to X$, given by:

$$\alpha(z) = \begin{cases} \mathrm{e}^{i\frac{2}{3}\pi}.z & k \text{ Even} \\ -z & k \text{ Odd} \end{cases}$$

is periodic with period 6, but here the point O is fixed (with period 1), there are three periods other than zero for the points corresponding to even k, 2 periods other than zero for the points corresponding to odd k and no points with period 6.

A topological space X is said to be α- reducible if there exists a partition of X into two closed non-empty subsets X' and X'' which are invariant with respect to the α application. A topological space X is said to be α- connected if such a partition is impossible. The problem examined is also linked to the algebraicity property of the operator introduced by Van Neumann. If the α application is periodic, then any weighted constant-coefficient displacement operator is algebraic. This is why the necessary condition leading to a coefficient operator is its algebraicity. A linear operator A is said to be algebraic if there exists a polynomial

$$P(z) = p_\ell z^\ell + p_{\ell-1} z^{\ell-1} + \ldots + p_0, \quad p_k \in \mathbb{C} \quad \text{such that} \quad P(A) = 0$$

. Such a polynomial of lowest degree is called a characteristic polynomial and is denoted by $Ch_A(z)$. The roots of $Ch_A(z)$ are called the characteristic numbers of the operator A.

In a finite-dimensional space, any operator is algebraic because it is the root of its characteristic polynomial (Caley-Hamilton theorem). The special cases of algebraic operators are nilpotent operators ($A^m = 0$), idempotent operators ($A^2 = A$), involutive operators ($A^2 = I$) and generalised involutive operators ($A^m = I$). The theory of algebraic operators is given, for example, in [8]. The equations related to generalised involutive operators have been studied in [3]. The algebraicity condition of an operator is sufficiently strong. This algebraicity gives rise to a series of properties that are not satisfied for any operator, but are typical for operators in finite-dimensional spaces. The spectrum of an algebraic operator is a finite set and coincides with the set of characteristic numbers. In this case the image of the operator $A - \lambda I$ is closed for any spectral value λ, which is not true for any operator whose spectrum is a finite set.

The necessary and sufficient conditions for the algebraicity of composition operators (without the weighted coefficient) are obtained in [9]. In [10], algebraicity conditions were obtained for more complex weighted displacement operators and the description of their characteristic polynomial. Here we need the main result from [10]

Let's call it:

$$a_k(x) = \prod_{j=0}^{k-1} a(\alpha(x))$$

Theorem 2.1 *Let B be a weighted displacement operator with continuous coefficient $a(\cdot)$. The following conditions are equivalent:*

i) There exists a polynomial:

$$P(z) = p_\ell z^\ell + p_{\ell-1} z^{\ell-1} + \cdots + p_0, \quad p_k \in \mathbb{C} \quad \textit{where} \quad p_0 \neq 0 \quad \textit{such that} \quad P(B) = 0$$

.

ii) The application alpha is periodic of period m, $a(x) \neq 0$ for all x and the function $a_m(x)$ has a finite number of values.

If these conditions are satisfied, the characteristic polynomial $Ch_B(z)$ has the form :

$$Ch_B(z) = \prod_{k=1}^{n} (z - \lambda_k) \tag{2.3}$$

where $n \leq m, \quad n \leq \ell, \quad \lambda_k \neq 0 \quad \lambda_k \neq \lambda_j \quad si \quad k \neq j$. i.e. all the characteristic numbers are simple.

If, on the other hand, the space X is *alpha*- connected, then for the algebraic operator $a(x) \equiv C = constant$ and $\lambda_k^m = C$ for all k. Consequently, not all roots of power m of the number C are characteristic.

3 Reducible weighted displacement operators

The link between the factorisation problem and the homology equation for positive-valued functions has been shown above. In the case of complex-valued functions, additional complications arise in obtaining the homology equation, due to the fact that the logarithm is a multivariate function. We will say that there is a continuous determination of the logarithm of the function $a(x)$, if there is a real-valued continuous function ψ on X such that

$$a(x) = \mathrm{e}^{\ln|a(x)|+i\psi(x)}$$

Theorem 3.1 *Let X be a α-connected space, α a periodic application and $a(x) \neq 0$ for all x. If there is a continuous determination of the logarithm of the function a, then the operator aT_α becomes an operator with a constant coefficient if, and only if, it is algebraic.*

Proof: Let's look at the homologous equation

$$\varphi(\alpha(x)) - \varphi(x) = f(x) \tag{3.1}$$

where $f(x) = g(x) - \xi(x), \quad g(x) = \ln|a(x)| + i\psi(x)$. Here g is a given continuous function φ and $\xi(x)$ are unknown functions.

By virtue of the periodicity of the α application, the T_α operator is algebraic and has, according to Theorem 2.1, a simple spectrum. So we can apply the general methods for finding algebraic operators [8].

On the other hand, here we have the equality $T_\alpha^m = I$, hence the application

$$\mathbb{Z}_m \ni k \longrightarrow T_\alpha^k \tag{3.2}$$

is a linear representation of the finite cyclic group $\mathbb{Z}_m$ in the space $\mathcal{C}(X)$. The application of the theory of representations of groups [12] allows us to obtain much more explicit results than in the case of any algebraic operators.

Note that we generally examine linear representations of groups in Hilbertian space. But in the case of finite groups, the main elements of the theory of representations have an algebraic character of their own and are true in the case of representations in Banach spaces, in particular, for linear representations in the space $\mathcal{C}(X)$. The finite commutative group $\mathbb{Z}_m$ has m irreducible representations ρ_j, these representations are one-dimensional and act according to the form :

$$\mathbb{Z}_m \ni k \longrightarrow \rho_j(k) = \omega^{kj}, \quad \text{où} \quad \omega = \mathrm{e}^{i\frac{2\pi}{m}}, \quad j = 0, \cdots, m-1 \tag{3.3}$$

Any linear representation of the group $\mathbb{Z}_m$ can be decomposed into irreducible representations, which allows us to study the equation (3.1) in detail. This decomposition is performed as follows:

The operators

$$P_j = \frac{1}{m}\sum_{k=0}^{m-1} \omega^{-kj} T_\alpha^k \tag{3.4}$$

are bounded projectors and therefore

$$\sum_{j=1}^{m-1} P_j = I, \quad P_k P_j = 0 \quad \text{si} \quad k \neq j; \quad T_\alpha = \sum_{j=0}^{m-1} \omega^j P_j \tag{3.5}$$

The last two equalities mean that the space $\mathcal{C}(X)$ decomposes into a direct sum of closed vector subspaces $E_j = I_m P_j$, and the last equality means that on the subspace E_j, the operator $T\alpha$ acts as a multiplication by the number ω^j. Note again that here we have $T_\alpha^m = I$ where all the characteristic numbers are roots of power m of 1 i.e. are of form ω^j which are characteristic. In other words, there are periodic applications of period m, such that the characteristic polynomial of T_α is

$$Ch_{T_\alpha}(z) = \prod_{j=1}^{p}(z^{m_j} - 1)$$

where $m = \prod_{j=1}^{p} m_j$, and the degree of the characteristic polynomial is the number $\sum_{j=1}^{p} m_j < m$. In this case, the projector P_j is non-zero if and only if ω^j is a characteristic number of the operator T_α.

An application with such properties was examined in the example 2.1. In this example, the application α is periodic with period $m = 6$ and the characteristic polynomial is of degree 4.

$$Ch_{T_\alpha}(z) = (z+1)(z^3 - 1),$$

The characteristic numbers being $\omega^0 = 1$, ω^2, $\omega^3 = -1$, ω^4 and the numbers ω and ω^5 are not characteristic numbers of the T_α operator.

From the point of view of the theory of representations, this remark means that in general the decomposition of the representation (3.2) does not include all irreducible representations. But the number $\omega^0 = 1$ is always characteristic and the projector

$$P_0 = \frac{1}{m}\sum_{k=0}^{m-1} T_\alpha^k$$

is always non-zero.

From the decomposition (3.5) we obtain that

$$T_\alpha - I = \sum_{j=1}^{m-1}(\omega^j - 1)P_j$$

and that

$$I_m(T_\alpha - I) = I_m\left[\sum_{j=1}^{m-1} P_j\right] = I_m(I - P_0) = \ker P_0$$

so therefore, the condition:

$$P_0 f = 0 \tag{3.6}$$

is a necessary and sufficient condition for the existence of a solution to the equation (3.1).

In examining the homology equation, the right-hand side $f(x) = g(x) - \xi(x)$ contains the unknown function ξ. This is why the solvency condition:

$$P_0 f = P_0 g - P_0 \xi = 0 \tag{3.7}$$

will be studied as an equation with respect to the function ξ. There are many ξ functions for which this equation is satisfied. From the invariance condition ($T_\alpha \xi = \xi$) it follows that $P_0\xi = \xi$; this is why from (3.7), in a unique way we obtain the following function:

$$\xi(x) = (P_0 g)(x) = \frac{1}{m}\sum_{j=0}^{m-1} g(\alpha_j(x)) \tag{3.8}$$

which satisfies the solvency condition. With this choice of function ξ the condition for solving the equation (3.1) is satisfied and consequently the other solutions differ by the invariance of the function. To construct the Lyapounov transformation, all we need to do is construct one of these solutions. Such a solution can be given by the expression:

$$\varphi(x) = \sum_{j=1}^{m-1} \frac{1}{\omega^j - 1} P_j f = \sum_{j=1}^{m-1} \frac{1}{\omega^j - 1}\left[\frac{1}{m}\sum_{k=0}^{m-1} \omega^{-kj} T_\alpha^k\right] f$$

By virtue of the invariance of the function ξ, we obtain that

$$\sum_{k=0}^{m-1} \omega^{-kj} T_\alpha^k \xi = \left[\sum_{k=0}^{m-1} \omega^{-kj}\right] \xi = 0.$$

hence

$$\varphi(x) = \sum_{j=1}^{m-1} \frac{1}{\omega^j - 1}\left[\frac{1}{m}\sum_{k=0}^{m-1} \omega^{-kj} T_\alpha^k\right] = \frac{1}{m}\sum_{k=0}^{m-1}\left[\sum_{j=1}^{m-1} \frac{\omega^{-kj}}{\omega^j - 1}\right] T_\alpha^k g. \tag{3.9}$$

Now, let $d(x) = \mathrm{e}^{\varphi(x)}$ and $a_0(x) = \mathrm{e}^{\xi(x)}$. From the homological equation we obtain the factorisation with displacement of the coefficient a, which we needed to prove.

Here the equality is realised:

$$a_0^m = \prod_{j=1}^{m-1} a(\alpha_j(x))$$

meaning that the function $a_0(x)$ is a continuous determination of the root of degree m of the function $\prod_{j=1}^{m-1} a(\alpha_j(x))$. The function a_0 is constant (and the operator reduces to an operator with a constant coefficient) if and only if $\prod_{j=1}^{m-1} a(\alpha_j(x))$ is constant. According to Theorem 1.1, this is the algebraicity of the operator B. The theorem is proved.

Consequence: If the application is periodic, then any weighted displacement operator reduces to an operator $a_0 T_\alpha$ in which $|a_0(x)|$ is an invariant function.

Proof: Let us examine the homological equation:

$$\varphi(\alpha(x)) - \varphi(x) = f(x) \tag{3.10}$$

where $f(x) = g(x)\xi(x), \quad g(x) = \ln|a(x)|$. This equation is solvable if, as above, we take

$$\xi(x) = (P_0 g)(x) = \frac{1}{m}\sum_{j=0}^{m-1} g(\alpha_j(x)).$$

. In this case the function $d(x) = \mathrm{e}^{\varphi(x)}$ gives rise to the factorisation with displacement of the coefficient a. Thus the question of reducibility boils down to a question of reducibility of operators for which $|a(x)| \equiv 1$. Below, we look at operators with such coefficients.

4 Topological obstacles to reducibility

. The condition used in Theorem 3.1 for the existence of a continuous determination of the logarithm is necessary. Let us show on an example that this condition is essential.

Example 4.1 *Let* $X = S^1$ *and* $\alpha(z) = \bar{z}$*. This is an example of an application that changes the orientation of the circle. For the coefficient* $a(z) = z$ *we have here:* $a(z)a(\alpha(z)) = z\bar{z} = 1$ *and the operator*

$$Bu(z) = zu(\bar{z})$$

is algebraic. But for the coefficient $a(z) = z$*, there is no form factorisation:*

$$a(z) = a_0(z)\frac{d(\bar{z}}{d(z)} \tag{4.1}$$

Here the obstacle to factorization is the Cauchy index $ind[a]$ *of the non-degenerate continuous function* a*, which is defined as the increase in the argument as it travels along the contour, divided by* 2π*. In this example, the condition for the existence of a continuous determination of the logarithm is the condition* $ind[a] = 0$*; for the function* $a(z) = z$ *this condition is not verified, so* $ind[a] = 1$*.*

Suppose (4.1) is realised where the function $a_0(z)$ is invariant:

$$a_0(\bar{z}) = a_0(z)$$

From the invariance of the function $a_(z)$ it follows that $ind[a_0] = 0$ On the other hand,

$$ind[d(\bar{z})] = ind[\frac{1}{d(z)}] = -ind[d(z)]$$

Therefore

$$ind[a_0(z)\frac{d(\bar{z}}{d(z)}] = -2ind[d]$$

Thus, the Cauchy index of the right-hand side of (4.1) is an even number. Therefore, if the Cauchy index of the coefficient a is odd, factorisation is impossible. In this example $ind[a] = 1$ and equality (4.1) is impossible.

In general, similar obstacles arise for operator regularisation. Let X be any compact space and

$$\gamma : [0, 1] \ni t \to \gamma(t) \in X$$

a non-trivial yaw on X (i.e. a continuous application such that $\gamma(0) = \gamma(1)$, not homotopic to a constant). In this case the function $a(\gamma(t))$ is a complex-valued continuous function on $[0, 1]$ such that $a(\gamma(0)) = a(\gamma(1))$. The increase in the continuous determination of the argument of this function on $[0, 1]$ is a multiple of 2π; this makes it possible to define the notion of Cauchy index on the yaw. Thus there can exist a large number of topological invariants (the Cauchy indexes on each non-trivial yaw) on which the regularization of the operator depends.

5 Operator generated by the symmetry of the square

Let's look in more detail at the question of obstacles to regularization using a concrete example. Let X be a graph, represented by a square in the plane with two median lines:

$$X = \{(x_1, x_2); x_1 \in \{-1, 0, 1\}, x_2 \in [-1, 1]\} \cup \{(x_1, x_2) : x_1 \in [-1, 1], x_2 \in \{-1, 0, 1\}$$

Let's construct the graph of Y, obtained by cutting the graph of X at the vertices of the square. This means that instead of each of the vertices $(\pm 1, \pm 1)$, we examine the two points $(\pm 1, \pm 1)^{\pm}$, considering that one of these points belongs to a side of the square merging with the vertex, and the other point belongs to the other side of the square, merging with this same vertex. The graph Y can be realized as a subset of $\mathbb{R}^3$, made up of six segments:

$Y = \{(0, x_2, 0) : x_2 \in [-1, 1]\} \cup \{(x_1, 0, 0) : x_1 \in [-1, 1]\} \cup \{(-1, x_2, x_2) : x_2 \in [-1, 1]\}$
$\cup \{(1, x_2, -x_2)x_2 \in [-1, 1]\} \cup \{(x_1, -1, -x_1) : x_1 \in [-1, 1]\} \cup \{(x_1, 1, x_1) : x_1 \in [-1, 1]\}$.

For such a realization of the graph, we obtain that :

$$(\pm 1, \pm 1)^{\pm} = (\pm 1, \pm 1, \pm 1) \in Y$$

The choice of signs is such that if we go through the sides of the square in a counter-clockwise direction (direct direction) from each vertex, we pass from the point $(\pm 1, \pm 1)^-$ to the point $(\pm 1, \pm 1)^+$. The function $a \in \mathcal{C}(X)$ naturally gives a function $\tilde{a}(x_1, x_2, x_3) = a(x_1, x_2)$ continuous on Y and

$$\tilde{a}((\pm 1, \pm 1)^+) = \tilde{a}((\pm 1, \pm 1)^-)$$

The graph of Y contains no trivial laces, so for the function $\tilde{a}$ on Y there is a continuous determination of the logarithm. As the regularization question reduces to the case where $|a(x)| \equiv 1$, for this case we obtain $\tilde{a}(x) = \mathrm{e}^{i2\pi\psi(x)}$ and the difference

$$\chi(a; (\pm 1, \pm 1)) = \psi((\pm 1, \pm 1)^-) - \psi((\pm 1, \pm 1)^-)$$

is an integer. For the space X, we have four Cauchy indexes $\psi(a; (\pm 1, \pm 1))$, representing topological invariants. The reducibility of the operator depends on these topological invariants; this dependence for different applications has various characteristics.

Theorem 5.1 *Let α be an application with respect to the diagonal $x_1 = x_2$, i.e. $\alpha(x_1, x_2) = (x_1, x_2)$. The operator $B = aT_\alpha$ on X is reducible to an operator with an invariant coefficient if and only if the three conditions are satisfied:*

1) The number $\psi(a; (1, 1))$ is even

2) The number $\psi(a; (-1, 1))$ is even

3) The number $\psi(a; (-1, 1)) + \psi(a : (1, -1))$ is even.

Proof: Since on Y there exists a continuous determination of the logarithm of the function *tildea* on Y, then for this function and by virtue of Theorem 3.1, there exists a factorisation with displacement:

$$\tilde{a}(x) = \tilde{a_0}(x)\frac{\tilde{d}(\alpha(x))}{\tilde{d}(x)} \tag{5.1}$$

Here the α application has period 2, and the T_α operator generates a representation of the $\mathbb{Z}_2$ group. This group has only two irreducible representations.

$$\tilde{a}_0(x) = e^{i2\pi\xi(x)}, \quad \xi(x) = \frac{1}{2}\left[\psi(x) + \psi(\alpha(x))\right] \tag{5.2}$$

$$\tilde{d}(x) = e^{i2\pi\varphi(x)}, \quad \varphi(x) = \frac{-1}{4}\left[\psi(x) - \psi(\alpha(x))\right] \tag{5.3}$$

The invariant function $\tilde{a_0}$ on Y generates on X a continuous invariant function $a_0(x_1, x_2) = \tilde{a}(x_1, x_2, x_3)$ if and only if:

$$\tilde{a_0}((\pm 1, \pm 1)^+) = \tilde{a_0}((\pm 1, \pm 1)^-)$$

This condition is satisfied if, and only if, the jump of the function ξ at each of the four points $(\pm 1, \pm 1)$ is an integer. Let us denote by $K(\xi; (\pm 1, \pm 1))$ the jump of the function ξ at the point $(\pm 1, \pm 1)$.
The function ξ is continuous at the points $(1, 1)$ and $(-1, -1)$ i.e.

$$K(\xi, (1, 1)) = K(\xi, (-1, -1)) = 0$$

The calculation shows that

$$K(\xi, (-1, 1)) = K(\xi, (1, -1)) = \frac{1}{2}\left[\chi(a; (-1, 1)) - \chi(a; (1, -1))\right]$$

Thus, the condition of continuity of the function a_0 is the parity of the number $\chi(a; (-1, 1)) - \chi(a; (1, -1))$. Similarly, the function $\tilde{d}$ generates a continuous function d on X, if

$$\tilde{d}((\pm 1, \pm 1)^+) = \tilde{d}((\pm 1, \pm 1)^-)$$

This condition is fulfilled if and only if the jump $K(\varphi; (\pm 1, \pm 1))$ of the function *varphi* at each point of $(\pm 1, \pm 1)$ is an integer. The calculation shows that these jumps are numbers:

$K(\varphi; (1, 1)) = K(\xi; (1, 1) = 0$
$K(\varphi; (-1, 1)) = 0$
$K(\varphi; (-1, 1)) = 0.\frac{1}{2}[\chi(a; (-1, 1)) - \chi(a; (1, -1))]$
$K(\varphi; (1, -1)) = 0$

Thus, the condition of continuity of the function a_0 is the parity of the number $\chi(a; (-1, 1)) - \chi(a; (1, -1))$. Similarly, the function *tilded* generates a continuous function d on X, if

$$\tilde{d}((\pm 1, \pm 1)^+) = \tilde{d}((\pm 1, \pm 1)^-).$$

This condition is met if, and only if, the jump of the function ξ at each point of $(\pm 1, \pm 1)$ is an integer. These jumps are the numbers :

$K(\xi; (-1,1)) = \frac{1}{2}[K(a; (-1,1)) - K(a; (1,-1))]$

$K(\xi; (1,-1)) = \frac{1}{2}[K(a; (-1,1)) - K(a; (1,-1))]$ and the theorem is proved.

We note that, from the formula (5.2), we have

$$a_0(x) = [a(x)a(\alpha(x))]^{\frac{1}{2}}$$

and that the conditions of the theorem are only the existence of a continuous determination on X of the square root.

From the formula (5.3) we obtain that

$$d_0(x) = \left[\frac{a(x)}{a(\alpha(x))}\right]^{\frac{1}{2}}$$

Moreover, the conditions of the theorem are the existence conditions of a continuous determination on X of the fourth root.

Acknowledgement

One of the authors, Serigne Aliou LO, would like to express his gratitude to the BTY Chair of Functional Analysis for all the attention paid to him during his stay at Belarus State University.

References

[1] A. B. Antonevich. *Linear functional Equations. Operator approach.* Universitetskoe, Minsk, 1988, 231 p.[in Russian]

[2] A. Katok A., B. Hasselblatt.*Introduction to the modern theory of dynamical systems.*Cambridge. Cambridge University Press.1998.

[3] N. Karapetiants and S. Samko. *Equation with involutive operators.*Birkhäuser Boston, 2001.

[4] V. G. Kravchenko and G. S. Litvinchuk. *Introduction to the theory of singular integral operators with shift.* Dordrecht. Kluver Acad. Publ. 1994.

[5] Erougin N.P. *Systèmes réductibles.* Moscou-Leningrad,1946. Tr.Matem.in ta AH SSSR, T.13(traduit du russe).

[6] Ahocob D. B. *Équations homologiques fonctionnelles additives liées à une rotation ergodique du cercle.* IZV. AN.SSSR. série Mat. T.37 (1973) N° 6, 1259-1274.(traduit du russe)

[7] Gordon A.Y. *Condition nécessaire de non solvabilité d'une équation homologique fonctionnelle additive, liée à une rotation ergodique du cercle.* Analyse Fonctionnelle et applications.Appl. T.9(1975). 71-72. (traduit russe)

[8] Serigne Aliou LO and Moussa O.A.Salem. *Conditions d'algébricité d'un opérateur de déplacement pondéré engendré par une application potentiellement périodique.* Conf. NAN Biélorussie 2011. T.55 N° 3, p. 17-20(traduit du russe).

[9] D. Przeworska and D. Rolewicz.*Equations with transformed argument* Elsevier Scientific Publ. Comp. and Polish Scientific Publishers,Amsterdam and WARSAW 1973.

[10] A. Bottcher and H. Heidler. *Algebraic compositions operators.* Integral equations and operator theory 15 (1992), 389-411.

[11] G.Belitskii and Y.Lyubich. *On the normal solvability of cohomological equations on topological spaces.* Operator theory: Advances and applications 103, 75-87 (1998).

[12] Gelobenko D.P. *Introduction à la Théorie des représentations* . Moscou: Presse Factorielle, 2001. 136 p.(traduit du russe)

FEW-SHOT LEARNING MEETS EXPLAINABLE AI: TOWARDS SMARTER ANOMALY DETECTION

Erhan YILMAZ [1,2]

[1] Department of Computer Engineering, Graduate School of Natural and Applied Sciences, Ege University, Izmir, Turkiye

[2] Kron Technologies, Izmir, Turkiye

erhan.yilmaz@itu.edu.tr

Özgü CAN [1]

[1] Department of Computer Engineering, Ege University, Izmir, Turkiye

ozgu.can@ege.edu.tr

Abstract

Anomaly detection in cybersecurity is essential for recognizing anomalies that indicate risks, including network intrusions and insider attacks. However, it faces significant challenges, including limited labeled data and the necessity for transparent decision-making. This study examines the integration of few-shot learning (FSL) and explainable AI (XAI) to address these issues by synthesizing recent advancements and proposing future research directions. FSL approaches, including gated networks, meta-learning, and Siamese architectures, effectively generalize from limited labeled examples, demonstrating success across diverse datasets. Concurrently, XAI fosters user trust, compliance, and actionable insights through techniques such as feature-attribution (e.g., SHAP, LIME), attention mechanisms, and deviation-based learning, providing clear rationales behind anomaly detections. Therefore, this study highlights contemporary trends in data-efficient FSL models and interpretable XAI methods, outlining essential future directions: enhancing generalizability to unseen anomaly classes, scaling frameworks to manage diverse datasets, and developing inherently interpretable models. Integrating solutions for data scarcity with improved interpretability represents a promising trajectory toward building resilient, transparent, and reliable cybersecurity frameworks, capable of effectively responding to the rapidly evolving landscape of cyber threats.

Keywords: *anomaly detection, cybersecurity, few-shot learning, explainable artificial intelligence* .

1. INTRODUCTION

Anomaly detection in cybersecurity is recognizing activity patterns that significantly deviate from expected behavior, whether in network traffic, database queries, or user actions, to reveal breaches, fraud, and other nefarious activities. In recent years, high-profile data breaches have underscored both the frequency and sophistication of cyberattacks: Verizon’s 2024 Data Breach Investigations Report documents over 10,000 confirmed breaches worldwide in a single year, with web-application exploits and stolen credentials among the most common initial vectors (Verizon, 2024). Incidents involving insider threats, in which authorized users misuse their privileges, cost an average of $17.4 million and take more than 80 days to contain (Ponemon Institute & DTEX Systems, 2025).

Traditional supervised detectors often rely on large volumes of labeled attack examples, yet acquiring representative samples for every threat type is impractical in dynamic environments (Guo & Zhao, 2008). Unsupervised methods can flag deviations without labels but frequently suffer high false-alarm rates and offer little guidance on remediation (Bo Liu et al., 2014). Semi-supervised and weakly-supervised approaches that leverage a handful of known anomalies alongside abundant unlabeled data have demonstrated promising gains in both accuracy and robustness. For instance, pairwise-relation networks learn discriminative patterns by contrasting anomalous and normal pairs, thereby extending detection to novel attack classes unseen during training (Pang et al., 2023).

Transparency is equally significant, since cybersecurity analysts need to understand the rationale behind a model's decision to flag a session or transaction as suspicious, enabling them to validate alerts, meet compliance requirements, and effectively respond to incidents (Drugan, 2016). By utilizing attention and feature-attribution algorithms, the signs that support anomaly scores can be revealed, which can strengthen analyst confidence. These indicators may include unexpected command sequences or file-access patterns (Bin Sarhan & Altwaijry, 2022).

This study examines the convergence of few-shot learning (FSL) paradigms, which seek to generalize from limited labeled instances, with explainable AI (XAI) techniques in the context of cybersecurity anomaly detection. This study analyzes key architectures and investigates the potential of post-hoc and inherently interpretable mechanisms to enhance the actionability of model outputs. The main goal of the study is to synthesize current advances, identify gaps in deploying data-efficient, transparent detectors in real-world cyber-defense, and outline directions for research that can meet the twin challenges of scarce labels and the imperative for explainability.

The remainder of this paper is organized as follows: Section 2 examines the implementation of FSL in anomaly detection, analyzing diverse approaches and their efficacy in contexts with limited labeled data. Section 3 focuses on XAI techniques, discussing feature-attribution methods, attention-based explanations, and other strategies that enhance the interpretability of anomaly detection models. Section 4 examines the integration of FSL and XAI, highlighting how these approaches can be combined to create more transparent and efficient anomaly detection systems. Section 5 discusses future research directions, emphasizing the need for enhanced data efficiency, scalability, and generalizability in FSL methods, as well as the importance of developing inherently interpretable models in XAI. Finally, Section 6 concludes the paper by summarizing the key findings and the potential of integrating FSL and XAI in addressing the challenges of cybersecurity anomaly detection.

2. FEW-SHOT LEARNING IN ANOMALY DETECTION

FSL has emerged as an innovative approach to anomaly detection, particularly valuable when limited labeled data is available. Traditional anomaly detection methods typically require extensive labeled datasets for training, a condition often impractical due to the scarcity of anomalous data. FSL methods address this limitation by effectively leveraging minimal examples to generalize to unseen anomaly classes (Yu & Bian, 2020).

The gated FSL technique that Huang et al. (2020) presented was created especially to deal with issues brought on by an imbalance in data between known and unknown anomaly classes. Their gated network structure facilitates the aggregation of known anomaly types with novel, unseen anomalies, significantly enhancing anomaly detection performance under few-shot conditions. Experiments conducted on the NSL-KDD dataset highlighted the model's superior capability in detecting new types of anomalies using limited labeled data.

Another application by Yu & Bian (2020) demonstrated a FSL-based intrusion detection system achieving remarkable accuracy with less than 1% of training data compared to traditional methods. Their approach employed balanced resampling and an adapted deep neural network architecture, significantly improving detection rates, especially for rare anomaly classes such as User-to-Root (U2R) and Remote-to-Local (R2L) attacks.

Moreover, Ding et al. (2021) expanded the few-shot anomaly detection paradigm by introducing cross-network meta-learning. Their Graph Deviation Network (GDN), combined with a meta-learning framework, effectively transferred anomaly detection knowledge from auxiliary networks. This method leveraged labeled anomalies from related networks to significantly enhance the detection capability in target networks with few or even one labeled anomaly sample.

Feng et al. (2021) also contributed significantly by developing a Few-shot Class-adaptive Anomaly Detection (FCAD) framework that employs Model-Agnostic Meta-Learning (MAML). Their system effectively extracted statistical, and time-series features from encrypted network traffic, demonstrating strong generalization abilities for unseen anomaly classes during testing phases.

Yuan et al. (2020) explored the domain of insider threat detection through a novel few-shot approach, combining self-supervised pre-training and metric-based learning. They effectively captured activity-type and time information from audit logs to pre-train models, subsequently fine-tuning them with limited malicious session data to accurately identify insider threats.

Bovenzi et al. (2024) addressed IoT-specific security challenges through FSL, demonstrating how advanced deep learning architectures could substantially enhance the classification accuracy of IoT attack traffic, even when limited labeled data were available. Their comprehensive empirical evaluations across diverse attack scenarios further emphasized FSL's practical applicability in IoT environments.

Additionally Gong et al. (2020) introduced a meta-learning approach for user profiling, leveraging time-heatmap encodings to capture temporal and behavioral patterns. This technique excelled at few-shot personalization, demonstrating robust performance under conditions of data imbalance and distribution shifts. The method was evaluated on internal Rakuten user behavior datasets, where it effectively adapted to unseen user behaviors with minimal labeled data.

Lastly, Zhou et al. (2022) presented a Siamese Few-Shot Learning (SFSL) architecture, enhanced by an improved contrastive loss function, to tackle insider threat detection. Their approach focused on addressing dataset imbalance by employing pairs classification, which allowed the model to distinguish between normal and malicious activity with limited labeled examples.

In summary, FSL has provided robust solutions for anomaly detection challenges stemming from scarce labeled data. Traditional machine learning approaches often rely extensively on large datasets with sufficient labeled examples to train accurate models, which can be a substantial obstacle in scenarios where labeled data is limited or difficult to obtain. FSL addresses this challenge by enabling models to effectively learn from a small number of labeled instances, thus significantly reducing the dependency on large datasets. This capability is particularly valuable in real-world cybersecurity applications, where the costs and time associated with labeling data can be restrictive. By leveraging FSL, anomaly detection systems can identify previously unseen threats and detect rare or emerging attacks that may not be well-represented in the training data. The integration of FSL into anomaly detection methodologies has proven to enhance the accuracy and robustness of these systems, making them more adaptable and efficient in dynamic and data-constrained environments. Consequently, FSL is becoming increasingly indispensable in various cybersecurity contexts, such as intrusion detection, fraud prevention, and network security, where rapid identification of anomalies is crucial. The ability of FSL to generalize from a few examples offers considerable promise for improving the scalability and effectiveness of anomaly detection mechanisms in real-world settings. As a result, the literature highlights the substantial potential of FSL in diverse cybersecurity contexts, significantly enhancing anomaly detection capabilities in real-world applications.

3. EXPLAINABLE AI IN ANOMALY DETECTION

In safety-critical and mission-critical applications such as healthcare monitoring, financial fraud prevention, and industrial control, the mere identification of anomalies is insufficient without insight into why a model has flagged a particular instance. XAI techniques address this need by translating opaque detection scores into human-interpretable rationales, thereby fostering user trust, facilitating root-cause analysis, and guiding effective remediation (Li et al., 2024; Salih et al., 2025).

3.1.Feature-Attribution Methods

Feature-attribution methods are a cornerstone of XAI, particularly in anomaly detection. These techniques aim to quantify the contribution of individual features to the anomaly score produced by a model. These methods are as follows:

- **SHAP (SHapley Additive exPlanations):** SHAP employs cooperative game theoretic Shapley values to quantify each feature's marginal contribution to an anomaly score. By averaging contributions over all possible feature coalitions, SHAP delivers both local (per instance) and global (dataset wide) explanations (Salih et al., 2025). In cybersecurity contexts, SHAP has been used to dissect complex ensemble and deep models—such as tree based classifiers and recurrent neural networks—revealing which traffic features or log events drive anomaly detections (Alenezi & Ludwig, 2021; Zou & Petrosian, 2020).

- **LIME (Local Interpretable Model Agnostic Explanations):** LIME constructs a sparse surrogate model—typically linear—around a single prediction by perturbing inputs and observing output changes. The resulting feature weights indicate their local influence on anomaly flags. While highly flexible and model-agnostic, LIME's linear approximation may overlook nonlinear interactions intrinsic to many anomaly detectors (Lee et al., 2024; Salih et al., 2025).

3.2.Attention-Based Explanations

Attention mechanisms, when integrated into sequence models (e.g., LSTMs or Transformers), inherently highlight the temporal or spatial regions most influential in triggering an anomaly alert. For instance, in Exathlon's benchmark for multivariate time series anomaly detection, attention weights have been leveraged to pinpoint root cause intervals within high dimensional streams, offering direct, model internal explanations without post hoc surrogates (Jacob et al., 2021).

3.3.Post Hoc Perturbation and Prototype Based Methods

XAI that relies on perturbation methods, such as LIME, can employ prototype-focused strategies. These strategies allow for the comparison of unusual instances with examples that are considered "normal". In the context of few shot anomaly detection, Siamese network explainers perturb input features to assess their effect on learned similarity metrics, thereby isolating feature combinations that most discriminate anomalies from normal samples (Fedele et al., 2024).

3.4.Prior-Driven Anomaly Score Learning

Weakly-supervised frameworks such as Deviation Networks integrate Shapley-inspired attributions directly into the training of anomaly scores. By enforcing normal samples to follow a chosen prior distribution and pushing labeled anomalies into the upper tail, these models yield anomaly scores that are inherently interpretable: deviations from the prior directly signal anomalousness, and feature-level gradients can be traced back to input dimensions (Pang et al., 2021).

4. INTEGRATION OF FEW-SHOT LEARNING AND EXPLAINABLE AI

The convergence of few-shot learning and explainable artificial intelligence (XAI) in anomaly detection research represents a significant advancement in addressing two critical challenges: data scarcity and model interpretability. Several recent studies have explored this intersection, developing methodologies that not only generalize from limited labeled data but also offer transparent, human-interpretable explanations of anomaly detection decisions.

A primary method is enhancing FSL frameworks using post-hoc explanation strategies. For example, in remote sensing applications, researchers have integrated few-shot classifiers with attention mechanisms and prototype analysis to not only detect rare or novel anomalies (such as invasive species or environmental changes) but also to highlight the key features that drive these decisions. This integration has proven particularly valuable in domains where obtaining large, annotated datasets is impractical. In such settings, explainable few-shot workflows enable models to generalize from minimal examples while simultaneously providing interpretable evidence for each prediction (Lee et al., 2024).

A common technique involves the integration of specialized network structures, such as Siamese networks, within the few-shot paradigm. These architectures are designed to learn discriminative representations that can differentiate subtle variations between normal and anomalous instances. By embedding attention modules within these networks, researchers have been able to derive visual or quantitative explanations that pinpoint which aspects of an input most strongly influenced the detection outcome. Such integrated systems facilitate a deeper understanding of the underlying decision processes, thereby enhancing trust and offering actionable insights for human analysts (Fedele et al., 2024).

Innovative methodologies also emerge from the fusion of deviation-based learning and explainability. In these approaches, anomaly scores are derived by contrasting the representations of normal samples—modeled under an assumed prior distribution—with those of anomalies. This deviation framework not only enhances detection performance under few-shot conditions but also inherently provides a rationale for why a particular sample deviates from expected behavior. The resulting explanations, often presented through gradient or Shapley-value analyses, offer a direct link between the detected anomaly and its contributing features, addressing the interpretability challenge head on (Pang et al., 2021).

Themes that frequently arise in the academic literature highlight the importance of employing attention mechanisms, the use of substitute models for local explanations, and the investigation of metric-learning frameworks suitable for both few-shot learning and post-hoc interpretability (Cholopoulou & Iakovidis, 2024; Meng et al., 2023). The integration of these approaches not only mitigates the challenges posed by limited labeled data but also empowers stakeholders by elucidating the inner workings of complex detection models (Adadi & Berrada, 2018). This dual benefit is particularly crucial in critical applications, where understanding the "why" behind an anomaly detection decision can be as important as the decision itself (J. Feng et al., 2021).

In summary, the integration of few-shot learning with XAI techniques in anomaly detection reflects a promising research direction. By combining the strengths of data-efficient learning with robust interpretability methods, recent studies have laid the groundwork for more transparent, trustworthy, and practical anomaly detection systems. Such systems are better equipped to operate in real-world scenarios characterized by scarce labels and a high demand for decision transparency.

5. FUTURE TRENDS AND DIRECTIONS

Anomaly detection in cybersecurity is crucial for identifying deviations from expected behavior, such as network intrusions and insider threats, especially given the increasing sophistication of cyberattacks. The lack of labeled data for new risks has sparked a growing interest in FSL techniques. Additionally, the demand for transparency has highlighted the importance of XAI. This section elaborates on the prior discussion regarding FSL and XAI, highlighting potential future research directions.

Future research in FSL for anomaly detection should focus on enhancing data efficiency and generalizability. One key direction is improving models to handle small training sets that do not contain all anomaly classes, as suggested by Pang et al. (2023) particularly noting the need for methods that can identify anomalies based on very few known class examples. This includes advancing domain adaptation mechanisms, as proposed by Komisarek et al. (2022) to leverage multi-domain network-flow-based knowledge transfer, extracting general patterns to improve model decision boundaries across domains.

Scaling FSL frameworks is another critical area. Aharon et al. (2025) suggests future work in optimizing ANN search for larger datasets and handling multiple baselines concurrently (e.g., API endpoints, domains), which could enhance scalability and adaptability to evolving threats. Additionally, integrating techniques like self-supervised pre-training, as explored by Yuan et al. (2020) could further enhance FSL by leveraging unlabeled data, potentially improving detection of novel anomalies.

The integration of advanced XAI techniques is essential for future anomaly detection systems. Research should focus on designing inherently interpretable models, moving beyond post-hoc explanations. Future work could explore attention mechanisms and feature attribution methods, such as SHAP or LIME, to highlight key factors contributing to anomaly scores, as suggested by Salih et al. (2025). This would enhance transparency, foster user confidence and facilitating effective incident response, particularly in critical applications where understanding the "why" behind detections is as important as the detection itself. Moreover, as cyber threats become more complex, future research should address the trustworthiness and fairness of XAI models, ensuring compliance with ethical standards. This includes developing methods to identify and mitigate biases, as highlighted by (Zhao et al., 2025) which discusses the use of large language models (LLMs) for anomaly detection in tabular cybersecurity data, emphasizing zero-shot and few-shot scenarios.

The convergence of FSL and XAI in anomaly detection represents a promising research direction for cybersecurity. Current trends highlight the development of data-efficient frameworks and the integration of interpretable models, while future directions focus on enhancing scalability, generalizability, and transparency. By mitigating the lack of data and improving model interpretability, these improvements can promote the creation of resilient and reliable systems. These systems will be effective in countering advanced cyber threats, therefore responding to the current and progressive demands of the domain.

6. CONCLUSIONS

This study explores the integration of FSL and XAI within cybersecurity anomaly detection, highlighting their combined potential in addressing critical challenges posed by limited labeled data and the necessity for interpretability. Few-shot learning techniques have shown considerable promise in effectively identifying anomalies from minimal labeled examples, overcoming traditional limitations in supervised and unsupervised anomaly detection methods. Approaches such as gated networks, meta-learning, and Siamese architectures have demonstrated impressive adaptability, particularly in scenarios where anomalous instances are scarce or evolve rapidly.

Simultaneously, the integration of XAI techniques into these few-shot methodologies has proven essential for translating complex, data-driven anomaly detections into actionable insights. Methods like SHAP, LIME, attention mechanisms, and prototype-based explanations have provided valuable transparency into model decision-making processes, significantly improving analyst confidence, supporting effective incident responses, and meeting regulatory compliance demands.

As a result, the future research directions should focus on further enhancing data efficiency, scalability, and generalizability of FSL methods while refining the interpretability of detection outputs. Efforts toward inherently explainable models rather than relying solely on post-hoc explanations will be increasingly critical as cybersecurity threats grow more sophisticated. Furthermore, addressing ethical concerns, fairness, and bias in anomaly detection models will be pivotal to maintaining stakeholder trust and compliance.

The integration of FSL and XAI presents a robust framework for the development of advanced and transparent anomaly detection systems. These integrated methodologies not only enhance cybersecurity resilience against emerging threats but also enable proactive and informed decision-making processes in real-world operational contexts.

7. ACKNOWLEDGEMENTS

This study is supported by The Scientific and Technological Research Council of Türkiye (TÜBİTAK) under grant number 125E156.

REFERENCES

1. Adadi, A., & Berrada, M. (2018). Peeking Inside the Black-Box: A Survey on Explainable Artificial Intelligence (XAI). *IEEE Access*, *6*, 52138–52160. https://doi.org/10.1109/ACCESS.2018.2870052

2. Aharon, U., Dubin, R., Dvir, A., & Hajaj, C. (2025). A classification-by-retrieval framework for few-shot anomaly detection to detect API injection. *Computers & Security*, *150*, 104249. https://doi.org/10.1016/j.cose.2024.104249

3. Alenezi, R., & Ludwig, S. A. (2021). Explainability of Cybersecurity Threats Data Using SHAP. *2021 IEEE Symposium Series on Computational Intelligence (SSCI)*, 01–10. https://doi.org/10.1109/SSCI50451.2021.9659888

4. Bin Sarhan, B., & Altwaijry, N. (2022). Insider Threat Detection Using Machine Learning Approach. *Applied Sciences*, *13*(1), 259. https://doi.org/10.3390/app13010259

5. Bo Liu, Yanshan Xiao, Yu, P. S., Zhifeng Hao, & Longbing Cao. (2014). An Efficient Approach for Outlier Detection with Imperfect Data Labels. *IEEE Transactions on Knowledge and Data Engineering*, *26*(7), 1602–1616. https://doi.org/10.1109/TKDE.2013.108

6. Bovenzi, G., Di Monda, D., Montieri, A., Persico, V., & Pescapè, A. (2024). Classifying attack traffic in IoT environments via few-shot learning. *Journal of Information Security and Applications*, *83*, 103762. https://doi.org/10.1016/j.jisa.2024.103762

7. Cholopoulou, E., & Iakovidis, D. K. (2024). *MeLIAD: Interpretable Few-Shot Anomaly Detection with Metric Learning and Entropy-based Scoring* (Version 1). arXiv. https://doi.org/10.48550/ARXIV.2409.13602

8. Ding, K., Zhou, Q., Tong, H., & Liu, H. (2021). Few-shot Network Anomaly Detection via Cross-network Meta-learning. *Proceedings of the Web Conference 2021*, 2448–2456. https://doi.org/10.1145/3442381.3449922

9. Drugan, M. M. (2016). A Bayesian model for anomaly detection in SQL databases for security systems. *2016 IEEE Symposium Series on Computational Intelligence (SSCI)*, 1–8. https://doi.org/10.1109/SSCI.2016.7849905

10. Fedele, A., Guidotti, R., & Pedreschi, D. (2024). Explaining Siamese networks in few-shot learning. *Machine Learning*, *113*(10), 7723–7760. https://doi.org/10.1007/s10994-024-06529-8

11. Feng, J., Liang, Y., & Li, L. (2021). Anomaly Detection in Videos Using Two-Stream Autoencoder with Post Hoc Interpretability. *Computational Intelligence and Neuroscience*, *2021*(1), 7367870. https://doi.org/10.1155/2021/7367870

12. Feng, T., Qi, Q., Wang, J., & Liao, J. (2021). Few-Shot Class-Adaptive Anomaly Detection with Model-Agnostic Meta-Learning. *2021 IFIP Networking Conference (IFIP Networking)*, 1–9. https://doi.org/10.23919/IFIPNetworking52078.2021.9472814

13. Gong, H., Zhao, Q., Li, T., Cho, D., & Nguyen, D. (2020). Learning to Profile: User Meta-Profile Network for Few-Shot Learning. *Proceedings of the 29th ACM International Conference on Information & Knowledge Management*, 2469–2476. https://doi.org/10.1145/3340531.3412722

14. Guo, S.-Q., & Zhao, Z.-H. (2008). An Anomaly Intrusion Detection Model Based on Limited Labeled Instances. *2008 International Symposium on Electronic Commerce and Security*, 283–287. https://doi.org/10.1109/ISECS.2008.26

15. Huang, S., Liu, Y., Fung, C., An, W., He, R., Zhao, Y., Yang, H., & Luan, Z. (2020). A Gated Few-shot Learning Model For Anomaly Detection. *2020 International Conference on Information Networking (ICOIN)*, 505–509. https://doi.org/10.1109/ICOIN48656.2020.9016599

16. Jacob, V., Song, F., Stiegler, A., Rad, B., Diao, Y., & Tatbul, N. (2021). *Exathlon: A Benchmark for Explainable Anomaly Detection over Time Series* (arXiv:2010.05073). arXiv. https://doi.org/10.48550/arXiv.2010.05073

17. Komisarek, M., Kozik, R., Pawlicki, M., & Choraś, M. (2022). Towards Zero-Shot Flow-Based Cyber-Security Anomaly Detection Framework. *Applied Sciences*, *12*(19), 9636. https://doi.org/10.3390/app12199636

18. Lee, G. Y., Dam, T., Ferdaus, Md. M., Poenar, D. P., & Duong, V. N. (2024). Unlocking the capabilities of explainable few-shot learning in remote sensing. *Artificial Intelligence Review*, *57*(7), 169. https://doi.org/10.1007/s10462-024-10803-5

19. Li, Z., Zhu, Y., & Van Leeuwen, M. (2024). A Survey on Explainable Anomaly Detection. *ACM Transactions on Knowledge Discovery from Data*, *18*(1), 1–54. https://doi.org/10.1145/3609333

20. Meng, Y., Lu, K.-C., Dong, Z., Li, S., & Shao, C. (2023). Explainable few-shot learning for online anomaly detection in ultrasonic metal welding with varying configurations. *Journal of Manufacturing Processes*, *107*, 345–355. https://doi.org/10.1016/j.jmapro.2023.10.047

21. Pang, G., Ding, C., Shen, C., & Hengel, A. van den. (2021). *Explainable Deep Few-shot Anomaly Detection with Deviation Networks* (arXiv:2108.00462). arXiv. https://doi.org/10.48550/arXiv.2108.00462

22. Pang, G., Shen, C., Jin, H., & Hengel, A. van den. (2023). *Deep Weakly-supervised Anomaly Detection* (arXiv:1910.13601). arXiv. https://doi.org/10.48550/arXiv.1910.13601

23. Ponemon Institute & DTEX Systems. (2025). *Cost of Insider Risks Global Report*.

24. Salih, A. M., Raisi-Estabragh, Z., Galazzo, I. B., Radeva, P., Petersen, S. E., Lekadir, K., & Menegaz, G. (2025). A Perspective on Explainable Artificial Intelligence Methods: SHAP and LIME. *Advanced Intelligent Systems*, *7*(1), 2400304. https://doi.org/10.1002/aisy.202400304

25. Verizon. (2024). *2024 Data Breach Investigations Report*.

26. Yu, Y., & Bian, N. (2020). An Intrusion Detection Method Using Few-Shot Learning. *IEEE Access*, *8*, 49730–49740. https://doi.org/10.1109/ACCESS.2020.2980136

27. Yuan, S., Zheng, P., Wu, X., & Tong, H. (2020). Few-shot Insider Threat Detection. *Proceedings of the 29th ACM International Conference on Information & Knowledge Management*, 2289–2292. https://doi.org/10.1145/3340531.3412161

28. Zhao, X., Leng, X., Wang, L., Wang, N., & Liu, Y. (2025). Efficient anomaly detection in tabular cybersecurity data using large language models. *Scientific Reports*, *15*(1), 3344. https://doi.org/10.1038/s41598-025-88050-z

29. Zhou, S., Wang, L., Yang, J., & Zhan, P. (2022). SITD: Insider Threat Detection Using Siamese Architecture on Imbalanced Data. *2022 IEEE 25th International Conference on Computer Supported Cooperative Work in Design (CSCWD)*, 245–250. https://doi.org/10.1109/CSCWD54268.2022.9776049

30. Zou, J., & Petrosian, O. (2020). Explainable AI: Using Shapley Value to Explain Complex Anomaly Detection ML-Based Systems. In A. J. Tallón-Ballesteros & C.-H. Chen (Eds.), *Frontiers in Artificial Intelligence and Applications*. IOS Press. https://doi.org/10.3233/FAIA200777

DETECTION of the E-COMMERCE CREDIT CARD FRAUD with DATA MINING

Khayyam Heydarov[1]

Şükrü Kitiş[2*]

[1]Kütahya Dumlupınar University, Postgraduate Education Institute, Kütahya

khayyam.heydarov0@ogr.dpu.edu.tr

[2*]Kütahya Dumlupınar University, Simav Technology Faculty, Kütahya

sukru.kitis@dpu.edu.tr

Abstract

In this study, a machine learning-based framework was developed to identify fraudulent credit card transactions using a dataset containing 1,615 purchase records obtained from an e-commerce company. Feature selection techniques including GainRatio, InfoGain, and Chi-Squared were applied, and classification was carried out using various algorithms such as K-Nearest Neighbors (KNN), Naive Bayes, J48, NBTree, Radial Basis Function (RBF) Network, and Artificial Neural Networks (ANN) within the WEKA software environment. Among the four distinct feature sets examined, the combination of the B attribute set with the KNN algorithm achieved the highest F1-score, with a success rate of 95.75%. The findings suggest that traditional and cost-efficient approaches can yield results that rival more complex deep learning methods. This underlines the model's practical effectiveness and its suitability for integration into real-time fraud detection systems.

Keywords: Data Mining, Credit Card Fraud, E-Commerce, Classification Algorithms, WEKA

1.INTRODUCTION

According to the 14th annual report by CyberSource, a Visa subsidiary, approximately 0.9% of total online revenues are lost due to fraudulent activities, translating to an estimated $3.5 billion in losses across North America alone [1]. Additionally, a study by Aouada, Stojanovic, Ottersten, and Bahnsen found that the use of non-traditional payment systems such as mobile and internet-based channels has contributed to a 14% increase in fraud incidents since

2014, making detection and prevention more complex [2]. These developments indicate that fraudsters continually evolve their tactics, giving rise to new forms of deception. As such, fraud detection strategies must be tailored for each new dataset to remain effective.

In this context, the current study aims to develop a machine learning model capable of identifying fraudulent e-commerce transactions. The classification process adopted is primarily rule-based and semi-manual. Section 2 provides an overview of related academic studies; Section 3 introduces the dataset and explains the selected features; Section 4 presents the methodology and experimental results; and the final section summarizes the key findings and offers concluding remarks. All data analysis was conducted using the WEKA software platform (Version 3.8.4) [3].

While fraud detection in banking systems is relatively straightforward due to access to extensive customer data, e-commerce platforms face significant limitations in this regard. This data scarcity makes it more difficult to analyze user behavior and transaction legitimacy. Raj and Portia explored a variety of fraud detection methods and categorized them by algorithmic approach, including Bayesian learning, Hidden Markov Models, Artificial Neural Networks, and hybrid systems [4].

Chan proposed a cost-sensitive fraud detection framework that integrates multiple fraud detectors to enhance accuracy while managing operational cost [5]. Bhattacharyya et al. also contributed by combining Support Vector Machines (SVM), Random Forests, and Logistic Regression to effectively classify fraudulent activities [6].

Furthermore, Adepoju et al. assessed the applicability of supervised machine learning techniques on corrupted datasets to improve fraud detection accuracy [7]. Vidanelage et al. examined different classification models using Python's Scikit-learn library to uncover anomalies in transaction data [8]. Lastly, Seemakurthi et al. introduced a novel approach that employs text classification to identify fraud in financial documents [9].

2. GENERAL PROPERTIES OF METHOD

In this section, the dataset used for the study is introduced, followed by a brief explanation of the applied methods. The relational database structure utilized in the analysis is illustrated in Figure 1, while Table 1 outlines the list of selected attributes and their respective descriptions, all derived from the main order table.

In the context of data mining, the process of selecting relevant feature subsets plays a critical role in ensuring accurate and efficient analysis. As the volume and dimensionality of data grow, it becomes increasingly difficult to test and validate models effectively. Feature selection aims to reduce this complexity by identifying a minimal yet informative subset of attributes that contribute most to predictive accuracy. Including too few attributes may lead to information loss, while an excessive number of irrelevant features can introduce noise, complicate the model, and decrease classification performance. By removing unnecessary or redundant features, both the training time and accuracy of the classifiers can be improved, leading to more efficient model development [10].

This study employs three widely used statistical feature selection techniques—Gain Ratio, Chi-Squared, and Information Gain—to filter and rank the importance of input variables. These filtering methods help simplify the feature set prior to classification. All classification and performance evaluations were conducted using the WEKA data mining toolkit. For consistency and comparability, default parameter settings were used across all classifiers.

Information Gain Ratio

Information Gain Ratio is a standard metric in feature selection, designed to eliminate non-contributory variables. It works by calculating the entropy of the dataset and measuring the information gain for each attribute. Attributes with higher gain ratios are preferred, as they contribute more to predicting the target class. The method creates a decision subspace based on class entropy and ranks features according to their discriminative power [11].

Chi-Squared Test (χ^2 MapReduce)

The Chi-Squared method evaluates the statistical independence between an attribute and the target class. It determines whether the observed distribution of class labels differs significantly across attribute values. Attributes that show a strong dependency are considered valuable predictors for classification tasks [11].

Gain Ratio Feature Selection

This method builds on Information Gain by normalizing it with the intrinsic information of an attribute. It is particularly effective in mitigating the bias that occurs when attributes with many distinct values dominate the selection process. Gain Ratio is univariate, asymmetric, and entropy-based, and is widely used for its ability to balance information richness with attribute generality [11].

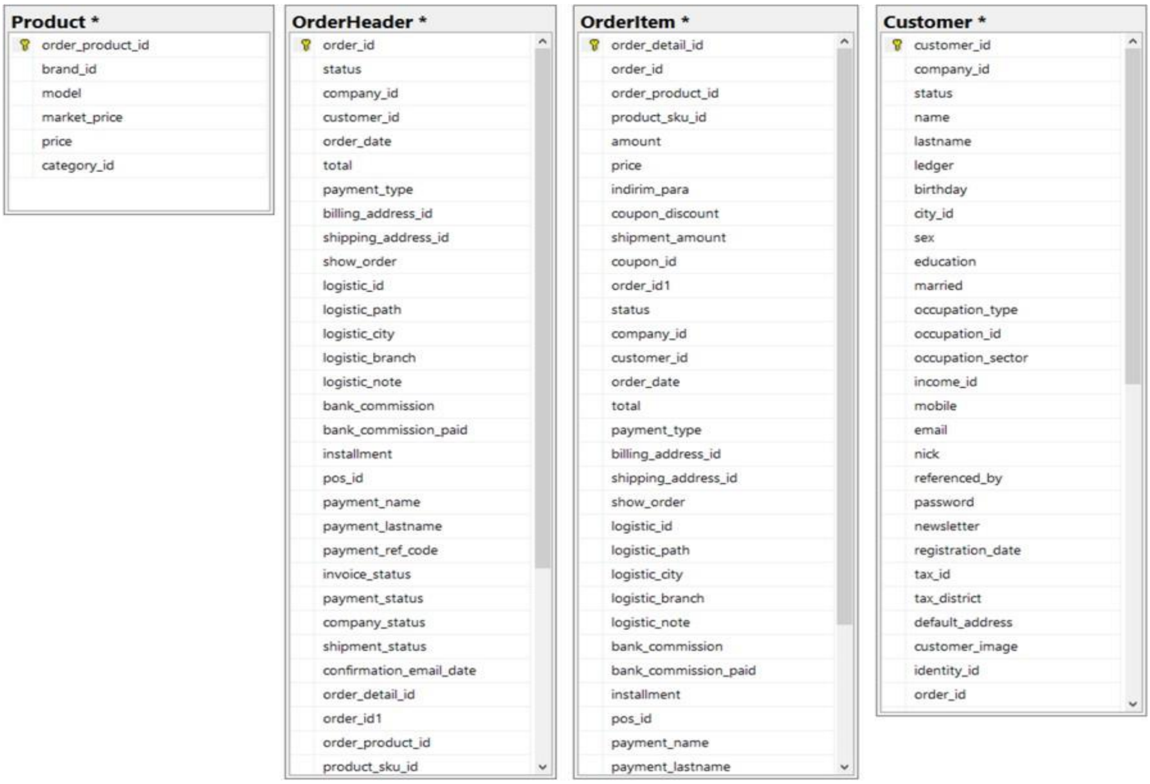

Figure 1. Relational Area and Tablos of E-Commerce Sites

Table 1. Impact of Attributes on Classification Based on Selection Methods

Variable Name	Meaning	GainRatio	ChiSquared	InfoGain
Total	Total purchase amount	2	1	1
Payment_ref_code	Bank response code	3	5	4
Amount	Product price	9	12	13
OrderHour	Order hour (normalized 1–24)	13	9	9
OrderDayOfWeek	Day of the order (1–7)	14	10	11
NameSurnameLen	Customer's name and surname length	1	2	2
Discount_money	Discount amount	15	15	15
Coupon_Discount	Coupon discount amount	16	16	16
Shipped_Amount	Shipping cost	8	11	10
CouponID	Coupon ID	17	17	17
EmailConfirmTime	Email confirmation time (1–24)	11	14	14
CustomerCityID	Customer city code	5	4	6
CustomerEmailFormat	Email format (classified by domain)	7	7	7
OrderBrandID	Product brand ID	6	6	5
CategoryID	Product category ID	4	3	3
CustomerAge	Customer’s age	10	8	8
Gender	Customer gender	12	12	12
IsFraud	Fraud label (0: genuine, 1: fraud)	Class Attribute	Class Attribute	Class Attribute

Table 1 summarizes the impact of each attribute on the classification performance, as determined by three different statistical feature selection techniques: GainRatio, Chi-Squared, and Information Gain. The rankings indicate the relative importance of each attribute in terms of its contribution to detecting fraudulent transactions. For instance, the attribute "NameSurnameLen" (length of customer's name and surname) received the top rank in GainRatio and a strong ranking in both Chi-Squared and InfoGain, suggesting a significant discriminative influence. Similarly, "Total" (total purchase amount) consistently ranked among the most influential features across all three methods. In contrast, features such as "CouponID" and "Discount_money" showed minimal impact on the classification and were ranked lowest.

These differences highlight how each selection method evaluates features based on distinct criteria—GainRatio balances information gain with entropy, Chi-Squared focuses on statistical independence, and InfoGain measures the reduction in uncertainty. By leveraging these rankings, the study aimed to reduce dimensionality without sacrificing predictive accuracy, thereby optimizing both model performance and processing efficiency [10][11].

2.1. Datasets and Methods

The dataset obtained from the e-commerce company originally contained 38 variables across 1,615 order records. The final column, labeled as "IsFraud", was defined by the company's IT department based on banking system flags. Following the application of the GainRatio feature selection method, several attributes with a high proportion of missing values were excluded. After this initial filtering, 17 features were retained for further analysis, as shown in Table 1.

Selecting the optimal set of attributes significantly influences model performance particularly in neural network-based classifiers since fewer attributes typically reduce computational load and improve efficiency [12]. To enhance the quality of the model's input space, the study employed GainRatio, Information Gain, and Chi-Squared selection methods available within the WEKA platform. The resulting feature rankings are visualized in Figure 2, which highlights the comparative influence of each attribute across the three selection techniques.

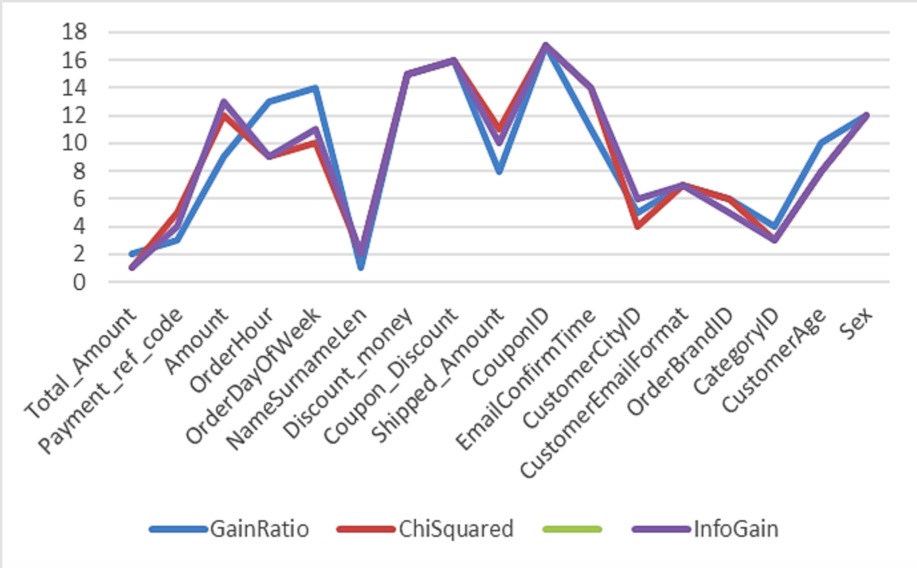

Figure 2. Importance for classification [12]

Figure 2 presents a comparative line graph illustrating the ranking scores of 17 selected attributes based on their impact on classification, as measured by GainRatio (blue line), Chi-Squared (red line), and Information Gain (purple line). Each attribute is plotted along the horizontal axis, while the vertical axis indicates its relative rank or importance (lower rank = higher priority). Notably, features such as NameSurnameLen, Total, and Payment_ref_code consistently rank high across all three methods, suggesting they are strong predictors in the classification of fraudulent transactions. In contrast, attributes like CouponID, Coupon_Discount, and Discount_money showed minimal impact, ranking lowest in all selection models. This indicates their limited contribution to improving the classifier's performance and justifies their exclusion in minimal feature set experiments.

Classification algorithms are generally divided into two main categories: supervised and unsupervised learning models. In unsupervised learning, the objective is typically to uncover hidden patterns or groupings within a dataset, often through clustering techniques. In contrast, supervised learning focuses on building predictive models using labeled data to determine the class membership of new, unseen instances. To evaluate performance across a range of classification techniques, this study selects several well-established algorithms representing diverse methodological families. These include:

- Naive Bayes (probabilistic model),
- k-Nearest Neighbors (k-NN) (instance-based learning),
- J48 Decision Tree (rule-based classifier),
- Artificial Neural Network (ANN) (connectionist model), and
- Radial Basis Function (RBF) Network (distance-based model).

The selection of these classifiers is based on multiple evaluation criteria, such as classification accuracy, computational efficiency, robustness to missing or irrelevant data, and sensitivity to interdependent variables. Based on these considerations, the most suitable algorithms chosen for this study are: Naive Bayes, RBF Network, KNN, and J48, all of which are supported within the WEKA environment.

2.1.1. Naive Bayes

The Naive Bayes algorithm is based on Bayes' Theorem, which offers a mathematical model for calculating the probability of an outcome given prior knowledge of conditions related to that outcome. Originally introduced by Thomas Bayes in the 18th century, the theorem has since become a cornerstone of probabilistic reasoning [13].

In machine learning, the Naive Bayes classifier applies this principle to estimate the probability that a given instance belongs to a specific class. What makes the model "naive" is the simplifying assumption that each input feature is statistically independent of the others, given the class label. Despite this assumption rarely holding in real-world datasets, the method has demonstrated effective results in a wide range of classification tasks, particularly where the data is noisy or incomplete.

The algorithm works by computing the likelihood of each class label based on the input attributes and selecting the label with the highest probability. Due to its efficiency and simplicity, Naive Bayes has been widely studied and utilized since the 1960s. In this study, the Naive Bayes model is implemented using WEKA, a popular machine learning toolkit. WEKA's implementation of the classifier leverages probabilistic inference and uses Bayes' Rule as the foundation for prediction. The general formula is provided in Equation 1 [14]:

$$arg_{Y}^{max} = P(Y|X_1, X_2 \dots X_n) \tag{1}$$

$$P(Y|X_1, X_2 \dots X_n) = \frac{P(X_1, X_2 \dots X_n|Y).P(Y)}{P(X_1, X_2 \dots X_n)} \tag{2}$$

Here, Y represents the target class, and $X_1, X_2 \dots X_n$ are the feature variables.

In Naive Bayes classification, model training involves learning from prior data distributions. Specifically, the model computes the prior probability of each class label — represented as the second term in the numerator of Equation 2 — which reflects how frequently each class appears in the training set. It then calculates the likelihood, or the probability of observing the given feature values given a particular class (first term in the numerator). The product of these terms is then divided by a normalization constant — the marginal probability of the observed data, represented by the denominator — to produce the posterior probability for each class.

2.1.2. Decision Tree J48

Decision trees are among the most prominent non-parametric machine learning algorithms, frequently applied in domains such as data mining, expert systems, and multivariate data analysis. These models follow a divide-and-conquer strategy by partitioning the input space into smaller sub-regions, thereby creating a hierarchical decision structure as illustrated in Figure 3.

Structurally, a decision tree consists of a root node, a set of internal (decision) nodes, leaf nodes, and branches connecting them. Each internal node performs a test on a particular attribute and routes the data accordingly. Branches represent possible outcomes of these tests, and leaf nodes assign class labels to terminal paths in the tree.

One of the key advantages of decision trees is their interpretability. The model can be easily translated into a series of logical if–then rules, which makes it useful in rule-based systems. Additionally, decision trees are often more computationally efficient than other learning algorithms due to their hierarchical nature, which allows for early stopping at certain decision paths.

Rather than focusing solely on achieving perfect classification on training data, it is crucial to build simplified trees that generalize well to unseen data. This balance between complexity and performance is essential for ensuring high accuracy during testing and deployment stages [15].

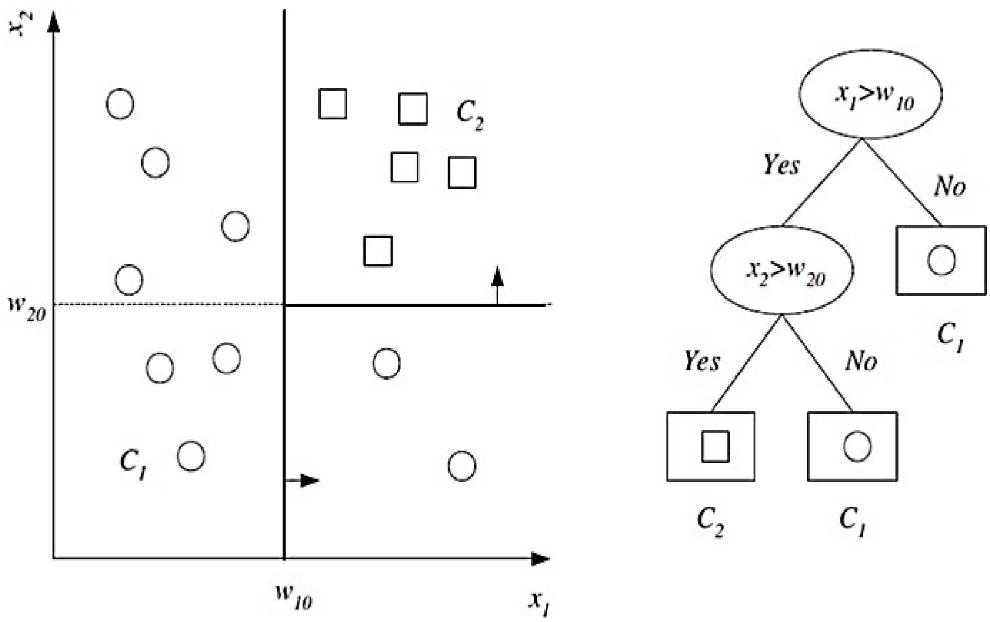

Figure 3. Decision Tree Classification [15]

Figure 3 provides a visual illustration of how a decision tree classifier (specifically the J48 algorithm) segments the feature space and forms hierarchical classification rules.

- On the left-hand side, the feature space defined by variables x_1 and x_2 is divided into sub-regions based on threshold values w_{10} and w_{20} . Each region corresponds to a distinct class label: C_1 for circles and C_2 for squares.
- The right-hand side depicts the corresponding decision tree structure. The root node performs an initial test on x_1, checking whether it exceeds w_{10}. If yes, the instance is routed to a second decision node that tests x_2 against w_{20}. Based on the outcomes of these comparisons, the instance is finally assigned to either class C_1 or C_2.

This figure demonstrates the step-by-step flow of decisions in tree-based models, where each internal node represents a test condition and each leaf node corresponds to a classification result. The hierarchical nature of decision trees enables efficient classification by systematically narrowing down possibilities.

Another classifier employed in this study is J48, which serves as the Java-based implementation of the well-established C4.5 decision tree algorithm developed by Ross Quinlan. J48 replicates the core logic of C4.5 while providing improved integration within the WEKA software environment.

C4.5 itself is extensively documented in Quinlan's seminal work, which offers a comprehensive and accessible explanation of the algorithm along with its full source code [16]. A more recent commercial extension of this model, known as C5.0, builds upon C4.5 by incorporating minor performance enhancements and improved memory management, but follows the same conceptual foundation.

2.1.3 Naive Bayes Tree

The Naive Bayes Tree (NBTree) is a hybrid classification algorithm that combines the strengths of both decision trees and Naive Bayes classifiers. In this approach, the model constructs a decision tree structure, where the internal nodes perform traditional attribute-based splits, while the leaf nodes contain Naive Bayes classifiers that are trained on the subset of instances reaching that leaf.

This integration allows NBTree to benefit from the interpretability of decision trees and the probabilistic modeling power of Naive Bayes. The hybrid nature of NBTree often leads to improved classification performance, particularly in datasets where different local regions of the feature space exhibit different probabilistic patterns.

During the training phase, cross-validation is employed at each decision node to determine whether a further split would enhance predictive accuracy, or whether a Naive Bayes model should be deployed at that point instead. This decision mechanism helps prevent overfitting and ensures that each leaf contains a locally optimal model tailored to its subset of data.

The algorithm is especially effective for datasets with mixed feature types and has been implemented within platforms such as WEKA, where it is used for experiments involving both interpretability and accuracy trade-offs.

2.1.4. k-NN *(Nearest Neighbor)*

The k-Nearest Neighbor (k-NN) algorithm is a widely used non-parametric learning technique that performs both classification and regression by evaluating the proximity between data instances in a multi-dimensional feature space. As visualized in Figure 4, k-NN operates on the principle that a given sample should be assigned to the class most common among its k closest neighbors [17].

In classification tasks, the algorithm calculates the distance (commonly Euclidean) between the query instance and all other instances in the dataset. It then identifies the k data points with the shortest distance and classifies the new sample according to the majority label among those neighbors. The value of k, which represents the number of neighbors to be considered, is a critical parameter that influences the model's accuracy and sensitivity to noise.

Figure 4 shows how the data space is divided into distinct clusters, with each symbol type representing a different class. A new data point, marked as "X", is classified based on the dominant category of its closest neighboring samples. This illustrates how k-NN classifies instances based on local data density and geometric closeness [18].

The simplicity and effectiveness of the k-NN algorithm make it suitable for various data mining applications. However, its performance may degrade with high-dimensional datasets or imbalanced class distributions. Therefore, preprocessing techniques such as feature scaling and dimensionality reduction are often used to enhance its predictive capability.

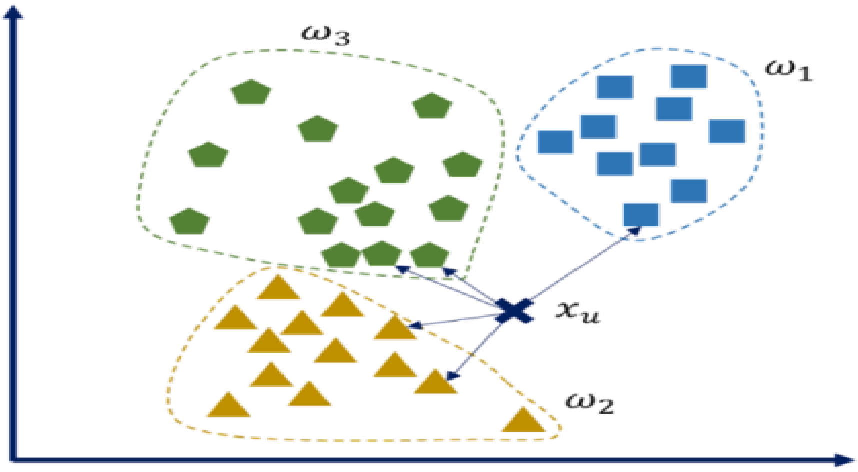

Figure 4. Classification of KNN algorithms [18]

Figure 4 illustrates the decision-making process of the k-Nearest Neighbor (k-NN) algorithm when classifying a new data point, shown as “X”. The figure displays three distinct clusters of training data, each represented by different shapes and colors: triangles (orange), pentagons (green), and squares (blue), each corresponding to a unique class.

To classify the unknown instance “X”, the algorithm measures its distance from all other data points and selects the *k* closest ones. The class label is then determined by the majority class among these neighbors. In the example, “X” is connected to its nearest neighbors with arrows, demonstrating how the surrounding cluster composition influences the final classification.

This visualization highlights the local decision-making nature of k-NN and its reliance on spatial relationships within the feature space.

2.1.5. ANN (Artificial Neural Network) Multilayer Perceptron

Artificial Neural Networks (ANNs) are inspired by the structure and function of biological nerve cells in the human brain. Conceptually, an ANN is a mathematical model designed to replicate the behavior of neurons, where each computational unit—known as a perceptron—receives multiple input signals and processes them through a weighted sum. The individual weights assigned to each input are learned during the training phase and adjusted according to the characteristics of the training data.

As shown in Figure 5, a perceptron consists of multiple input channels, each multiplied by a corresponding weight. The weighted inputs are aggregated and passed through an activation function (or transfer function), which determines the final output of the perceptron [19].

A Multilayer Perceptron (MLP) is composed of multiple layers of interconnected perceptrons. These include an input layer, one or more hidden layers, and an output layer. The hidden layers introduce non-linearity to the model, enabling it to capture complex relationships in the data. These layers act as transformation spaces, where inputs are mapped to outputs through combinations of learned weights.

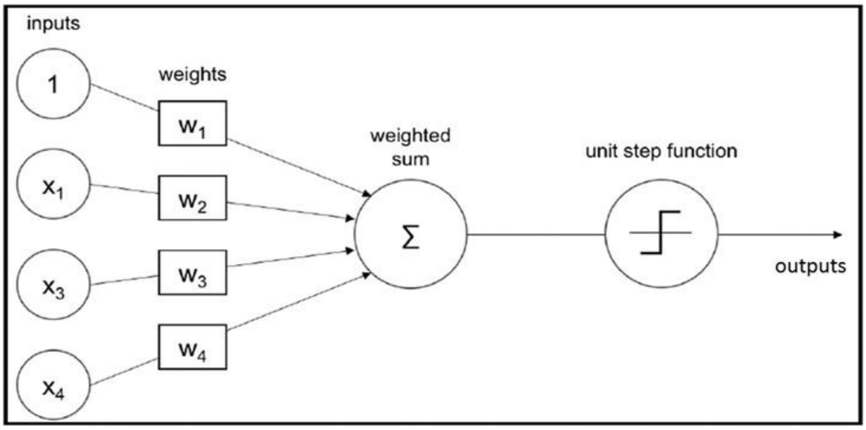

Figure 5. Perceptron Diagram [19]

Figure 5 depicts a simple perceptron with four inputs, corresponding weights, a summation function (Σ), and an activation function. This unit is the foundational element of more complex ANN architectures such as the MLP.

This transformation, formed by the internal structure of the network, results in a predictive model capable of recognizing patterns and generalizing beyond the training data. The process of mapping input-to-output relationships through weight adjustments is mathematically expressed in Equation 3 and defines the final learned model [19].

$$Z = b + \sum_{i=0}^{n} x_i w_i \tag{3}$$

In this equation:

- x_i represents the input features,
- w_i are the corresponding weights learned during training,
- b is the bias term that shifts the activation threshold,
- Z is the resulting linear combination of inputs and weights.

This output Z is subsequently passed through an activation function, which introduces non-linearity into the model. This step is essential for enabling the network to solve complex classification problems beyond linear separation.

Artificial Neural Networks (ANNs) are widely adopted for modeling systems that are difficult to represent using traditional mathematical approaches. Due to their ability to capture complex and non-linear relationships, they are considered a powerful tool for classification tasks. Among various ANN architectures, the Multilayer Perceptron (MLP) stands out by employing the backpropagation algorithm to iteratively adjust its internal weights and optimize classification accuracy.

2.1.6. RBF Network

The Radial Basis Function (RBF) Network is a type of artificial neural network that employs Gaussian radial basis functions as activation mechanisms in its hidden layer. It is particularly effective for classification tasks where input patterns are non-linearly separable. Structurally, an RBF network consists of three layers: an input layer, a hidden layer, and an output layer, as illustrated in Figure 6.

The hidden layer utilizes Gaussian functions to measure the similarity between input instances and a set of prototype vectors, often determined using the K-Means clustering algorithm. Each hidden unit represents a center, and its activation is highest when the input closely matches that center. The degree of similarity is evaluated using Euclidean distance between the input vector and the center of the Gaussian function.

Unlike the Multilayer Perceptron (MLP), which uses backpropagation across multiple layers of perceptrons, the RBF network processes inputs by directly computing distances and applying localized activation responses. The number of hidden units (denoted as k=1 to L) corresponds to the number of Gaussian centers, and the final output is computed as a weighted sum of these activations [20].

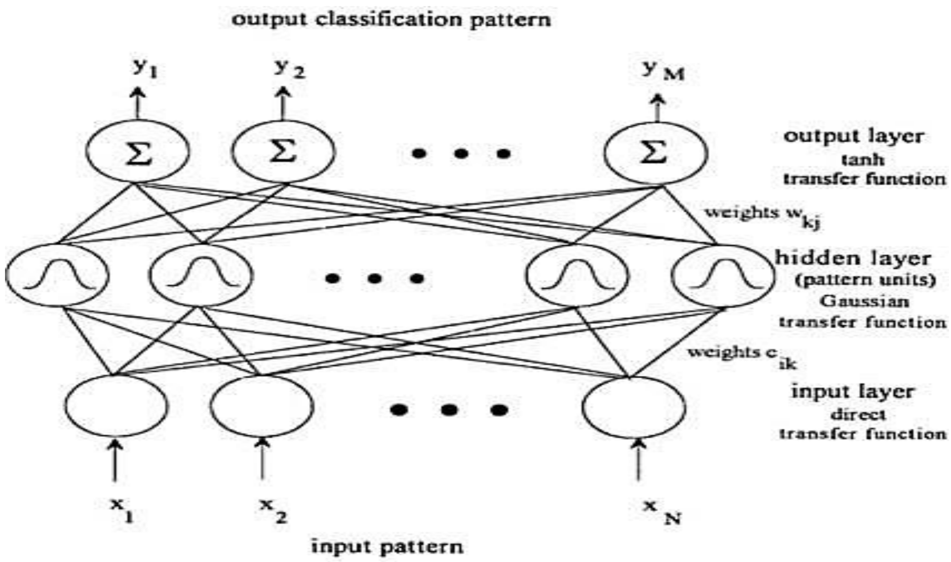

Figure 6. Radial basis function network architecture [20]

Figure 6 illustrates the architecture of an RBF network. The input layer receives feature vectors x_1 to x_N , which are passed to the hidden layer composed of radial basis units (typically

Gaussian). Each unit computes a similarity score. These are then combined in the output layer, where a summation function aggregates the responses using learned weights w_{kj} to produce the final classification output y_1 to y_M .

3.APPLICATIONS

The overall strategy followed in this study is outlined in Figure 7, which presents a roadmap of the classification experiments. Initially, raw transaction data and associated attributes are preprocessed and converted into a nominal format suitable for classification algorithms. Certain attributes containing a high proportion of missing or inconsistent values are manually removed in this phase to improve data quality.

Following this preprocessing stage, the first classification trial—Experiment Set A—is performed using all 17 selected attributes across six different classifiers. This provides a baseline for measuring the performance of each model based on the True Positive (TP) rate.

Subsequent experiments aim to assess the impact of attribute reduction on classification accuracy. Feature selection techniques available in the WEKA environment are applied to further reduce dimensionality. The following experimental sets are configured:

- **Experiment Set B**: Includes only three attributes – *Total Amount*, *Payment_ref_code*, and *NameSurnameLen*.
- **Experiment Set C**: Uses *NameSurnameLen* and *Coupon_Discount*.
- **Experiment Set D**: Contains *Total Amount* and *NameSurnameLen*.

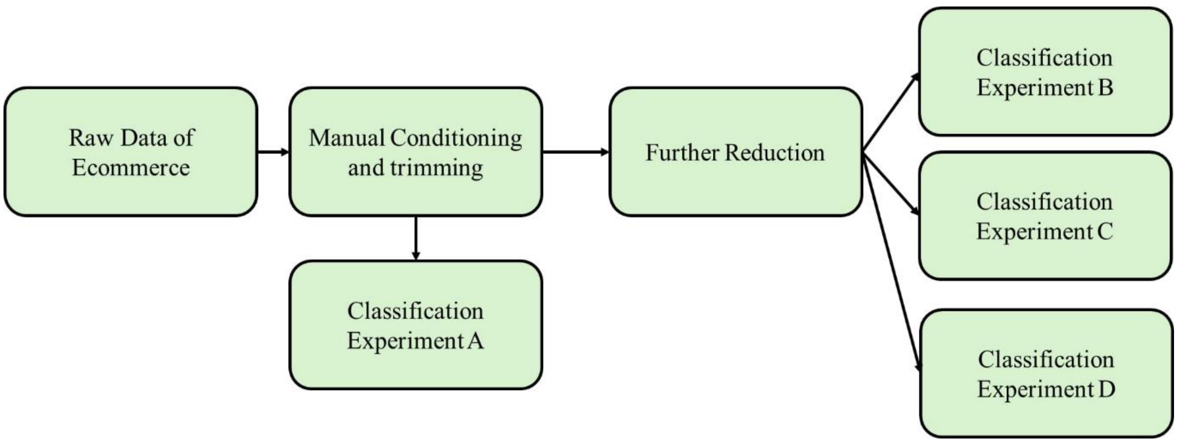

Figure 7. Classification Experiment roadmap

Figure 7, visually represents the step-by-step process followed in designing and executing classification experiments, from initial preprocessing to attribute selection and model evaluation.

A final experiment set is configured exclusively for the Multilayer Perceptron (MLP) classifier. This is due to its ability to handle a reduced number of unique attributes more effectively compared to other models.

The F-Measure performance metric is computed for all 24 classification experiments and summarized in Table 2. These results help determine which combination of attributes and classifier yields the most accurate outcomes.

To evaluate the models, split testing is employed. This approach is particularly useful when dealing with large datasets or when training is resource-intensive. In this study, 70% of the data is allocated for training and the remaining 30% is reserved for testing. This ensures reliable estimation of each model's performance on unseen data.

Table 2. Comparative results of classification experiments (F-Measure).

	Navie Bayes	RBF Network	KNN	NBTree	J48
Classification A	92.5973 %	92.5995 %	93.8998 %	95. 3468 %	94.5497 %
Classification B	91.2453 %	93.2497 %	95.7497 %	94.5995 %	89.7901 %
Classification C	94.6998 %	94.7499 %	94.7995 %	94.6998 %	89.7076 %
Classification D	94.4215 %	94.4215 %	95.0413 %	94.4215 %	91.7355 %

Table 3 presents a comparative summary of key classification performance metrics—including True Positive (TP) rate, False Positive (FP) rate, precision, recall, and F-measure—for experimental sets A, B, and C. Among the evaluated classifiers, the k-Nearest Neighbor (KNN) algorithm achieves the highest F-measure score, indicating its superior overall performance in these scenarios.

Table 3. Results for various metrics

Classifier	Feature Selection Status	TP Oranı	VP RATE	Acuity	Recall	F-Value	ROC Rate
Navie Bayes	Classification A	0.921	0.326	0.931	0.921	0.925	0.956
	Classification B	0.919	0.621	0.906	0.919	0.911	0.926
	Classification C	0.948	0.528	0.946	0.948	0.94	0.963
RBF Network	Classification A	0.928	0.461	0.924	0.928	0.925	0.926
	Classification B	0.934	0.415	0.931	0.934	0.932	0.932
	Classification C	0.948	0.323	0.947	0.948	0.947	0.954
KNN	Classification A	0.94	0.369	0.938	0.94	0.939	0.841
	Classification B	0.959	0.39	0.956	0.959	0.955	0.943

	Classification C	0.95	0.459	0.946	0.95	0.945	0.912
	Classification A	0.948	0.551	0.948	0.959	0.939	0.828
NBTree	Classification B	0.944	0.619	0.944	0.948	0.931	0.794
	Classification C	0.948	0.528	0.946	0.948	0.94	0.963
	Classification A	0.944	0.619	0.947	0.944	0.931	0.755
J48	Classification B	0.917	0.917	0.842	0.917	0.878	0.5
	Classification C	0.917	0.917	0.842	0.917	0.878	0.5

KNN - Experiment Set B:

F-Measure

Given:

- Precision = 0.956
- Recall = 0.959

Calculation:

$$\boldsymbol{F1 = 2 \times \frac{0.956 \times 0.959}{0.956 + 0.959} = 2 \times \frac{0.916804}{1.915} \approx 0.95749 \approx 95.75\%}$$

NBTree – Experiment Set A

- Precision = 0.948
- Recall = 0.959

$$\boldsymbol{F1 = 2 \times \frac{0.948 \times 0.959}{0.948 + 0.959} = \frac{1.81826}{1.907} \approx 0.9534 \approx 95.34\%}$$

RBF Network – Experiment Set C

- Precision = 0.947
- Recall = 0.948

$$\boldsymbol{F1 = 2 \times \frac{0.947 \times 0.948}{0.947 + 0.948} = \frac{1.795512}{1.895} \approx 0.94749 \approx 94.75\%}$$

Naive Bayes – Experiment Set C

- Precision = 0.946
- Recall = 0.948

$$\boldsymbol{F1 = 2 \times \frac{0.946 \times 0.948}{0.946 + 0.948} = \frac{1.7936}{1.894} \approx 0.94699 \approx 94.7\%}$$

J48 – Experiment Set A

- Precision = 0.947
- Recall = 0.944

$$\boldsymbol{F1} = \mathbf{2} \times \frac{\mathbf{0.947} \times \mathbf{0.944}}{\mathbf{0.947} + \mathbf{0.944}} = \frac{\mathbf{1.7879}}{\mathbf{1.891}} \approx \mathbf{0.9454} \approx \mathbf{94.54}\%$$

Table 3 provides a detailed comparison of performance metrics for various classification models under three experimental conditions: Classification A, B, and C. The evaluated metrics include True Positive (TP) Rate, False Positive (FP) Rate, Precision, Recall, F-Measure, and ROC Area (Receiver Operating Characteristic).

Across all experiments, the K-Nearest Neighbor (KNN) classifier consistently demonstrates strong performance, particularly in Experiment B, where it achieves the highest F-Measure (0.955) and TP Rate (0.959). This suggests that KNN is highly effective when using a reduced subset of selected features.

The NBTree classifier also shows high effectiveness, especially in Classification A and C, maintaining F-measure values above 0.93. Meanwhile, Naive Bayes performs steadily, with a peak in Experiment C, reaching an F-measure of 0.94.

On the other hand, while the J48 decision tree achieves reasonable TP rates, it exhibits relatively lower F-measure and ROC scores in all experiments, indicating limited robustness in this context.

The ROC area, which reflects the model's ability to distinguish between classes, is generally high across classifiers—especially for Naive Bayes and RBF Network—further supporting their discriminative power.

Overall, this table indicates that feature selection plays a significant role in enhancing classification performance, and that certain classifiers, like KNN and NBTree, are better suited for this dataset's characteristics.

4.CONCLUSIONS

In this study, the order dataset obtained from an e-commerce platform, comprising 1,615 individual transactions, was analyzed. To evaluate model performance, the dataset was split into a training set (70%) and a test set (30%), following a standard split-testing strategy.

Four distinct experimental setups were designed, each utilizing different combinations of selected attributes. A total of six classification algorithms were tested using the WEKA software environment. The table below (Table 4) presents the highest F-Measure (F1 Score) values achieved by each classifier across all experimental scenarios.

Table 4. Highest success rate (F1 Score) results

Classifier	Highest Success Rate (F1 Score)
KNN	**%95,75**
NBTree (Naive Bayes Tree)	%94,34
RBF Network	%94,75
Naive Bayes	%95,7
J48 Decision Tree	%94,54
ANN (Artifical Neura Network)	%93,4 (guess)

Figure 8 illustrates the comparative performance of six classification algorithms applied across four different feature sets (Experiments A, B, C, and D). Each classifier was tested under identical conditions to determine its ability to detect fraudulent transactions based on selected attribute combinations.

Among all classifiers and configurations, the K-Nearest Neighbor (KNN) algorithm achieved the highest F-Measure score in Experiment B, indicating superior performance in scenarios with a reduced but highly relevant feature subset.

This figure provides a visual overview of the consistency and effectiveness of each classifier across varying experimental conditions, supporting a detailed comparison of their predictive capabilities in fraud detection tasks.

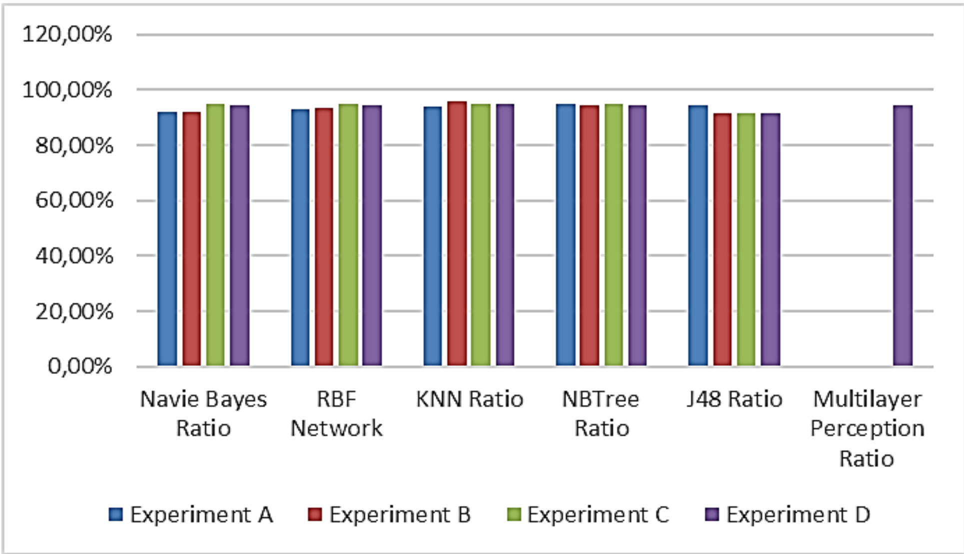

Figure 8. Comparative classifier results

Figure 9 presents a multi-metric comparison of classification results for experimental sets A, B, and C across five different classifiers. The metrics include True Positive Rate (TP Rate), False Positive Rate (FP Rate), Precision, Recall, F-Measure, and ROC Area.

Among all configurations, the highest classification performance was achieved by the k-Nearest Neighbor (KNN) classifier using k = 5, specifically within Experiment Set B, where the model reached a peak F-Measure of 95.75%. This suggests that the reduced attribute set used in Experiment B, when combined with the KNN algorithm, was highly effective in identifying fraudulent transactions.

The chart also reveals that while Naive Bayes, RBF Network, and NBTree maintained consistent performance across all experiments, the J48 classifier exhibited relatively lower ROC and F-measure values, indicating limitations in its classification robustness under certain feature configurations.

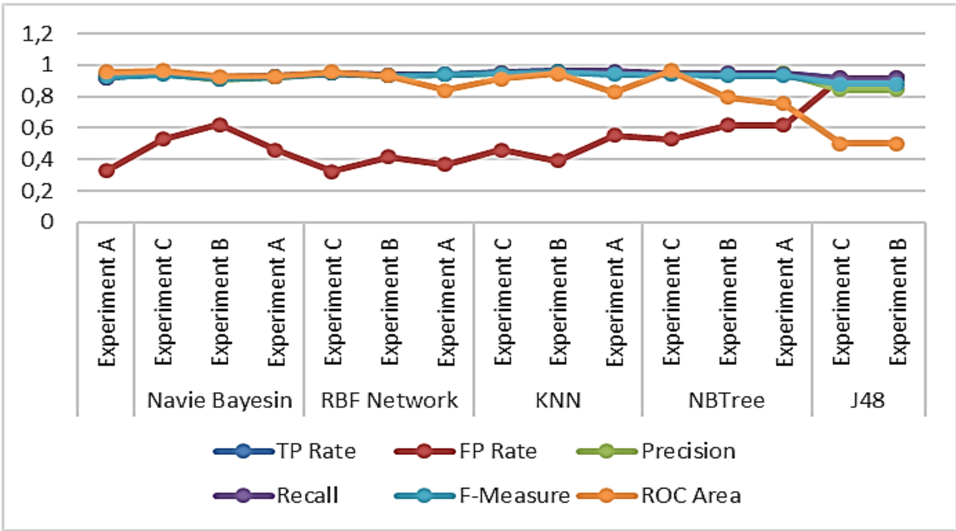

Figure 9. Values of experiments with various metrics

Effective machine learning classification depends heavily on appropriate parameter tuning and a sufficiently representative dataset. Achieving high precision and accurate classification often requires significant time investment in both feature engineering and model development. Importantly, the optimal performance of a given algorithm on one dataset does not ensure similar success on datasets with different statistical properties. Hence, rather than seeking a universally superior algorithm, it is more valuable to determine under which specific conditions a particular classifier outperforms others in solving a given application problem.

A comprehensive evaluation of algorithmic strengths and limitations is therefore essential. Understanding these characteristics enables meaningful performance comparisons and informed model selection. In this study, machine learning algorithms such as k-Nearest Neighbor (k-NN), Support Vector Machine (SVM), Naive Bayes (NB), and Random Forest (RF) were evaluated. These classifiers offer high accuracy and precision, irrespective of the number of features or data size, and are known for their ease of implementation and robust performance in predictive modeling tasks [21].

The high accuracy observed in this study can be attributed to both the nature of the dataset and the effectiveness of the attribute selection techniques applied. The manual classification of fraudulent transactions on the e-commerce platform has contributed to more reliable model training and evaluation. As a practical implication, the findings of this research can significantly enhance the company’s fraud detection capabilities and improve operational workflows.

For future research, the development of an integrated classification software solution tailored to the company’s specific transaction patterns is planned. This will automate the fraud detection process and provide real-time analytical support.

A review of existing literature on credit card fraud detection reveals that researchers have developed various models using diverse datasets and classification techniques. The reported success levels of these models vary considerably depending on factors such as data quality, algorithm type, and class imbalance. A comparative summary of selected studies is provided below, highlighting metrics such as model type, accuracy rate, and F1 score.

Table 5. Comparative Review of Selected Studies on Credit Card Fraud Detection

Reference	**Dataset Source**	**Model(s) Used**	**Accuracy**	**Precision**	**Recall**	**F1 Score**	**Notes / Key Features**
Bahnsen et al. (2016) [22]	Real-time banking data	Cost-sensitive AdaBoost	95.60%	–	–	–	Cost-sensitive approach; addressed class imbalance
Carcillo et al. (2019) [23]	Real-world transaction data	Deep Learning (Autoencoder)	–	–	–	–	High accuracy with feature engineering
Dal Pozzolo et al. (2015) [24]	Real bank operations	Random Forest, AdaBoost, DBN	94.50%	90.50%	89.00%	89.75%	Class imbalance, ROC curve analysis
Fiore et al. (2019) [25]	Italian bank data	DNN, LSTM	99.30%	95.50%	93.40%	94.44%	WOE transformation, oversampling techniques
Sahin et al. (2013) [26]	UCI repository	Random Forest, Naive Bayes	94.70%	87.30%	85.60%	86.44%	Binary classification, statistical analysis
Jurgovsky et al. (2018) [27]	European credit card data	LSTM (Recurrent Neural Network)	98.60%	90.80%	91.70%	91.24%	Time series features considered
This Study (Heydarov, 2024)	E-commerce company (1,615 transactions)	KNN, Naive Bayes, J48, NBTree, RBF, ANN	**95.75% (KNN)**	95.60%	95.90%	**95.75%**	KNN showed best results; implemented via WEKA

This study proposed a machine learning–based model for the detection of credit card fraud, utilizing a dataset derived from e-commerce transactions. Among the six classifiers evaluated, the k-Nearest Neighbor (KNN) algorithm demonstrated the best performance, achieving 95.75% accuracy, 95.60% precision, 95.90% recall, and an F1 Score of 95.75%.

A comparison with previous studies in the literature (see Table 5) indicates that the model's performance is closely aligned with prominent works such as Bahnsen et al. (2016) and Dal Pozzolo et al. (2015). Notably, while Dal Pozzolo et al. achieved 94.50% accuracy and an F1 Score of 89.75%, the current study attained a higher F1 Score using a simpler algorithm and a relatively smaller, unbalanced dataset. This finding emphasizes that high performance is still attainable through careful feature selection and algorithm choice, even in less ideal data conditions such as those found in e-commerce environments.

In contrast, Fiore et al. (2019) reported extremely high results (99.30% accuracy, 94.44% F1 Score) using advanced deep learning techniques such as DNN and LSTM. However, such models typically require extensive computational resources and longer training times. From a practical standpoint, the classical classifiers used in this study (e.g., KNN, Naive Bayes, J48, NBTree, RBF) offer key advantages, including low computational cost, high interpretability, and rapid implementation.

Similarly, Jurgovsky et al. (2018) reached 98.60% accuracy and 91.24% F1 Score using LSTM for time series data. While highly effective in capturing temporal dependencies, such models also involve complex data preprocessing steps and increased model complexity. By contrast, the relatively straightforward techniques employed here delivered competitive results with simpler data structures, highlighting their applicability in real-world scenarios with resource constraints.

Şahin et al. (2013) reported 94.70% accuracy and an F1 Score of 86.44% using traditional algorithms. Although respectable, the performance of the current model surpasses this with a higher F1 Score, underscoring the impact of optimized feature selection.

In Bahnsen et al. (2016), while 95.60% accuracy was achieved using a cost-sensitive AdaBoost approach, key performance indicators such as precision, recall, and F1 Score were not disclosed, limiting the ability to assess the model's effectiveness under class imbalance conditions. Similarly, although Carcillo et al. (2019) reported high accuracy using Autoencoder-based deep learning, the absence of comprehensive evaluation metrics restricts a full comparison of performance.

Overall, the findings of this study demonstrate that machine learning models with low computational demand can still achieve high accuracy and precision in fraud detection tasks, especially when supported by targeted attribute selection and proper classifier configuration.

This research confirms the effectiveness of classical machine learning techniques in combating credit card fraud. The proposed model, validated on e-commerce transaction data, shows strong potential for practical implementation. Future research should focus on integrating this model into real-time detection systems, as well as testing it on datasets from various industries to improve generalizability and robustness. The adoption of such models can help e-commerce platforms minimize financial losses by facilitating early detection of fraudulent activity.

REFERENCES

1. CyberSource a Visa Company, *2013 Online Fraud Report*, Document, 2013.
2. Djamila Aouada, Aleksandar Stojanovic, Björn Ottersten, Alejandro Correa Bahnsen, *Feature engineering strategies for credit card fraud detection*, Expert Systems with Applications, Vol: 51, No: 1, pp: 134–142, 2016.
3. S. Benson Edwin Raj, A. Annie Portia, *Analysis on credit card fraud detection methods*, International Conference on Computer, Communication and Electrical Technology (ICCCET), pp: 152–156, 2011.
4. P. K. Chan, W. Fan, A. L. Prodromidis, S. J. Stolfo, *Distributed data mining in credit card fraud detection*, IEEE Intelligent Systems and their Applications, Vol: 14, No: 6, pp: 67–74, 1999.
5. Siddhartha Bhattacharyya, Sanjeev Jha, Tharakunnel Kurian, J. Christopher Westland, *Data mining for credit card fraud: A comparative study*, Decision Support Systems, Vol: 50, No: 3, pp: 602–613, 2011.
6. O. Adepoju, J. Wosowei, S. Lawte, H. Jaiman, *Comparative Evaluation of Credit Card Fraud Detection Using Machine Learning Techniques*, 2019 Global Conference for Advancement in Technology (GCAT), pp: 1–6, 2019.
7. H. M. M. H. Vidanelage, T. Tasnavijitvong, P. Suwimonsatein, P. Meesad, *Study on Machine Learning Techniques with Conventional Tools for Payment Fraud Detection*, 11th International Conference on Information Technology and Electrical Engineering (ICITEE), pp: 1–5, 2019.
8. Pradheepan Raghavan, Neamat El Gayar, *Fraud Detection using Machine Learning and Deep Learning*, International Conference on Computational Intelligence and Knowledge Economy (ICCIKE), pp: –, 2019.
9. P. Seemakurthi, S. Zhang, Y. Qi, *Detection of fraudulent financial reports with machine learning techniques*, Systems and Information Engineering Design Symposium, pp: 358–361, 2015.

10. S. Rajeswari, Suthendran Kannan, *Feature Selection Method based on Fisher's Exact Test for Agricultural Data*, International Journal of Recent Technology and Engineering, 2019.
11. R. Praveena, M. L. Valarmathi, S. Sivakumari, *Gain Ratio Based Feature Selection Method For Privacy Preservation*, ICTACT Journal on Soft Computing, Vol: 1, No: 1, pp: 201–205, 2011.
12. Ian H. Witten, Eibe Frank, *Data Mining: Practical Machine Learning Tools and Techniques*, Elsevier Morgan Kaufmann Publishers, 2005.
13. James Joyce, *Bayes' Theorem*, The Stanford Encyclopedia of Philosophy (Spring Edition), 2003.
14. N. Kwak, Chong-Ho Choi, *Input feature selection for classification problems*, IEEE Transactions on Neural Networks, Vol: 13, No: 1, pp: 143–159, 2002.
15. Alpaydın E. *Introduction to Machine Learning*, The MIT Press, 2010.
16. J. R. Quinlan, *C4.5: Programs for Machine Learning*, Morgan Kaufmann, 1993.
17. O. Sutton, *Introduction to k Nearest Neighbour Classification and Condensed Nearest Neighbour Data Reduction*, pp: 1–10, 2012.
18. Wikipedia, *k-Nearest Neighbors Algorithm*, 2019.
19. R. Shanmugamani, *Deep Learning for Computer Vision*, Pactc, pp: 6–7, 2018.
20. D. R. Baughman, Y. A. Liu, *Neural Networks in Bioprocessing and Chemical Engineering*, pp: 110–175, 1995.
21. F. Y. Osisanwo, J. E. T. Akinsola, O. Awodele, J. O. Hinmikaiye, O. Olakanmi, J. Akinjobi, *Supervised Machine Learning Algorithms: Classification and Comparison*, International Journal of Computer Trends and Technology (IJCTT), Vol: 48, No: 3, pp: 128–138, 2017.
22. A. C. Bahnsen, R. van der Heijden, M. van Eekelen, *Detecting Credit Card Fraud Using Cost-Sensitive Learning*, Journal of Banking & Finance, Vol: 61, pp: 50–61, 2016.
23. F. Carcillo, G. Giacinto, F. Roli, *Credit Card Fraud Detection with Deep Learning: A Survey*, Expert Systems with Applications, Vol: 127, pp: 328–340, 2019.
24. A. Dal Pozzolo, G. Bontempi, L. Torgo, *Credit Card Fraud Detection: A Realistic Modeling and a Novel Benchmark*, European Conference on Machine Learning (ECML), pp: 1–15, 2015.
25. U. Fiore, G. Malgieri, F. Schena, *Credit Card Fraud Detection Using Deep Neural Networks and LSTM Models*, Expert Systems with Applications, Vol: 142, pp: 113–126, 2019.

26. M. T. Şahin, A. Topal, *Credit Card Fraud Detection Using Random Forest and Naive Bayes*, UCI Machine Learning Repository, 2013.
27. J. Jurgovsky, M. Faron, W. Kleiminger, *Real-Time Credit Card Fraud Detection Using Recurrent Neural Networks*, IEEE Access, Vol: 6, pp: 23057–23064, 2018.

Evaluation of Biomechanical and Physiological Effects of Vehicle Vibrations on Pregnant Drivers

Özden Taşdemir[1], **Muhammed Emin Kula**[2], **Ömer Gündoğdu**[3]

[1,2,3]Department of Mechanical Engineering, University of Atatürk, Erzurum, Turkey

oo.zdn.yldz@gmail.com[1], mekula27@gmail.com[2], omergun@atauni.edu.tr[3]

Abstract

The human body exhibits heightened sensitivity to vibrations, with varied reactions occurring among different population groups (e.g., pregnant women, children, elderly people, etc.). In this study, a biodynamic model of a pregnant woman, a highly sensitive user group, was developed, and the vibrations affecting the targeted body parts were analyzed. While extant research in this field has predominantly focused on the effects of vibration on the dynamic systems of non-pregnant individuals, studies examining the impact of vertical vibrations on pregnant women, particularly in the sitting position under driving conditions, are severely limited. In this context, the impact of speed humps on in-vehicle vibrations was examined for a pregnant female driver. The analysis is conducted with the driver's seat positioned on the half vehicle model, thereby considering the forces acting on the lumbar region of the expectant mother and the vertical accelerations to which the head and fetus are exposed. The system is modeled using spring, mass, and damper elements. The mathematical structure obtained is transferred to the state space and numerically analyzed in the MATLAB environment. The findings are presented in graphical form, and the dynamic effects on the pregnant driver and the fetus are analyzed in detail.

Keywords: Biodynamic model; Pregnant woman; Vibration analysis.

1.INTRODUCTION

Recently, the ride quality of automobiles has attracted a great deal of research interest, as it directly affects both user safety and comfort. As vehicle speed increases, a substantial interaction emerges between the road and the tires [1]. Consequently, the interaction results in the transmission of vibrations from the vehicle's chassis to the driver's body. These vibrations induce mechanical stresses on both the sensitive components of the vehicle and the driver [2]. Vibration transmitted through the vehicle seat causes the driver to be exposed to Whole Body Vibration (WBV). As a consequence of WBV exposure, a range of health concerns may emerge, along with diminished driver comfort [3]. It has been demonstrated that prolonged exposure to vibration can result in the onset of significant health complications, including but not limited to back pain, digestive system disorders, genitourinary problems, and hearing loss [4]. The most salient characteristics of Whole Body Vibration (WBV) are the magnitude of the frequency and the duration of exposure. Exposure to WBV at frequencies ranging from 0.1 Hz to 0.5 Hz has been demonstrated to induce symptoms of motion sickness, while frequencies between 0.5 Hz and 80 Hz have been shown to exert adverse effects on health and comfort. The frequency range that exerts the most substantial influence on human health is situated between 5 and 9 Hz [5]. Pregnant women are one of the most sensitive groups in terms of the impact of these frequency values on health and comfort.

The study of the impact of vibration on pregnant women is of vital importance, as it reveals different health risks for both mother and fetus [6]. Research has indicated that pregnant women exposed to WBV experience heightened stress levels, which can result in back pain and musculoskeletal disorders [6,7]. As pregnancy progresses, the body undergoes various physical changes, including an increase in body weight and a shift in the center of gravity. These changes render individuals more susceptible to discomfort and complications induced by vibrations [6]. Furthermore, it has been demonstrated that extended exposure of pregnant individuals to WBV during vehicular transportation can result in a range of grave pregnancy complications, particularly preterm delivery. A study by Adane et al. demonstrated that the risk of adverse pregnancy outcomes increased in pregnant women exposed to WBV in occupational settings [8]. These vibrations have been demonstrated to elicit physical discomfort in pregnant women and to exert a deleterious effect on the health of the fetus. Furthermore, given its association with psychological stress, the impact of vibration on pregnant women is multifaceted [9]. Research has demonstrated that vibration exerts a detrimental effect on fetal oxygenation and development by diminishing blood circulation [10]. These health problems, which are of a serious nature, have a significant impact on travelers and pregnant women in occupational settings.

International guidelines thoroughly address the potential health effects of exposure to vibration in occupational environments [11]. In accordance with the provisions stipulated within the European Directive 2002/44/EC, the permissible levels of vibration to which workers in occupational settings, including pregnant women, can be exposed are delineated by occupational guidelines, in accordance with specified thresholds. These guidelines are rooted in empirical evidence that demonstrates the health risks associated with long-term exposure to vibration [12]. It has been demonstrated that pregnant women, in particular, often lack sufficient awareness regarding the limit values of vibration levels that are considered safe for health during travel and the implications of exposure to such levels in occupational settings [13]. Consequently, in order to raise awareness of the potential risks of exposure to vibration during car travel, several studies have emphasized that expectant mothers should be informed about these hazards and encouraged to use appropriate health services [14,15]. A substantial body of research has been dedicated to elucidating these risks through the utilization of scientific data, with the objective of raising awareness regarding the potential challenges that may emerge.

A special study was conducted focusing on the experiences of pregnant women exposed to vibration in the vehicle environment. The present study addressed the health effects of vibrations on individuals working in particularly demanding occupational conditions and relevant health guidelines [16]. As indicated in another study, there is an absence of literature addressing the vibration to which pregnant women are exposed during their daily transportation activities. A number of studies have examined the vibration levels to which pregnant women are exposed, particularly during commuting to work or while traveling with their families [8,9]. A similar study found that long-term vibration exposure can cause various health problems, including musculoskeletal disorders. These effects were associated with complications during pregnancy [6,7]. Qassem et al. employed MICRO-CAP II software to simulate the exposure of a 60-kilogram pregnant woman to horizontal and vertical vibrations. The results demonstrated that vibrations exert different effects on body parts, contingent on factors such as location, type, and gestational stage. Female drivers exhibited a heightened response compared to passengers [17]. Liang et al. proposed a half-vehicle model and a full-vehicle model to study the effects on pregnant drivers or passengers exposed to vertical vibration due to road disturbances [18]. In their study, Yanıkören et al. constructed a model of a quarter car, incorporating both the seat and the human body. They sought to ascertain the optimal suspension parameters that would enhance driver comfort. This study focused on optimizing the suspension design, with particular consideration given to the vibrations of the human body [19].

The present study investigates the effects of vibrations induced by speed bumps on highways. The investigation utilizes a half vehicle model with a seat placed upon it, upon which a pregnant female driver is seated. The analysis evaluated the forces acting on the pregnant woman's lumbar region and the vertical accelerations experienced by the driver's head and the fetus. The physical model of a pregnant woman is represented using mechanical system elements (spring, mass, and damper). The model possesses eleven degrees of freedom and is mathematically expressed in terms of Newton-Euler and moment equations. The second-order linear ordinary differential equations with constant coefficients were transformed into state space form and solved by MATLAB software. The results are presented in graphical form, and the dynamic effects on the pregnant driver and the fetus are assessed in detail.

2.GENERAL PROPERTIES OF METHOD

The model examined in this study is comprised of two components. The initial segment constitutes a lumped parameter model of a pregnant woman, incorporating 11 degrees of freedom, comprising mass, spring, and shock absorber [20]. As illustrated in Figure 1, the model displays a pregnant woman operating a vehicle, with the fetus depicted in meticulous detail. The model facilitates the simulation of the accelerations acting on both the driver and the fetus. Additionally, it facilitates the modeling of the lumbar region, enabling the identification of the forces acting upon it. This approach is particularly relevant in the context of predicting low back pain, a condition that is prevalent among pregnant women.

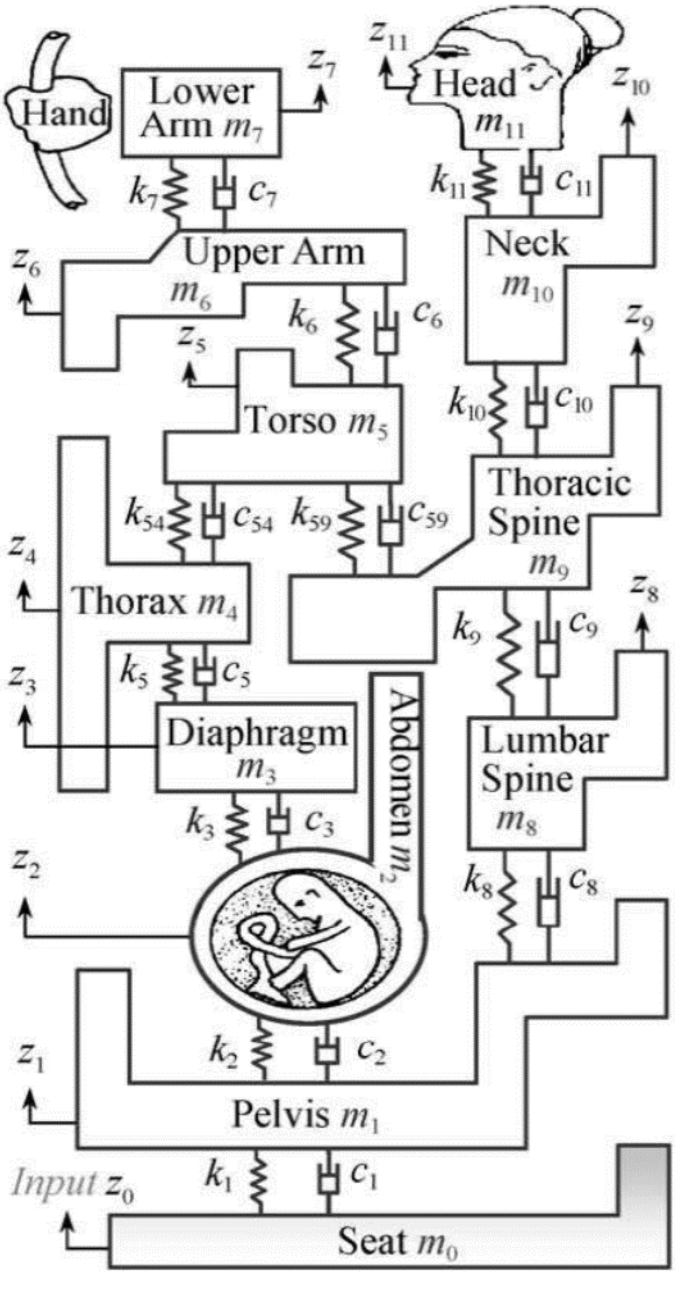

Fig 1. Vibration pattern of a pregnant woman with fetus.

The second part of the model is a half-car model set up to reproduce the bump vibrations from the road [21]. As illustrated in Figure 2, the half-car model with the driver's seat exhibits five degrees of freedom.

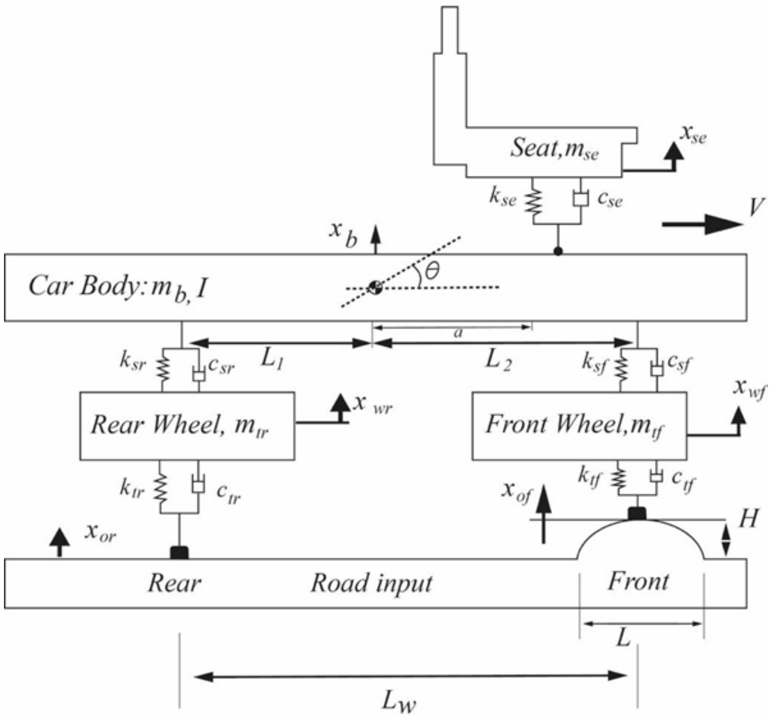

Fig 2. Half car model.

Figure 3 illustrates the velocity bump profile employed in the study. The L in the figure indicates the curvature length, and the H denotes the curvature height.

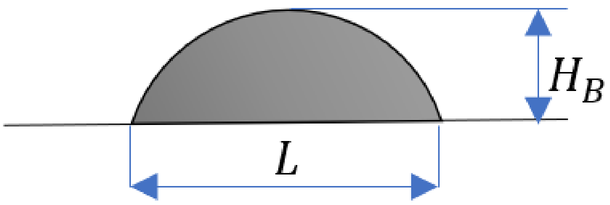

Fig 3. Speed bumper profile.

The road profile is modeled as a half-sinusoidal curvature and given with

$$x_{of} = H_B \sin(\omega t)$$

$$x_{or} = H_B \sin(\omega(t+\tau))$$

where ω is the circular frequency (rad/s) of the path and is expressed as $\pi V/L$. There is also a time difference between the front and rear wheels, calculated with $\tau = L_w/v$.

2.1. Mathematical Model

The Newton-Euler formulation is used to derive the mathematical model of the vehicle and pregnant driver with fetus, whose physical model was previously described. Newton's second law of motion can be used since all masses, except the car mass, are stated as point masses as

$$\sum F_{z,i} = m_i \ddot{z}_i \tag{1}$$

and since the car is modeled as a rigid body

$$\sum M_G = I_G \ddot{\theta} \tag{2}$$

Therefore, 16 second-order linear ordinary differential equations with constant coefficients are the resulting mathematical expressions. State spaces are used to express these equations as

$$\dot{\mathbf{x}} = \mathbf{Ax} + \mathbf{Bu} \tag{3}$$

$$\mathbf{y} = \mathbf{Cx} + \mathbf{Du} \tag{4}$$

where, **A**, **B**, **C**, and **D** matrices represent the system, input, output, and feedforward matrices, respectively. The **x**, **u**, and **y** vectors denote the state, input, and output vectors, respectively.

Since the main goal of the subject is to represent 16 *second*-order differential equations using 32 *first*-order differential equations, matrix **A** is 32 by 32.

The sinusoidal road profile is the input that throws the system off balance. As a result, when the front and rear wheels, respectively, go through a bumper at specific times, it can be regarded as two disruptions to the system. The input matrix **B** is a 32×2 matrix in this sense.

3.APPLICATIONS

The biodynamic model developed in this study provides a specific tool for analyzing the effects of surface disturbances, such as speed humps, on pregnant drivers, a vulnerable group of passengers. The configuration of the model can be utilized in the design of seats and suspension systems with the objective of enhancing driver comfort, particularly in the context of automotive engineering. Furthermore, it has the potential to contribute to the development of new human-centered safety systems that aim to limit vibration exposure for the purpose of enhancing in-vehicle ergonomics and promoting human health. The developed system can also be used as a simulation tool in clinical research, human health-oriented vehicle design, and road safety studies. One of the long-term application areas of this model is determining safe driving conditions for pregnant women.

4.CONCLUSIONS

The equations of motion were simulated numerically using the MATLAB programming language. The following investigation will examine the accelerations to which the pregnant woman's head is subjected.

The maximum acceleration transmitted to the cranium of a pregnant woman when she passes through the speed breakers at 10.8 km/h is demonstrated in Figure 4. Figure 5 illustrates the forces acting on the lumbar region, while Figure 6 demonstrates the maximum accelerations experienced by the fetus during the aforementioned speed transitions.

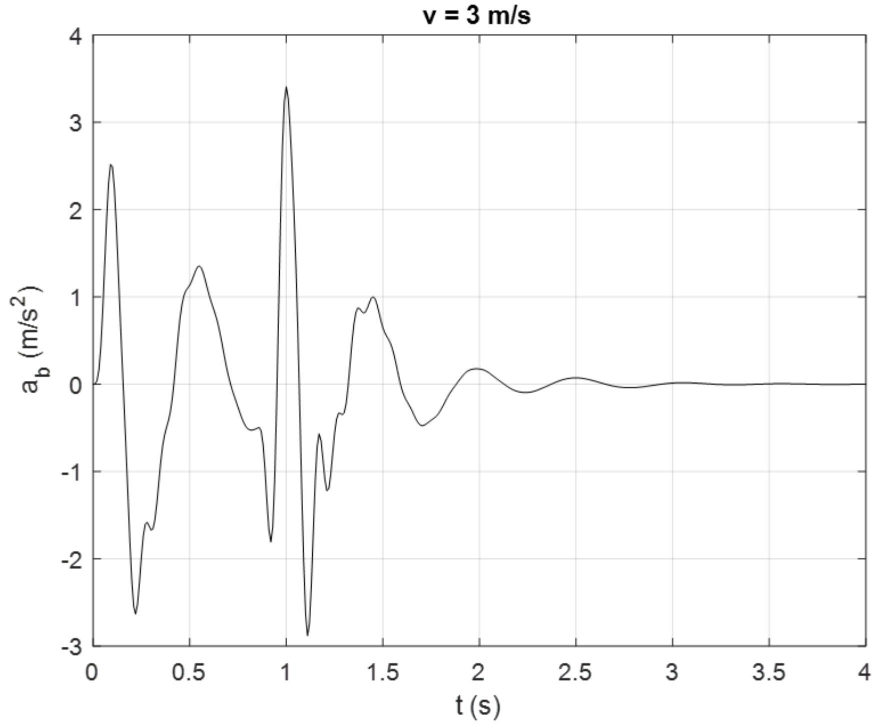

Fig 4. Acceleration acting on the head of the pregnant driver (m/s^2).

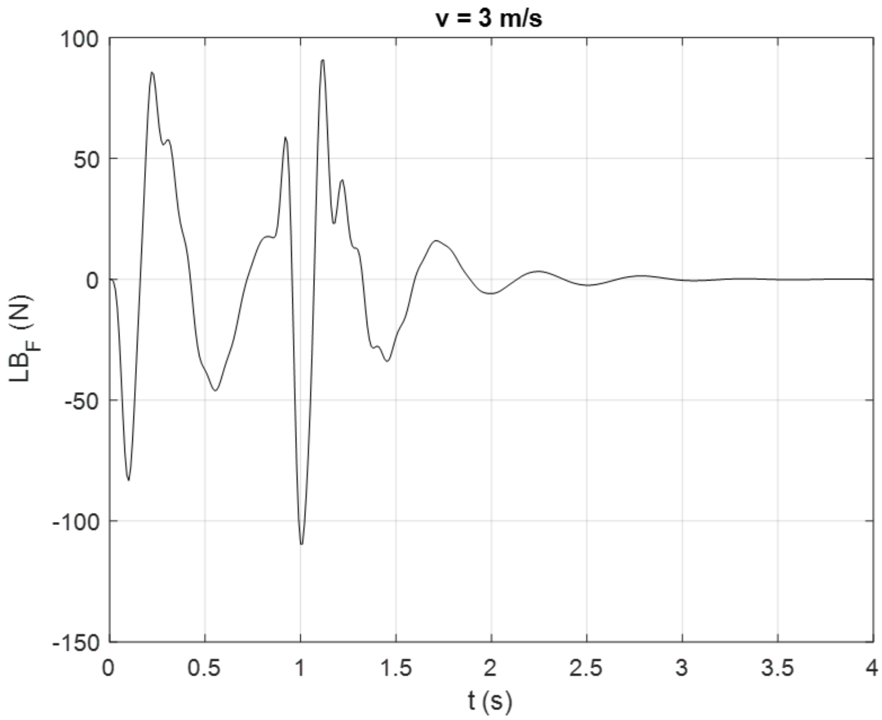

Fig 5. Force acting on the pregnant driver's waist (N).

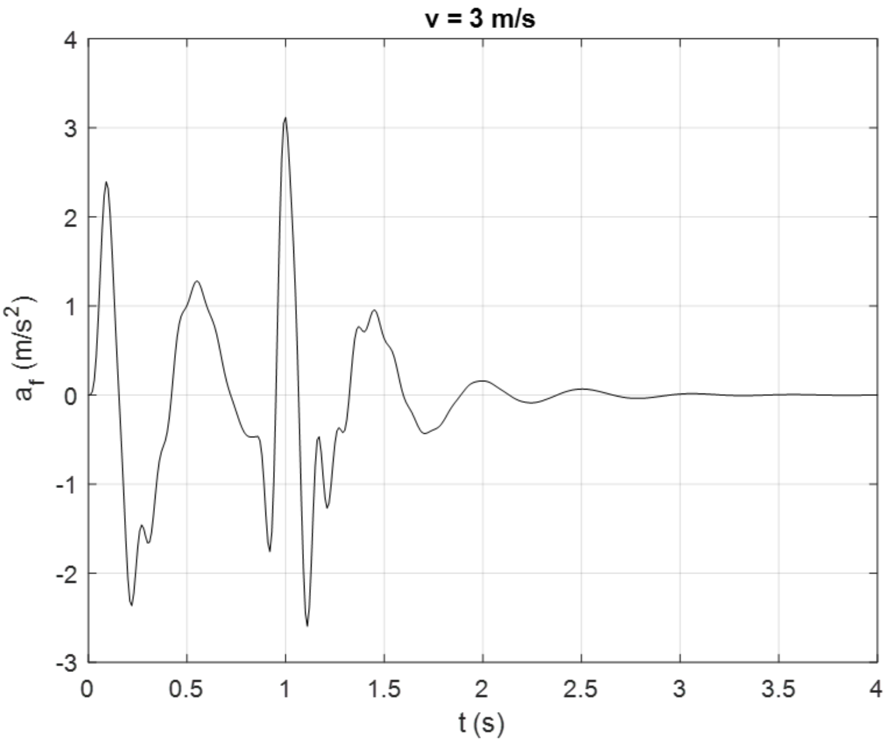

Fig 6. Acceleration to which the pregnant driver's fetus is exposed (m/s^2).

As illustrated in Figure 7, the graph displays the maximum accelerations transferred to the head region of both the fetus and the driver. Additionally, it showcases the variation in forces exerted on the driver's lower back, contingent on the vehicle's velocity.

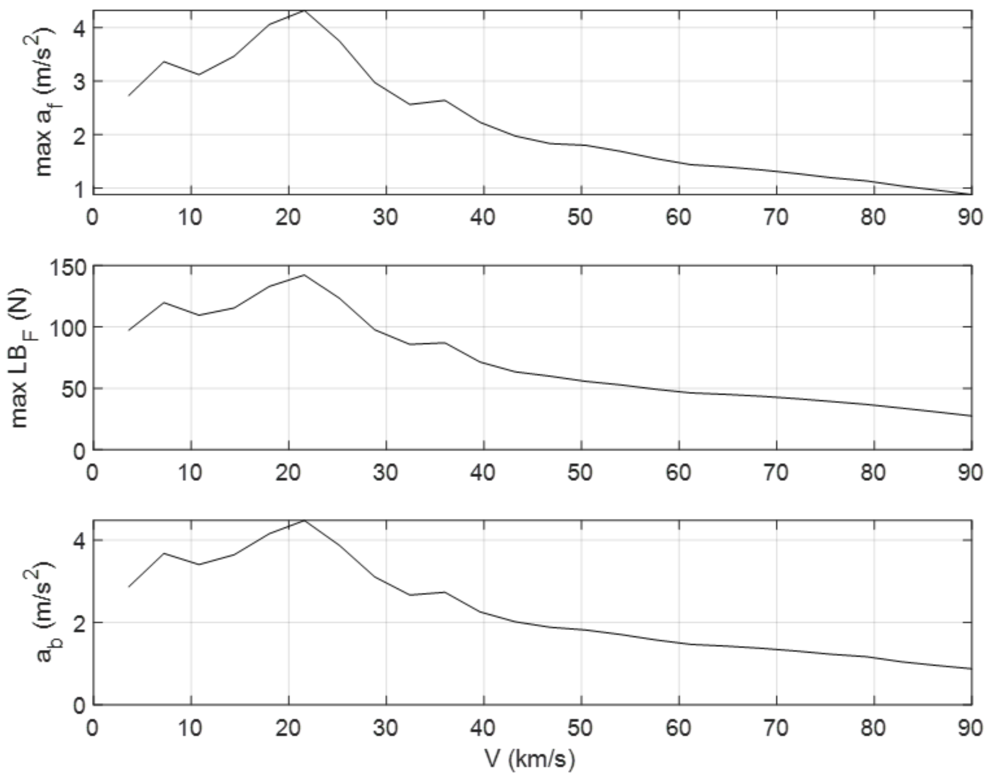

Fig 7. Maximum accelerations acting on the fetus and head at different speeds.

A close examination of the graphs reveals that acceleration and force values reach a maximum at approximately 22 km/h, after which they demonstrate a pronounced downward trend at higher speeds.

This suggests that pregnant individuals operating motor vehicles should avoid velocities of approximately 22 km/h when traversing speed humps. To ensure optimal safety during crossing, it is recommended that speeds be maintained at low levels (e.g., 5 km/h) or at relatively high levels (e.g., 40-50 km/h).

During the modeling process, the damping force is defined by the relation ($F_d = cv$), where c is a constant. This relation demonstrates a direct proportionality between the damping force and the velocity. While this assertion is theoretically valid, it is not supported by empirical evidence. In practice, vehicle shock absorbers dampen more at high speeds. Consequently, despite the model's precision, the mechanical components of the vehicle may sustain damage when traversing speed breakers at high speeds. It is recommended that low-speed operation be maintained for two reasons. Firstly, this practice is intended to avert potential mechanical damage to the vehicle. Secondly, it is intended to minimize the adverse dynamic effects on the pregnant driver and fetus.

REFERENCES

1. Abbas, W., Abouelatta, O. B., El-Azab, M., El-Saidy, M., & Megahed, A. A. (2011). Optimal seat suspension design using genetic algorithms. Journal of Mechanics Engineering and Automation, 1(1), 44–52.

2. Kula, M. E., Usanmaz, B., & Gündoğdu, Ö. (2024). Calculation of maximum accelerations to the head and internal organs of a cyclist. In Proceedings of the 5th International Conference on Advanced Engineering Technologies (ICADET 2024) (ss. 813–818). Bayburt University

3. Griffin, M. J. (1990). Handbook of human vibration. Academic Press.

4. Kula, M. E., Usanmaz, B., & Gündoğdu, Ö. (2024). INVESTIGATION OF HAND-ARM VIBRATION EXPOSED TO A DRIVER IN TERMS OF OCCUPATIONAL HEALTH AND SAFETY. In D. B. Sarıipek (Ed.), Proceedings of the 1st International Ayasofya Scientific Researches and Innovation Congress (16–17 November 2024, Istanbul, Türkiye) (ss. 165–175). BİLSEL Yayıncılık.

5. International Organization for Standardization. (1997). ISO 2631-1:1997 – Mechanical vibration and shock – Evaluation of human exposure to whole-body vibration – Part 1: General requirements.

6. Eger, T. R., & Dickey, J. P. (2015). Vibration exposure characteristics and health risk prevention strategies associated with vibration exposure during mining applications. The Journal of the Acoustical Society of America, 137(4_Supplement), 2378. https://doi.org/10.1121/1.4920640

7. J., & Lott, M. (2000). Work-Relatedness and Threshold Limit Values for Back Disorders due to Exposure to whole Body Vibration. Proceedings of the Human Factors and Ergonomics Society Annual Meeting, 44(30), 5–620. https://doi.org/10.1177/154193120004403079

8. Adane, H. A., Iles, R., Boyle, J. A., Gelaw, A., & Collie, A. (2023). Maternal Occupational Risk Factors and Preterm Birth: A Systematic Review and Meta-Analysis. Public Health Reviews, 44. https://doi.org/10.3389/phrs.2023.1606085

9. Wójcik, M., Jarząbek-Bielecka, G., Merks, P., Luwański, D., Plagens-Rotman, K., Pisarska-Krawczyk, M., Mizgier, M., & Kędzia, W. (2022). Visceral Therapy and Physical Activity for Selected Dysfunctions, with Particular Emphasis on Locomotive Organ Pain in Pregnant Women—Importance of Reducing Oxidative Stress. Antioxidants, 11(6), 1118. https://doi.org/10.3390/antiox11061118

10. Croteau, A. (2020). Occupational lifting and adverse pregnancy outcome: a systematic review and meta-analysis. Occupational and Environmental Medicine, 77(7), 496–505. https://doi.org/10.1136/oemed-2019-106334

11. Yunitasari, E., Matos, F., Zulkarnain, H., Kumalasari, D. I., Kusumaningrum, T., Putri, T. E., Yusuf, A., & Astuti, N. P. (2022). PREGNANT WOMAN IN DEVELOPING COUNTRY

AWARENESS OF OBSTETRIC DANGER SIGNS: SYSTEMATIC REVIEW. Research Square (Research Square). https://doi.org/10.21203/rs.3.rs-2195143/v1

12. Munera, M., Chiementin, X., Crequy, S., & Bertucci, W. (2014). Physical risk associated with vibration at cycling. Mechanics & Industry, 15(6), 535–540. https://doi.org/10.1051/meca/2014057

13. Maseresha, N., Woldemichael, K., & Dube, L. (2016). Knowledge of obstetric danger signs and associated factors among pregnant women in Erer district, Somali region, Ethiopia. BMC Women S Health, 16(1). https://doi.org/10.1186/s12905-016-0309-3

14. Sardasht, F. G., Motaghi, Z., Shariati, M., Keramat, A., & Akbari, N. (2022). The Status, policies, and Programs of Preconception Risk Assessment in Iran: A Narrative review. Journal of Caring Sciences, 11(2), 105–117. https://doi.org/10.34172/jcs.2022.15

15. Mbalinda, S. N., Nakimuli, A., Kakaire, O., Osinde, M. O., Kakande, N., & Kaye, D. K. (2014). Does knowledge of danger signs of pregnancy predict birth preparedness? A critique of the evidence from women admitted with pregnancy complications. Health Research Policy and Systems, 12(1). https://doi.org/10.1186/1478-4505-12-60

16. Munera, M., Chiementin, X., Crequy, S., & Bertucci, W. (2014b). Physical risk associated with vibration at cycling. Mechanics & Industry, 15(6), 535–540. https://doi.org/10.1051/meca/2014057

17. Qassem, W., & Othman, M. O. (1996). Vibration effects on sitting pregnant women—subjects of various masses. Journal of Biomechanics, 29(4), 493–501.

18. Liang, C.-C., Chiang, C.-F. ve Nguyen, T.-G., 2007. Biodynamic responses of seated pregnant subjects exposed to Vertical Vibrations in Driving Conditions. Vehicle System Dynamics. 45, 1017–1049.

19. Yanıkören, M., Tezgel, S., Usanmaz, B., & Gündoğdu, Ö. (2020). The effect of vehicle vibrations on driver comfort: Half car and driver model. Gümüşhane University Journal of Science and Technology, 10(3), 796–803.

20. Liang, C., & Chiang, C. (2006). A study on biodynamic models of seated human subjects exposed to vertical vibration. International Journal of Industrial Ergonomics, 36(10), 869–890.

21. Abbas, W., Emam, A., Badran, S., Shebl, M., & Abouelatta, O. (2013). Optimal Seat and Suspension Design for a Half-Car with Driver Model Using Genetic Algorithm. Intelligent Control and Automation, 04(02), 199–205. https://doi.org/10.4236/ica.2013.42024

ON SOME FRACTIONAL INTEGRAL INEQUALITIES FOR STRONGLY MODIFIED $(\alpha, h-m)$-CONVEX FUNCTIONS

Ayşe Kübra DEMİREL [1]

[1] Department of Mathematics, Ordu University, Ordu, Turkey

aysekubrademirel@gmail.com,

Abstract

This paper introduces strongly modified $(\alpha, h-m)$-convex functions, which generalization strongly modified h-convex functions, and proves some of their properties. Hermite–Hadamard type inequalities are obtained for these functions. Furthermore, the Riemann-Liouville integral is used to prove Hermite-Hadamard inequalities.

Keywords: Convex function; Hermite-Hadamard inequality; Riemann-Liouville integral.

1.INTRODUCTION

Convex functions play an important role in many areas of mathematics. They are particularly significant in engineering and in the study of optimization problems. There are many generalizations of convex functions in the literature. For instance, strongly convexity is a key concept in this field of study. Various studies on strongly convexity can be found in the literature (see [2,4-6,9-10]).

Definition 1. [7] Let $J \subseteq \mathbb{R}$ be an interval and let $h: J \to \mathbb{R}$ be a nonnegative function. Then the function $f: [0,r] \to \mathbb{R}$ with $r > 0$ is a modified h-convex function, if

$$f\left(tx+(1-t)y\right) \leq h(t) f(x) + \left(1-h(t)\right) f(y),$$

holds $x, y \in [0,r]$ and $t \in [0,1]$.

Definiton 2. [8] Let $I \subset \mathbb{R}$ be an interval and let c be a positive number. A function $f: I \to \mathbb{R}$ is called strongly convex function with modulus $c > 0$, if

$$f\left(tx+(1-t)y\right) \leq tf(x) + (1-t) f(y) - ct(1-t)(y-x)^2,$$

for all $x, y \in I$ and $t \in [0,1]$.

Definition 3. [2] A function $f:[0,r]\to\mathbb{R}$ with $r>0$ is a strongly modified (h,m)-convex function with modulus $c>0$, if

$$f(tx+m(1-t)y)\le h(t)f(x)+m(1-h(t))f(y)-mct(1-t)(y-x)^2,$$

holds $x,y\in[0,r]$, $c>0$, $m\in[0,1]$ and $t\in[0,1]$.

2.GENERAL PROPERTIES OF METHOD

One of the best-known inequalities in the field of convex analysis is the Hermite–Hadamard inequality. First presented by J. Hadamard in 1893 as the Hadamard inequality. It was later widely used as the Hermite–Hadamard inequality. This inequality provides an estimate of the mean value of a convex function. [1-3].

Theorem 1. [3] Let $f:[a,b]\to\mathbb{R}$ be a convex function for $a<b$. Then the following inequality holds:

$$f\left(\frac{a+b}{2}\right)\le\frac{1}{b-a}\int_a^b f(x)\,dx\le\frac{f(a)+f(b)}{2}.$$

In [8], N. Merentes and K. Nikodem presented Hermite-Hadamard inequality via strongly convex function:

Theorem 2. Let $f:[a,b]\to\mathbb{R}$ be a strongly convex function with modulus $c>0$, then

$$f\left(\frac{a+b}{2}\right)+\frac{c}{12}(b-a)^2\le\frac{1}{b-a}\int_a^b f(x)\,dx\le\frac{f(a)+f(b)}{2}-\frac{c}{6}(b-a)^2.$$

Definition 4. [11] Let $f\in L[a,b]$. Then the Riemann-Liouville fractional integrals of order $\beta>0$ are described as:

$$M_{a+}^{\beta}f(x)=\frac{1}{\Gamma(\beta)}\int_a^x (x-t)^{\beta-1}f(t)\,dt,\quad x>a$$

$$M_{b-}^{\beta}f(x)=\frac{1}{\Gamma(\beta)}\int_x^b (t-x)^{\beta-1}f(t)\,dt,\quad x<b,$$

where $\Gamma(\beta)$ is the Gamma function.

3.APPLICATIONS

In this section, we will present some properties of the strongly modified $(\alpha, h-m)$-convex functions. Then we will prove some integral inequalities for this class of functions.

Definition 5. Let $J \subseteq \mathbb{R}$ be an interval, and let $h: J \to \mathbb{R}$ be a nonnegative function. Then the function $f:[0,r] \to \mathbb{R}$ is called strongly modified $(\alpha, h-m)$-convex function with modulus $c>0$, if

$$f(tx+m(1-t)y) \leq h(t^\alpha) f(x) + m(1-h(t^\alpha)) f(y) - mct(1-t)(y-x)^2,$$

holds for all $x, y \in [0,r]$, $(\alpha, m) \in [0,1]^2$ and $t \in [0,1]$.

Remark 1. a) If we set $\alpha = 1$, we obtain the strongly modified (h,m)-convex function (see [2]),

b) If we set $\alpha = m = 1$, we obtain the strongly modified h-convex function.

c) If we set $\alpha = 1$ and $c = 0$, we obtain the modified (h,m)-convex function.

Proposition 1. Let f and g are strongly modified (SM) $(\alpha, h-m)$-convex function, then their sum $f+g$ is also SM-$(\alpha, h-m)$-convex function.

Proof. For $x, y \in [0,r]$, we get

$$(f+g)(tx+m(1-t)y) = f(tx+m(1-t)y) + g(tx+m(1-t)y).$$

Since f and g are SM-$(\alpha, h-m)$-convex function,

$$\begin{aligned}(f+g)(tx+m(1-t)y) &\leq h(t^\alpha) f(x) + m(1-h(t^\alpha)) f(y) - mct(1-t)(y-x)^2 \\ &\quad + h(t^\alpha) g(x) + m(1-h(t^\alpha)) g(y) - mct(1-t)(y-x)^2 \\ &= h(t^\alpha)(f+g)(x) + m(1-h(t^\alpha))(f+g)(y) - mct(1-t)(y-x)^2.\end{aligned}$$

Proposition 2. Let f be a SM-$(\alpha,h-m)$-convex function, then for scalar $n>0$, nf is also SM-$(\alpha,h-m)$-convex function.

Proof. For $x,y\in[0,r]$, we get

$$nf\left(tx+m(1-t)y\right)\le n\left(h\left(t^{\alpha}\right)f(x)+m\left(1-h\left(t^{\alpha}\right)\right)f(y)-mct(1-t)(y-x)^{2}\right)$$

$$=h\left(t^{\alpha}\right)nf(x)+m\left(1-h\left(t^{\alpha}\right)\right)nf(y)-mct(1-t)(y-x)^{2}.$$

Proposition 3. Let h_1 and h_2 nonnegative function on J and $h_2(t)\le h_1(t)$. If f is SM-(α,h_2-m)-convex function, then f is also SM-(α,h_1-m)-convex function.

$$f\left(tx+m(1-t)y\right)\le h_2\left(t^{\alpha}\right)f(x)+m\left(1-h_2\left(t^{\alpha}\right)\right)f(y)-mct(1-t)(y-x)^{2}$$

$$\le h_1\left(t^{\alpha}\right)f(x)+m\left(1-h_1\left(t^{\alpha}\right)\right)f(y)-mct(1-t)(y-x)^{2}.$$

Proposition 4. Let $f_i:[0,r]\to\mathbb{R}$ are SM-$(\alpha,h-m)$-convex function for $i\in\mathbb{N}$ and $\sum_{i=1}^{d}n_i=1$; then their linear combination $\Omega(u)=\sum_{i=1}^{d}n_if_i(u)$, $\forall t\in[0,r]$ is also SM-$(\alpha,h-m)$-convex function.

Proof. By choosing $x,y\in[0,r]$ with $r>0$ and $u=tx+m(1-t)y$;

$$\Omega\left(tx+m(1-t)y\right)=\sum_{i=1}^{d}n_if_i\left(tx+m(1-t)y\right).$$

Since f_i is SM-$(\alpha,h-m)$-convex function,

$$\Omega\left(tx+m(1-t)y\right)\le h\left(t^{\alpha}\right)\sum_{i=1}^{d}n_if_i(x)+m\left(1-h\left(t^{\alpha}\right)\right)\sum_{i=1}^{d}n_if_i(y)-\sum_{i=1}^{d}n_imct(1-t)(y-x)^{2}$$

$$=h\left(t^{\alpha}\right)\Omega(x)+m\left(1-h\left(t^{\alpha}\right)\right)\Omega(y)-mct(1-t)(y-x)^{2}.$$

Theorem 3. Let $f:[0,r]\to\mathbb{R}$ with $r>0$ be a strongly modified $(\alpha,h-m)$-convex function such that for $a,b\in[0,r]$, $a<b$, then

$$f\left(\frac{a+mb}{2}\right)+\frac{mc}{4}F_t\le h\left(\frac{1}{2^\alpha}\right)\frac{1}{mb-a}\int_a^{mb}f(x)dx+m^2\left(1-h\left(\frac{1}{2^\alpha}\right)\right)\frac{1}{mb-a}\int_{a/m}^{b}f(x)dx$$

$$\le h\left(\frac{1}{2^\alpha}\right)\int_0^1\left(h(t^\alpha)f(a)+m\left(1-h(t^\alpha)\right)f(b)-mct(1-t)(b-a)^2\right)dt$$

$$+m\left(1-h\left(\frac{1}{2^\alpha}\right)\right)\int_0^1\left(m\left(1-h(t^\alpha)\right)f\left(\frac{a}{m^2}\right)+h(t^\alpha)f(b)-mct(1-t)\left(b-\frac{a}{m^2}\right)^2\right)dt. \quad (1)$$

where

$$F_t=\int_0^1\left(t(b-a)+(1-t)\left(\frac{a}{m}-mb\right)\right)^2dt.$$

Proof. For $x,y\in[0,r]$ with $r>0$, we get

$$f(tx+m(1-t)y)\le h(t^\alpha)f(x)+m\left(1-h(t^\alpha)\right)f(y)-mct(1-t)(y-x)^2 \quad (2)$$

If we put $t=\frac{1}{2}$ in (2), we get

$$f\left(\frac{x+my}{2}\right)\le h\left(\frac{1}{2^\alpha}\right)f(x)+m\left(1-h\left(\frac{1}{2^\alpha}\right)\right)f(y)-\frac{mc}{4}(y-x)^2 \quad (3)$$

By choosing $x=ta+m(1-t)b$ and $y=(1-t)\frac{a}{m}+tb$ in (3), we obtain

$$f\left(\frac{a+mb}{2}\right)\le h\left(\frac{1}{2^\alpha}\right)f(ta+m(1-t)b)+m\left(1-h\left(\frac{1}{2^\alpha}\right)\right)f\left((1-t)\frac{a}{m}+tb\right)$$

$$-\frac{mc}{4}\left(t(b-a)+(1-t)\left(\frac{a}{m}-mb\right)\right)^2. \quad (4)$$

By integrating (4) with respect to "t" from *0* to *1*, we have

$$f\left(\frac{a+mb}{2}\right)\int_0^1 1dt\le h\left(\frac{1}{2^\alpha}\right)\int_0^1 f(ta+m(1-t)b)dt+m\left(1-h\left(\frac{1}{2^\alpha}\right)\right)\int_0^1 f\left((1-t)\frac{a}{m}+tb\right)dt$$

$$-\frac{mc}{4}\int_0^1\left(t(b-a)+(1-t)\left(\frac{a}{m}-mb\right)\right)^2dt.$$

$$f\left(\frac{a+mb}{2}\right)+\frac{mc}{4}F_t \le h\left(\frac{1}{2^\alpha}\right)\int_0^1 f\left(ta+m(1-t)b\right)dt+m\left(1-h\left(\frac{1}{2^\alpha}\right)\right)\int_0^1 f\left((1-t)\frac{a}{m}+tb\right)dt. \quad (5)$$

Put $x=ta+m(1-t)b$ in the first integral of (5) and $x=(1-t)\frac{a}{m}+tb$ in the second integral of (5), to get

$$f\left(\frac{a+mb}{2}\right)+\frac{mc}{4}F_t \le h\left(\frac{1}{2^\alpha}\right)\frac{1}{mb-a}\int_a^{mb} f(x)dx+m^2\left(1-h\left(\frac{1}{2^\alpha}\right)\right)\frac{1}{mb-a}\int_{a/m}^{b} f(x)dx. \quad (6)$$

By comparing the right-hand side of (5) and (6),

$$h\left(\frac{1}{2^\alpha}\right)\frac{1}{mb-a}\int_a^{mb} f(x)dx+m^2\left(1-h\left(\frac{1}{2^\alpha}\right)\right)\frac{1}{mb-a}\int_{a/m}^{b} f(x)dx$$

$$=h\left(\frac{1}{2^\alpha}\right)\int_0^1 f\left(ta+m(1-t)b\right)dt+m\left(1-h\left(\frac{1}{2^\alpha}\right)\right)\int_0^1 f\left((1-t)\frac{a}{m}+tb\right)dt.$$

Since f is a SM-$(\alpha,h-m)$-convex function, we have

$$h\left(\frac{1}{2^\alpha}\right)\frac{1}{mb-a}\int_a^{mb} f(x)dx+m^2\left(1-h\left(\frac{1}{2^\alpha}\right)\right)\frac{1}{mb-a}\int_{a/m}^{b} f(x)dx$$

$$\le h\left(\frac{1}{2^\alpha}\right)\int_0^1\left(h(t^\alpha)f(a)+m\left(1-h(t^\alpha)\right)f(b)-mct(1-t)(b-a)^2\right)dt \quad (7)$$

From (6) and (7), we obtain

$$f\left(\frac{a+mb}{2}\right)+\frac{mc}{4}F_t \le h\left(\frac{1}{2^\alpha}\right)\frac{1}{mb-a}\int_a^{mb} f(x)dx+m^2\left(1-h\left(\frac{1}{2^\alpha}\right)\right)\frac{1}{mb-a}\int_{a/m}^{b} f(x)dx$$

$$\le h\left(\frac{1}{2^\alpha}\right)\int_0^1\left(h(t^\alpha)f(a)+m\left(1-h(t^\alpha)\right)f(b)-mct(1-t)(b-a)^2\right)dt$$

$$+m\left(1-h\left(\frac{1}{2^\alpha}\right)\right)\int_0^1\left(m\left(1-h(t^\alpha)\right)f\left(\frac{a}{m^2}\right)+h(t^\alpha)f(b)-mct(1-t)\left(b-\frac{a}{m^2}\right)^2\right).$$

Remark 2. a) If $\alpha=1$ in (1), we obtain Theorem 2 of [2].

b) If $\alpha=m=1$ and $h(t)=t$ in (1), we obtain Theorem 6 of [8].

c) If $\alpha=m=1$ and $c=0$ in (1), we obtain Theorem 3 of [7].

Corollary 1. a) If we take $c=0$ and $m=1$ in (1), we have

$$f\left(\frac{a+b}{2}\right)\le\frac{1}{b-a}\int_a^b f(x)dx\le\left(1-2h\left(\frac{1}{2^\alpha}\right)\right)\left(f(b)-f(a)\right)\int_0^1 h(t^\alpha)dt+f(a).$$

b) If we take $m=1$ and $h(t)=t$ in (1), we have

$$f\left(\frac{a+b}{2}\right)+\frac{c(b-a)^2}{12}\le\frac{1}{b-a}\int_a^b f(x)dx$$

$$\le\frac{\left[\alpha 2^\alpha-\alpha+1\right]f(a)}{2^\alpha(\alpha+1)}+\frac{\left[\alpha+2^\alpha-1\right]f(b)}{2^\alpha(\alpha+1)}-\frac{c(b-a)^2}{6}.$$

Theorem 4. Assume that $f:[0,r]\to\mathbb{R}$ is a SM-$(\alpha,h-m)$-convex function for $a,b\in[0,r]$ with $a<b$, then we have

$$f\left(\frac{a+mb}{2}\right)+\frac{mc\beta}{4}F_\beta\le\frac{\Gamma(\beta+1)}{(mb-a)^\beta}\left[\left(1-h\left(\frac{1}{2^\alpha}\right)\right)M_{a+}^\beta f(mb)+m^{\beta+1}M_{b-}^\beta f\left(\frac{a}{m}\right)\right]$$

$$\le\beta\left[\left(1-h\left(\frac{1}{2^\alpha}\right)\right)f(a)-m\left(1-h\left(\frac{1}{2^\alpha}\right)\right)f(b)-m^2h\left(\frac{1}{2^\alpha}\right)f\left(\frac{a}{m^2}\right)\right]\int_0^1 t^{\beta-1}h(t^\alpha)dt$$

$$+m\left[\left(1-h\left(\frac{1}{2^\alpha}\right)\right)f(b)+mh\left(\frac{1}{2^\alpha}\right)f\left(\frac{a}{m^2}\right)\right] \tag{8}$$

where

$$F_\beta=\int_0^1 t^{\beta-1}\left(t(b-a)+(1-t)\left(\frac{a}{m}-mb\right)\right)^2dt.$$

Proof. Since f is a SM-$(\alpha,h-m)$-convex function, then

$$f\left((1-t)x+mty\right)\le\left(1-h(t^\alpha)\right)f(x)+mh(t^\alpha)f(y)-mct(1-t)(y-x)^2. \tag{9}$$

By choosing $t=\frac{1}{2}$, we get

$$f\left(\frac{x+my}{2}\right)\le\left(1-h\left(\frac{1}{2^\alpha}\right)\right)f(x)+mh\left(\frac{1}{2^\alpha}\right)f(y)-\frac{mc}{4}(y-x)^2. \tag{10}$$

Assume that $x=ta+m(1-t)b$ and $y=(1-t)\frac{a}{m}+tb$ in (10) to get

$$f\left(\frac{a+mb}{2}\right)\leq\left(1-h\left(\frac{1}{2^{\alpha}}\right)\right)f\left(ta+m(1-t)b\right)+mh\left(\frac{1}{2^{\alpha}}\right)f\left((1-t)\frac{a}{m}+tb\right)$$

$$-\frac{mc}{4}\left(t(b-a)+(1-t)\left(\frac{a}{m}-mb\right)\right)^{2}. \tag{11}$$

Multiplying (11) with $t^{\beta-1}$ and then integrating with respect to "t" from *0* to *1*, we get

$$\int_0^1 f\left(\frac{a+mb}{2}\right)t^{\beta-1}dt\leq\left(1-h\left(\frac{1}{2^{\alpha}}\right)\right)\int_0^1 t^{\beta-1}f\left(ta+m(1-t)b\right)dt+mh\left(\frac{1}{2^{\alpha}}\right)\int_0^1 t^{\beta-1}f\left((1-t)\frac{a}{m}+tb\right)dt$$

$$-\frac{mc}{4}\int_0^1 t^{\beta-1}\left(t(b-a)+(1-t)\left(\frac{a}{m}-mb\right)\right)^{2}dt.$$

$$\frac{1}{\beta}f\left(\frac{a+mb}{2}\right)+\frac{mc}{4}F_{\beta}\leq\left(1-h\left(\frac{1}{2^{\alpha}}\right)\right)\int_0^1 t^{\beta-1}f\left(ta+m(1-t)b\right)dt$$

$$+mh\left(\frac{1}{2^{\alpha}}\right)\int_0^1 t^{\beta-1}f\left((1-t)\frac{a}{m}+tb\right)dt. \tag{12}$$

Put $x=ta+m(1-t)b$ in the first integral of (12) and $x=(1-t)\frac{a}{m}+tb$ in the second integral of (12), to have

$$\frac{1}{\beta}f\left(\frac{a+mb}{2}\right)+\frac{mc}{4}F_{\beta}\leq\left(1-h\left(\frac{1}{2^{\alpha}}\right)\right)\int_a^{mb}\left(\frac{mb-x}{mb-a}\right)^{\beta-1}\frac{f(x)}{mb-a}dx$$

$$+m^{2}h\left(\frac{1}{2^{\alpha}}\right)\int_{a/m}^{b}\left(\frac{mx-a}{mb-a}\right)^{\beta-1}\frac{f(x)}{mb-a}dx. \tag{13}$$

Since,

$$\int_a^{mb}(mb-x)^{\beta-1}f(x)dx=\Gamma(\beta)M_{a+}^{\beta}f(mb)$$

$$\int_{a/m}^{b}(mx-a)^{\beta-1}f(x)dx=\Gamma(\beta)m^{\beta-1}M_{b-}^{\beta}f\left(\frac{a}{m}\right)$$

Consequently (13) becomes,

$$f\left(\frac{a+mb}{2}\right)+\frac{mc\beta}{4}F_{\beta}\le\frac{\Gamma(\beta+1)}{(mb-a)^{\beta}}\left[\left(1-h\left(\frac{1}{2^{\alpha}}\right)\right)M_{a+}^{\beta}f(mb)+m^{\beta+1}h\left(\frac{1}{2^{\alpha}}\right)M_{b-}^{\beta}f\left(\frac{a}{m}\right)\right]. \quad (14)$$

Also f is SM-$(\alpha,h-m)$-convex function, then

$$f(ta+m(1-t)b)\le h(t^{\alpha})f(a)+m(1-h(t^{\alpha}))f(b)-mct(1-t)(b-a)^{2}, \quad (15)$$

and

$$f\left((1-t)\frac{a}{m}+tb\right)\le m(1-h(t^{\alpha}))f\left(\frac{a}{m^{2}}\right)+h(t^{\alpha})f(b)-mct(1-t)\left(b-\frac{a}{m^{2}}\right)^{2}. \quad (16)$$

Multiplying (15) with $\left(1-h\left(\frac{1}{2^{\alpha}}\right)\right)$ and multiplying (16) with $h\left(\frac{1}{2^{\alpha}}\right)$, then adding (15) and (16), we get

$$\left(1-h\left(\frac{1}{2^{\alpha}}\right)\right)f(ta+m(1-t)b)+mh\left(\frac{1}{2^{\alpha}}\right)f\left((1-t)\frac{a}{m}+tb\right)$$

$$\le\left(1-h\left(\frac{1}{2^{\alpha}}\right)\right)\left[h(t^{\alpha})f(a)+m(1-h(t^{\alpha}))f(b)-mct(1-t)(b-a)^{2}\right]$$

$$+h\left(\frac{1}{2^{\alpha}}\right)\left[m^{2}(1-h(t^{\alpha}))f\left(\frac{a}{m^{2}}\right)+mh(t^{\alpha})f(b)-m^{2}ct(1-t)\left(b-\frac{a}{m^{2}}\right)^{2}\right]$$

$$=h(t^{\alpha})\left[\left(1-h\left(\frac{1}{2^{\alpha}}\right)\right)(f(a)-mf(b))-m^{2}h\left(\frac{1}{2^{\alpha}}\right)f\left(\frac{a}{m^{2}}\right)\right]$$

$$+m\left[\left(1-h\left(\frac{1}{2^{\alpha}}\right)\right)f(b)+mh\left(\frac{1}{2^{\alpha}}\right)f\left(\frac{a}{m^{2}}\right)\right]$$

$$-\left(1-h\left(\frac{1}{2^{\alpha}}\right)\right)mct(1-t)(b-a)^{2}-h\left(\frac{1}{2^{\alpha}}\right)m^{2}ct(1-t)\left(b-\frac{a}{m^{2}}\right)^{2}. \quad (17)$$

Multiplying (17) with $t^{\beta-1}$ and then integrating with respect to "t" from *0* to *1*, we have

$$\left(1-h\left(\frac{1}{2^{\alpha}}\right)\right)\int_{0}^{1}t^{\beta-1}f(ta+m(1-t)b)dt+mh\left(\frac{1}{2^{\alpha}}\right)\int_{0}^{1}t^{\beta-1}f\left((1-t)\frac{a}{m}+tb\right)dt$$

$$\le\left[\left(1-h\left(\frac{1}{2^{\alpha}}\right)\right)(f(a)-mf(b))-m^{2}h\left(\frac{1}{2^{\alpha}}\right)f\left(\frac{a}{m^{2}}\right)\right]\int_{0}^{1}t^{\beta-1}h(t^{\alpha})dt$$

$$+m\left[\left(1-h\left(\frac{1}{2^{\alpha}}\right)\right)f(b)+mh\left(\frac{1}{2^{\alpha}}\right)f\left(\frac{a}{m^2}\right)\right]\int_0^1 t^{\beta-1}dt$$

$$-\left(1-h\left(\frac{1}{2^{\alpha}}\right)\right)mc(b-a)^2\int_0^1 t^{\beta}(1-t)\,dt-h\left(\frac{1}{2^{\alpha}}\right)m^2c\left(b-\frac{a}{m^2}\right)^2\int_0^1 t^{\beta}(1-t)\,dt. \qquad (18)$$

Put $x=ta+m(1-t)b$ in the first integral of (18) and $x=(1-t)\frac{a}{m}+tb$ in the second integral of (18), we obtain

$$\left(1-h\left(\frac{1}{2^{\alpha}}\right)\right)\int_a^{mb}\left(\frac{mb-x}{mb-a}\right)^{\beta-1}\frac{f(x)}{mb-a}dx+m^2h\left(\frac{1}{2^{\alpha}}\right)\int_{a/m}^{b}\left(\frac{mx-a}{mb-a}\right)^{\beta-1}\frac{f(x)}{mb-a}dx$$

$$\leq\left[\left(1-h\left(\frac{1}{2^{\alpha}}\right)\right)\left(f(a)-mf(b)\right)-m^2h\left(\frac{1}{2^{\alpha}}\right)f\left(\frac{a}{m^2}\right)\right]\int_0^1 t^{\beta-1}h\left(t^{\alpha}\right)dt$$

$$+\frac{m}{\beta}\left[\left(1-h\left(\frac{1}{2^{\alpha}}\right)\right)f(b)+mh\left(\frac{1}{2^{\alpha}}\right)f\left(\frac{a}{m^2}\right)\right]$$

$$-\frac{mc\left[\left(1-h\left(\frac{1}{2^{\alpha}}\right)\right)(b-a)^2+mh\left(\frac{1}{2^{\alpha}}\right)\left(b-\frac{a}{m^2}\right)^2\right]}{(\beta+1)(\beta+2)}.$$

$$\frac{\Gamma(\beta+1)}{(mb-a)^{\beta}}\left[\left(1-h\left(\frac{1}{2^{\alpha}}\right)\right)M_{a+}^{\beta}f(mb)+m^{\beta+1}h\left(\frac{1}{2^{\alpha}}\right)M_{b-}^{\beta}f\left(\frac{a}{m}\right)\right]$$

$$\leq\beta\left[\left(1-h\left(\frac{1}{2^{\alpha}}\right)\right)\left(f(a)-mf(b)\right)-m^2h\left(\frac{1}{2^{\alpha}}\right)f\left(\frac{a}{m^2}\right)\right]\int_0^1 t^{\beta-1}h\left(t^{\alpha}\right)dt$$

$$+m\left[\left(1-h\left(\frac{1}{2^{\alpha}}\right)\right)f(b)+mh\left(\frac{1}{2^{\alpha}}\right)f\left(\frac{a}{m^2}\right)\right]$$

$$-\frac{mc\beta\left[\left(1-h\left(\frac{1}{2^{\alpha}}\right)\right)(b-a)^2+mh\left(\frac{1}{2^{\alpha}}\right)\left(b-\frac{a}{m^2}\right)^2\right]}{(\beta+1)(\beta+2)}. \qquad (19)$$

From (14) and (19), we obtain

$$f\left(\frac{a+mb}{2}\right)+\frac{mc\beta}{4}F_{\beta}\leq\frac{\Gamma(\beta+1)}{(mb-a)^{\beta}}\left[\left(1-h\left(\frac{1}{2^{\alpha}}\right)\right)M_{a+}^{\beta}f(mb)+m^{\beta+1}h\left(\frac{1}{2^{\alpha}}\right)M_{b-}^{\beta}f\left(\frac{a}{m}\right)\right]$$

$$\leq \beta\left[\left(1-h\left(\frac{1}{2^{\alpha}}\right)\right)\left(f(a)-mf(b)\right)-m^{2}h\left(\frac{1}{2^{\alpha}}\right)f\left(\frac{a}{m^{2}}\right)\right]\int_{0}^{1}t^{\beta-1}h\left(t^{\alpha}\right)dt$$

$$+m\left[\left(1-h\left(\frac{1}{2^{\alpha}}\right)\right)f(b)+mh\left(\frac{1}{2^{\alpha}}\right)f\left(\frac{a}{m^{2}}\right)\right]$$

$$-\frac{mc\beta\left[\left(1-h\left(\frac{1}{2^{\alpha}}\right)\right)(b-a)^{2}+mh\left(\frac{1}{2^{\alpha}}\right)\left(b-\frac{a}{m^{2}}\right)^{2}\right]}{(\beta+1)(\beta+2)}.$$

Remark 3. a) If $\alpha=1$ in (8), we obtain Theorem 3 of [2].

b) If $\alpha=m=1$ and $h(t)=t$ in (1), we obtain the result of strongly convex function.

c) If $\alpha=m=1$ and $c=0$ in (1), we obtain the result of convex function.

Corollary 2. a) If we take $m=1$ and $c=0$, we have

$$f\left(\frac{a+b}{2}\right)\leq\frac{\Gamma(\beta+1)}{(b-a)^{\beta}}\left[\left(1-h\left(\frac{1}{2^{\alpha}}\right)\right)M_{a+}^{\beta}f(b)+h\left(\frac{1}{2^{\alpha}}\right)M_{b-}^{\beta}f(a)\right]$$

$$\leq \beta\left[\left(1-h\left(\frac{1}{2^{\alpha}}\right)\right)\left(f(a)-f(b)\right)-h\left(\frac{1}{2^{\alpha}}\right)f(a)\right]\int_{0}^{1}t^{\beta-1}h\left(t^{\alpha}\right)dt$$

$$+\left(1-h\left(\frac{1}{2^{\alpha}}\right)\right)f(b)+h\left(\frac{1}{2^{\alpha}}\right)f(a).$$

b) If we take $m=1$ and $h(t)=t$ in (1), we have

$$f\left(\frac{a+b}{2}\right)+\frac{c\beta(b-a)^{2}\left(\beta^{2}-\beta+2\right)}{4\beta(\beta+1)(\beta+2)}\leq\frac{\Gamma(\beta+1)}{(b-a)^{\beta}}\left[\left(1-\frac{1}{2^{\alpha}}\right)M_{a+}^{\beta}f(b)+\frac{1}{2^{\alpha}}M_{b-}^{\beta}f(a)\right]$$

$$+\frac{\beta}{\alpha+\beta}\left[\left(1-\frac{1}{2^{\alpha}}\right)\left(f(a)-f(b)\right)-\frac{1}{2^{\alpha}}f(a)\right]-\frac{c\beta(b-a)^{2}}{(\beta+1)(\beta+2)}.$$

c) If we take $\alpha=m=1$ in (1), we have

$$f\left(\frac{a+b}{2}\right)+\frac{c\beta(b-a)^{2}\left(\beta^{2}-\beta+2\right)}{4\beta(\beta+1)(\beta+2)}\leq\frac{\Gamma(\beta+1)}{(b-a)^{\beta}}\left[\left(1-h\left(\frac{1}{2}\right)\right)M_{a+}^{\beta}f(b)+h\left(\frac{1}{2}\right)M_{b-}^{\beta}f(a)\right]$$

$$\le \beta\left[\left(1-h\left(\frac{1}{2}\right)\right)\left(f(a)-f(b)\right)-h\left(\frac{1}{2}\right)\left(f(a)+f(b)\right)\right]\int_0^1 t^{\beta-1}h(t)\,dt$$

$$+\left(1-h\left(\frac{1}{2}\right)\right)f(b)+h\left(\frac{1}{2}\right)f(a)-\frac{c\beta(b-a)^2}{(\beta+1)(\beta+2)}.$$

d) If we take $m=1$, $h(t)=t$ and $c=0$ in (1), we have

$$f\left(\frac{a+b}{2}\right)\le\frac{\Gamma(\beta+1)}{(b-a)^{\beta}}\left[\left(1-\frac{1}{2^{\alpha}}\right)M_{a+}^{\beta}f(b)+\frac{1}{2^{\alpha}}M_{b-}^{\beta}f(a)\right]$$

$$\le\frac{\beta}{\alpha+\beta}\left[\left(1-\frac{1}{2^{\alpha}}\right)\left(f(a)-f(b)\right)-\frac{1}{2^{\alpha}}f(a)\right]$$

$$+\left(1-\frac{1}{2^{\alpha}}\right)f(b)+\frac{1}{2^{\alpha}}f(a).$$

4.CONCLUSIONS

In this paper, we presented the term of strongly modified $(\alpha,h-m)$-convex function, which generalizes the term of a strongly convex function, and examined some of its properties. We then proved some integral inequalities that this class of functions. In future, it will be possible to derive several inequalities and describe new classes of convex functions using fractional operators on this class of convex functions.

REFERENCES

1. Abdallah El Farissi, Simple Proof and Refinement of Hermite-Hadamard Inequality, Journal of Mathematical Inequalities, Vol:4, No:3, 365-369, 2010.
2. Ali N. A. Koam, Ammara Nosheen, Khuram Ali Khan, Mudassir Hussain Bukhari, Ali Ahmad, Maryam Salem Alatawi, On Riemann–Liouville Integral via Strongly Modified (h,m)-Convex Functions, Fractal and Fractional, Vol:2024, No:8, 680, 2024.
3. Baburao G. Pachpatte, Mathematical Inequalities, Elsevier, Vol:67, 2005.
4. Constantin Niculescu, Lars-Erik Persson, Convex Functions and Their Applications, New York: Springer, Vol:23, 2006.

5. Daniel Breaz, Çetin Yıldız, Luminita-Ioana Cotirla, Gauhar Rahman, Büşra Yergöz, New Hadamard Type Inequalities for Modified h-Convex Functions, Fractal and Fractional, Vol:7, No:3, 216, 2023.
6. Muhammad Ajmal, Muhammad Rafaqat, Labeeb Ahmed, Caputo Fractional Derivative Inequalities for Modified (h,m)-Convex Functions, Journal of Corrosion and Materials, Vol. 2023, No:48, 101-115, 2023.
7. Muhammad Aslam Noor, Khalida Inayat Noor, Muhammad Uzair Awan, Hermite-Hadamard Inequalities for Modified h-Convex Functions, Transylvanian Journal Of Mathematics And Mechanics, Vol:6, No:2, 171-180, 2014.
8. Nelson Merentes, Kazimierz Nikodem, Remarks on Strongly Convex Functions, Aequat. Math. Vol:2010, No:80, 193-199, 2010.
9. Peiyu Yan, Qi Li, Yu Ming Chu, Sana Mukhtar, Shumaila Waheed, On Some Fractional Integral Inequalities for Generalized Strongly Modified h-Convex Functions, AIMS Mathematics, Vol:5, No:6, 6620-6638, 2020.
10. Xiaobin Wang, Muhammad Shoaib Saleem, Kiran Naseem Aslam, Xingxing Wu, Tong Zhou, On Caputo-Fabrizio Fractional Integral Inequalities of Hermite-Hadamard Type for Modified h-Convex Functions, Journal of Mathematics, Vol:2020, Article ID 8829140, 17p, 2020.
11. Ghulam Farid, Study of a Generalized Riemann-Liouville Fractional Integral via Convex Functions, Commun. Fac. Sci. Univ. Ank. Ser. A1 Math. Stat, Vol:69, No:1, 37-48, 2020.

EXAMINING THE GOLDEN RATIO-AESTHETIC RELATIONSHIP IN HISTORICAL BRIDGES IN DIYARBAKIR

Bilge Su ÇİFÇİ[1] Samet GÜNDÜZ[2]

[1]Bismil BİLSEM, Ministry of Education, Diyarbakir, Türkiye

bilgesuc8@gmail.com

[2]Bismil BİLSEM, Ministry of Education, Diyarbakir, Türkiye

asametgunduz@gmail.com

Abstract

The golden ratio is a special numerical proportion that is considered aesthetically pleasing and harmonious in both mathematics and art. The golden ratio, approximately equal to 1.618, appears widely in nature and everyday life, ranging from art to sculpture and graphic design. Throughout history, it has often been used in architecture to ensure aesthetic integrity and visual harmony. This research aims to examine the arches of historical bridges based on the concept of the golden ratio and evaluate these structures aesthetically. This study is significant in revealing the aesthetic balance in the design of historical bridges through the use of the golden ratio, thereby contributing to the preservation and evaluation of cultural heritage. The study was carried out on three historical bridges located in Diyarbakır, a city rich in historical and cultural heritage, hosting numerous civilizations throughout history. The presence of the golden ratio in the arches of the examined bridges was analyzed using span-to-height ratios. Deviations from the golden ratio were calculated, and these values were evaluated in terms of the golden ratio-aesthetic relationship. The results showed that the design principles used in bridge construction could be related to the golden ratio and aesthetic criteria. Thus, the importance of examining the aesthetic values of historical structures from a mathematical perspective was highlighted. Additionally, this study makes a significant contribution to the field by combining the aesthetic aspect of historical structures with mathematical analysis.

Keywords: Golden ratio; Aesthetic evaluation; Historic bridges.

1. INTRODUCTION

Culture is the entirety of thought and artistic works unique to a society or community. Heritage is defined as something that one generation leaves to subsequent generations (TDK, 2024). Underlying the characterization of culture as heritage is the transfer of values held by societies to future generations (Kurtar & Somuncu, 2013). From this perspective, we can define cultural heritage as the thoughts and artworks transmitted from previous societies or communities to the present day. Institutions such as the United Nations Educational, Scientific, and Cultural Organization (UNESCO) categorize cultural heritage as "tangible cultural heritage, intangible cultural heritage, underwater cultural heritage, and natural cultural heritage." Tangible cultural heritage is further divided into movable and immovable categories. Sculptures, manuscripts, coins, and archaeological artifacts constitute movable cultural heritage, while immovable cultural heritage includes historical urban fabrics, monuments, and archaeological sites (Kuşçuoğlu & Taş, 2017).

Türkiye is a country that has hosted numerous civilizations throughout history, thus housing significant cultural heritage. Among the important tangible cultural heritages in Türkiye are historical bridges, categorized under immovable cultural heritage. Historical bridges reflect the architectural, engineering, and aesthetic understanding of different periods and constitute a vital part of the country's rich cultural heritage. Bridges are among the most significant structures in human history, constructed to overcome natural obstacles such as rivers, straits, and valleys, playing a crucial role in transportation. Bridges not only facilitate crossings but also contribute to shortening travel distances (Tanrıverdi & Gürel, 2019). Diyarbakır is one of the provinces in Türkiye that houses a significant portion of these historical bridges. Diyarbakır is a strategic intersection point linking the Mediterranean to the Persian Gulf and the Black Sea to Mesopotamia, as well as connecting to Azerbaijan and Iran via the Bitlis and Van Lake basins. Due to its location on important trade routes, the city has always been a center of commerce, maintaining this characteristic across different historical periods (Kutlay, 2012). Consequently, the city's cultural heritage preserves traces of numerous communities and civilizations, including the Assyrians, Urartians, Hittites, Persians, Romans, Byzantines, Umayyads, Abbasids, Artuqids, Seljuks, Aq Qoyunlu (aka. White Sheep Turkomans), Ottomans, and ultimately, the Republic of Türkiye (Kamuran, 2017; Kutlay, 2012). Historical structures in the city hold significant value in terms of regional cultural and engineering heritage. Bridges in Diyarbakır are noteworthy both functionally and aesthetically. Among the historical bridges constructed during various periods in the city are the Dicle Bridge, Haburman Bridge, Halilivran Bridge, Sinek Bridge, Kara Köprü, Malabadi Bridge, and Ambarçayı Bridge. The locations of historical bridges in Diyarbakır are shown in Figure 1.

1. Ambarcay Bridge 2. Cungus Bridge 3. Devegecidi Bridge 4. Tigris (Dicle) Bridge 5. Haburman Bridge
6. Halilviran Bridge 7. Black Bridge 8. Karasu Bridge 9. Malabadi Bridge 10. Sancak Bridge
11. Sinek Bridge

Figure 1. Locations of historical bridges in Diyarbakır (Dalkılıç and Halifeoğlu, 2009).

It can be stated that these bridges are significant due not only to their functional roles in connecting different regions but also to their aesthetic values and engineering techniques. Among these, Dicle Bridge, Malabadi Bridge, and Haburman Bridge are particularly notable in terms of engineering techniques and aesthetic values, thus forming the focus of this research.

The Dicle Bridge, named after the Tigris River over which it stands, is a significant structure that has become a symbol of the city with its size and architecture. Because it has ten arches, it is also known among the public as the “Ten-Arched Bridge.” The bridge was built using cut basalt stone (Ministry of Culture and Tourism [MoCT], 2024). According to the inscription on the bridge, one of the oldest in Diyarbakır, it was constructed in 1065 during the Marwanid period, although some claims suggest that it may belong to different periods as well (Yeşilbaş, 2007). Halifeoğlu and Dalkılıç (2009) also stated that the bridge had been destroyed and restored multiple times, and that three arches with wider spans were built in place of four arches that collapsed in the middle. They suggested that the original bridge may have had eleven arches. A visual of the Dicle Bridge is provided in Figure 2.

Figure 2. Dicle Bridge (MoCT, 2024)

Located 104 km from the city center over the Batman Creek, which flows into the Tigris, the Malabadi Bridge was constructed in 1147–48 by Timurtaş, the ruler of the Mardin Artuqids (Ilgazids), according to the inscription on it (Beysanoğlu, 1990). The Malabadi Bridge extends in a broken east-west axis, is steeply arched, and consists of a large central arch and four adjacent smaller arches, making five in total (Kutlay, 2012). With its pointed main arch spanning 40.86 meters, it is the stone arch bridge with the largest span in the world that has survived to the present day (Silvan District Governorship, 2024). With its internal rooms, the structure served not only the purpose of crossing the river but also provided accommodation and resting spaces for travelers using the road (Halifeoğlu, Toprak & Kavak, 2011). A visual of the Malabadi Bridge is presented in Figure 3.

Figure 3. Malabadi Bridge (MoCT, 2024)

The Haburman Bridge is located on the Sinek Creek, which flows into the Euphrates, along the old Çermik-Siverek road. According to the inscription on the bridge, it was built by the Artuqids in 1179 (Halifeoğlu, Toprak & Kavak, 2011). The bridge consists of a total of three arches, with a large pointed central arch and two smaller relieving arches on the sides. A visual of the Haburman Bridge is presented in Figure 4.

Figure 4. Haburman Bridge (MoCT, 2024)

These bridges are notable in the region not only for their functionality but also for their aesthetic and engineering qualities. Throughout history, the golden ratio has been used as an important element to ensure aesthetic integrity in the construction of many structures (Akın, 2021). The golden ratio is a mathematical proportion, approximately equal to 1.618, obtained by dividing a line such that the ratio of the larger part to the smaller part is equal to the ratio of the whole line to the larger part (Livio, 2002; as cited in Yılmaz, 2017). This ratio is considered the mathematical representation of aesthetics and balance in natural entities (Akın, 2021). Indeed, the existence of this aesthetic proportion has been observed in many architectural structures. The Egyptian pyramids are among the first architectural structures where the golden ratio was predominantly used (Hastürk, 2014). Other examples where the golden ratio has been identified include the Parthenon, considered the greatest work of Greek architecture; the Florence Cathedral in Italy; the Notre Dame Cathedral, a prime example of French Gothic architecture; the Eiffel Tower, the symbol of France; and the Taj Mahal, completed in the 1650s in India (Yılmaz, 2017). This ratio has also been identified in some historical structures in Türkiye. It is frequently observed in Seljuk-era structures, especially in portal designs; in the plan and facade layouts of Ottoman-era buildings; and in the architectural works of Mimar Sinan (Akın, 2021). Yılmaz (2017) identified the use of the golden ratio in three Seljuk-era madrasas in Konya in his study. In another study, Akın (2021) found that the golden ratio was used in Ottoman-era mosques in Diyarbakır. Other verified examples of the golden ratio include the Divriği Complex, Sultan Han, Sivas Gök Medrese, Istanbul Davut Pasha Mosque, and Konya Sahip Ata Mosque (Gürsoy, 2018).

Whether the golden ratio, as a principle providing aesthetic and mathematical harmony, is also found in historical bridges built with engineering skills—not just monumental and religious buildings—has been a subject of curiosity. Historical bridges in Diyarbakır such as the Dicle Bridge, Malabadi Bridge, and Haburman Bridge reflect the engineering and architectural understanding of different periods and serve as significant examples for exploring the relationship between aesthetic order and the golden ratio in these structures. The aim of this study is to examine the span-to-height ratios of the arches of three historical bridges in Diyarbakır based on the concept of the golden ratio and to evaluate these structures aesthetically. The research aims to analyze how closely the obtained ratios align with the golden ratio and to reveal the relationship between aesthetic and mathematical harmony in the architectural designs of these bridges. When reviewing studies in the literature that examine the golden ratio-aesthetic relationship in architectural facades (Akın, 2021; Akın & Aykal, 2022; Salık, 2024; Selçuk, Sorguç & Akan, 2009; Yılmaz, 2017), it is seen that most of the research focuses on structures such as mosques, madrasas, and mausoleums, and no study has been found related to historical bridges. In this respect, this study is expected to fill that gap in the literature by focusing on the aesthetic and mathematical analysis of historical bridges in Diyarbakır. Demonstrating the aesthetic balances in the designs of historical bridges through the use of the golden ratio is important for the preservation and evaluation of cultural heritage. Evaluating these bridges in terms of engineering and aesthetics will not only help us understand past architectural and aesthetic perspectives but may also serve as an inspiration for modern architectural designs.

2. GENERAL PROPERTIES OF METHOD

This research was conducted using a quantitative analysis method due to its focus on examining the golden ratio—an aesthetic proportion—in historical bridges located in Diyarbakır. The study is based on a descriptive approach and a scanning model that incorporates a mathematical analysis process. By examining the architectural characteristics of the historical bridges, the study aimed to determine their relationship with the golden ratio. This model seeks to present the existing situation as it is and interpret it using an analytical approach.

The research was carried out on three historical bridges located within the borders of Diyarbakır Province. These bridges are the Dicle Bridge, known among the public as the "Ten-Arched Bridge," the Malabadi Bridge, and the Haburman Bridge. The selected bridges represent different historical periods of Diyarbakır and are architecturally prominent structures of the city.

To conduct the related studies, historical bridges in Diyarbakır were first examined, and then consultations were held with a field expert faculty member at the Faculty of Architecture and Engineering at Dicle University. As a result, these three bridges were determined as the study sites. A detailed investigation was conducted on the selected bridges. The numerical data related to these bridges were obtained from the 9th Regional Directorate of Highways in Diyarbakır on October 18, 2024. In this context, the presence of the golden ratio in the arches of the specified bridges was examined through span-to-height ratios. The process was supported by a literature review and photographs.

The study began with the assumption that the golden ratio is one of the important aesthetic factors in historical bridges. Based on this assumption, the span-to-height ratios of the arches of historical bridges were calculated, and their deviations from the golden ratio were determined. The amounts of deviation were identified using the absolute difference method, and the results were visualized with tables for each bridge. These analyses provided a basis for interpreting the aesthetic and mathematical features of the bridges. Thus, by identifying how closely these ratios approach the golden ratio value of 1.618 and determining the deviations, golden ratio-aesthetic evaluations were made for each arch. Ideally, if a ratio is close to 1.618, it indicates that the structure uses the golden ratio.

3. APPLICATIONS

The historical bridges examined within the scope of this study were evaluated based on their arches. These evaluations were made using the span-to-height ratios of the arches. The data for the Dicle Bridge (Ten-Arched Bridge), one of the bridges examined in the study, are presented in Table 1.

Table 1. Data for Dicle Bridge

Arch	Span	Height	Ratio	Deviation Amount
Arch 1	8.48	4.98	1.703	0.085
Arch 2	8.04	5.01	1.605	0.013
Arch 3	13.84	7.97	1.737	0.119
Arch 4	11.97	6.97	1.717	0.099
Arch 5	13.92	7.76	1.794	0.176
Arch 6	8.38	4.77	1.757	0.139
Arch 7	8.73	4.74	1.842	0.224

Arch 8	8.45	5.53	1.528	0.090
Arch 9	8.59	4.93	1.742	0.124
Arch 10	8.15	4.92	1.657	0.039

Table 1 shows the span-to-height ratios of the arches of the Dicle Bridge. It can be seen that arches 1, 2, 6, 7, 8, 9, and 10 are of similar dimensions, while arches 3, 4, and 5 have noticeably wider spans. As observed in the table, the span-to-height ratios of the arches range between 1.528 and 1.842. The lowest deviation amount was found in arch 2 (0.013), while the highest deviation was in arch 7 (0.224). To better illustrate the deviations from the golden ratio, these data are shown in the bar graph in Figure 5.

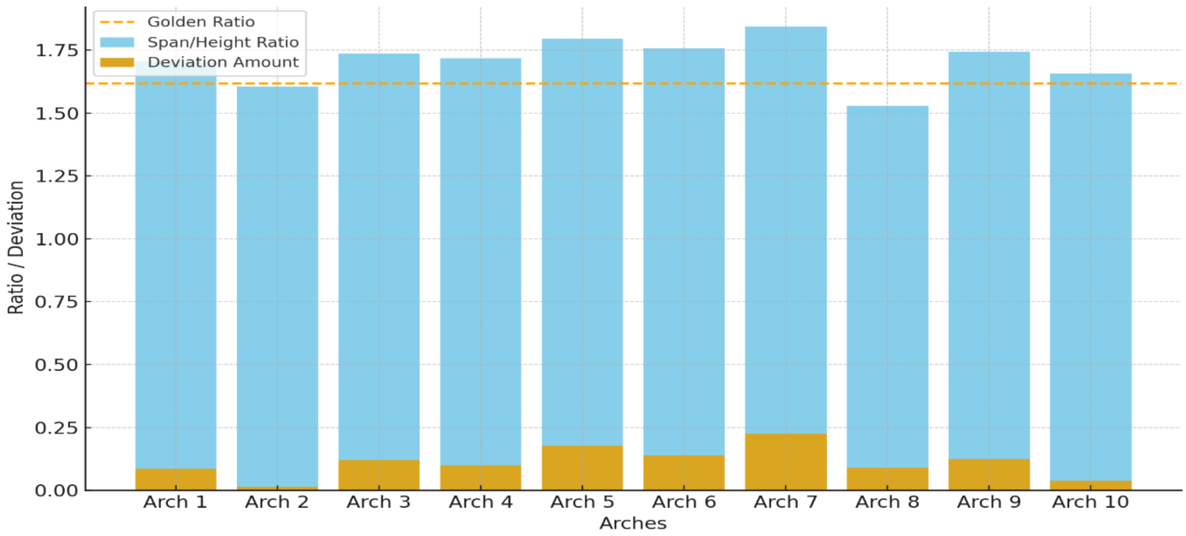

Figure 5. Span-to-Height Ratios and Golden Ratio Deviations of Dicle Bridge

The arches of the Dicle Bridge generally exhibit a close alignment with the golden ratio. The overall proximity of the arches to the golden ratio suggests that the arches were not designed randomly, that the golden ratio may have been used deliberately, and that aesthetic concerns were considered. The data for the Malabadi Bridge, another bridge examined in this study, are presented in Table 2.

Table 2. Data for Malabadi Bridge

Arch	Span	Height	Ratio	Deviation Amount
Arch 1	40.85	23.78	1.718	0.100
Arch 2	4.28	6.81	1.591	0.027
Arch 3	5.67	10.18	1.795	0.177
Arch 4	5.66	7.66	1.353	0.265

The Malabadi Bridge consists of a main arch (Arch 1) and four smaller arches. The fifth arch was closed in 1955 with the construction of a reinforced concrete bridge, so data for this arch were not included in the analysis. In the smaller arches (2, 3, and 4), height exceeds span, so height-to-span ratios were calculated instead of span-to-height ratios. As shown in Table 2, the ratios range from 1.353 to 1.795. The lowest deviation amount was found in arch 2 (0.027), and the highest in arch 4 (0.265). The deviation of the main arch from the golden ratio was determined to be 0.1. To better illustrate the deviations from the golden ratio, these values are shown in the bar graph in Figure 6.

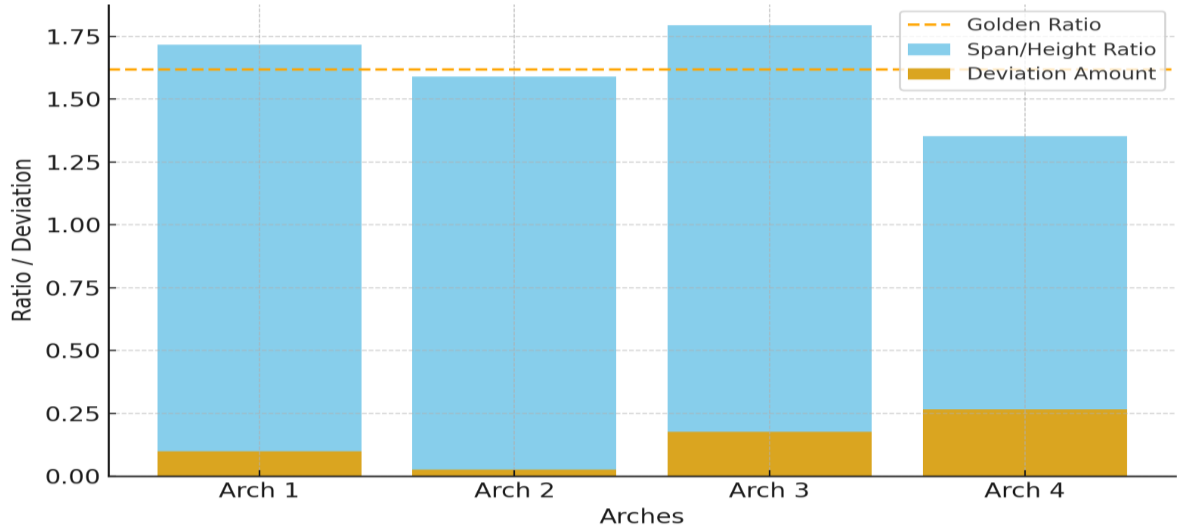

Figure 6. Span-to-Height Ratios and Golden Ratio Deviations of Malabadi Bridge

As shown in Figure 6, the arches of the Malabadi Bridge generally exhibit proximity to the golden ratio. Arch 2 is the closest to the golden ratio. While arches 1 and 2 reflect the aesthetic effect of the golden ratio, arches 3 and 4 show greater deviation. Therefore, the significant deviations in some arches make it difficult to determine whether these proportions were used intentionally or resulted from functional requirements. However, it can be said that while aesthetic aspects were prioritized in the main and second arches, engineering requirements had more influence on the design of the other two. The data for the Haburman Bridge, another bridge examined in the study, are presented in Table 3.

Table 3. Data for Haburman Bridge

Arch	Span	Height	Ratio	Deviation Amount
Central Arch	19.00	11.20	1.696	0.078
East Arch	5.30	4.50	1.778	0.160
West Arch	7.10	5.50	1.291	0.327

The Haburman Bridge consists of a central arch, referred to as the main arch, and two smaller arches. As seen in Table 3, the lowest deviation amount is in the central arch (0.078). The other two arches show higher deviations compared to the central arch. In particular, the west arch deviates significantly from the golden ratio. To better illustrate the deviations from the golden ratio, these data are shown in the bar graph in Figure 7.

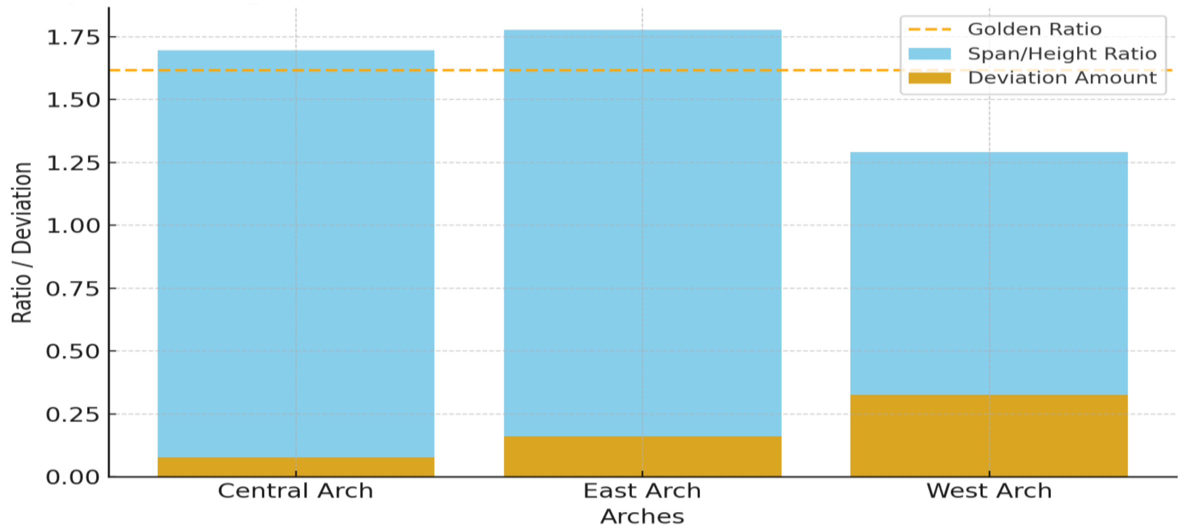

Figure 7. Span-to-Height Ratios and Golden Ratio Deviations of Haburman Bridge

As also shown in Figure 3, the central arch of the Haburman Bridge, which can be considered the main arch, is close to the golden ratio. However, the west arch exhibits a higher deviation, and its span-to-height ratio diverges from the golden ratio. This suggests that while overall attention was paid to aesthetics in the bridge, in the west arch in particular, engineering requirements took precedence over aesthetics.

4. CONCLUSIONS

In this study, based on the idea that the golden ratio can be an effective universal aesthetic criterion in architectural structures, three historical bridges located in Diyarbakır were examined in the context of the compatibility of their arch structures with the golden ratio and their aesthetic relationship. The span-to-height ratios of the arches in the historical bridges were calculated, and the deviations from the golden ratio were determined for each arch individually. In this way, it was aimed to better understand the relationship between the arches and the golden ratio and their aesthetic harmony.

In the Dicle Bridge, it was observed that seven of the arches have similar span sizes, while three arches are significantly wider. Halifeoğlu et al. (2009) stated that these three spans were constructed in place of four arches of similar size that previously existed but had collapsed, and that the original bridge possibly had eleven arches. Although the arches of the Dicle Bridge display different ratios, they generally exhibit a balanced structure both functionally and aesthetically due to their closeness to the golden ratio. Proximity to the golden ratio can be considered an indicator of aesthetic harmony in historical structures. This suggests that the bridge should be evaluated not only from an engineering perspective but also as a product of artistic design.

The arches of the Malabadi and Haburman Bridges show variation in their closeness to the golden ratio. In the Malabadi Bridge, arches 1 and 2 present strong aesthetic value, whereas arches 3 and especially 4 are more distant from the golden ratio. In the Haburman Bridge, the central arch has a value close to the golden ratio, but the third arch deviates more significantly. This indicates that both aesthetics and functionality were considered in the design of these bridges. While general attention was paid to aesthetic harmony, it appears that in the smaller arches—compared to the main arches—engineering requirements were prioritized over aesthetics. Thus, it can be said that each arch plays a different role in terms of aesthetic harmony and engineering necessities.

As a result, it was found that the span-to-height ratios of the arches in the examined bridges generally show values close to the golden ratio. While aesthetic concerns are thought to have influenced all the arches in the Dicle Bridge, in the Malabadi and Haburman Bridges, the main arches stand out more in terms of aesthetics, and in some of the smaller arches, engineering necessities appear to be more dominant. These findings suggest that the golden ratio may have been used consciously or intuitively as an aesthetic design element in the examined bridges. Therefore, although the influence of the golden ratio on the aesthetic structure is generally observable in these bridges, whether this was a conscious design decision or a natural result of functional requirements remains open to discussion. Nevertheless, it can be concluded that the relationship between the golden ratio and aesthetics has had a significant impact on these historical structures.

Based on the results of the study, the following recommendations are proposed:

This study is limited to three historical bridges in Diyarbakır. The presence of a golden ratio–aesthetic relationship in historical bridges can also be examined in bridges built in different periods or located in different provinces.

In this research, the presence of the golden ratio in historical bridges was determined through the span-to-height ratio of the arches. The presence of the golden ratio and its aesthetic relationship can also be examined using different methods, such as the solid-void ratio of facades.

The presence of the golden ratio in the design of the Dicle, Malabadi, and Haburman Bridges demonstrates that aesthetic factors were considered during their construction processes. Accordingly, it is recommended that aesthetic concerns be considered alongside engineering requirements during the restoration and preservation of historical bridges.

The historical use of the golden ratio as an aesthetic element can also serve as a valuable guide for modern engineering and architectural design. Therefore, taking aesthetic principles and the golden ratio into account in today's bridge projects may result in more harmonious structures in both functional and aesthetic terms.

The fact that engineering requirements took precedence in some arches indicates a compromise on aesthetics. In this context, a multidisciplinary approach can be adopted during the design phase of new bridges to balance engineering and aesthetic considerations.

REFERENCES

1. Akın, R. B. (2021). *Ottoman era mosque facades in Diyarbakir occupancyvacancy rates examination of the relationship between the golden ratio and aesthetics* (Publication No. 664813). [Master's thesis, Dicle University]. Turkish Council of Higher Education Thesis Center.
2. Akın, R. B. & Aykal, F. D. (2022). Behram Paşa Camii cephelerinin doluluk-boşluk oranlarında altın oran-estetik ilişkisinin incelenmesi [An analysis of the golden ratio–aesthetic relationship in the solid-void ratios of Behram Pasha Mosque facades]. *Online Journal of Art & Design*, *10*(2), 241-255.
3. Beysanoğlu, Ş, (1990). *Anıtları ve Kitabeleri ile Diyarbakır Tarihi [The History of Diyarbakır with Its Monuments and Inscriptions]* (Vol. 1), Ankara.
4. Dalkılıç, N. & Halifeoğlu, F. M. (2009). *Historical bridges located in Diyarbakır province and towns*. I. Uluslararası Nebiler, Sahabiler, Azizler ve Krallar Kenti Diyarbakır Sempozyumu, Diyarbakır.
5. Halifeoğlu, F. M., Toprak, Z. F. & Kavak, O. (2011). *Tarihi Diyarbakır köprülerinin mimari, hidrolojik ve jeolojik açıdan değerlendirilmesi [Architectural, hydrological, and geological evaluation of historical bridges in Diyarbakır]*. II. Su Yapıları Sempozyumu, Diyarbakır.
6. Hastürk, E. (2014). Golden ratio in anthropometric data. *Mesleki Bilimler Dergisi, 3*(2), 173-177.
7. Salık, M. G. (2024). Golden ratio-aesthetic relationship analysis of the facades of Veysel Karani Building. *Tasarım Mimarlık ve Mühendislik Dergisi*, *4*(2), 105-116.
8. Gürsoy, E. (2018). The relationship of measure-ratio at the models of mosques. *Türk Dünyası Araştırmaları, 118*(232), 211-228.
9. Kurtar, C. & Somuncu, M. (2013). Conservation and sustainability of urban cultural heritage: The Ankara Hamamönü example. *Journal of Ankara Studies, 1*(2): 35-47.
10. Kuşçuoğlu, G. Ö. & Taş, M. (2017). Sustainable cultural heritage management. *Yalvaç Akademi Dergisi*, *2*(1), 58-67.
11. Kutlay, Ş. (2012). *Bridges in Diyarbakır.* (Publication No. 324997). [Master's thesis, Gazi University]. Turkish Council of Higher Education Thesis Center.
12. Ministry of Culture and Tourism (MoCT) (2024). Bridges. Retrieved August 25, 2024, from https://diyarbakir.ktb.gov.tr/TR-56900/kopruler.html

13. Sami, K. (2017). Diyarbakır historical Suriçi: A Cultural heritage with its color having disappeared in the urban, spatial and social life. *Journal of International Social Research*, *10*(53), 390-400.
14. Selçuk, S. A., Sorguç, A. G. & Akan, A. E. (2009). Designing by Golden Ratio:φ Code in Nature, Architecture and Structural Design. *Trakya Üniversitesi Fen Bilimleri Dergisi*, *10*(2), 149-157.
15. Silvan District Governorship (2024). *Malabadi Bridge*. Retrieved August 26, 2024, from http://www.silvan.gov.tr/malabadi-koprusu adresinden 26.08.2024
16. Tanrıverdi, M. & Gürel, M. A. (2019). Arch Bridges From Past To Present. *Harran University Journal of Engineering, 4*(3), 156-167.
17. Turkish Language Association (TDK) (2024). *Current Turkish Dictionary*. Retrieved December 18, 2024, from https://sozluk.gov.tr
18. Yeşilbaş, E. (2007). *Water architecture in Diyarbakir*. (Publication No. 211550). [Master's thesis, Selçuk University]. Turkish Council of Higher Education Thesis Center.
19. Yılmaz, E. M. (2017). *The relationship between golden ratio and aesthetics in madrasas of Seljuk period: The case of Konya*. (Publication No. 453524). [Master's thesis, Selçuk University]. Turkish Council of Higher Education Thesis Center.

STATISTICAL LITERACY IN MIDDLE SCHOOL VIA INTERDISCIPLINARY CONNECTIONS

Özlem Ayça Kaplan[1], Fatma Nur Gürbüz[2], Elif Yıldırım[3], Zerrin Toker[4]

[1]Department of Elementary Mathematics Education, University of TED, Ankara, Turkey

oayca.kaplan@tedu.edu.tr

[2]Department of Mathematics Education, Middle East Technical University, Ankara, Turkey

fatma.gurbuz@metu.edu.tr

[3]Department of Statistics and Quality Coordinator, Konya Technical University, Konya, Turkey

edil@ktun.edu.tr

[4]Department of Mathematics and Science Education, Çanakkale Onsekiz Mart University, Çanakkale, Turkey

zerrin.toker@comu.edu.tr

Abstract

One of the most essential goals of mathematics instruction is to help students develop and apply statistical literacy skills. However, several research studies indicate that mathematics teachers and students struggle with statistics when it comes to teaching and learning. Developing approaches is essential to overcome these struggles and increase statistical literacy. This article presents a review of the literature on statistical literacy among middle school students and provides an informative guide to statistics education researchers and statistics/mathematics teachers alike. This systematic review, using the PRISMA framework, analyses 20 research articles to provide an overview of studies on statistical literacy among middle school students. It examines six key themes in detail: year of the study, research method, grade level, data collection tools, data analysis method, interdisciplinary concept in statistical literacy, and methods and strategies used in developing it. Furthermore, this research primarily concentrates on studies that emphasise interdisciplinary approaches. The main outcome of this review is to lay the groundwork for an effort to create an interdisciplinary educational program. According to the results of the present review, we conclude that improvements in data literacy and different methods have been developed to increase middle school students' statistical literacy.

Keywords: interdisciplinary, mathematics, PRISMA, teaching statistics

1.INTRODUCTION

The concept of statistical literacy, which began to develop quite small and technically in the late 1970s, was expanded by Statistical Association (ASA) in the late 1990s [1]. The concept of statistical literacy was originally used to describe the information people need to technically understand statistics and make decisions based on analysis of data. This aspect of the concept was measured using statistics in daily life. However, only the technical aspects of the concept were considered with these measurements. Afterward, the broad definition of the concept was expressed as "statistical literacy is the ability to understand and critically evaluate statistical results that permeate our daily lives – coupled with the ability to appreciate the contributions that statistical thinking can make in public and private, professional and personal decisions" by ASA.

In recent years, statistical literacy has grown in importance. Statistics, which we encounter even in the most ordinary issues in daily life, are one of the most feared and regarded as too difficult to comprehend by societies [2]. One of the primary reasons for this could be the simple and direct transmission of statistical information without adequate communication with the students. Students cannot understand and interpret statistical knowledge in this situation because the information is given directly to them, and they are not permitted to interpret that knowledge [2]. Changing students' attitudes toward statistics and increasing their statistical literacy; practices involving statistics concepts and processes.

The capacity to critically assess and apply statistics in daily life is known as statistical literacy. These skills include arranging data, making and displaying tables, and analyzing various data visualizations [3]. Data literacy is defined in the paper "Beyond Data Literacy," which was released in September 2015, as the capacity to read data, work with data, analyze data, and discuss data. According to this paper, data literacy interacts with statistical literacy and consists of a combination of the technical, critical, mathematical, and conceptual skills that serve as the foundation for statistical literacy.

The recognition of the importance of statistics in daily life, as well as the relationship between statistical literacy, has focused attention on mathematics curricula and program developers [4] [5][6]. Statistics are taught in schools for three important reasons: (1) Statistics is useful in everyday life, (2) it is a tool used in other disciplines, and (3) it is essential in the development of critical thinking [5]. For these reasons, some communities frequently emphasize statistics' specific role in mathematics curricula and make special recommendations on statistical education [7] [8].

Six important recommendations are made for school statistics courses in the Guidelines for Assessment and Instruction in Statistics Education (GAISE) [9] study. The development of statistical thinking and statistical literacy should be emphasized more in the classroom, real data should be used, conceptual understanding should be valued above procedural knowledge, active learning techniques should be used, technology should be used to develop data analysis and conceptual understanding, and assessments that measure and improve student learning should be combined [10]. Only the first of the six suggestions from the original GAISE [11]. study have been changed, adding two new emphases in the GAISE II report [12]. These skills—statistics, problem-solving, and decision-making—should be taught to students as part of the research process, and they should have opportunities to practice multivariate thinking. The GAISE II [12] report retains the characteristics of the GAISE I report and includes the new skills needed to make sense of data today.

In consistency with the GAISE report, interdisciplinary interaction is emphasized as one of the important elements in the teaching process in mathematics curricula designed and used by many countries, including Turkey [13]. Interdisciplinary connections stand for a variety of intelligences and approaches to offering various solutions to the world's complicated problems. By combining several subjects, such as art, math, science, and social studies, it improves students' abstract thinking, cognitive growth, problem-solving abilities, and creativity [14]. Students may see and learn about the connections between each discipline and the real world thanks to the interdisciplinary approach. Additionally, it enables individuals to acquire the knowledge and abilities required to adapt to cultures that are continually undergoing cultural, economic, and technological change. These abilities enable students to think critically and solve problems creatively [15]. Thus, curriculum documents in all disciplines refer to some competencies that students will need at the national and international levels in their personal, social, academic, and work lives [13]. Furthermore, research studies in various disciplines revealed an increase in students' academic achievement as a result of interdisciplinary interactions in teaching [16].

However, it is difficult to go beyond transferring these learning outcomes to students with a teaching approach that focuses solely on the learning outcomes defined in the mathematics curriculum. Concrete examples of teaching materials relating to the use of interdisciplinary connections are required instead. Interdisciplinary connections and connections to daily life to statistics can be built in this context by relating statistics content to content in other disciplines such as social studies, science, technology, physical education, and arts. The interdisciplinary analysis of statistics concepts will connect two seemingly independent disciplines while also increasing the time allocated for teaching the topic, improving students' daily lives and mathematical connections. Tasks that are designed to promote students' learning of statistics concepts related to real-life situations and integrated with concepts to be learned in other disciplines.

A. The Rationale for the study

Students must define, organize, and interpret numerical data obtained in various contexts within statistics [10]. The GAISE identifies statistics teaching, the development of statistical thinking, as well as the emphasis on statistical literacy, the use of active learning methods within the classroom, the encouragement of technology use, the analysis of student learning, the availability of conceptual understanding rather than operational knowledge, and the use of real data as methods to develop statistical literacy [10]. Interdisciplinary teaching can be used as a foundation for providing context for students while dealing with real data and having conceptual understanding. Interdisciplinary teaching is a method of assisting students in combining and integrating knowledge from various fields, as well as enabling students to think by synthesizing and analyzing them through concepts [17].

In recent years, the concept of statistical literacy has expanded beyond its traditional boundaries to include interdisciplinary perspectives and a variety of educational approaches. This expansion has led to increased research interest in how statistical literacy is developed, particularly at the secondary school level, where basic skills are developed. In this context, it is critical to examine the literature for research-based examples of interdisciplinary connections, identify activities, and identify effective methods for developing statistical literacy. In conclusion, this study formulates five primary research questions that systematically examine various dimensions of statistical literacy development among secondary school students. Tracking the publication years of studies on statistical literacy provides valuable insights into the evolution of research interest over time. By mapping trends in publication frequency, this study aims to identify periods of increased academic focus and potential gaps where further research is needed. Understanding these trends can help contextualize the evolution of statistical literacy research and reveal how changes in educational policy, technological advances, and pedagogical innovations have impacted the field.

RQ1: What years have manuscripts in this field been published?

Methodological approaches in statistical literacy research are essential for uncovering effective teaching practices and understanding the cognitive and pedagogical mechanisms that shape student learning. This question seeks to examine the variety of sample types, ranging from individual case studies to large-scale experimental designs, and the variety of data collection tools used, such as surveys, interviews, and performance assessments. In addition, methods such as qualitative and quantitative research and mixed methods approaches help identify key factors that influence learning outcomes and the relationships between different learning methods.

RQ2: What sample types, data collection tools and data analysis methods, were used to identify the most effective practices for improving statistical literacy in middle school students?

Developing statistical literacy in secondary school students presents several pedagogical and conceptual challenges. This research question aims to explore challenges identified in the literature, including students' misconceptions about statistical concepts, limitations in curriculum design, and varying effectiveness of teaching methods. Additionally, the study examines the role of interdisciplinary connections in overcoming these challenges and evaluates how integrating statistics with subjects such as science, social studies, and economics can increase student understanding and engagement.

Q3: What are the main issues identified in the literature review concerning the development of statistical literacy in middle school students and the use of interdisciplinary connections?

Interdisciplinary approaches offer a promising avenue for improving statistical literacy by addressing statistical concepts in real-world contexts. This research question aims to investigate specific strategies used to integrate statistics across disciplines, such as project-based learning, inquiry-based activities, and technology-enhanced instruction. By identifying successful interdisciplinary approaches, the study provides a framework for developing curricula that integrate statistical literacy with broader educational goals.

Q4: What methods have been used to support the statistical literacy of middle school students with interdisciplinary approaches?

Effective pedagogical strategies are essential to promoting statistical literacy and enabling students to develop the critical thinking skills necessary for data-driven decision making. This research question synthesizes evidence on instructional methods including active learning techniques, real and easily accessible data in classroom tasks, and assessment-focused feedback mechanisms. By evaluating the effectiveness of these strategies, the study aims to provide actionable recommendations for educators seeking to improve statistical literacy instruction in secondary school settings.

Q5: What are the methods and strategies that are useful in the development of statistical literacy?

By addressing these research questions, this study contributes to a deeper understanding of how statistical literacy is conceptualized, taught, and assessed within an interdisciplinary framework. The findings aim to inform educators, curriculum designers, and policy makers about best practices and emerging trends in statistical literacy education and ultimately support the development of more effective teaching methodologies.

2.GENERAL PROPERTIES OF METHOD

In this study, a systematic review with PRISMA protocol was used to determine the results related to the improvement of the statistical literacy of middle school students, which interdisciplinary methods are used for statistical literacy and to determine what kind of studies have been done in this field. A systematic review is a determination of which studies will be included in the compilation using various inclusion and elimination criteria of all studies on a particular subject and the synthesis of the identified studies according to the research question [18][19]. The purpose of the systematic review is to synthesize the studies on a particular subject, reveal the general trend on that subject, and identify the deficiencies and possible studies on the subject [18][20].

The PRISMA protocol was developed by reviewers, clinicians, medical editors, and methodologists in 2005 for a more clear and complete reporting of systematic reviews and consists of a 27-item checklist and a 4-step flowchart [21]. PRISMA contributes to the quality and reproducibility of the process in studies such as systematic review and meta-analysis [22][23]. PRISMA offers three benefits: 1) it describes the research questions included in the systematic review, 2) it identifies inclusion and exclusion criteria, and 3) it allows for the investigation of a large database of literature.

Review and inclusion criteria

In this study, various combinations of keywords such as "statistical literacy, data literacy, middle school, material, method, strategy, process/steps" were used to search in Turkish and English in ERIC, Web of Science (WOS), and ULAKBIM (national database) databases to determine the methods used to improve the statistical literacy of middle school students. To reach more studies, studies after 2010 were considered, as well as relevant studies, practices, and compilations published in national and international journals. Only studies in which participants were middle school students were included.

Elimination criteria

This study included studies with English and Turkish texts; studies written in other languages were excluded. Selected articles are only included in WOS, ERIC and ULAKBIM databases. Articles outside of these databases are not included. The study excluded case reports, case texts, conference papers, reviews, theses, and reprinted publications. In order to develop more comprehensive research, the word interdisciplinary was not included in the inclusion criteria. However, the articles determined according to the inclusion criteria were not included in the study if they do not include an interdisciplinary approach.

Selection process of the studies

Two of the researchers worked independently to identify and select the studies. As a result, the same selection procedure was followed twice. When there was a disagreement among the researchers, the expert opinion was sought. 1128 studies were obtained from ERIC (n=139), WOS (n=827) and ULAKBIM (n=162) electronic databases in accordance with the keywords determined in the first step of the study conducted in accordance with the PRISMA checklist. In the second step, 69 studies were determined according to the study title and abstract according to the inclusion and exclusion criteria, and 29 duplicates studies were excluded. In the third step, 20 articles were screened in detail according to inclusion and exclusion criteria. In the fourth step, the full text of the remaining 20 articles was examined in detail in accordance with the determined criteria and research questions (The list of articles included in the study is given in the Appendix). The applied PRISMA process is summarized in the flow chart in Figure 1.

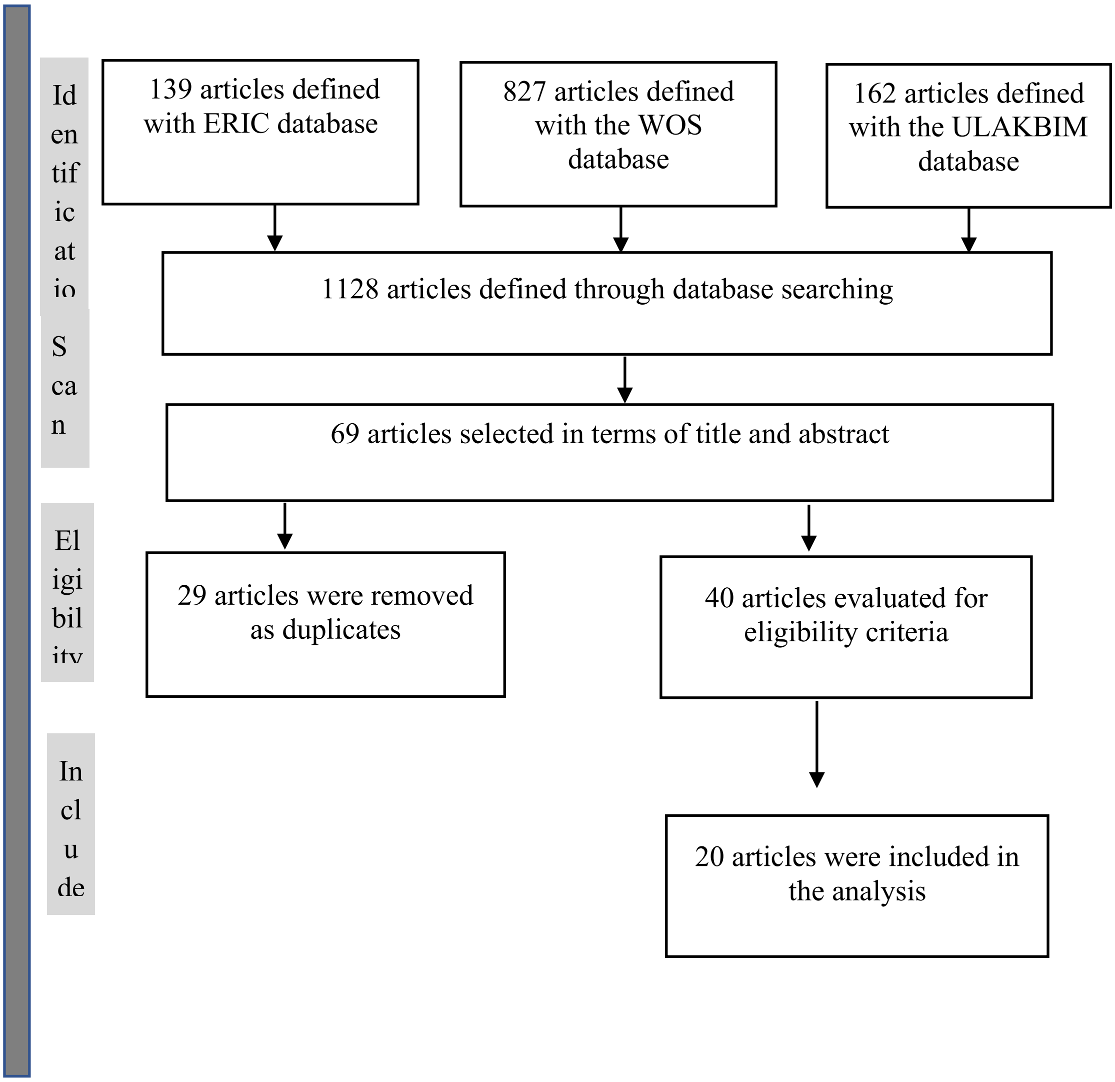

Figure 1. The selection process of the articles

20 articles included in the study comprise different types including practitioner papers. The practitioner papers are often produced for educators working in the field by educators or occasionally by researchers. Real classroom experiences and observations are highlighted in practitioner articles, which also primarily cover useful teaching advice and classroom ideas.

Coding and analysis of data

The researchers thoroughly examined all the studies included in the study, and some categories were established to analyze the subject. These were determined to be "year of the study, research method, grade level, data collection tools, data analysis method, interdisciplinary concept in statistical literacy and methods and strategies used in developing statistical literacy." The researchers then determined the codes for each study independently based on these pre-determined categories. The coding was done independently by two researchers, and the validity and reliability of the coding were also examined. The percentage of agreement among researchers was calculated as 0.91 (Reliability = Consensus / (Agreement + Disagreement) x 100). The Excel program was used for all coding and analysis. As a result, for analysis and interpretation, the frequency percentage values of the data belonging to each category were calculated, and a graphical method was used to better understand and interpret some results.

3.APPLICATIONS

Using the selection criteria, a total of 20 research articles that fit the research framework were analyzed in two main sections: research and teaching elements. In order to answer the research question of when the studies included in the study were conducted, 20 studies were examined in terms of publication year. The distribution of articles by year is shown in Table 1 and Figure 2.

Table 1. Distribution of years of studies within the scope of the research

Year	n	%	Year	n	%
2010	0	0	2016	1	5
2011	2	10	2017	1	5
2012	1	5	2018	1	5
2013	3	15	2019	0	0
2014	3	15	2020	1	5
2015	1	5	2021	4	20
			2022	2	10

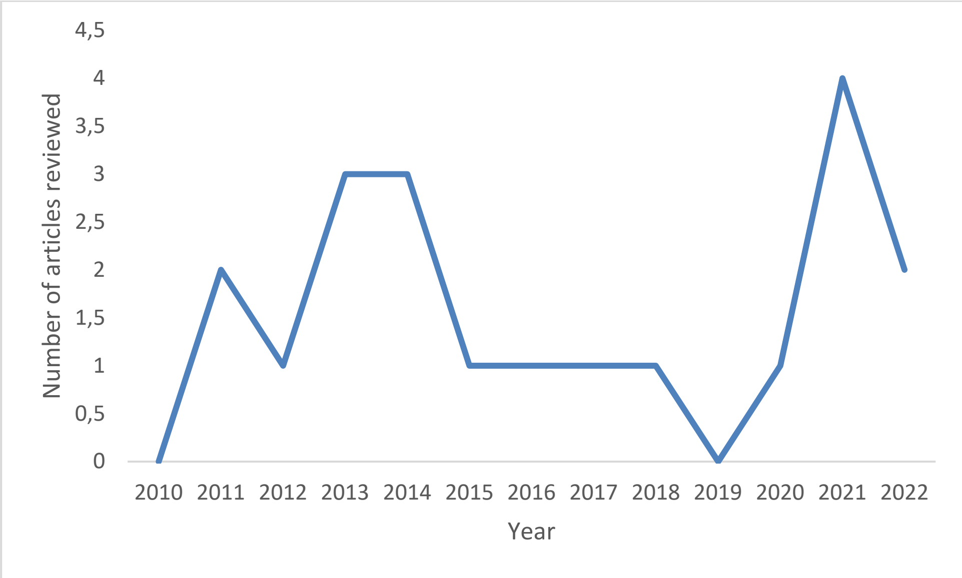

Figure 2. Number of articles reviewed over time

When the publication years of the articles are considered, it is discovered that every year except 2010 and 2019, there is at least one article published on this subject, though it is higher in some years. The year with the most articles appears to be 2021 (n = 4).

The study also looked into the research method or approach used in the 20 articles that were the subject of the study. Looking at all 20 studies, it is clear that some use a quantitative approach while others use a qualitative approach. Table 2 describes the various types of studies.

Table 2. Distribution of research methods/approaches used in studies within the scope of the research

Method	n	%	Method	n	%
Case study	4	20	Experimental research	6	30
Practitioner paper	4	20	Design-based/developmental research	3	15
			Mixed method research	3	15

When Table 2 is examined, it is clear that the selected studies use a variety of research designs. While case studies are common in qualitative research, experimental studies are more common in quantitative research. Furthermore, roughly one-fifth of the studies (n=4) were designed as practitioner papers. The sample types were examined in terms of grade level to answer the fourth research question. Table 3 depicts the situation for this analysis.

Table 3. Distribution of sample types used in studies within the scope of the research

Grade Level	n	%
4-6	1	5
5-8	3	15
6-8	3	15
7	7	35
8	4	20
Middle years	1	5
Upper elementary	1	5

Table 3 shows that sample types are defined differently in the articles reviewed. Some studies include students from multiple grade levels, while others concentrate on a single grade level. Although some grade levels overlapped with others in the table because the definition of grade level varies by country, how grade level was defined in the study is provided here. When the studies are analyzed by grade level, it is discovered that the majority of them are in the seventh grade (n=6). The next grade level (n=4) is eighth grade. Studies focusing on a single level outnumber studies focusing on multiple levels, accounting for approximately 55 percent of all studies.

When the data collection tools used in the 20 articles studied are examined, it is discovered that different data collection tools were used depending on the study's research method. Table 4 presents the distribution of data collection tools used in studies within the scope of the research.

Table 4. Distribution of data collection tools used in studies within the scope of the research

	n	%		n	%
Questionnaire	2	6.8	Interview	7	24.1
Test	6	20.7	Artifacts/written documents	13	44.8
			Observation	1	3.4

Table 4 shows that multiple data collection tools were used in some of the studies. As a result, there are more data collection tools than studies. Artifacts and written documents are the most preferred data collection tools in qualitative studies, mixed-method research, developmental research, and case studies (n=13). In other words, artifacts/written documents made up roughly half of the total data collection tools used in the studies. After artifacts and written documents, interviews are the most used data collection tool in studies with a qualitative dimension (n=7). Tests are mostly used as data collection tools for quantitative dimension (n=6).

When the studies' data analysis methods are examined, it is discovered that a variety of methods are used. Table 5 shows the data analysis methods used in the studies.

Table 5. Distribution of data analysis methods used in studies within the scope of the research

	n	%		n	%
Document analysis/ Content analysis	7	41.1	Chi-square	1	5.8
			T-test	2	11.8
			Anova	2	11.8
			Ancova	1	5.8
Frequency table	3	17.6	Manova	1	5.8

The data analysis methods used in the studies vary, as shown in Table 5. However, some studies use separate analysis methods for quantitative and qualitative data, and content analysis is the most used data analysis method (41.1%). The t-test is preferred over other analysis methods for quantitative analysis, but the percentage is not as high. Because data analysis and presentation take the form of student work and process explanation, practical articles are not included in this section.

The findings to this point are for analyzing the studies investigated in the research dimension. The details of the findings discussed in the studies are included in the second part of the findings. Table 6 shows the analysis of articles in terms of the concept of interdisciplinary connections.

Table 6. Analysis of Articles in Terms of the Concept of Interdisciplinary Connections

Article (Authors, publication year)	How did the author(s) handle interdisciplinary connections?	How did the author(s) use it?	Scope/concept and procedures focused	Instructional process (if any)
Akar, N., & Övez, F. T. D. (2018)	Mentioning the importance of concepts in mathematics in other disciplines and in daily life	Including own views or the views of other authors in the literature on this subject	Graphs (Examining how this concept is included in course materials)	None
Blagdanic, C., & Chinnappan, M. (2013)	Presenting an example of practice to improve statistical literacy	Using activities that require learning graphs by using real-life situations as a context	Creating and interpreting graphs with real-life contexts	Implementing activities to experience the process
Çakıroğlu, Ü., & Güler, M. (2021)	Using gamification as an interdisciplinary concept	Using gamification as a tool in statistics teaching	Line graph, pie graph, median, mode	Teaching the concepts of statistics with gamification
Çakmak, Z. T. & Durmuş, S. (2015)	Mentioning the importance of concepts in mathematics in other disciplines and in daily life	Revealing the concepts and reasons that are difficult to learn about statistics and probability	All concepts related to probability and statistics in the national curriculum in grades 6-8	None
Conti, K. C., & De Carvalho, D. L. (2014)	Taking a discipline as a basis and supporting it with another discipline (Using Technology in Mathematics)	Making use of technology in activities in the project carried out to improve statistical literacy	Formulating research questions, creating tables	Conducting three activities (preparing a questionnaire, tabulating the data and presenting it as a poster) to improve statistical literacy as part of a project

Güler, H. K., & Kabar, M. G. D. (2021)	Mentioning the importance of concepts in mathematics in other disciplines	Including own views or the views of other authors in the literature on this subject	Reading and interpreting graphs	Implementation of activities for reading and interpreting graphs
Gürbüz, R., Yıldırım, İ., & Doğan, M. F. (2021)	Mentioning the importance of concepts in mathematics in other disciplines and in daily life	Including own views or the views of other authors in the literature on this subject	Line graph, mean, median, and mod	Using error-based activities in teaching
Koparan, T., & Güven, B. (2014)	Selecting topics in a way to include interdisciplinary themes during the project process	Conducting the project around an interdisciplinary theme	Generating research questions, data collection and data analysis	Project-based learning process
Martí, E., García-Mila, M., Gabucio, F., & Konstantinidou, K. (2011)	Not mentioning the interdisciplinary connection	Not mentioning the interdisciplinary connection	Creating binary tables	Activities requiring asking students to create a table for the given situation
Mota, A. I., Oliveira, H., & Henriques, A. (2016)	Taking a discipline as a basis and supporting it with another discipline (Using Technology in Mathematics)	Using Tinker plots software in teaching	Data interpretation	Activities including analyzing and predicting the real data by using Tinker plots
Ozmen, Z. M., Guven, B., & Kurak, Y. (2020)	Not mentioning the interdisciplinary connection	Not mentioning the interdisciplinary connection	Reading, interpreting, creating, comparing and evaluating graphs (Descriptive analysis of students' solutions)	None

Selmer, S. J., Bolyard, J. J., & Rye, J. A. (2011)	Connecting mathematics and another discipline (Science)	Using the science theme as a context in the process of activities to develop statistical literacy	Statistical literacy cycle consisting of creating research questions, collecting data, presenting and interpreting data	Teaching process consisting of a series of activities in the context of nutrition theme
Selmer, S. J., Rye, J. A., Malone, E., Fernandez, D., & Trebino, K. (2014)	Connecting mathematics and another discipline (Science)	Using the science theme as a context in the process of activities within project process to develop statistical literacy	Statistical literacy cycle consisting of creating research questions, collecting data, presenting and interpreting data	Project-based learning process including gardening and local product market activities at school
Sharma, S. (2013)	Building on one discipline and supplementing it with another (use of strategies related to Reading and writing in Mathematics)	Associating reading and writing strategies with the statistics teaching process	Data evaluation	Performing a series of activities that require students to evaluate statistical discoveries made by others in terms of data collection method, measurement tool, and validity of findings
Swan, K., Vahey, P., van't Hooft, M., Kratcoski, A., Rafanan, K., Stanford, T., & Cook, D. (2013)	Integration of Social Studies, Science, Mathematics and Language teaching	Consecutive teaching processes of four disciplines within the framework of a common theme	Asking appropriate questions, using appropriate data representation methods, using data processing methods, making data-based comments and explanations	Teaching process with the Preparation for the Future Learning Framework (interdisciplinary unit processing with a problem-based approach)

Utomo, D. P. (2021)	Mentioning the importance of concepts in mathematics in other disciplines and in daily life	Including own views or the views of other authors in the literature on this subject	Understanding the problem, presenting the data, interpreting the data (Examining student solutions to TIMSS problems)	None
Vahey, P., Rafanan, K., Patton, C., Swan, K., van't Hooft, M., Kratcoski, A., & Stanford, T. (2012)	Integration of Social Studies, Science, Mathematics and Language teaching	Consecutive teaching processes of four disciplines within the framework of a common theme	Asking appropriate questions, using appropriate data representation methods, using data processing methods, making data-based comments and explanations	Teaching process with the Preparation for the Future Learning Framework (interdisciplinary unit processing with a problem-based approach)
Yanık, H. B., Özdemir, G., & Eryılmaz-Çevirgen, A. (2017)	Mentioning the importance of concepts in mathematics in other disciplines and in daily life	Including own views or the views of other authors in the literature on this subject	Data processing (Examining how data processing is included in activities in textbooks)	None
Büscher, C. (2022)	Presenting an example of practice to improve statistical literacy	Using activities that require the use of statistical literacy	Basic statistical concepts (i.e. mean)	Online course structure
Morris,B.J., Masnick, A. M., & Was, C. A. (2022)	Connecting mathematics and another discipline (Sports)	Using activities that require the use of statistical literacy	Basic statistical concepts (i.e. average)	Computerized testing

When the studies are examined in terms of how they handle multidisciplinary interaction, it is seen that there are several approaches. These include highlighting the value of connections, successive teaching across disciplines, performing projects within the context of a common theme including several disciplines, and employing other disciplines to support it based on mathematics. Interdisciplinary connections occurred in the studies in a variety of ways, including by conducting common lesson processes, taking it into account during project planning, carrying out classroom activities, and including it in the literature review section. Some of the studies covered the statistical literacy cycle as a whole, while others focused on a particular subject. In studies on a particular topic, graphics is the most popular subject. Activities predominated in terms of instructional procedures, and project-based learning is frequently preferred.

The studies analyzed in the scope of this study underlined some methods and strategies that worked on the development of statistical literacy. These practices are provided in Table 7.

Table 7. Methods and strategies found useful on the development of statistical literacy

#	Methods and Strategies
1	Using real life activities enriched with gamification elements
2	Using relevant, interesting, familiar, attractive and authentic contexts
3	Engaging students in the complex and demanding tasks
4	Connecting the statistical concepts with other concepts in mathematics
5	Giving emphasis to interpretation of the data
6	Incorporating real experiences into learning process
7	Using project-based learning
8	Providing opportunity to communicate the data in a detailed manner
9	Using erroneous examples
10	Using cooperative learning activities
11	Using student centered teaching principles
12	Using real and readily available data in classroom tasks
13	Using technology to perform tasks easily and faster
14	Providing scaffolding support

4.CONCLUSIONS

The goal of this study is to present an analysis of studies dealing with statistical literacy and incorporating interdisciplinary interaction. In order to achieve this goal, the studies were scanned using specific keywords, and 20 articles that fit the purpose of the study were examined in terms of the year they were published, the grade level, the research design, the type of data collection tools used, data analysis methods, and the results they discussed.

This study discovered that studies were conducted almost every year, with more studies conducted in the previous year. Statistical literacy is a process that has received attention [4][10][5][6]. Thus, increase in the number of studies focusing on statistical literacy is expected. Despite the interdisciplinary emphasis discussed in this study, studies on statistical literacy in the article scanning process have become more common in recent years, regardless of this emphasis.

When it comes to the research design preferred in the studies, case studies are preferred more in qualitative studies, while experimental studies are preferred more in quantitative studies. Because case studies in qualitative studies are a frequently preferred method in various fields of education to analyze the current situation [24] the fact that they are also preferred in the studies under consideration is a situation that overlaps with the general preferences. Likewise, experimental studies that deal with the effect appear to be preferred at this point. Practitioner papers make up a significant portion of the 20 studies. Four papers, or about a quarter of the total, are practitioner papers. It is critical that such articles present evidence-based educational practices and findings particularly useful for practitioners such as teachers and teacher candidates [25].

When we look at the grade levels where the studies are conducted, we can conclude that studies are conducted at various levels. The number of studies focusing on a single grade level, on the other hand, is greater than the number of studies focusing on more than one grade level. Different sample selection strategies may have been preferred based on the different nature of the studies [26].

When the findings about the data collection tools are examined, we see that the studies use more than one data collection tool. From this perspective, it is possible to state that more than one source [26] was used to improve the validity and reliability of the data in the studies. When the studies are evaluated in terms of data analysis, it is discovered that the analysis method varies depending on the research questions and data type, and the most prominent data analysis methods chosen in accordance with the nature of the studies are t-test and content analysis. This is not surprising result since these are among the common approaches [27][28] in educational research.

When examining how the studies use the interdisciplinary approach, it is seen that they generally combine statistical literacy with different approaches such as mathematical concepts, social sciences, and daily life. It has been discovered that the authors generally take the interdisciplinary approach with the project-based approach, combining with technology, their own views and those of other authors in the literature. While most of the studies dealing with statistical literacy and interdisciplinary approach focused on creating and interpreting graphs or tables, few studies focused on concepts such as mode, median, and mean. In teaching these concepts with interdisciplinary approaches, it is seen that project-based approach, teaching with activity and teaching methods with gamification are frequently used. These findings are consistent with many different studies in the literature [10] [29]. Besides, several studies underlined the importance of student centeredness in learning by strategies such as using collaborative learning environments. Thus, statistical literacy is said to be developed by means of activity enriched learning environments as indicated in other studies [10].

In conclusion, in studies on statistical literacy, it has been determined that themes such as the use of real-life data, project-based learning, student-centered teaching, associating statistical concepts with other concepts in mathematics have emerged. From the findings, it can be said that the use of real-life data to explain statistical concepts and show the application of statistics is related to the types of student learning experience. In addition, it can be said that the use of interdisciplinary approaches such as social sciences, natural sciences or mathematical sciences in statistics teaching supports the approaches most commonly used in statistics teaching in schools (using real-life data, project-based learning, etc.).

Limitations and future research directions

Although statistical literacy has gained more attention in recent years than in previous years, the number of studies in this field is quite limited, particularly when viewed in the context of interdisciplinary interaction. In this context, it is critical to consider studies aimed at improving statistical literacy at various grade levels, different conceptual focuses, or procedural processes, as well as designing and implementing research processes. This study could handle 20 studies that were appropriate for the purpose. A greater number of studies in this area in the future may allow for the collection of different types of data.

Another issue was the lack of longitudinal studies in the small sample size. Because Statistical Literacy development, like other literacy development, is a long-term process, longitudinal studies are considered important in terms of understanding the various stages and tools that are beneficial in the process. In this context, data from other studies and longitudinal studies can be included. Although a limited number of studies were examined here, the data from those studies provide a picture of the processes, strategies, and tools for improving statistical literacy through interdisciplinary interactions. With an increase in the number of practitioner papers, experimental studies, qualitative studies, and longitudinal studies containing such practices, a useful toolbox for researchers and practitioners would be created.

REFERENCES

1. François, K., Monteiro, C., & Allo, P. Big-data literacy as a new vocation for statistical literacy, Statistics Education Research Journal, Vol. 9, No. 1, 194–205, 2020.
2. Tishkovskaya, S., & Lancaster, G. Statistical education in the 21st century: A review of challenges, teaching innovations and strategies for reform, Journal of Statistics Education, Vol. 20, No. 2, 1–56, 2012. https://doi.org/10.1080/10691898.2012.1188964
3. Garfield, J., Delmas, R., & Chance, B. The web-based artist: assessment resource tools for improving statistical thinking, Assessment Resources for Statistics, AERA Annual Meeting, 2003.
4. Gal, I. Statistical tools and statistical literacy: The case of the average, Teaching Statistics, Vol. 17, 97–99, 1995. https://doi.org/10.1111/j.1467-9639.1995.tb00720.x
5. Koparan, T. İstatistiksel okuryazarlık modelleri ve bileşenlerinin incelenmesi [Analysis of statistical literacy models and their components], Turkish Journal of Education, Vol. 4, No. 3, 16–28, 2015. https://doi.org/10.19128/turje.181131
6. Rumsey, D. J. Discussion: Statistical literacy: Implications for teaching, research and practice, International Statistical Review, Vol. 70, 32–36, 2002.

7. American Statistical Association. Guidelines for assessment and instruction in statistics education: College report, Alexandria, 2005.
8. National Council of Teachers of Mathematics. Principles and standards for school mathematics, Reston, VA, 2000.
9. Franklin, C., Kader, G., Mewborn, D., Moreno, J., Peck, R., Perry, M., & Scheaffer, R. Guidelines for Assessment and Instruction in Statistics Education (GAISE) report, American Statistical Association, 2005
10. Koparan, T., & Akıncı, M. İstatistik öğretiminde yeni yaklaşımlar [New approaches in teaching statistics], Journal of Research in Education and Teaching, Vol. 4, No. 1, 36–45, 2015.
11. GAISE College Report ASA Revision Committee Guidelines for Assessment and Instruction in Statistics Education (GAISE) College Report, American Statistical Association, 2016.
12. Bargagliotti, A., Franklin, C., Arnold, P., Gould, R., Johnson, S., Perez, L., & Spangler, D. A. Pre-K-12 Guidelines for Assessment and Instruction in Statistics Education (GAISE) report II, American Statistical Association and National Council of Teachers of Mathematics, 2020.
13. Milli Eğitim Bakanlığı (MEB) (MoNE). İlköğretim kurumları matematik dersi öğretim programı [Elementary school mathematics curriculum], MEB, 2018.
14. Alpaslan, B. Disiplinlerarası öğretim yaklaşımına göre hazırlanmış bilim etkinliklerinin 5. sınıf öğrencilerinin yaratıcı problem çözme becerilerine ve 21. yüzyıl becerilerine etkisi [The effects of science activities prepared according to the interdisciplinary teaching approach on the creative problem solving and 21st century skills of 5th graders], MA thesis, Marmara University, 2021.
15. Özkök, A. Effects of interdisciplinary creative problem solving teaching program on creative problem solving skills, Hacettepe University Journal of Education, Vol. 28, 159–167, 2005.
16. Gouvea, J. S., Sawtelle, V., Geller, B. D., & Turpen, C. A framework for analyzing interdisciplinary tasks: Implications for student learning and curricular design, CBE - Life Sciences Education, Vol. 12, No. 2, 187–205, 2013. https://doi.org/10.1187/cbe.12-08-0135
17. Kanatlı, F., & Çekici, Y.E. Türkçe öğretiminde disiplinler arası olanaklar [Interdisciplinary opportunities in Turkish teaching], Mersin University Journal of the Faculty of Education, Vol. 9, No. 2, 223–234, 2013. https://doi.org/10.17860/efd.20911
18. Petticrew, M., & Roberts, H. Systematic reviews in the social sciences: A practical guide, Blackwell Publishing, 2006. https://doi.org/10.1002/9780470754887
19. Torgerson, C. Systematic Reviews, Continuum, 2003.
20. Gough, D., Thomas, J., & Oliver, S. Clarifying differences between review design and methods, Syst Rev, Vol. 1, No. 28, 1–9, 2012. https://doi.org/10.1186/2046-4053-1-28
21. Liberati, A., Altman, D. G., Tetzlaff, J., Mulrow, C., Gotzsche, P. C., Ioannidis, J. P. A., Clarke, M., Devereaux, P. J., Kleijnen, J., & Moher, D. The PRISMA statement for reporting systematic reviews and meta-analyses of studies that evaluate healthcare interventions: explanation and elaboration, BMJ, Vol. 339, b2700, 2009. https://doi.org/10.1136/bmj.b2700

22. Moher, D., Shamseer, L., Clarke, M., Ghersi, D., Liberati, A., Petticrew, M., Shekelle, P., & Stewart, L. A. Preferred reporting items for systematic review and meta-analysis protocols (PRISMA-P) 2015 statement, Systematic Reviews, Vol. 4, No. 1, 1–9, 2015. https://doi.org/10.1186/2046-4053-4-1
23. Abelha, M., Fernandes, S., Mesquita, D., Seabra, F., Ferreira-Oliveira, A.T. Graduate employability and competence development in higher education—a systematic literature review using PRISMA, Sustainability, Vol. 12, No. 15, 5900, 2020. https://doi.org/10.3390/su12155900
24. Ozan Leymun, Ş., Odabaşı, H. F., & Kabakçı Yurdakul, I. Eğitim ortamlarında durum çalışmasının önemi [The importance of case study research in educational settings], Journal of Qualitative Research in Education, Vol. 5, No. 3, 369–385, 2017. https://doi.org/10.14689/issn.2148-2624.1.5c3s16m
25. Lastrapes, E.R., & Mooney, P. Teachers' use and perceptions of research-to-practice articles, Exceptionality, Vol. 29, No. 5, 375–389, 2021. https://doi.org/10.1080/09362835.2020.1772068
26. Cohen, L., Manion, L., & Morrison, K. Research methods in education (8th ed.), Routledge, 2018.
27. Dinçer, S. Content analysis in scientific research: meta-analysis, meta-synthesis, and descriptive content analysis, Bartın University Journal of Faculty of Education, Vol. 7, No. 1, 176–190, 2018. https://doi.org/10.14686/buefad.363159
28. Hsu, T. Research methods and data analysis procedures used by educational researchers, International Journal of Research & Method in Education, Vol. 28, No. 2, 109–133, 2005. https://doi.org/10.1080/01406720500256194
29. Koparan, T., & Güven, B. The effect of new approaches in statistics teaching on statistical literacy: Project-based learning, Journal of Research in Education and Teaching, Vol. 3, No. 4, 356–377, 2014.

SOME SPECIAL CONDITION FOR PSEUDOSYMMETRIC KENMOTSU MANIFOLDS

Pakize Uygun[1], **Mehmet Atçeken**[2], **Tuğba Mert**[3]

[1] Department of Mathematics, University of Aksaray, Aksaray, Turkey

pakizeuygun@hotmail.com,

[2] Department of Mathematics, University of Aksaray, Aksaray, Turkey

mehmetatceken@aksaray.edu.tr,

[3] Department of Mathematics, University of Sivas Cumhuriyet, Sivas, Turkey

tmert@cumhuriyet.edu.tr,

Abstract

In this paper pseudosymmetric and Ricci pseudosymmetric of a Kenmotsu manifolds are researched. We have achieved the necessary and sufficient conditions for a Kenmotsu manifold, W_8-pseudosymmetric, W_8-Ricci pseudosymmetric, W_9-pseudosymmetric and W_9-Ricci pseudosymmetric. Additionally, some interesting results on Kenmotsu manifolds are obtained.

Keywords: Kenmotsu Manifold; Pseudosymmetric Manifold; Ricci Pseudosymmetric Manifold.

1.INTRODUCTION

U.C. De and A. K. Gazi studied pseudo Ricci symmetric manifolds. They obtained a sufficient condition for a pseudo Ricci symmetric manifold to be a quasi Einsteain manifold. They proved that in a pseudo Ricci symmetric quasi Einstein manifold the scalar curvature vanishes and pseudo Ricci symmetric quasi Einstein perfect fluid spacetime has also been considered [8].

In a Riemannian manifold, the Riemannian curvature tensor is R and for each $X, Y \in \chi(M)$, if $R(X,Y) \cdot R = 0$, then the manifold is said to be semisymmetric. Similarly, if $R(X,Y) \cdot S = 0$, the manifold is called Ricci semisymmetric, if $R(X,Y) \cdot P = 0$, the manifold is called projective semisymmetric, $R(X,Y) \cdot \tilde{Z} = 0$ and the manifold is called concircular semisymmetric, where S is the Ricci curvature tensor, P is the projective curvature tensor and $\tilde{Z}$ is the concircular curvature tensor. Studies on the symmetric Riemannian manifolds started with Cartan [5]. In the following periods, many authors have studied the curvature tensors of various manifolds [4, 6, 11, 14, 15, 16].

K. Kenmotsu studied a class of a contact Riemannian manifold and call them Kenmotsu manifold [13]. He studied that if Kenmotsu manifold satisfies the condition $R(X,Y).R=0$, then the manifold is of negative curvature -1, where R is the Riemannian curvature tensor of type $(1,3)$ and $R(X,Y)$ denotes the derivation of the tensor algebra at each point of the tangent space. The properties of Kenmotsu manifolds have been studied by several authors [7, 9, 20, 22, 23].

In this article, we have researched the pseudosymmetric and Ricci pseudosymmetric of Kenmotsu manifold. For Kenmotsu manifold, W_8 pseudosymmetric, W_8 Ricci pseudosymmetric, W_9 pseudosymmetric and W_9 Ricci pseudosymmetric cases are considered. Then some results are obtained and classifications have been made.

2.PRELIMINARIES

Let M be a $(2n+1)-$dimensional almost contact metric manifold with an almost contact metric structure (ϕ,ξ,η,g), that is, ϕ is an $(1,1)$ tensor field, ξ is a vector field, η is a 1-form and the Riemanniann metric g on M satisfy

$$\phi^2(X)=-X+\eta(X)\xi,\quad \eta(\phi X)=0, \tag{2.1}$$

$$\eta(\xi)=1,\quad \phi\xi=0,\ \eta(\phi)=0 \tag{2.2}$$

for all $X,Y\in\chi(M)$ [17]. Let g be Riemannian metric compatible with (ϕ,ξ,η), that is

$$g(\phi X,\phi Y)=g(X,Y)-\eta(X)\eta(Y), \tag{2.3}$$

or equivalently,

$$g(X,\phi Y)=-g(\phi X,Y)\quad \text{and}\quad g(X,\xi)=\eta(X) \tag{2.4}$$

for all $X,Y\in\chi(M)$ [2]. If in addition to above relation

$$(\nabla_X\phi)Y=-\eta(Y)\phi X-g(X,\phi Y)\xi, \tag{2.5}$$

and

$$\nabla_X\xi=X-\eta(X)\xi, \tag{2.6}$$

where ∇ denotes the Riemannian connection of g hold, then $M(\phi,\xi,\eta,g)$ is called Kenmotsu manifold. Kenmotsu manifold becomes a Kenmotsu manifold if

$$g(X,\phi Y) = d\eta(X,Y). \tag{2.7}$$

In a Kenmotsu manifold M, the following relation holds [13, 9]:

$$(\nabla_X \eta)Y = g(X,Y) - \eta(X)\eta(Y), \tag{2.8}$$

$$R(X,Y)\xi = \eta(X)Y - \eta(Y)X, \tag{2.9}$$

$$R(\xi,X)Y = \eta(Y)X - g(X,Y)\xi, \tag{2.10}$$

$$S(X,\xi) = -2n\eta(X), \tag{2.11}$$

$$Q\xi = -2n\xi, \tag{2.12}$$

where R is the Riemannian curvature tensor and S is Ricci tensor defined by $S(X,Y) = g(QX,Y)$, where Q is Ricci operator. It yields to

$$S(\phi X,\phi Y) = S(X,Y) + 2n\eta(X)\eta(Y). \tag{2.13}$$

Definition 2.1 *A Kenmotsu manifold M is said to be an* η *−Einstein manifold if its Ricci tensor S of the form*

$$S(X,Y) = \alpha g(X,Y) + \beta\eta(X)\eta(Y) \tag{2.14}$$

for arbitrary vector fields X,Y; where α and β are functions on (M^{2n+1},g). If $\beta = 0$, then $\eta-$ Einstein manifold becomes Einstein manifold [3].

On a semi-Riemannian manifold (M,g), for a $(0,k)-$type tensor field $(0,k)$-type tensor field T and (0,2)-type tensor field A, $(0,k+2)$-type Tachibana tensor field $Q(A,T)$ is defined as

$$Q(A,T)(X_1,X_2,\ldots,X_k;X,Y) = -T((X\wedge_A Y)X_1,X_2,\ldots,X_k)$$

$$-T(X_1,(X\wedge_A Y)X,X_3,\ldots,X_k)\ldots -T(X_1,X_2,\ldots,(X\wedge_A Y)X_k),$$

.

.

$$-T(X_1,X_2,\ldots,(X\wedge_A Y)X_k), \tag{2.15}$$

for all $X_1, X_2, \dots, X_k, X, Y \in \chi(M)$, where

$$(X \wedge_A Y)Z = A(Y,Z)X - A(X,Z)Y. \tag{2.16}$$

for all $X, Y, Z \in \chi(M)$.

3. CHARACTERIZATION OF PSEUDOSYMMETRIC AND RICCI PSEUDOSYMMETRIC KENMOTSU MANIFOLD

In this section, the case of pseudosymmetry and Ricci pseudosymmetry of Kenmotsu manifold are investigated. According to W_8 curvature tensor, W_9 curvature tensor and concircular curvature tensors, the pseudosymmetrical and Ricci pseudosymmetrical cases of the Kenmotsu manifold can be given as follows.

Let (M, g) be an $(2n+1)$-dimensional Riemannian manifold. Then the W_8 curvature tensor is defined by [19]. Furthermore, W_8 the curvature tensor for Riemannian manifold (M^{2n+1}, g) is given by

$$W_8(X,Y)Z = R(X,Y)Z - \frac{1}{2n}[S(Y,Z)X - S(X,Y)Z] \tag{3.1}$$

for all $X, Y, Z \in \chi(M)$ [19]. If we choose, respectively, $X = \xi$ and $Z = \xi$ in (3.1), then we obtain as follows:

$$W_8(\xi,Y)Z = \eta(Z)Y - \eta(Y)Z - g(Y,Z)\xi - \frac{1}{2n}S(Y,Z)\xi, \tag{3.2}$$

$$W_8(X,Y)\xi = \eta(X)Y + \frac{1}{2n}S(X,Y)\xi. \tag{3.3}$$

In addition, we choose $Z = \xi$ in (3.2), we obtain as follows:

$$W_8(\xi,Y)\xi = Y - \eta(Y)\xi. \tag{3.4}$$

Definition 3.1 *Let M be Kenmotsu manifold with $(2n+1)$ −dimensional, R be the Riemannian curvature tensor of M, S be the Ricci curvature tensor of M.*

(i) If the pair $R \cdot W_8$ and $Q(g, W_8)$ are linearly dependent, that is, if a λ_1 function can be found on the set

$M_1 = \{x \in M | g(x) \neq W_8(x)\}$ such that

$$R.W_8 = \lambda_1 Q(g, W_8), \tag{3.5}$$

the M manifold is called a W_8 pseudosymmetric manifold.

(ii) If the pair $R \cdot W_8$ and $Q(S, W_8)$ are linearly dependent, that is, if a λ_2 function can be found on the set

$M_2 = \{x \in M | S(x) \neq W_8(x)\}$ such that

$$R.W_8 = \lambda_2 Q(S, W_8), \tag{3.6}$$

the M manifold is called a W_8 Ricci pseudosymmetric manifold. Particularly, if $\lambda_1 = 0$, then this manifold is said to be semisymmetric [10].

Let us now investigate the cases of W_8 pseudosymmetry and W_8 Ricci pseudosymmetry.

Theorem 3.2 *If a* $(2n+1)$ *−dimensional* M *Kenmotsu manifold is a* W_8 *pseudosymmetric manifold, then* M *is a semisymmetric manifold.*

Proof. Let us suppose that Kenmotsu manifold M is a W_8 pseudosymmetric manifold. Then, we can write

$$(R(X,Y) \cdot W_8)(Z,U,W) = \lambda_1 Q(g, W_8)(W,U,Z;X,Y), \tag{3.7}$$

for each $X, Y, Z, U, W \in \chi(M)$. This means that

$$\begin{aligned}
&R(X,Y)W_8(Z,U)W - W_8(R(X,Y)Z,U)W - W_8(Z,R(X,Y)U)W \\
&-W_8(Z,U)R(X,Y)W \\
&= -\lambda_1\{W_8((X \wedge_g Y)W,U)Z + W_8(W,(X \wedge_g Y)U)Z \\
&+W_8(W,U)(X \wedge_g Y)Z\}.
\end{aligned} \tag{3.8}$$

Here taking $X = Z = \xi$ and by using (2.9), (2.10) and (2.16) in (3.8), we reach at

$$\begin{aligned}
&\eta(W_8(\xi,U)W)Y - g(Y, W_8(\xi,U)W) - R(Y - \eta(Y)\xi, U)W \\
&-W_8(\xi, \eta(U)Y - g(U,Y)\xi)W - \eta(W_8(\xi,Y)W)U + g(U, R(\xi,Y)W) \\
&= -\lambda_1\{W_8(g(Y,W)\xi - \eta(W)Y, U)\xi + W_8(W, g(Y,U)\xi - \eta(U)Y) \\
&+W_8(W,U)(\eta(Y)\xi - Y)\}.
\end{aligned} \tag{3.9}$$

If we use (3.2), (3.3) and taking $W=\xi$ in (3.9) and make the necessary abbreviations, then we have

$$\eta(U-\eta(U)\xi)Y-g(Y,U-\eta(U)\xi)\xi-W_8(Y,U)\xi+\eta(Y)W_8(\xi,U)\xi$$
$$-\eta(U)W_8(\xi,Y)\xi-W_8(\xi,U)Y+\eta(Y)W_8(\xi,U)\xi$$
$$=-\lambda_1\{\eta(Y)(U-\eta(U)\xi)-(\eta(Y)U+\tfrac{1}{2n}S(U,Y)\xi)-\eta(U)(Y-\eta(Y)\xi)$$
$$-\eta(Y)(U-\eta(U)\xi)-W_8(\xi,U)Y\}. \tag{3.10}$$

Taking the inner product with $\xi\in\chi(M)$ on both sides of (3.10) and make use of (3.2), then we can infer

$$\lambda_1[g(U,Y)-\eta(U)\eta(Y)]=0. \tag{3.11}$$

On the other hand, we know that from (2.3) and (3.11), we conclude

$$\lambda_1 g(\phi U,\phi Y)=0.$$

This completes our proof.

Theorem 3.3 *If a* $(2n+1)-$*dimensional* M *Kenmotsu manifold is a* W_8 *Ricci pseudosymmetric manifold, then* M *is a semisymmetric manifold.*

Proof. Let us assume that Kenmotsu manifold M is a W_8 Ricci pseudosymmetric manifold. This implies that

$$(R(X,Y)\cdot W_8)(Z,U,W)=\lambda_2 Q(S,W_8)(W,U,Z;X,Y), \tag{3.12}$$

for each $X,Y,Z,U,W\in\chi(M)$, that is,

$$R(X,Y)W_8(Z,U)W-W_8(R(X,Y)Z,U)W-W_8(Z,R(X,Y)U)W$$
$$-W_8(Z,U)R(X,Y)W$$
$$=-\lambda_2\{W_8((X\wedge_S Y)W,U)Z+W_8(W,(X\wedge_S Y)U)Z$$
$$+W_8(W,U)(X\wedge_S Y)Z\}. \tag{3.13}$$

Here, taking $X=Z=\xi$ and using (2.9), (2.16) in (3.13), we arrive at

$$\eta(W_8(\xi,U)W)Y - g(Y,W_8(\xi,U)W) - W_8(Y-\eta(Y)\xi,U)W$$

$$-W_8(\xi,\eta(U)Y - g(U,Y)\xi)W - \eta(W_8(\xi,Y)W)U + g(U,W_8(\xi,Y)W)$$

$$= -\lambda_2\{W_8(S(Y,W)\xi + 2n\eta(W)Y,U)\xi + W_8(W,S(Y,U)\xi$$

$$+2n\eta(U)Y)\xi + 2nW_8(W,U)(Y-\eta(Y)\xi)\}. \tag{3.14}$$

If ξ is taken of W at (3.14), considering (2.11), (3.2), then we get

$$\eta(U-\eta(U)\xi)Y - g(Y,U-\eta(U)\xi)\xi - W_8(Y,U)\xi + \eta(Y)W_8(\xi,U)\xi$$

$$-\eta(U)W_8(\xi,Y)\xi - W_8(\xi,U)Y + \eta(Y)W_8(\xi,U)\xi$$

$$= -\lambda_2\{-4n\eta(Y)(U-\eta(U)\xi) + 2n(\eta(Y)U + \tfrac{1}{2n}S(U,Y)\xi)$$

$$+2n\eta(U)(Y-\eta(Y)\xi) + 2nW_8(\xi,U)Y\}. \tag{3.15}$$

Inner product both sides of (3.15) by $\xi \in \chi(M)$ and make the necessary adjustments, we obtain

$$\lambda_2[g(U,Y) - \eta(U)\eta(Y)] = 0. \tag{3.16}$$

Additionally, from (2.3) we reach at

$$\lambda_2 g(\phi U,\phi Y) = 0,$$

which proves our assertion.

Let (M,g) be an $(2n+1)$-dimensional Riemannian manifold. Then the W_9 curvature tensor is defined by [19]. Furthermore, W_9 the curvature tensor for Riemannian manifold (M^{2n+1},g) is given by

$$W_9(X,Y)Z = R(X,Y)Z + \tfrac{1}{2n}[S(X,Y)Z - g(Y,Z)QX] \tag{3.17}$$

for all $X,Y,Z \in \chi(M)$ [19]. If we choose, respectively, $X=\xi$ and $Z=\xi$ in (3.17), then we obtain as follows:

$$W_9(\xi,Y)Z = \eta(Z)Y - \eta(Y)Z, \tag{3.18}$$

$$W_9(X,Y)\xi = \eta(X)Y - \eta(Y)X - \frac{1}{2n}(S(X,Y)\xi - \eta(Y)QX). \tag{3.19}$$

In addition, we choose $Z = \xi$ in (3.18), we obtain as follows:

$$W_9(\xi, Y)\xi = Y - \eta(Y)\xi. \tag{3.20}$$

Definition 3.4 *Let M be Kenmotsu manifold with $(2n+1)$ $-$dimensional, R be the Riemannian curvature tensor of M, S be the Ricci curvature tensor of M and W_9 be the W_9 $-$curvature tensor.*

(i) If the pair $R \cdot W_9$ and $Q(g, W_9)$ are linearly dependent, that is, if a λ_3 function can be found on the set

$M_3 = \{x \in M | g(x) \neq W_9(x)\}$ such that

$$R.W_9 = \lambda_3 Q(g, W_9), \tag{3.21}$$

the M manifold is called a W_9 pseudosymmetric manifold.

(ii) If the pair $R \cdot W_9$ and $Q(S, W_9)$ are linearly dependent, that is, if a λ_4 function can be found on the set

$M_4 = \{x \in M | S(x) \neq W_9(x)\}$ such that

$$R.W_9 = \lambda_4 Q(S, W_9), \tag{3.22}$$

the M manifold is called a W_9 Ricci pseudosymmetric manifold [10].

Let us now investigate the cases of W_9 pseudosymmetry and W_9 Ricci pseudosymmetry.

Theorem 3.5 *If a $(2n+1)$ $-$dimensional M Kenmotsu manifold is a W_9 pseudosymmetric manifold, then M is an η $-$Einstein manifold provided $\lambda_3 \neq -1$ and $\lambda_3 \neq 0$.*

Proof. Let us suppose that Kenmotsu manifold M is a W_9 pseudosymmetric manifold. Then, we can write

$$(R(X,Y) \cdot W_9)(Z,U,W) = \lambda_3 Q(g, W_9)(W,U,Z;X,Y), \tag{3.23}$$

for each $X, Y, Z, U, W \in \chi(M)$. This means that

$$R(X,Y)W_9(Z,U)W - W_9(R(X,Y)Z,U)W - W_9(Z,R(X,Y)U)W$$

$$-W_9(Z,U)R(X,Y)W$$

$$= -\lambda_3\{W_9((X \wedge_g Y)W,U)Z + W_9(W,(X \wedge_g Y)U)Z$$

$$+W_9(W,U)(X \wedge_g Y)Z\}, \tag{3.24}$$

that is, in the last equality taking $X = Z = \xi$ and using (2.9), (2.10) and (3.18) in (3.24), we obtain

$$\eta(W_9(\xi,U)W)Y - g(Y,W_9(\xi,U)W) - W_9(Y-\eta(Y)\xi,U)W$$

$$-W_9(\xi,\eta(U)Y - g(U,Y)\xi)W - \eta(W_9(\xi,Y)W)U + g(U,W_9(\xi,Y)W)$$

$$= -\lambda_3\{W_9(g(Y,W)\xi - \eta(W)Y,U)\xi + W_9(W,g(Y,U)\xi - \eta(U)Y)$$

$$+W_9(W,U)(\eta(Y)\xi - Y)\}. \tag{3.25}$$

If we use (3.18), (3.19) and taking $W = \xi$ in (3.25) and make the necessary abbreviations, then we have

$$\eta(U-\eta(U)\xi)Y - g(Y,U-\eta(U)\xi)\xi - W_9(Y,U)\xi$$

$$+\eta(Y)W_9(\xi,U)\xi - \eta(U)W_9(\xi,Y)\xi - W_9(\xi,U)Y$$

$$+\eta(Y)W_9(\xi,U)\xi$$

$$= -\lambda_3\{2\eta(Y)(U-\eta(U)\xi) - (\eta(Y)U - \eta(U)Y - \tfrac{1}{2n}S(U,Y)\xi$$

$$+\eta(U)\tfrac{QY}{2n}) - \eta(U)(Y-\eta(Y)\xi) - (\eta(Y)U - \eta(U)Y)\}. \tag{3.26}$$

Taking the inner product with $\xi \in \chi(M)$ on both sides of (3.26) and make use of (3.20), then we arrive

$$S(U,Y) = \tfrac{2n}{1+\lambda_3}g(U,Y) - \tfrac{2n\lambda_3}{1+\lambda_3}\eta(U)\eta(Y). \tag{3.27}$$

This completes our proof.

Corollary 3.6 *Let M be a $(2n+1)$ −dimensional Kenmotsu manifold. If M is a W_9-semisymmetric manifold, M is an Einstein manifold.*

Corollary 3.7 *Let M be a $(2n+1)-$dimensional Kenmotsu manifold. If M is a W_9-pseudosymmetric manifold, M is an Einstein manifold, provided $\lambda_3 = 0$.*

Theorem 3.8 *If a $(2n+1)-$dimensional M Kenmotsu manifold is a W_9 Ricci pseudosymmetric manifold, then M is an $\eta-$Einstein manifold, provided $\lambda_4 \neq 1$ and $\lambda_4 \neq 0$*

Proof. Let us assume that Kenmotsu manifold M is a W_9 Ricci pseudosymmetric manifold. This implies that

$$(R(X,Y)\cdot W_9)(Z,U,W) = \lambda_4 Q(S,W_9)(W,U,Z;X,Y), \tag{3.28}$$

for each $X,Y,Z,U,W \in \chi(M)$, that is,

$$\begin{aligned}
&R(X,Y)W_9(Z,U)W - W_9(R(X,Y)Z,U)W - W_9(Z,R(X,Y)U)W \\
&-W_9(Z,U)R(X,Y)W \\
&= -\lambda_4\{W_9((X\wedge_S Y)W,U)Z + W_9(W,(X\wedge_S Y)U)Z \\
&+W_9(W,U)(X\wedge_S Y)Z\}.
\end{aligned} \tag{3.29}$$

Taking $X = Z = \xi$ and using (2.9), (3.18) in (3.29), we have

$$\begin{aligned}
&\eta(W_9(\xi,U)W)Y - g(Y,W_9(\xi,U)W) - W_9(Y-\eta(Y)\xi,U)W \\
&-W_9(\xi,\eta(U)Y - g(U,Y)\xi)W - \eta(W_9(\xi,Y)W)U + g(U,W_9(\xi,Y)W) \\
&= -\lambda_4\{W_9(S(Y,W)\xi + 2n\eta(W)Y,U)\xi + W_9(W,S(Y,U)\xi \\
&+2n\eta(U)Y)\xi + 2nW_9(W,U)(Y-\eta(Y)\xi)\}.
\end{aligned} \tag{3.30}$$

If we use (3.18), (3.20) and setting $W = \xi$ in (3.30), then we get

$$\begin{aligned}
&\eta(U-\eta(U)\xi)Y - g(Y,U-\eta(U)\xi)\xi - W_9(Y,U)\xi \\
&+\eta(Y)W_9(\xi,U)\xi - \eta(U)W_9(\xi,Y)\xi - W_9(\xi,U)Y \\
&+\eta(Y)W_9(\xi,U)\xi \\
&= -\lambda_4\{-4n\eta(Y)(U-\eta(U)\xi) + 2n(\eta(Y)U - \eta(U)Y \\
&-\tfrac{1}{2n}S(U,Y)\xi + \eta(U)\tfrac{QY}{2n}) + 2n(\eta(Y)U - \eta(U)Y)
\end{aligned}$$

$$+2n\eta(U)(Y-\eta(Y)\xi)\}. \tag{3.31}$$

Inner product both sides of (3.31) by $\xi \in \chi(M)$, we obtain

$$S(U,Y) = -\frac{2n}{1-\lambda_4}g(U,Y) + \frac{\lambda_4-4n}{1-\lambda_4}\eta(Y)\eta(U).$$

which proves our assertion.

Corollary 3.9 *Let M be a $(2n+1)-$dimensional Kenmotsu manifold. If M is a W_9-semisymmetric manifold, M is an $\eta-$Einstein manifold.*

Corollary 3.10 *Let M be a $(2n+1)-$dimensional Kenmotsu manifold. If M is a W_9-pseudosymmetric manifold, M is an Einstein manifold provided $\lambda_4 = 4n$.*

4.CONCLUSIONS

In this paper pseudosymmetric and Ricci pseudosymmetric of a Kenmotsu manifolds are researched. We have achieved the necessary and sufficient conditions for a Kenmotsu manifold, W_8-pseudosymmetric, W_8-Ricci pseudosymmetric, W_9-pseudosymmetric and W_9-Ricci pseudosymmetric. Additionally, some interesting results on Kenmotsu manifolds are obtained.

REFERENCES

1. M. Atçeken, On generalized Sasakian space forms satisfying certain conditions on the concircular curvature tensor, Bulletin of Mathematical Analysis and Applications, Vol:6(1), 1-8, 2014.

2. D. E. Blair, Contact manifolds in Riemannian geometry, Lecture Note in Mathematics, 509, Springer-Verlag, Berlin-New York, 1976.

3. W. M. Boothby, An Introduction to Differentiable Manifolds and Riemannian Geometry, Academic Press, Inc, London, UK, 1986.

4. E. Boeckx, P. Buecken and L. Vanhecke, ϕ-symmetric contact metric spaces, Glasgow Mathematical Journal, Vol:41, 409-416, 1999.

5. E. Cartan, Sur one classe remarquable despaces de Riemannian, Bulletin de la Societe Mathematique de France, Vol:54, 214-264, 1926.

6. M.C. Chaki, On pseudo Ricci symmetric manifolds, Bulgarian Journal of Physics, Vol:15, 526-531, 1988.

7. K. De and U. C. De, Conharmonic curvature tensor on Kenmotsu manifolds, In Bulletin of the Transilvania University of Brasov, Vol: 6(55), No:1, 2013.

8. U. C. De and A. K. Gazi, On psudo Ricci symmetric manifolds, Analeles Tnt Ifcealeuniversit II, Matematica, 2012.

9. U. C. De and G. Pathak, On 3-dimensional Kenmotsu manifolds, Indian J. pure Appl. Math., Vol:35, 159-165, 2004.

10. R. Deszcz, On pseudosymmetric spaces, Bull. Soc. Belg. Math., Ser. A, Vol: 44, 1-34, 1992.

11. R. Deszcz, On Ricci warped products, Demonstratio Mathematica, Vol: 22 (4), 1053-1065, 1989.

12. A. Haseeb, Some results on projective on projective curvature tensor in an $\epsilon-$Kenmotsu manifold, Plestine Journal of Math., Vol: 6, 196-203, 2017.

13. K. Kenmotsu, A class of almost contact Riemannian manifolds, Tohoku Math. J., Vol: 24, 93-103, 1972.

14. T. Mert, On a Classification of Almost C(a)-manifolds, Journal of Mathematics, 2022, Article ID 5173330.

15. T. Mert and M. Atçeken, Almost $C(\alpha)$-manifold on $W_0^\star-$curvature tensor, Applied Mathematical Sciences, Vol:15(15), 693-703, 2021.

16. T. Mert and M. Atçeken, Characterizations for pseudoparalel submanifolds of Lorentz-Sasakian space forms, Malaya Journal of Matematık, Vol:12(1), 31-42, 2024.

17. R.S. Mishra, Structure on a Differentiable manifold and their applications, Chandrama Prakashan, 50-A Bairampur House Allahabad (1984).

18. C. Ozgür, On Kenmotsu manifolds satisfying certain pseudosymmetry conditions, World Applied Sciences Journal, Vol:1(2), 144-149, 2006.

19. G. P. Pokhariyal, Relativistic significance of curvature tensors, Internat. J. Math. Sci., Vol:5(1), 133-139, 1982.

20. D. G. Prakasha and B. S. Hadımanı, On the conharmonic curvature tensor of Kenmotsu manifolds with generalized Tanaka-Webster connection, Miskole Mathematical Notes, Vol: 19, 491-503, 2018.

21. R.N. Singh, , S. K. Pandey, and G. Pandey, On W_2-curvature tensor in a Kenmotsu manifold. Tamsui Oxf. J. Inf. Math. Sci, Vol:29(2), 129-141, 2013.

22. P.Uygun, M. Atceken and S. Dirik, On Kenmotsu metric spaces satisfying some conditions on the W_1-curvature tensor, Filomat, Vol:36(5), 1603-1613, 2022.

23. P.Uygun and M. Atceken, On Kenmotsu metric spaces satisfying some conditions on the W_7-curvature tensor, Malaya J. Mat., Vol:11(04), 447-456, 2023.

ON A HEAT EQUATION AND NEWTON- RAPHSON METHOD

İlayda Tarhanacı[1] **, Elif Başkaya**[2]

[1,2]Department of Mathematics, Karadeniz Technical University, Trabzon, Turkey

432131@ogr.ktu.edu.tr,

elifbekar@ktu.edu.tr,

Abstract

In this paper, we study a heat conduction problem in a rod that a boundary condition, which involves a linear combination of dependent variable and its derivative, arises when heat is lost from the end of the rod due to radiation into the surrounding medium. When we apply the seperation of variables method to solve the problem, Newton- Raphson method is used to calculate the eigenvalues of the equations we encounter.

Keywords: Heat equation; Eigenvalue problem; Newton- Raphson method.

1. INTRODUCTION

The heat equation

$$\nabla^2 u = a^{-2} u_t$$

where a^2 is a physical constant, arises in problems concerning the temperature distribution in homogeneous solids, electromagnetic theory, diffusion processes, and the propagation of current in transmission lines. A properly-posed problem consists this equation coupled with a single boundary condition and single initial condition, an example of which is given by

$$\nabla^2 u = a^{-2} u_t, \quad u \text{ in } R$$

$$u = g \text{ on } \partial R$$

$$u = f \text{ for } t = 0.$$

Here, R denotes the domain of the function u, and ∂R is the boundary of R.

In this work, we study with a one-dimensional model for heat equation. Let us consider the following heat conduction problem in a rod that a boundary condition, which involves a linear combination of dependent variable and its derivative, arises when heat is lost from the end of the rod due to radiation into the surrounding medium:

$$u_{xx} = a^{-2} u_t, \quad 0 < x < p \tag{1}$$

$$u(0,t) = 0, hu(p,t) + u_x(p,t) = 0, \quad t > 0 \tag{2}$$

$$u(x,0) = f(x) \tag{3}$$

where a^2 is a positive constant known as the diffusivity of the material forming the rod and $h > 0$. Negative values of h would physically correspond to thermal energy constantly put into the rod through the right end [1]. Our aim is to solve this problem for $a = 1, h = 1$ and $p = \pi$.

2. GENERAL PROPERTIES OF METHOD

In this paper, we consider a heat equation and we solve it by separating variables. At that case, we must obtain eigenvalues and eigenfunctions of a eigenvalue problem. For this, we use Newton-Raphson method.

The Newton-Raphson method is the best-known method of finding roots of a function. The method is simple and fast. One drawback of this method is that it uses the derivative of the function as well as the function f(x) itself. Hence, the Newton-Raphson method is usable only in problems where f(x) can be readily computed [2]. Newton-Raphson method is also called Newton's method. Here, f(x) is continuous and differentiable. In this method, the solution process starts by selecting point x_1 as the first estimate of the solution. The second estimate x_2 is found by drawing the tangent line to f(x) at the point $(x_1, f(x_1))$ and determining the intersection point of the tangent line with the x-axis. The next estimate x_3 is the intersection of the tangent line to f(x) at the point $(x_2, f(x_2))$ with the x-axis, and so on. Since the tangent line of the function f(x) at point x_n intersects the x-axis at point x_{n+1}, the slope here is written as:

$$f'(x_n) = \frac{f(x_n) - 0}{x_n - x_{n+1}}$$

and from this equation, one gains

$$x_{n+1} = x_n - \frac{f(x_n)}{f'(x_n)}.$$

3. APPLICATIONS

In this section, we solve the problem (1)-(3). Let's look for a solution for this equation in the form of $u(x,t) = X(x)T(t)$ by the separation of variables method. If this solution $u(x,t)$ is substituted into the heat equation:

$$X''(x)T(t) = a^{-2}X(x)T'(t),$$

that is

$$\frac{X''(x)}{X(x)} = \frac{a^{-2}T'(t)}{T(t)} = -\lambda.$$

From here, the following two equations are obtained:

1) $X''(x) + \lambda X(x) = 0$,

2) $T'(t) + a^2\lambda T(t) = 0$.

If the first boundary condition $u(0,t) = 0$ in the problem is applied, $X(0)T(t) = 0$ is found. For non- trivial solution $T(t) \neq 0$ and $X(0) = 0$ must be. When the second boundary condition $hu(p,t) + u_x(p,t) = 0$ is applied in the problem, the equation $hX(p)T(t) + X'(p) + T(t) = T(t)\{hX(p) + X'(p)\} = 0$ is found. For non- trivial solution $T(t) \neq 0$ and $hX(p) + X'(p) = 0$ must be. Thus, the following eigenvalue problem for X(x) is obtained:

$$X''(x) + \lambda X(x) = 0, \quad X(0) = 0, hX(p) + X'(p) = 0. \tag{4}$$

For the sake of brevity, we accept $a = 1, h = 1$ and $p = \pi$ in (1)-(3). Denoting the nth solution of $\sin(k\pi) + k\cos(k\pi) = 0$ by k_n, the eigenvalues and eigenfunctions of (4) are represented by

$$\lambda_n = {k_n}^2, \quad \phi_n(x) = \sin(k_n x), \quad n = 1,2,3, \ldots \tag{5}$$

Returning now to $T'(t) + \lambda T(t) = 0$, we obtain

$$T_n(t) = c_n e^{-{k_n}^2 t}, n = 1,2,3, \ldots$$

which, combined with (5), gives the formal solution

$$u(x,t) = \sum_{n=1}^{\infty} c_n \sin(k_n x) e^{-{k_n}^2 t}. \tag{6}$$

For the condition (2), setting $t = 0$ in (6) yields the relation

$$u(x,0) = f(x) = \sum_{n=1}^{\infty} c_n \sin(k_n x), 0 < x < \pi,$$

which is a generalized Fourier series. In this case the Fourier coefficients are calculated from

$$c_n = \|\phi_n(x)\|^{-2} \int_0^{\pi} f(x) \sin(k_n x) dx, n = 1,2,3, \ldots$$

where

$$\begin{aligned}
\|\phi_n(x)\|^2 &= \int_0^{\pi} \sin^2(k_n x) dx \\
&= \frac{1}{2}\left(\pi - \frac{\sin(2k_n\pi)}{2k_n}\right) \\
&= \frac{1}{2}\left(\pi - \frac{\sin(k_n\pi)\cos(k_n\pi)}{k_n}\right),
\end{aligned}$$

but since $\sin(k_n\pi) = k_n \cos(k_n\pi)$, we have

$$\|\phi_n(x)\|^2 = \frac{1}{2}[\pi - \cos^2(k_n\pi)], n = 1,2,3, \ldots$$

We remark that k_n is not exactly clear in (5). In this study, we calculate some k_n by using Newton-Raphson method, so that one writes the solution of the heat equation from (6).

Let us consider the problem (1)-(3) for $a = 1, h = 1$ and $p = \pi$. Hence, we have the following the eigenvalue problem $X(x)$ and the equation for $T(t)$:

$$X''(x) + \lambda X(x) = 0, \quad X(0) = 0, X(\pi) + X'(\pi) = 0, \tag{7}$$

$$T'(t) + \lambda T(t) = 0.$$

Firstly, we note that (7) has a symmetric operator, so the eigenvalues of (7) are real. The solution of the problem (7) is examined according to the values of the λ parameter as follows:

- If $\lambda = 0$,

the equation is $X'' = 0$ and the characteristic polynomial is $r^2 = 0$. The roots of the characteristic polynomial are found $r_1 = r_2 = 0$ and the general solution is $X(x) = c_1 + c_2 x$. If the first boundary condition $X(0) = 0$ is applied, $c_1 = 0$ is obtained; if the second boundary condition $X(\pi) + X'(\pi) = 0$ is applied, $c_2\pi + c_2 = c_2(1 + \pi) = 0$ is obtained. We know $1 + \pi \neq 0$, so $c_2 = 0$. That is, the solution $X \equiv 0$ is obtained. Thus, λ is not an eigenvalue.

- If $\lambda = -k^2 < 0$,

the equation $X'' - k^2 X = 0$ and the characteristic polynomial is $r^2 - k^2 = 0$. The roots of the characteristic polynomial are found $r_1 = -k$, $r_2 = k$ and the general solution is $X(x) = c_1 \cosh(kx) + c_2 \sinh(kx)$. If the first boundary condition $X(0) = 0$ is applied, $c_1 = 0$ is obtained; if the secondary boundary condition $X(\pi) + X'(\pi) = 0$ is applied, $c_2 \sinh(k\pi) + kc_2 \cosh(k\pi) = c_2\{\sinh(k\pi) + k\cosh(k\pi)\} = 0$ is obtained. Since we want to obtain a nontrivial solution $c_2 \neq 0$, it should be $\sinh(k\pi) + k\cosh(k\pi) = 0$. If k solved from this equation:

$$k = -\frac{\sinh(k\pi)}{\cosh(k\pi)} = -\tanh(k\pi).$$

Here, the graphs of the $u = k$ and $u = -\tanh(k\pi)$ functions are drawn, the intersection points of the two equations are investigated. The graph is as follows:

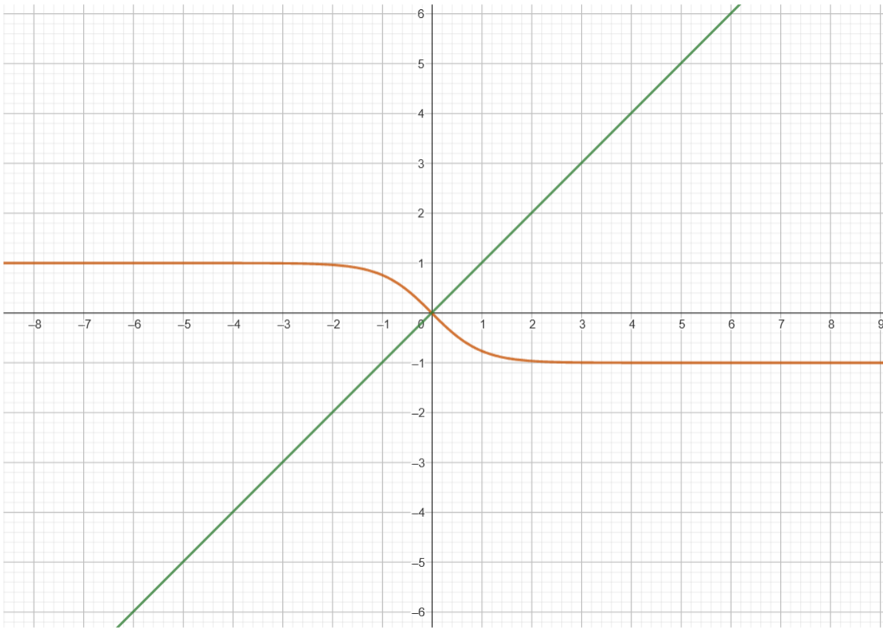

Figure 1. Graphs of the functions $u = k$ and $u = -\tanh(k\pi)$

As can be seen from the graph, the only intersection point is zero. But since $k \neq 0$, $\lambda = -k^2$ is not eigenvalue.

- If $\lambda = k^2 > 0$,

the equation $X'' + k^2X = 0$ and the characteristic polynomial is $r^2 + k^2 = 0$. The roots of the characteristic polynomial are found $r_1 = -ik, r_2 = ik$ and the general solution is $X(x) = c_1\cos(kx) + c_2\sin(kx)$. If the first boundary condition $X(0) = 0$ is applied, $c_1 = 0$ is obtained; if the second boundary condition $X(\pi) + X'(\pi) = 0$ is applied, $c_2\sin(k\pi) + kc_2\cos(k\pi) = c_2\{\sin(k\pi) + k\cos(k\pi)\} = 0$ is obtained. Since we want to obtain a nontrivial solution, $c_2 \neq 0$, it should be $\sin(k\pi) + k\cos(k\pi) = 0$. The k values that provide this equation will form the eigenvalues. To find the roots of the equation, that is, the k values that provide the equation, the Newton- Raphson method is applied. The iteration is constructed as follows:

Since $f(x) = \sin(\pi x) + x\cos(\pi x)$, $f'(x) = \pi\cos(\pi x) + \cos(\pi x) - x\pi\sin(\pi x)$. So from the formula $x_{n+1} = x_n - \frac{f(x_n)}{f'(x_n)}$,

$$x_{n+1} = x_n - \frac{\sin(\pi x_n) + x_n\cos(\pi x_n)}{\pi\cos(\pi x_n) + \cos(\pi x_n) - x_n\pi\sin(\pi x_n)},$$

and so

$$x_{n+1} = \frac{x_n \pi \cos(\pi x_n) - \sin(\pi x_n)\{{x_n}^2 \pi + 1\}}{\pi \cos(\pi x_n) + \cos(\pi x_n) - x_n \pi \sin(\pi x_n)}.$$

Let's determine the starting point for the iteration by using the graphs of the $\sin(\pi x)$ and $-x\cos(\pi x)$ functions:

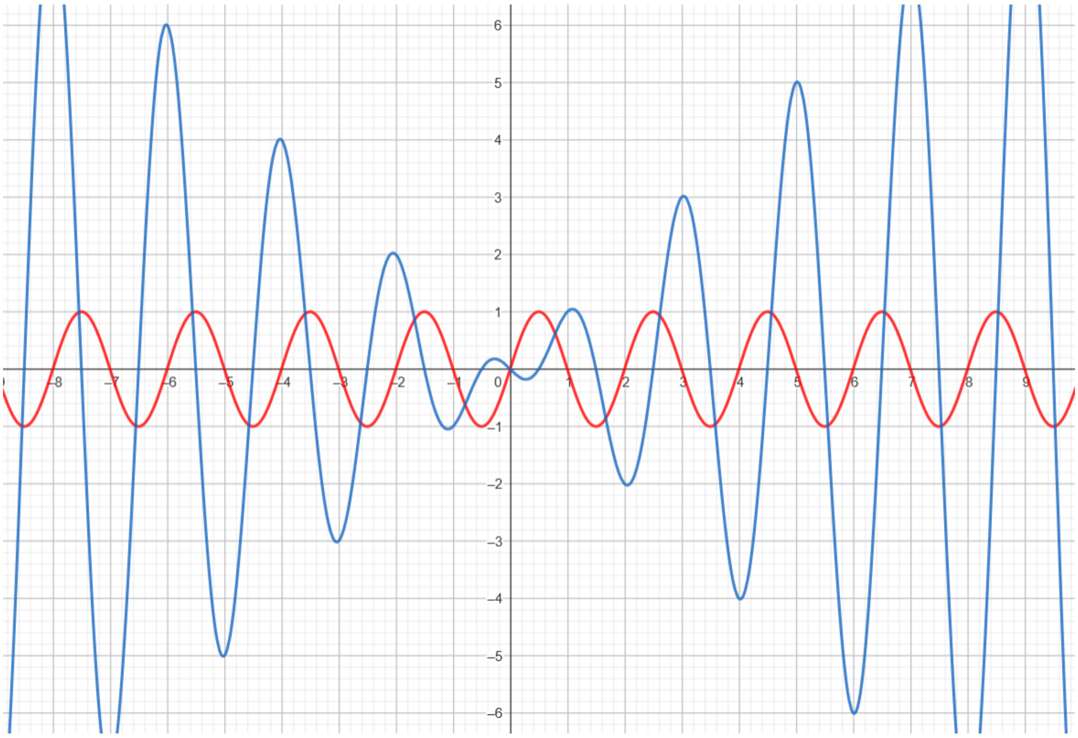

Figure 2. Graphs of the functions $\sin(\pi x)$ and $-x\cos(\pi x)$

Let's start the iteration with $x_0 = 0.6$:

- If $x_0 = 0.6$,

$f(x_0) = \sin(0.6\pi) + 0.6\cos(0.6\pi) = 0.765646.$

- If $x_1 = \frac{0.6\pi\cos(\pi 0.6) - \sin(\pi 0.6)\{0.6\pi + 1\}}{0.6\cos(\pi 0.6) + \cos(\pi 0.6) - 0.6\pi \sin(\pi 0.6)} = 0.849192,$

$f(x_1) = -0.299404.$

- If $x_2 = 0.788122,$

$f(x_2) = -0.002319.$

- If $x_3 = 0.787637,$

$f(x_3) = 0.000001.$

- $x_4 = 0.787637.$

Since here $x_i, i \geq 3$ values repeat and because it is $f(x_i) = 0.000001$, the root of the $\sin(\pi x) + x\cos(\pi x) = 0$ equation is found as $x \cong 0.787637$. Thus $\lambda = k^2 > 0$ is the eigenvalue and the first positive eigenvalue $\lambda_1 = (0.787637)^2$ is obtained. Also, substitution this value $k_1 = 0.787637$ into the equation (6), one gives the solution of the heat problem (1)-(3).

Let's start the iteration with $x_0 = 1.5$.

- If $x_0 = 1.5$,

$f(x_0) = \sin(1.5\pi) + 1.5\cos(1.5\pi) = -1.000000.$

- If $x_1 = \frac{1.5\pi\cos(\pi 1.5) - \sin(\pi 1.5)\{1.5\pi + 1\}}{1.5\cos(\pi 1.5) + \cos(\pi 1.5) - 1.5\pi\sin(\pi 1.5)} = 1.712207,$

$f(x_1) = 0.272892.$

- If $x_2 = 1.672007,$

$f(x_2) = 0.002663.$

- If $x_3 = 1.671606,$

$f(x_3) = 0.000002.$

- $x_4 = 1.671606.$

Since here $x_i, i \geq 3$ values repeat and because it is $f(x_i) = 0.000002$, the root of the $\sin(\pi x) + x\cos(\pi x) = 0$ equation is found as $x \cong 1.671606$. Thus $\lambda = k^2 > 0$ is the eigenvalue and the second positive eigenvalue $\lambda_2 = (1.671606)^2$ is obtained. Also, substitution this value $k_2 = 1.671606$ into the equation (6), one gives the solution of the heat problem (1)-(3).

Similarly, $\lambda_3 = -1.671606$ and $\lambda_4 = 2.616214$ are calculated.

We note that we also verify these values by using MAXIMA.

4. CONCLUSIONS

In this paper, we consider a heat problem so that when we apply the seperation of variables method to solve the problem, we see that the eigenvalues are not clear. We use Newton-

Raphson method to calculate approximation eigenvalues, and we find the first two eigenvalues and hence one writes the solution of the heat problem.

5. ACKNOWLEDGE

This work was supported by Office of Scientific Research Projects of Karadeniz Technical University. Project number: FYL-2024-11257.

REFERENCES

1. Larry C. Andrews, Elementary Partial Differential Equations with Boundary Value Problems, Academic Press Inc., London, 1986.
2. Rao V. Dukkipati, Numerical Methods, New Age International Publishers, New Delhi, 2010.

Generalized Lacunary Statistical Convergence of Modulus Function Sequences

Çiğdem A. Bektaş and Muhammet E. Aydın
Firat University, Department of Mathematics, Elazığ, Turkey
cbektas@firat.edu.tr aydinemin607@gmail.com

Abstract In this paper, we generalized structure for statistical convergence by the concept of density functions using sequences of modulus functions (f_t) of order $\mu \in (0,1]$. This method introduces a new density framework designed specifically for lacunary sequences, facilitating the definitions of strong $(f_t)-$lacunary summability of order μ and $(f_t)-$lacunary statistical convergence of order μ These newly defined concepts serve as a bridge between traditional convergence and statistical convergence in the context of lacunary sequences, providing a middle ground that enhances analytical versatility. Furthermore, we establish inclusion results and investigate the connections between these notions, offering a thorough exploration of their implications. This study extends the reach of statistical convergence theory and advances the field by presenting a more generalized analytical approach.

Keywords Lacunary statistical convergence, Lacunary summability, Modulus function, Weighted density, Difference sequence spaces.

Mathematics Subject Classification 40A05, 40A35 46A45, 40H05

1. Introduction

The notion of statistical convergence was first introduced by Zygmund [1]. Independently, Steinhaus [2] and Fast [3] also formulated similar ideas around the same time. Later, Schoenberg [4] and many other mathematicians expanded upon and analyzed this concept further. Statistical convergence, along with several related notions, has been studied in the context of various types of sequences. After the foundational work on statistical convergence, numerous perspectives were explored, leading to several generalizations and extensions. Notably, classes of sequences exhibiting statistical convergence have been developed using functions and sequences from specific categories. Additionally, a connection between statistical convergence and Cesàro summability was identified and rigorously studied. Salat [5] and Fridy [6] showed that statistical convergence has emerged as an active area of research within summability theory. The concept of asymptotic (or natural) density serves as a key tool in statistical convergence. The set of all sequences that are statistically convergent will be denoted by S, and the set of sequences that are statistically convergent of order μ will be denoted S^{μ}. Çolak [7] and Çolak and Bektaş [8] also conducted studies on this subject. The ideas of lacunary summability and convergence involving lacunary sequences were first introduced by Fridy and Orhan ([9] and [10]). The set of all lacunary statistically convergent sequences is denoted by S_θ and the set of sequences that are lacunary statistically convergent of order μ is denoted by S_θ^μ. The topics of lacunary statistical convergence, lacunary boundedness of order μ, and strong summability sequences of order μ have been extensively studied by Connor [11], Çolak [12], and Şengül and Et in [13, 14]. In their work, Pehlivan and Fisher [15] introduced the idea of lacunary strong convergence in Banach spaces, using a sequence of modulus functions. The modulus function is another concept that is central to our investigation. The concept of the modulus was first introduced by Nakano [16] and later, Ruckle [17] established new sequence spaces using a modulus function f, which were then applied in numerous studies (see [18, 19, 20, 21]). Altering the definition of the density function is one approach used to distinguish statistical convergence. Various generalizations of the concept of asymptotic density have been investigated. One such generalization is the density f introduced by Aizpuru et al. [22]: The f-density of a set $A \subseteq N$ is defined by

$$\delta_f(A) = \lim_{n\to\infty} \frac{f(|\{k \leq n : k \in A\}|)}{f(n)}$$

if the limit exists, where f is an unbounded modulus functions. Erdal and Bektaş [23] defined strongly $F^{\mu}-$lacunary summable and $F^{\mu}-$lacunary statistically convergent. Kizmaz [24] introduced difference sequence spaces .Difference sequence spaces are a class of sequence spaces studied in functional analysis, particularly within the theory of sequence spaces and summability. These spaces arise by considering sequences whose differences (typically first-order or higher-order) belong to a certain classical sequence space like ℓ_∞, c and c_0. After that Et and Çolak [25] generalized these spaces. Generalized difference sequence spaces extend the concept of ordinary difference sequence spaces by applying more flexible or higher-order difference operators often involving weights, matrices, or generalized difference operators or even using lacunary sequences, Orlicz functions, or modulus functions.

2. Main Results

For each $\mu \in R$ such that $\mu > 1$ lacunary statistical convergence is not properly defined (see [13], [14]). Therefore, in the remainder of this paper, we focus on the case where $\mu \in (0, 1]$. We introduce a slight extension of strongly lacunary summability of order μ by employing a sequence of modulus functions. Based on this definition, inclusion relationships are provided under specific conditions. We introduced a new concept of lacunary statistical convergence of order μ by using a sequence of modulus functions. By some given inclusion theorems, we establish some relations between lacunary summability and lacunary statistical convergence under certain conditions.

Let $F = (f_t)$ be a sequence of modulus functions, $\theta = (t_r)$ be a lacunary sequence and $\mu \in (0, 1]$ throughout the article.

Definition 2.1. The sequence (ζ_t) is strongly $F^{\mu}(\Delta^m)-$lacunary summable to some $L \in C$ provided that

$$\lim_{r\to\infty} \frac{1}{h_r^{\mu}} \sum_{t \epsilon I_r} f_t(|\Delta^m \zeta_t - L|) = 0.$$

The set of all $F^{\mu}(\Delta^m)-$lacunary summable sequences is denoted by $N_\theta^{\mu}(\Delta^m, F)$.

It is important to note that in this definition, the modulus functions f_k do not need to be unbounded.

Remark 2.2.

i) If we take $\mu = 1$, $m = 0$ and $f_t(\zeta) = \zeta$ for all $t \in N$, then $N_\theta^{\mu}(\Delta^m, F) = N_\theta$.

ii) If we take $m = 0$ and $f_t(\zeta) = \zeta$ for all $t \in N$, then $N_\theta^{\mu}(\Delta^m, F) = N_\theta^{\mu}$.

iii) If we take $\mu = 1$, $m = 0$ and $f_t = f$ for all $t \in N$, then $N_\theta^\mu(\Delta^m, F) = N_\theta(f)$.

In the following theorems and corollaries, supremum and infimum will be taken over all $u \in (0, \infty)$ and $t \in N$.

Theorem 2.3. For $\mu_1 \le \mu_2$ we have:

i) If $\sup_{u,t} \frac{f_t(u)}{g_t(u)} < \infty$, then $N_\theta^{\mu_1}(\Delta^m, G) \subset N_\theta^{\mu_2}(\Delta^m, F)$.

ii) If $\inf_{u,t} \frac{f_t(u)}{g_t(u)} > 0$, then $N_\theta^{\mu_1}(\Delta^m, F) \subset N_\theta^{\mu_2}(\Delta^m, G)$.

iii) If $0 < \inf_{u,t} \frac{f_t(u)}{g_t(u)} \le \sup_{u,t} \frac{f_t(u)}{g_t(u)} < \infty$, then $N_\theta^{\mu_1}(\Delta^m, F) = N_\theta^{\mu_1}(\Delta^m, G)$.

Proof i) Let $\zeta \in N_\theta^{\mu_1}(\Delta^m, G)$. If $p = \sup_{u,t} \frac{f_t(u)}{g_t(u)} < \infty$, then $0 < \frac{f_t(u)}{g_t(u)} \le p$ and hence $f_t(u) \le p g_t(u)$ for all $t \in N$ and for any $u \in R^+ \cup \{0\}$. Since $0 < \mu_1 \le \mu_2 \le 1$, we obtain

$$\frac{1}{h_r^{\mu_2}} \sum_{t \in I_r} f_t(|\Delta^m \zeta_t - l|) \le \frac{1}{h_r^{\mu_1}} \sum_{t \in I_r} f_t(|\Delta^m \zeta_t - l|) \le \frac{1}{h_r^{\mu_1}} \sum_{t \in I_r} p g_t(|\Delta^m \zeta_t - l|).$$

If we take limit as $r \to \infty$, we have $\zeta \in N_\theta^{\mu_1}(\Delta^m, F)$.

ii) If $\inf_{u,t} \frac{f_t(u)}{g_t(u)} > 0$, then $g_t(u) \le \frac{1}{q} f_t(u)$ for every $u \in R^+ \cup \{0\}$and for all $t \in N$. Thus, the rest of the proof is exactly similar to (i).

iii) is seen from (i) and (iii).

Corollary 2.4. For $F = (f_t)$ and $G = (g_t)$, if $\mu_1 \le \mu_2$, then $N_\theta^{\mu_1}(\Delta^m, F) \subset N_\theta^{\mu_2}(\Delta^m, F)$.

Corollary 2.5. For $F = (f_t)$, $G = (g_t)$ and μ, if $\sup_{u,t} \frac{f_t(u)}{g_t(u)} < \infty$, then $N_\theta^\mu(\Delta^m, G) \subset N_\theta^\mu(\Delta^m, F)$.

Corollary 2.6. For $F = (f_t)$ and $\mu_1 \le \mu_2$, the followings hold:

i) If $\sup_{u,t} \frac{f_t(u)}{u} < \infty$, then $N_\theta^{\mu_1} \subset N_\theta^{\mu_2}(\Delta^m, F)$.

iii) If $\inf_{u,t} \frac{f_t(u)}{u} > 0$, then $N_\theta^{\mu_1}(\Delta^m, F) \subset N_\theta^{\mu_2}$.

Corollary 2.7. For $F = (f_t)$ and $\mu_1 \le \mu_2 \le \gamma$, the followings hold:

i) If there exists a modulus function f such that $f_t \le f$ for every $t \in N$, then $N_\theta^{\mu_1}(\Delta^m, f) \subset N_\theta^{\mu_2}(\Delta^m, F)$.

ii) If there exists a modulus function f such that $g \le f_t$ for every $t \in N$, then $N_\theta^{\mu_1}(\Delta^m, F) \subset N_\theta^{\mu_2}(\Delta^m, g)$.

iii) If there exists a modulus function f and g such that $g \le f_t \le f$ for every $t \in N$, then $N_\theta^{\mu_1}(\Delta^m, f) \subset N_\theta^{\mu_2}(\Delta^m, F) \subset N_\theta^\gamma(\Delta^m, g)$.

Definition 2.8[23] The density of $A \subseteq N^+$ of order $\mu \in (0, 1]$ for unbounded modulus functions $F = (f_t)$ is denified by

$$\delta_{F_\mu}(A) = \lim_{r \to \infty} \frac{f_r(|\{t \le r : t \in A\}|)}{f_r(r^\mu)}$$

whenever the limit exists.

Here if $\mu = 1$ and $f_t(\zeta) = \zeta$ for all $t \in N$, then we have the natural density (see [3]). If $\mu \in (0, 1]$ and $f_t(\zeta) = \zeta$ for all $t \in N$, then we have the μ-density (see [7]).If $\mu = 1$ and

$f_t(\zeta) = f(\zeta)$ for all $t \in N$ and for $f \in M$, then we have the f-density (see [20]). If $\mu \in (0, 1]$ and $f_t(\zeta) = f(\zeta)$ for all $t \in N$ and for $f \in M$, then we have the f_μ-density (see[26]).

Definition 2.9. The sequence (ζ_t) is generalized F_μ-lacunary statistically convergent (or strongly $S_\theta^\mu(F)$-convergent) to some $l \in C$ provided that every $\varepsilon > 0$

$$\lim_{r\to\infty} \frac{1}{f_r(h_r^\mu)} f_r(|\{t \in I_r : |\Delta^m \zeta_t - l| \geq \varepsilon\}|) = 0.$$

This is represented by $\zeta \to l(S_\theta^\mu(\Delta^m, F))$ or $S_\theta^\mu(\Delta^m, F) - \lim \zeta_t = l$. The set of all sequences $S_\theta^\mu(\Delta^m, F)$-convergent sequences is denoted as $S_\theta^\mu(\Delta^m, F)$.

Theorem 2.10. For $F = (f_t)$, $G = (g_t)$ and $\mu_1 \leq \mu_2$, if $\inf_{u,t} \frac{f_t(u)}{g_t(u)} > 0$ and $\lim_{u\to\infty} \frac{g_t(u)}{u} > 0$ for all t, then $N_\theta^{\mu_1}(\Delta^m, F) \subset S_\theta^{\mu_2}(\Delta^m, G)$.

Proof. Let $\zeta \in N_\theta^{\mu_1}(\Delta^m, F)$. Since $q = \inf_{u,t} \frac{f_t(u)}{g_t(u)} > 0$ and hence $q g_t(u) \leq f_t(u)$, we have

$$\begin{aligned}
\frac{1}{h_r^{\mu_1}} \sum_{t\in I_r} f_t(|\Delta^m \zeta_t - l|) &\geq q \frac{1}{h_r^{\mu_1}} \sum_{t\in I_r} g_t(|\Delta^m \zeta_t - l|) \\
&\geq q \frac{1}{h_r^{\mu_2}} \sum_{t\in I_r} g_t(|\Delta^m \zeta_t - l|) \\
&\geq q \frac{1}{h_r^{\mu_2}} \sum_{\substack{t\in I_r \\ |\Delta^m z_t - l| \geq \epsilon}} g_t(|\Delta^m \zeta_t - l|) + q \frac{1}{h_r^{\mu_2}} \sum_{\substack{t\in I_r \\ |\Delta^m z_t - l| < \epsilon}} g_t(|\Delta^m \zeta_t - l|) \\
&\geq q \frac{1}{h_r^{\mu_2}} \sum_{\substack{t\in I_r \\ |\Delta^m z_t - l| \geq \epsilon}} g_t(|\Delta^m \zeta_t - l|) \\
&\geq q \frac{1}{h_r^{\mu_2}} |\{t \epsilon I_r : |\Delta^m \zeta_t - l| \geq \varepsilon\}| g_r(\varepsilon),
\end{aligned}$$

where $g_r(\varepsilon) = \inf_{t\in I_r} g_t(\varepsilon)$. If we make the necessary arrangements and take the limit as $r \to \infty$ of both sides, we obtain that $\zeta \in S_\theta^{\mu_1}(\Delta^m, G)$.

Corollary 2.11. If $\lim_{u\to\infty} \frac{f_t(u)}{u} > 0$ for all $t \in N$, then $N_\theta^{\mu_1}(\Delta^m, F) \subseteq S_\theta^{\mu_2}(\Delta^m, F)$.

Corollary 2.12. If $\inf_{u,t} \frac{f_t(u)}{g_t(u)} > 0$ and $\lim_{u\to\infty} \frac{f_t(u)}{u} > 0$ for all $t \in N$, then $N_\theta^\mu(\Delta^m, F) \subseteq S_\theta^\mu(\Delta^m, G)$.

Corollary 2.13. If $\inf_{u,t} \frac{f_t(u)}{u} > 0$, then $N_\theta^\mu(\Delta^m, F) \subseteq S_\theta^\mu$.

Theorem 2.14. Let $F = (f_t)$, $G = (g_t)$ be sequences of modulus functions, $0 < \mu_1 \leq \mu_2 \leq 1$, and $\theta = (t_r)$, $\Psi = (s_r)$ be lacunary sequences such that $I_r \subset J_r$ for each $r \in N$. If $\sup_{u,t} \frac{g_t(u)}{u} < \infty$ and $\lim_{r\to\infty} \frac{s_r - s_{r-1}}{(t_r - t_{r-1})^{\mu_2}} = 1$, then $l_\infty \cap s_\theta^{\mu_1}(\Delta^m, F) \subset N_\Psi^{\mu_2}(\Delta^m, G)$.

Proof. Let $I_r = (t_{r-1}, t_r]$, $J_r = (s_{r-1}, s_r]$, $h_r = t_r - t_{r-1}$, $v_r = s_r - s_{r-1}$, $0 < \mu_1 \leq \mu_2 \leq 1$ and $\zeta \in \ell_\infty \cap s_\theta^{\mu_1}(\Delta^m, F)$. Hence for every $\varepsilon > 0$, we have

$$\lim_{r\to\infty} \frac{1}{f_r(h_r^{\mu_1})} f_r(|\{t \in I_r : |\Delta^m \zeta_t - l| \geq \varepsilon\}|) = 0.$$

Therefore, for a given $p \in N$ we can determine a natural number r_0 such that

$$f_r(|\{t \in I_r : |\Delta^m \zeta_t - l| \geq \varepsilon\}|) \leq \frac{1}{p} f_r\left(h_r^{\mu_1}\right) \leq \frac{1}{p} p f_r\left(\frac{h_r^{\mu_1}}{p}\right) = f_r\left(\frac{h_r^{\mu_1}}{p}\right)$$

for $r > r_0$. Since f_r are sequences modulus functions, we have

$$\frac{1}{h_r^{\mu_1}} |\{t \in I_r : |\Delta^m \zeta_t - l| \geq \varepsilon\}| \leq \frac{1}{p}.$$

Then $s_\theta^{\mu_1}(\Delta^m, F) \subset s_\theta^{\mu_1}$ and hence $l_\infty \cap s_\theta^{\mu_1}(\Delta^m, F) \subset l_\infty \cap s_\theta^{\mu_1}$. Since $\lim_{r\to\infty} \frac{v_r}{h_r^{\mu_2}} = 1$ and $I_r \subset J_r$ for each $r \in N$, we have $l_\infty \cap s_\theta^{\mu_1}(\Delta^m, F) \subset N_\Psi^{\mu_2}$. Since $\sup_{u,k} \frac{g_t(u)}{u} < \infty$ we have $N_\theta^{\mu_2} \subset N_\psi^{\mu_2}(\Delta^m, G)$. Hence $l_\infty \cap s_\theta^{\mu_1}(\Delta^m, F) \subset N_\Psi^{\mu_2}(\Delta^m, G)$.

The inclusion $l_\infty \cap s_\theta^{\mu_1}(\Delta^m, F) \subset N_\Psi^{\mu_2}(\Delta^m, G)$ is strict. If we take $f_t(u) = g_t(u) = u$ for all $t \in N$, we can easily seen from Example 3.3 in [25].

Corollary 2.15. Let $\theta = (t_r)$, $\Psi = (\varpi_r)$ be lacunary sequences and $\mu_1 \leq \mu_2$. Then, the following statements hold:
i) $l_\infty \cap s_\theta^{\mu_1}(\Delta^m, F) \subset N_\Psi^{\mu_2}(\Delta^m, F)$,
ii) $l_\infty \cap s_\theta^{\mu_1}(\Delta^m, F) \subset N_\Psi^{\mu_1}(\Delta^m, F)$,
iii) $l_\infty \cap s_\theta^{\mu_1} \subset N_\Psi^{\mu_1}(\Delta^m, F)$.

Theorem 2.16. Lett $\mu_1 \leq \mu_2$. If $\sup_{u>0} \sup_{n\in N} f_n(u) < \infty$, then $S_\theta^\mu(\Delta^m, F) \subset N_\theta^\mu(\Delta^m, F)$.

Proof. Suppose that $\sup_{u>0} \sup_{n\in N} f_n(u) < \infty$ and $T = sup_{u>0} T(u)$ where $T(u) = sup_{n\in N} f_n(u)$. Let $\zeta \in S_\theta^\mu(\Delta^m, F)$. Since $S_\theta^\mu(\Delta^m, F) \subset S_\theta^\mu$, we have $lim_{r\to\infty} \frac{1}{h_r^\mu} |\{t \in I_r : |\Delta^m \zeta_t - l| \geq \varepsilon\}| = 0$. In addition, we have

$$\frac{1}{h_r^\mu} \sum_{t\in I_r} f_t(|\Delta^m \zeta_t - l|) = \frac{1}{h_r^\mu} \sum_{\substack{t\in I_r \\ |\Delta^m z_t - l| \geq \epsilon}} f_t(|\Delta^m \zeta_t - l|) + \frac{1}{h_r^\mu} \sum_{\substack{t\in I_r \\ |\Delta^m z_t - l| < \epsilon}} f_t(|\Delta^m \zeta_t - l|)$$
$$\leq \frac{1}{h_r^\mu} T |\{t \epsilon I_r : |\Delta^m \zeta_t - l| \geq \varepsilon\}| + \frac{1}{h_r^\mu} h_r T.$$

If we take limit for $r \to \infty$, we have

$$lim_{r\to\infty} \frac{1}{h_r^\mu} |\{t \in I_r : |\Delta^m \zeta_t - l| \geq \varepsilon\}| = 0$$

i.e, $\zeta \in N_\theta^\mu(\Delta^m, F)$.

3. Conclusions

In this study, we have introduced and analyzed the concepts of strongly lacunary summable sequences and lacunary statistically convergent sequences, using sequences of modulus functions. Throught this approach, we have established a set of inclusion theorems that serve to compare these sequences, based on various parameters, the structure of lacunary sequences, and the properties of sequences of modulus functions. Statistical convergence is a powerful and widely used concept in applied mathematics. A sequence is typically considered statistically convergent to a given point if, for the majority of its terms, the values approach this point as closely as desired. The traditional method of statistical convergence can sometimes be too rigid or abrupt, especially in contexts where it is necessary to retain as many terms as possible from the sequence. In these cases, the use of modulus functions provides a refined approach to handling statistical convergence. By utilizing a sequence of modulus functions, it is possible to retain terms without discarding them, even when they do not contribute significantly to the convergence. Moreover, this study introduces the concept of density functions defined by sequences of unbounded modulus functions, in combination with a real number. This allows for a more nuanced approach to statistical convergence, where instead of relying on a single constant modulus function, a sequence of modulus functions is employed. As a result, the number of terms that need to be excluded from the sequence is greatly reduced, improving the overall accuracy of the convergence process. This refinement helps to enhance both statistical convergence and summability methods, offering a more precise way to study sequences that do not fit neatly into traditional frameworks. In addition to providing an improved method for understanding convergence, this work also serves as a stepping stone for future research. By selecting different sequences of modulus functions tailored to specific applications, it may be possible to develop application-specific sequence spaces that better reflect the underlying structures of various problems. For example, in fields such as signal processing, data analysis, or numerical methods, the techniques introduced in this study can be applied to develop more efficient algorithms and models. Ultimately, this paper offers a deeper understanding of lacunary convergence and summability, while also presenting a foundation for further exploration in these areas.

References

[1] Zygmund, A. Trigonometric Series, Cambridge University Press, Cambridge, (1979).

[2] Steinhaus, H. Sur la convergence ordinaire et la convergence asymptotique. Colloquium Mathematicum. 2, 73-74 (1951).

[3] Fast, H. Sur la convergence statistique. Colloquium Mathematicum. 2, 241-244 (1951).

[4] Schoenberg, I.J. The integrability of certain functions and related summability methods. The American Mathematical Monthly. 66, 361-375 (1959).

[5] Salat, T. On statistically convergent sequences of real numbers. Mathematica Slovaca. 30, 139-150 (1980).

[6] Fridy, J. On statistical convergence. Analysis. 5, 301-313 (1985).

[7] Çolak, R. Statistical convergence of order α. In:Modern Methods in Analysis and Its Applications. Anamaya Publishers, New Delhi (2010).

[8] Çolak, R., Bektaş Ç.A. λ- Statistical convergence of order α. Acta Mathematica Scientia. 31(3), 953-959 (2011).

[9] Fridy, J., Orhan, C. Lacunary statistical convergence. Pacific Journal of Mathematics. 160(1), 43-51 (1993).

[10] Fridy, J., Orhan, C. Lacunary statistical summability. Journal of Mathematical Analysis and Applications. 173(2), 497-504 (1993).

[11] Connor, J. On strong matrix summability with respect to a modulus and statistical convergence. Canadian Mathematical Bulletin. 32(2), 194-198 (1989).

[12] Çolak, R. Lacunary strong convergence of difference sequences with respect to a modulus function. Filomat. 17, 9-14 (2003).

[13] Şengül, H., Et, M. On lacunary statistical convergence of order α. Acta Mathematica Scientia. 34(2), 473-482 (2014).

[14] Et, M., Şengül, H. Some Cesàro-Type Summability of order and Lacunary Statistical Convergence of order α. Filomat. 28, 1593-1602 (2014).

[15] Pehlivan, S., Fisher, B. Lacunary strong convergence with respect to a sequence of modulus functions. Commentationes Mathematicae Universitatis Carolinae. 36(1), 69-76 (1995).

[16] Nakano, H. Concave modulars. Journal of the Mathematical Society of Japan. 5, 29-49 (1953).

[17] Ruckle, W.H. FK-Spaces in which the sequence of coordinate vectors is bounded. Canadian Journal of Mathematics. 25, 973-978 (1973).

[18] Bhardwaj, V.K., Singh,N. On some sequence spaces defined by a modulus. Indian Journal of Pure and Applied Mathematics. 30, 809-817 (1999).

[19] Ghosh, D., Srivastava, P.D. On some vector valued sequence spaces defined using a modulus function. Indian Journal of Pure and Applied Mathematics. 30, 819-826 (1999).

[20] Maddox, I.J. Sequence spaces defined by a modulus. Mathematical Proceedings of the Cambridge Philosophical Society. 100, 161-166 (1986).

[21] Pehlivan, S., Fisher, B. Some sequence spaces defined by a modulus function. Mathematica Slovaca. 45(3), 275-280 (1995).

[22] Aizpuru, A., Listán-Garcia, M.C. Rambla-Barreno, F.: Density by moduli and statistical convergence. Quaestiones Mathematicae. 37, 525-530 (2014).

[23] Bayram, E., Bektaş, Ç.A. Lacunary Statistically Convergence via Modulus Function Sequences, Math. Sci. Appl-Notes, 12(4), 187-195 (2024).

[24] Kizmaz, H. On Certain Sequence Spaces Canad Math Bull. 24:2, 169-176 (1981).

[25] Et M., Çolak R., On some generalized difference sequence spaces, Soochow J. Math., 21(4), 377-386 (1995).

[26] Bhardwaj, V.K., Dhawan,S. f-Statistical convergence of order α and strong Cesàro summability of order with respect to a modulus. J. Ineq.and Appl. 332 (2015).

[27] Ibrahim I.S., Çolak, R. On strong lacunary summability of order with respect to modulus functions. Math. Comp. Sci. Series. 48(1), 127-136 (2021).

ROUGH QUOTIENT RINGS AND HOMOMORPHISMS OF ROUGH RINGS

M. Mustafa Beydağı[1], **A. Fatih Özcan**[1], **İlhan İçen**[1]

[1] Department of Mathematics, Inonu University, Malatya, Turkiye

mbeydagi23@gmail.com, abdullah.ozcan@inonu.edu.tr, ilhan.icen@inonu.edu.tr

Abstract

In this study, the concept of a ring, which is an algebraic structure, is combined with rough set theory. Along with the definitions and theorems of rough rings, rough subrings and rough ideals, rough quotient rings and homomorphisms of rough rings are introduced.

Keywords: Rough set theory; Rough rings; Rough ideals; Rough quotient rings; Homomorphisms of rough rings.

1.INTRODUCTION

Rough set theory, discovered by Pawlak in 1982, is a useful set model for understanding unclear information [1]. Rough set theory has been applied to most algebraic structures and successful results have been obtained [2-8]. In addition to mathematics, it is also used in fields such as medicine, data mining, artificial intelligence and machine learning [10-13]. In this section, the basic properties of the rough set model are discussed. Also, the adaptation of rough set theory to the concepts of group, ring and ideal is shown.

Definition 1.1 Let F is a universe (non-empty) set and θ is an equivalence relation on F. The set (F,θ) is said to be an approximation space. We denote the equivalence class of object $a \in F$ by $[a]_\theta$. Suppose (F,θ) is an approximation space and S is a subset of F. The sets $\underline{S} = \{\, a \in F : [a]_\theta \subseteq S\}$, $\overline{S} = \{\, a \in F : [a]_\theta \cap S \neq \emptyset\}$, $Bnd(S) = \overline{S} - \underline{S}$ are called upper approximation, lower approximation, and boundary region of S, respectively. If $Bnd(S) \neq \emptyset$, then S is rough set [1].

Definition 1.2 Let (F,θ) be an approximation space and $*$ be a binary operation on F. $A \subset F$ is called a rough group if the following properties are satisfied:

$i)$ $\forall \mu, \vartheta \in A,\ \mu * \vartheta \in \overline{A}$

$ii)$ $\forall \mu, \vartheta, \varepsilon \in A,\ (\mu * \vartheta) * \varepsilon = \mu * (\vartheta * \varepsilon)$ or associative property holds in $\overline{A}$.

$iii)$ $\forall \mu \in A$, such that $\exists e \in \overline{A},\ \mu * e = e * \mu = \mu$, where e is called the rough unit element of rough group A.

$iv)$ $\forall\mu \in A, \exists\rho \in A \ni \mu * \rho = \rho * \mu = e$, where ρ is said the rough inverse element of μ in A, we denote it by μ^{-1} [7,8].

Theorem 1.1 If B is a rough subgroup of rough group A, the following properties are satisfied:

$i)$ $\forall\theta, \vartheta \in B,\ \theta * \vartheta\ \in \overline{B}$.

$ii)$ $\forall\theta \in B,\ \theta^{-1} \in B$ [7,8].

Definition 1.3 Let $(G_1,*)$ and $(G_2, \blacksquare)$ be two rough groups. If there exists a surjective function $\varphi : \overline{\mathrm{G}_1} \to \overline{\mathrm{G}_2}$ such that $\varphi(x * y) = \varphi(x)\blacksquare\varphi(y)$ for $\forall\ x, y \in \overline{\mathrm{G}_1}$, then φ is called a rough group homomorphism and the rough groups G_1 and G_2 are called rough homomorphic groups.

Definition 1.4 Let $\mathcal{R}$ is a rough set. Define the operation in $\mathcal{R}$ as "$\oplus$" and "$\otimes$" are addition and multiplication in $\mathcal{R}$, respectively. Then, $(\mathcal{R}, \oplus,\otimes)$ triple is said to be a rough ring if all condition below are satisfied:

$i)$ $(\mathcal{R}, \oplus)$ is a rough commutative group,

$ii)$ $(\mathcal{R}, \otimes)$ is a rough semigroup or $\overline{\mathcal{R}}$ satisfied associative property,

$iii)$ For every $\theta, \vartheta, \mu \in \mathcal{R}$, then $\theta \otimes (\ \vartheta \oplus \mu) = \theta \otimes \vartheta \oplus \theta \otimes \mu$ and $(\theta \oplus \vartheta) \otimes \mu = \theta \otimes \mu \oplus \vartheta \otimes \mu$ holds in $\overline{\mathcal{R}}$ [9].

Definition 1.5 Let $\mathcal{R}$ be rough ring and $\mathrm{P} \subseteq \mathcal{R}$. P is said to be a rough subring of $\mathcal{R}$ if P is a rough ring with the same operation as $\mathcal{R}$ [9].

Theorem 1.2 Let $B \neq \emptyset$ is a rough subset of a rough ring $\mathcal{R}$. B is called a rough subring of $\mathcal{R}$ if and only if every $b_1, b_2 \in B$ the following condition is satisfied:

$i)$ For $\forall b_1, b_2 \in B, b_1 \oplus (-b_2) \in \overline{B}$,

$ii)$ For $\forall b_1, b_2 \in B, b_1 \otimes b_2 \in \overline{B}$ [9].

Definition 1.6 Let $(\mathcal{R},\oplus,\otimes)$ be a rough ring and $\mathfrak{D} \neq \emptyset$ is rough subset of $\mathcal{R}$. $\mathfrak{D}$ is called rough ideal of $\mathcal{R}$ if:

$i)$ For $\forall d_1, d_2 \in \mathfrak{D}, d_1 \oplus (-d_2) \in \overline{\mathfrak{D}}$,

$ii)$ For $\forall d \in \mathfrak{D}$ and $\forall r \in \mathcal{R}$, $d \otimes r, r \otimes d \in \overline{\mathfrak{D}}$ [9].

Definition 1.7 [9] Let $(\mathcal{R},\oplus,\otimes)$ be a rough ring and $\mathfrak{D} \subseteq \mathcal{R}$. A subset $\mathfrak{D}$ is said to be left-rough ideal in $\mathcal{R}$ if

$i)$ For $\forall d_1, d_2 \in \mathfrak{D}, d_1 \oplus (-d_2) \in \overline{\mathfrak{D}}$

$ii)$ For $\forall d \in \mathfrak{D}$ and $\forall r \in \mathcal{R}$, $r \otimes d \in \overline{\mathfrak{D}}$.

A subset $\mathfrak{D}$ is said to be right-rough ideal in $\mathcal{R}$ if

$i)$ For $\forall d_1, d_2 \in \mathfrak{D}$, $d_1 \oplus (-d_2) \in \overline{\mathfrak{D}}$

$ii)$ For $\forall d \in \mathfrak{D}$ and $\forall r \in \mathcal{R}$, $d \otimes r \in \overline{\mathfrak{D}}$.

Example 1.1 Let $F = \mathbb{Z}_{10}$. For every $x_1, x_2 \in F$, define an equivalence relation $\theta = x_1 - x_2 = 2k, k \in \mathbb{R}$. Then, the equivalence class of F is

$$F/\theta = \left\{ \{\overline{0}, \overline{2}, \overline{4}, \overline{6}, \overline{8}\}, \{\overline{1}, \overline{3}, \overline{5}, \overline{7}, \overline{9}\} \right\}$$

Let $\mathcal{R} = \left\{\overline{0}, \overline{1}, \overline{2}, \overline{3}, \overline{4}\right\} = \mathbb{Z}_5$. Then we obtain lower approximation and upper approximation of $\mathcal{R}$ are $\underline{\mathcal{R}} = \emptyset$ and $\overline{\mathcal{R}} = \{\overline{0}, \overline{1}, \overline{2}, \overline{3}, \overline{4}, \overline{5}, \overline{6}, \overline{7}, \overline{8}, \overline{9}\} = \mathbb{Z}_{10}$, respectively. Because $Bnd(\mathcal{R}) \neq \emptyset$, we can say that $\mathcal{R}$ is a rough set. Morever, it is clear that $\mathcal{R}$ is a rough ring.

Suppose that $\mathfrak{D} = \left\{\overline{0}, \overline{1}, \overline{4}\right\} \subseteq \mathcal{R}$. Thus, $\underline{\mathfrak{D}} = \emptyset$ and $\overline{\mathfrak{D}} = \left\{\overline{0}, \overline{1}, \overline{2}, \overline{3}, \overline{4}, \overline{5}, \overline{6}, \overline{7}, \overline{8}, \overline{9}\right\} = \mathbb{Z}_{10}$. Since $\overline{\mathfrak{D}} - \underline{\mathfrak{D}} \neq \emptyset$, $\mathfrak{D}$ is rough set. Now let's show that $\mathfrak{D}$ is a rough ideal.

$i)$ For $\forall d_1, d_2 \in \mathfrak{D}$, $d_1 \oplus (-d_2) \in \overline{\mathfrak{D}}$

$ii)$ For $\forall d \in \mathfrak{D}$ and $\forall r \in \mathcal{R}$, $d \otimes r, r \otimes d \in \overline{\mathfrak{D}}$.

Since conditions $i)$ and $ii)$ above are hold, it is clear that $\mathfrak{D}$ is the rough ideal of $\mathcal{R}$.

2.ROUGH QUOTIENT RINGS

In this section, we study rough quotient rings using rough rings and rough ideals.

Theorem 2.1 If $\mathcal{R}$ is a rough ring and $\mathfrak{D}$ is a rough ideal of $\mathcal{R}$ and $\theta, \vartheta \in \mathcal{R}$, the relation $\backsim$ defined as

$$\theta \backsim \vartheta \Leftrightarrow \theta \oplus (-\vartheta) \in \overline{\mathfrak{D}}$$

is an equivalence relation with respect to binary operations on $\mathcal{R}$. The equivalence classes obtained by this relation are right and left cosets. The set of equivalence classes is denoted by

$$\mathcal{R}/\mathfrak{D} = \left\{ \theta \oplus \overline{\mathfrak{D}} : \theta \in \mathcal{R} \right\}$$

Theorem 2.2 Let $\mathcal{R}$ be a rough ring and $\mathfrak{D}$ be a rough ideal of $\mathcal{R}$. For $\forall\, \theta \oplus \overline{\mathfrak{D}}, \vartheta \oplus \overline{\mathfrak{D}} \in \mathcal{R}/\mathfrak{D}$

$$\left(\theta \oplus \overline{\mathfrak{D}}\right) \oplus \left(\vartheta \oplus \overline{\mathfrak{D}}\right) = (\theta \oplus \vartheta) \oplus \overline{\mathfrak{D}}$$

$$\left(\theta \oplus \overline{\mathfrak{D}}\right) \otimes \left(\vartheta \oplus \overline{\mathfrak{D}}\right) = (\theta \otimes \vartheta) \oplus \overline{\mathfrak{D}}$$

the structure $(\mathcal{R}/\mathfrak{D}, \oplus, \otimes)$ defined by addition and multiplication operations is a rough ring.

Proof. 1) Let us show that the structure $(\mathcal{R}/\mathfrak{D}, \oplus)$ is a commutative rough group**.** For $\forall\, \theta \oplus \overline{\mathfrak{D}}, \vartheta \oplus \overline{\mathfrak{D}}, \mu \oplus \overline{\mathfrak{D}} \in \mathcal{R}/\mathfrak{D}$, it is defined by $\overline{\mathcal{R}/\mathfrak{D}} = \left\{ \theta \oplus \overline{\mathfrak{D}} : \theta \in \overline{\mathcal{R}} \right\}$.

$i)$ Since $\mathcal{R}$ is a rough ring, $\left(\theta \oplus \overline{\mathfrak{D}}\right) \oplus \left(\vartheta \oplus \overline{\mathfrak{D}}\right) = (\theta \oplus \vartheta) \oplus \overline{\mathfrak{D}} \in \overline{\mathcal{R}/\mathfrak{D}}$.

ii) The associative property is provided for $\overline{\mathcal{R}/\mathfrak{D}}$.
iii) There exists $\left(0 \oplus \overline{\mathfrak{D}}\right) \in \overline{\mathcal{R}/\mathfrak{D}}$ such that $\left(\theta \oplus \overline{\mathfrak{D}}\right) \oplus \left(0 \oplus \overline{\mathfrak{D}}\right) = (\theta \oplus 0) \oplus \overline{\mathfrak{D}} = \left(\theta \oplus \overline{\mathfrak{D}}\right)$.
iv) There exists $\left((-\theta) \oplus \overline{\mathfrak{D}}\right) \in \mathcal{R}/\mathfrak{D}$ such that $\left(\theta \oplus \overline{\mathfrak{D}}\right) \oplus \left((-\theta) \oplus \overline{\mathfrak{D}}\right) = \left(0 \oplus \overline{\mathfrak{D}}\right)$.
v) $\left(\theta \oplus \overline{\mathfrak{D}}\right) \oplus \left(\vartheta \oplus \overline{\mathfrak{D}}\right) = (\theta \oplus \vartheta) \oplus \overline{\mathfrak{D}}$

$$= (\vartheta \oplus \theta) \oplus \overline{\mathfrak{D}} \in \overline{\mathcal{R}/\mathfrak{D}}.$$

Therefore, the structure $(\mathcal{R}/\mathfrak{D}, \oplus)$ is a commutative rough group.

2) Let us show that the associative property of the structure $(\mathcal{R}/\mathfrak{D}, \otimes)$ is also satisfied in $\overline{\mathcal{R}/\mathfrak{D}}$.

Since $\mathcal{R}$ is a rough ring,

$$\begin{aligned}\left(\theta \oplus \overline{\mathfrak{D}}\right) \otimes \left[\left(\vartheta \oplus \overline{\mathfrak{D}}\right) \otimes \left(\mu \oplus \overline{\mathfrak{D}}\right)\right] &= \left(\theta \oplus \overline{\mathfrak{D}}\right) \otimes (\vartheta \otimes \mu) \oplus \overline{\mathfrak{D}} \\ &= (\theta \otimes \vartheta \otimes \mu) \oplus \overline{\mathfrak{D}} \\ &= [(\theta \otimes \vartheta) \otimes \mu] \oplus \overline{\mathfrak{D}} = (\theta \otimes \vartheta) \oplus \overline{\mathfrak{D}} \otimes \left(\mu \oplus \overline{\mathfrak{D}}\right) \\ &= \left[\left(\theta \oplus \overline{\mathfrak{D}}\right) \otimes \left(\vartheta \oplus \overline{\mathfrak{D}}\right)\right] \otimes \left(\mu \oplus \overline{\mathfrak{D}}\right) \in \overline{\mathcal{R}/\mathfrak{D}}.\end{aligned}$$

3) Let us show that the left and right distributive properties of the operation $\otimes$ on the operation $\oplus$ are also satisfied in $\overline{\mathcal{R}/\mathfrak{D}}$.

Since $\mathcal{R}$ is a rough ring,

$$\begin{aligned}\left(\theta \oplus \overline{\mathfrak{D}}\right) \otimes \left[\left(\vartheta \oplus \overline{\mathfrak{D}}\right) \oplus \left(\mu \oplus \overline{\mathfrak{D}}\right)\right] &= \left[\left(\theta \oplus \overline{\mathfrak{D}}\right) \otimes \left(\vartheta \oplus \overline{\mathfrak{D}}\right)\right] \oplus \left[\left(\theta \oplus \overline{\mathfrak{D}}\right) \otimes \left(\mu \oplus \overline{\mathfrak{D}}\right)\right] \\ &= \left[(\theta \otimes \vartheta) \oplus \overline{\mathfrak{D}}\right] \oplus \left[(\theta \otimes \mu) \oplus \overline{\mathfrak{D}}\right] \in \overline{\mathcal{R}/\mathfrak{D}}.\end{aligned}$$

Thus, multiplication is distributive from the left over addition. Similarly, multiplication is distributive from the right over addition.

Therefore, the structure $(\mathcal{R}/\mathfrak{D}, \oplus, \otimes)$ is a rough ring.

Remark 2.1 If the rough ring $\mathcal{R}$ is commutative and has identity, then the rough ring $\mathcal{R}/\mathfrak{D}$ is also commutative and a rough ring with identity for $\mathcal{R} \neq \mathfrak{D}$.

Proof For $\forall\, \theta \oplus \overline{\mathfrak{D}}, \vartheta \oplus \overline{\mathfrak{D}} \in \mathcal{R}/\mathfrak{D}$, since $\mathcal{R}$ is a rough ring

$$\begin{aligned}\left(\theta \oplus \overline{\mathfrak{D}}\right) \otimes \left(\vartheta \oplus \overline{\mathfrak{D}}\right) &= (\theta \otimes \vartheta) \oplus \overline{\mathfrak{D}} \\ &= (\vartheta \otimes \theta) \oplus \overline{\mathfrak{D}} \in \overline{\mathcal{R}/\mathfrak{D}}.\end{aligned}$$

Then, the rough ring $(\mathcal{R}/\mathfrak{D}, \oplus, \otimes)$ is commutative.

Let $\mathcal{R} \neq \mathfrak{D}$ and let the identity of the rough ring $\mathcal{R}$ be 1 with respect to multiplication. For $\forall\, \theta \oplus \overline{\mathfrak{D}} \in \mathcal{R}/\mathfrak{D}$, since $\left(\theta \oplus \overline{\mathfrak{D}}\right) \otimes \left(1 \oplus \overline{\mathfrak{D}}\right) = \left(1 \oplus \overline{\mathfrak{D}}\right) \otimes \left(\theta \oplus \overline{\mathfrak{D}}\right) = (\theta \otimes 1) \oplus \overline{\mathfrak{D}} = \left(\theta \oplus \overline{\mathfrak{D}}\right)$ is a identity element. Thus, the rough ring $(\mathcal{R}/\mathfrak{D},\oplus,\otimes)$ has identity.

Definition 2.1 Let $\mathcal{R}$ be a rough ring and $\mathfrak{D}$ be a rough ideal of $\mathcal{R}$. The rough ring $(\mathcal{R}/\mathfrak{D},\oplus,\otimes)$ is called a rough quotient ring.

Example 2.1 From Example 1.1, for $F = \mathbb{Z}_{10} = \left\{\overline{0},\overline{1},\overline{2},\overline{3},\overline{4},\overline{5},\overline{6},\overline{7},\overline{8},\overline{9}\right\}$ universal set, $F/\theta = \left\{\left\{\overline{0},\overline{2},\overline{4},\overline{6},\overline{8}\right\},\left\{\overline{1},\overline{3},\overline{5},\overline{7},\overline{9}\right\}\right\}$ equivalence classes, $\mathcal{R} = \left\{\overline{0},\overline{1},\overline{2},\overline{3},\overline{4}\right\} = \mathbb{Z}_5$ rough ring, $\mathfrak{D} = \left\{\overline{0},\overline{1},\overline{4}\right\} \subseteq \mathcal{R}$ rough ideal, $\mathcal{R}/\mathfrak{D} = \left\{0 \oplus \overline{\mathfrak{D}}\right\}$ and $\overline{\mathcal{R}/\mathfrak{D}} = \left\{0 \oplus \overline{\mathfrak{D}}\right\}$. Thus,

1) $(\mathcal{R}/\mathfrak{D},\oplus)$ is a commutative rough group.
2) The structure $(\mathcal{R}/\mathfrak{D},\otimes)$ satisfies the associative property in $\overline{\mathcal{R}/\mathfrak{D}}$.
3) The left and right distributive properties of the operation $\otimes$ on the operation $\oplus$ are also satisfied in $\overline{\mathcal{R}/\mathfrak{D}}$.

3.HOMOMORPHISMS OF ROUGH RINGS

In this section, homomorphisms, properties and theorems of rough rings are given using homomorphisms of rough groups.

Definition 3.1 For rough rings $(\mathcal{R}_1,\oplus,\otimes)$ and $(\mathcal{R}_2,\oplus,\otimes)$, the surjective map $\varphi : \overline{\mathcal{R}_1} \to \overline{\mathcal{R}_2}$ is called a rough ring homomorphism on φ if the following conditions are satisfied.

i) For $\forall\, \theta, \vartheta \in \overline{\mathcal{R}_1}$, $\varphi(\theta \oplus \vartheta) = \varphi(\theta) \oplus \varphi(\vartheta)$.

ii) For $\forall\, \theta, \vartheta \in \overline{\mathcal{R}_1}$, $\varphi(\theta \otimes \vartheta) = \varphi(\theta) \otimes \varphi(\vartheta)$.

Since $\varphi : \overline{\mathcal{R}_1} \to \overline{\mathcal{R}_2}$ is a rough ring homomorphism surjective map, $\mathcal{R}_2$ is called a homomorphic image of $\mathcal{R}_1$.

Definition 3.2 If the rough ring homomorphism $\varphi : \overline{\mathcal{R}_1} \to \overline{\mathcal{R}_2}$ is a injective map, then φ is called a rough ring isomorphism. Also, the rough rings $\mathcal{R}_1$ and $\mathcal{R}_2$ are said to be isomorphic and are denoted by $\mathcal{R}_1 \cong \mathcal{R}_2$.

Theorem 3.1 If $\varphi : \overline{\mathcal{R}_1} \to \overline{\mathcal{R}_2}$ is rough ring homomorphism, then

i) $\varphi\left(0_{R_1}\right) = 0_{R_2}$

ii) For $\forall\, \theta \in \overline{\mathcal{R}_1}$, $\varphi(-\theta) = -\varphi(\theta)$.

Proof i) $\varphi\left(0_{R_1}\right) = \varphi\left(0_{R_1}\right) \oplus 0_{R_2}$

$$= \varphi\left(0_{R_1}\right) \oplus \varphi\left(0_{R_1}\right) \oplus \left(-\varphi\left(0_{R_1}\right)\right)$$

$$= \varphi\left(0_{R_1} \oplus 0_{R_1}\right) \oplus \left(-\varphi\left(0_{R_1}\right)\right)$$

$$= \varphi(0_{R_1}) \oplus \left(-\varphi(0_{R_1})\right) = 0_{R_2}.$$

ii) For $\forall\ \theta \in \overline{\mathcal{R}_1}$, $\varphi(\theta) \oplus \varphi(\text{-}\theta) = \varphi(\theta \oplus (\text{-}\theta))$

$$= \varphi(0_{R_1}) = 0_{R_2}.$$

Since $(\mathcal{R}_2,\oplus)$ is a rough group and the inverse of an element in a rough group is unique, we obtain $\varphi(\text{-}\theta) = -\,\varphi(\theta)$.

Theorem 3.2 Let $\varphi : \overline{\mathcal{R}_1} \to \overline{\mathcal{R}_2}$ be a rough ring homomorphism.

i) If $\mathcal{R}_1$ is a commutative rough ring, then $\mathcal{R}_2$ is also a commutative rough ring.

ii) If $\mathcal{R}_1$ is a unitary rough ring with unit 1_{R_1}, then $\mathcal{R}_2$ is a unitary rough ring with unit $1_{R_2}$and $\varphi(1_{R_1}) = 1_{R_2}$.

iii) If $\mathcal{R}_1$ is a rough ring with unity and $\theta \in \overline{\mathcal{R}_1}$ has a multiplicative inverse in $\mathcal{R}_1$, then $\varphi(\theta)$ also has a multiplicative inverse in $\mathcal{R}_2$ and $\varphi(\theta^{-1}) = [\varphi(\theta)]^{-1}$.

Proof i) Let $\mathcal{R}_1$ be a commutative rough ring. Since $\varphi : \overline{\mathcal{R}_1} \to \overline{\mathcal{R}_2}$ is a rough ring homomorphism,

For $\forall\alpha \in \overline{\mathcal{R}_2}$, there exists $\theta \in \overline{\mathcal{R}_1}$ such that $\varphi(\theta) = \alpha$.

For $\forall\beta \in \overline{\mathcal{R}_2}$, there exists $\vartheta \in \overline{\mathcal{R}_1}$ such that $\varphi(\vartheta) = \beta$.

$\alpha \otimes\ \beta = \varphi(\theta) \otimes \varphi(\vartheta) = \varphi\ (\theta \otimes \vartheta) = \varphi\ (\vartheta \otimes \theta) = \varphi(\vartheta) \otimes \varphi(\theta) =\ \beta \otimes \alpha$ is obtained.

Thus, the rough ring $\mathcal{R}_2$ is commutative.

ii) Let $\mathcal{R}_1$ be a unitary rough ring with unit 1_{R_1}. Since φ is a rough ring homomorphism, for $\forall\alpha \in \overline{\mathcal{R}_2}$, there exists $\theta \in \overline{\mathcal{R}_1}$ such that $\varphi(\theta) = \alpha$.

$\varphi(1_{R_1}) \otimes\ \alpha = \varphi(1_{R_1}) \otimes \varphi(\theta) = \varphi(1_{R_1} \otimes \theta) = \varphi(\theta) = \alpha$ is obtained.

Likewise, $\alpha \otimes\ \varphi(1_{R_1}) = \varphi(\theta) \otimes\ \varphi(1_{R_1}) =\ \varphi(\theta \otimes 1_{R_1}) =\ \varphi(\theta) = \alpha$.

Since $\varphi(1_{R_1}) \otimes\ \alpha =\ \alpha \otimes\ \varphi(1_{R_1})$ for $\forall\alpha \in \overline{\mathcal{R}_2}$, $\varphi(1_{R_1})$ is the unit for the rough ring $\mathcal{R}_2$, and since there is only one unit element in the rough ring, $\varphi(1_{R_1}) = 1_{R_2}$is obtained for the unit element 1_{R_2} of $\mathcal{R}_2$.

iii) Let $\mathcal{R}_1$ be a rough ring with unity and let $\theta^{-1} \in \overline{\mathcal{R}_1}$ be for $\theta \in \overline{\mathcal{R}_1}$.

$\varphi(1_{R_1}) = \varphi(\theta \otimes \theta^{-1}) = \varphi(\theta) \otimes \varphi(\theta^{-1}) = 1_{R_2}$ and

$\varphi(1_{R_1}) = \varphi(\theta^{-1} \otimes \theta) = \varphi(\theta^{-1}) \otimes \varphi(\theta) = 1_{R_2}$ is obtained.

Hence, since $\varphi(\theta) \otimes \varphi(\theta^{-1}) = \varphi(\theta^{-1}) \otimes \varphi(\theta) = 1_{R_2}$, the inverse of $\varphi(\theta)$ becomes $\varphi(\theta^{-1})$.

Also, since the inverse of $\varphi(\theta)$ is given by $[\varphi(\theta)]^{-1}$, we have $\varphi(\theta^{-1}) = [\varphi(\theta)]^{-1}$.

Theorem 3.3 If $\mathcal{R}$ is a rough ring and $0 \neq \theta \in \overline{\mathcal{R}}$; the map defined as $\varphi_\theta : \overline{\mathcal{R}} \to \overline{\mathcal{R}}, \vartheta \mapsto \varphi_\theta(\vartheta) = \theta \otimes \vartheta$ is injective if and only if the element θ is not a zero divisor of the rough ring $\mathcal{R}$.

Proof Let $\mathcal{R}$ be a rough ring and let $0 \neq \theta \in \overline{\mathcal{R}}$.

($\Longrightarrow$:)Let the map φ_θ be injective. For $\forall\, \vartheta, \mu \in \overline{\mathcal{R}}$, if $\varphi_\theta(\vartheta) = \varphi_\theta(\mu)$, then $\vartheta = \mu$.

$$\begin{aligned} \varphi_\theta(\vartheta) = \varphi_\theta(\mu) &\Longrightarrow \theta \otimes \vartheta = \theta \otimes \mu \\ &\Longrightarrow (\theta \otimes \vartheta) \oplus -(\theta \otimes \mu) = (\theta \otimes \mu) \oplus -(\theta \otimes \mu) \\ &\Longrightarrow \theta(\vartheta \oplus -\mu) = 0 \text{ is written.} \end{aligned}$$

Since $\vartheta = \mu$, we obtain $\vartheta \oplus -\mu = 0$. Thus, it can be seen that the element θ is not a zero divisor of the rough ring $\mathcal{R}$.

($\Longleftarrow$:) Suppose that the element θ is not a zero divisor of the rough ring $\mathcal{R}$.

$$\begin{aligned} \varphi_\theta(\vartheta) = \varphi_\theta(\mu) &\Longrightarrow \theta \otimes \vartheta = \theta \otimes \mu \\ &\Longrightarrow (\theta \otimes \vartheta) \oplus -(\theta \otimes \mu) = (\theta \otimes \mu) \oplus -(\theta \otimes \mu) \\ &\Longrightarrow \theta(\vartheta \oplus -\mu) = 0 \text{ is written.} \\ &\Longrightarrow \vartheta \oplus -\mu = 0 \\ &\Longrightarrow \vartheta = \mu \text{ is obtained.} \end{aligned}$$

Thus, it can be seen that φ_θ is injective map.

Definition 3.3 Let $\varphi : \overline{\mathcal{R}_1} \to \overline{\mathcal{R}_2}$ be a rough ring homomorphism. The set

$$Ker\varphi = \{\theta \in \overline{\mathcal{R}_1} : \varphi(\theta) = 0_{R_2}\}$$

is called the kernel of φ and the set

$$Im\varphi = \{\varphi(\theta) : \theta \in \overline{\mathcal{R}_1}\}$$

is called the image of φ.

Theorem 3.4 If $\varphi : \overline{\mathcal{R}_1} \to \overline{\mathcal{R}_2}$ is a rough ring homomorphism, then $Ker\varphi$ is a rough ideal of $\mathcal{R}_1$.

Proof If $\varphi : \overline{\mathcal{R}_1} \to \overline{\mathcal{R}_2}$ is a rough ring homomorphism, then it is clear that $\varphi\left(0_{R_1}\right) = 0_{R_2}$. From Definition 3.3 we obtain $0_{R_1} \in Ker\varphi$ and $Ker\varphi \neq \emptyset$. Let us now show that $Ker\varphi$ is a rough ideal of $\mathcal{R}_1$.

i) If $\forall d_1, d_2 \in Ker\varphi$, then $\varphi(d_1) = 0_{R_2}$ and $\varphi(d_2) = 0_{R_2}$.

$\varphi(d_1 \oplus -d_2) = \varphi(d_1) \oplus -\varphi(d_2)$

$= 0_{R_2} \oplus -0_{R_2} = 0_{R_2}$ is obtained. Thus, it is seen that $(d_1 \oplus -d_2) \in \overline{Ker\varphi}$.

ii) If $\forall d \in Ker\varphi$, then $\varphi(d) = 0_{R_2}$. For $\forall r \in \mathcal{R}$, $\varphi(rd) = \varphi(r) \otimes \varphi(d) = \varphi(r) \otimes 0_{R_2} = 0_{R_2}$ is obtained. Thus, it is seen that $rd \in \overline{Ker\varphi}$.

Likewise, $\varphi(dr) = \varphi(d) \otimes \varphi(r) = 0_{R_2} \otimes \varphi(r) = 0_{R_2}$ is obtained. Thus, it is seen that $dr \in \overline{Ker\varphi}$.

Hence, $Ker\varphi$ is a rough ideal of $\mathcal{R}_1$.

Theorem 3.5 Let $\mathcal{R}$ be a rough ring and $\mathfrak{D}$ be a rough ideal of $\mathcal{R}$. In this case, the map defined by

$$\varphi : \overline{\mathcal{R}} \to \overline{\mathcal{R}/\mathfrak{D}}, r \mapsto \varphi(r) = r \oplus \overline{\mathfrak{D}}$$

is a rough ring homomorphism with kernel $\overline{\mathfrak{D}}$.

Proof For $r \oplus \overline{\mathfrak{D}} \in \overline{\mathcal{R}/\mathfrak{D}}$, there exists $r \in \overline{\mathcal{R}}$ such that $\varphi(r) = r \oplus \overline{\mathfrak{D}}$. Thus, φ is surjective.

For $\forall\, \vartheta, \mu \in \overline{\mathcal{R}}$, $\varphi(\theta \oplus \vartheta) = (\theta \oplus \vartheta) \oplus \overline{\mathfrak{D}} = \left(\theta \oplus \overline{\mathfrak{D}}\right) \oplus \left(\vartheta \oplus \overline{\mathfrak{D}}\right) = \varphi(\theta) \oplus \varphi(\vartheta)$ and

$\varphi(\theta \otimes \vartheta) = (\theta \otimes \vartheta) \oplus \overline{\mathfrak{D}} = \left(\theta \oplus \overline{\mathfrak{D}}\right) \otimes \left(\vartheta \oplus \overline{\mathfrak{D}}\right) = \varphi(\theta) \otimes \varphi(\vartheta)$ is obtained.

Thus, φ is a rough ring homomorphism. It seen that,

$$\begin{aligned} Ker\varphi &= \left\{r \in \overline{\mathcal{R}} :\ \varphi(r) = 0 \oplus \overline{\mathfrak{D}}\right\} \\ &= \left\{r \in \overline{\mathcal{R}} :\ r \oplus \overline{\mathfrak{D}} = \overline{\mathfrak{D}}\right\} \\ &= \left\{r \in \overline{\mathcal{R}} :\ r \in \overline{\mathfrak{D}}\right\} = \overline{\mathfrak{D}}. \end{aligned}$$

4.CONCLUSIONS

In this study, rough quotient rings and homomorphisms of rough rings are studied using the concepts of rough rings and rough ideals. It is thought that by using this information, theorems of isomorphisms of rough rings and transformations between rough fields and rough fields can be defined.

REFERENCES

1. Z. Pawlak, “Rough Sets,” Int. J. Comput. Inf. Sci., vol. 11, no. 5, pp. 341–356, 1982, doi: 10.1007/978-1-4613-1461-5_1.
2. T. Iwinski, Algebraic approach to rough sets, Bull. Polish Acad. Sci. Math. 35 (1987) 673-683.
3. Z. Bonikowaski, Algebraic structures of rough sets, in: W.P. Ziarko (Ed.), Rough Sets, Fuzzy Sets and Knowledge Discovery, Springer-Verlag, Berlin, 1995, pp. 242-247.
4. J. Pomykala, J. A. Pomykala, The stone algebra of rough sets, Bull. Polish Acad. Sci. Math. 36 (1998) 495-508.
5. N. Kuroki, P. P. Wang, The lower and upper approximations in a fuzzy group, Information Sciences 90 (1996) 203-220.
6. W. Cheng, Z. Mo, J. Wang, Notes on “the lower and upper approximations in a fuzzy group" and “rough ideals in semigroups", Inform. Sci. 177 (2007) 5134-5140.
7. D. Miao, S. Han, D. Li, and L. Sun, Rough Group, Rough Subgroup and Their Properties, D. Ślkezak et al. (Eds.): RSFDGrC 2005, LNAI 3641, pp. 104–113, 2005.© Springer-Verlag Berlin Heidelberg 2005.
8. N. Bağırmaz and A.F. Özcan, “Rough Semigroups on Approximation Spaces”, Int. J. of Algebra Vol: 9 no.7 (2015), 339-350.
9. Agusfrianto, F.A., Fitriani, Mahatma, Y., Rough Rings, Rough Subrings and Rough Ideals, Journal of Fundamental Mathematıcs and Applıcatıons (JFMA) Vol. 5 No. 2 (Nov 2022), https://doi.org/10.14710/jfma.v5i2.15194.
10. Hong TP, Tseng LH, Wang SL. Learning rules from incomplete training examples by rough sets. Expert Systems with Applications Volume 22, Issue 4, May 2002, Pages 285-293. https://doi.org/10.1016/S0957-4174(02)00016-7
11. Lingras P, Yao Y. Data Mining Using Extensions of the Rough Set Model. J. Am. Soc. Inf. Sci. 49(5): 415-422 (1998). https://doi.org/10.1002/(SICI)1097-4571(19980415)49:5<415::AID-ASI4>3.0.CO;2-Z
12. Pattaraintakorn P, Cercone N. Integrating rough set theory and medical applications. Applied Mathematics Letters Volume 21, Issue 4, April 2008, Pages 400-403. https://doi.org/10.1016/j.aml.2007.05.010
13. Zhang H, Li D. Applications of computer vision techniques to cotton foreign matter inspection: A review. Computers and Electronics in Agriculture Volume 109, November 2014, Pages 59-70. https://doi.org/10.1016/j.compag.2014.09.004

This study is supported by Inonu University Scientific Research Project unit within the scope of project number 3971.

THE SOFT FIBRE OF GROUPOIDS

Semih GEÇEN[1], **İlhan İÇEN**[2], **A. Fatih ÖZCAN**[3]

[1]Department of Mathematics, University of Inonu, Malatya, Türkiye, semihgecen44@gmail.com

[2]Department of Mathematics, University of Inonu, Malatya, Türkiye, ilhan.icen@inonu.edu.tr

[3]Department of Mathematics, University of Inonu, Malatya,Türkiye, abdullah.ozcan@inonu.edu.tr

Abstract

Soft set theory has brought a new perspective to contemporary mathematics. In this way, new analyzes have been developed regarding the complex structure of contemporary problems that are incomplete and uncertain. The concept of covering space corresponds to the concept of groupoid, which is an algebraic structure, and due to this feature, it has found a wide field of study in topology In this study, the concept of soft set and the concept of fibre, which finds a place in covering spaces, are discussed together and various concepts such as soft quotient map, soft fibre, and soft fibre groupoid, each of which are original concepts, are introduced.

Keywords: Soft set, Soft groupoid, Soft quotient map, Concept of fibre, Concept of soft fibre.

1.INTRODUCTION

Complex and uncertain problems in modern life have entered the fields of study of both thinkers and scientists dealing with mathematics and logic. Classical methods of mathematics have been inadequate to solve some uncertainty problems of the modern age. In order to overcome this situation, various set theories, starting with G. Cantor, have added a new perspective to mathematics, produced themselves in a new language and offered new and practical solutions to problems related to uncertainty situations.

D. A. Molodtsov put forward the "Soft set" theory in 1999, which gave a new perspective to the concepts of completeness and precision in mathematics [1]. This theory proposes more specific and easier to classify solutions by parameterizing some incomplete and imprecise concepts encountered in practical life. After soft set theory was introduced, it was studied by many mathematicians from topological, categorical and algebraic perspectives [2-16].

The concept of covering space is remarkable in many respects. First of all, this concept allows obtaining the $\tilde{X}$ space, which has a simpler structure than a given X space. More importantly, this concept corresponds to the concept of groupoid, which is an algebraic structure, and due to this feature, it has found a wide field of study in topology. [17-22].

In this study, the concept of soft set and the concept of fibre, which finds a place in covering spaces, are discussed together and various concepts such as soft quotient map, soft fibre, and soft fibre groupoid, each of which are original concepts, are introduced.

2. SOFT SETS

Soft set theory defined by D.A. Molodtsov has found a wide place in contemporary mathematics. After the introduction of soft set theory, which gave a new perspective to the concepts of completeness and precision in mathematics, it was studied by many mathematicians from topological, categorical and algebraic perspectives. [2-16].

Let the set of all subsets of X be $P(X)$ and $A \subset E$, where X is a universal set and E is the set of parameters. Thus, the definition of a soft set is given as follows.

Definition 2.1. The pair (F, A) given with any $F : A \longrightarrow P(X)$ transformation is called a soft set on X [1]. For the above definition, it can be said that a soft set on X is a parameterized family of subsets of the universal set X. For $\theta \in A$, the $F(\theta)$ family can be defined as a set of α approximation elements of the soft set (F, A) [1]. Here, for convenience, a soft set (F, A) on X will sometimes be denoted by (X, F, A).

Example 2.1. Let the universal set X be the set of shoes. Also, let the set of E parameters be defined as $E = \{$summer, seasonal, winter, beautiful, comfortable, bright, colorful, expensive, cheap$\}$. In this case, a soft set to be defined; will indicate shoes such as summerly shoes, seasonal shoes, winterly shoes, beautiful shoes, … etc.
Suppose there are six shoes in the universal set $X = \{h_1, h_2, h_3, h_4, h_5, h_6\}$.

For the parameter set $A = \{e_1, e_2, e_3, e_4, e_5\}$,
e_1 parameter is 'summer',
e_2 parameter is 'winter',
e_3 parameter is 'expensive',

e_4 parameter is 'beautiful',

e_5 parameter is 'comfortable' and

$F(e_1) = \{ h_1\}$

$F(e_2) = \{ h_2, h_4 \}$

$F(e_3) = \{ h_2, h_3, h_5\}$

$F(e_4) = \{ h_1, h_2, h_3, h_4, h_5\}$

$F(e_5) = \{h_2, h_3, h_5, h_6\}$

be defines as. Here;

$F(e_1) = \{h_1\}$ summer shoes,

$F(e_2) = \{h_2, h_4\}$ winter shoes,

$F(e_3) = \{h_2, h_3, h_5\}$ expensive shoes,

$F(e_4) = \{ h_1, h_2, h_3, h_4, h_5\}$ beautiful shoes,

$F(e_5) = \{h_2, h_3, h_5, h_6\}$ comfortable shoes.

Accordingly, the soft set (F, A) is a parameterized $\{F(e_i)$, i = 1, 2, 3, 4, 5$\}$ family of subsets of the universal set X.

Thus, the (F, A) soft set becomes $(F, A) =$ {Summer shoes = $\{h_1\}$, winter shoes = $\{ h_2, h_4 \}$, expensive shoes = $\{h_2, h_3, h_5\}$, beautiful shoes = $\{h_1, h_2, h_3, h_4, h_5\}$, comfortable shoes = $\{h_2, h_3, h_5, h_6\}$}.

Definition 2.2. For two soft sets (F, A) and (H, B) over a common universe X, we say that (H, B) is a soft subset of (F, A) if

- **i.** $B \subset A$.
- **ii.** $\forall \theta \in B$, $H(\theta)$ and $F(\theta)$ are identical approximations.

We write $(H, B) \; \tilde{\subset} \; (F, A)$ [2].

3. SOFT GROUPOIDS

Definition 3.1. Let H be a groupoid and A the set of parameters, and let the family of all subgroupoids of this groupoid be denoted by $P(H)$. If the set $F(\theta)$ is a subgroupoid of H with the $F: A \longrightarrow P(H)$ transformation for every $\theta \in A$, the (F, A) pair is called a soft groupoid on H [23].

Definition 3.2. Let (H, F, A) and (G, F', B) be two soft groupoids, $g: A \longrightarrow B$ is a surjective morphism and $\mathfrak{R}: H \longrightarrow G$ is a functor. If the following conditions exist, the $(\mathfrak{R}, g)$ pair is called a soft groupoid homomorphism:

i. $\mathfrak{R}$ functor is full,

ii. For every $\theta \in A$, $\mathfrak{R}\left(F(\theta)\right) = F'\left(g(\theta)\right)$[23].

Definition 3.3. Let (H, F, A) and (G, F', B) be two soft groupoids. If for $B \subseteq A$ and every $\theta \in B$, the groupoid $F'(\theta)$ is a subgroupoid of $F(\theta)$, (G, F', B) is called a soft subgroupoid of (H, F, A) [23].

Definition 3.4. Let (G, F', B) be a soft subgroupoid of the soft groupoid (H, F, A). In this case, for each $\theta \in B$;

i. If the groupoid $F'(\theta)$ is a full subgroupoid of $F(\theta)$, (G, F', B) is called a full soft subgroupoid of (H, F, A).

ii. If the groupoid $F'(\theta)$ is a wide subgroupoid of $F(\theta)$, (G, F', B) is called a wide soft subgroupoid of (H, F, A).

iii. If the groupoid $F'(\theta)$ is a normal subgroupoid of $F(\theta)$, (G, F', B) is called a normal soft subgroupoid of (H, F, A) [23].

Definition 3.5. Let (G, F', B) be a soft subgroupoid of the soft groupoid (H, F, A), where (G, F', B) is totally disconnected. In this case, if the $F(\theta)/F'(\theta)$ structure is a quotient groupoid for each $\theta \in B$, with the structure transformations reduced from the H/G quotient groupoid and the transformation defined as,

$$F'' : B \longrightarrow P(H/G)$$
$$\theta \mapsto F''(\theta) = F(\theta)/F'(\theta)$$

the $(H/G, F'', B)$ structure is called a soft quotient groupoid [23].

4. THE SOFT FIBRE OF GROUPOIDS

In this section, the concept of fibre was first examined, then the concept of soft set and the concept of fibre that found a place in covering spaces were discussed together, and various concepts such as soft quotient map, soft fibre, and soft fibre groupoid, each of which are original concepts, were defined.

Definition 4.1. Let $\varphi: H \longrightarrow G$ be a morphism of groupoids. A morphism $\varphi: H \longrightarrow G$ is *faithfull* (resp *full*) if the restrictions of φ mapping $H(x, y) \longrightarrow G(\varphi(x), \varphi(y))$ are injective (resp surjective) for all objects x, y of H [24].

Definition 4.2. Let $\varphi: H \longrightarrow G$ be a morphism of groupoids. The fibre of φ at an object y of G is the suhgroupoid of H whose elements are mapped by φ to the identity at y; this fibre is written $\varphi^{-1}(y)$. Clearly the kernel of φ, ker φ, is the sum (or disjoint union, as it is also called) of the fibres $\varphi^{-1}(y)$ for all objects y of G [24].

Definition 4.3. Let $\varphi : H \longrightarrow G$ be a soft groupoid homomorphism. Im φ is the set of elements $\varphi(a)$ for $a \in H$. Let the structure $(H/G, F'', B)$ be a soft quotient groupoid as given in Definition 3.5. The $p: H \longrightarrow H/G$ projection is the soft homomorphism of soft groupoids that is universal for homomorphisms from H to φ such that Im φ is disjoint.

Any such universal soft homomorphism of the form p, which must be followed by a soft isomorphism, is called a **soft quotient map**.

Definition 4.4. Let $\varphi : H \longrightarrow G$ be a soft groupoid homomorphism. The **soft fibre** of φ at an object y of G is the subgroupoid of H whose elements are mapped by φ to the identity at y; this soft fibre is written $S\varphi^{-1}(y)$.

Clearly the kernel of φ, kerφ, is corresponds to the soft fibre $S\varphi^{-1}(y)$ for all objects y of G, and kerφ is also called the disjoint union of fibres $\varphi^{-1}(y)$ and can be shown as follows:

$$ker\varphi = \{\varphi^{-1}(y) : y \in Ob(G)\} = \cup_{y \in Ob(G)} \{\varphi^{-1}(y)\}$$

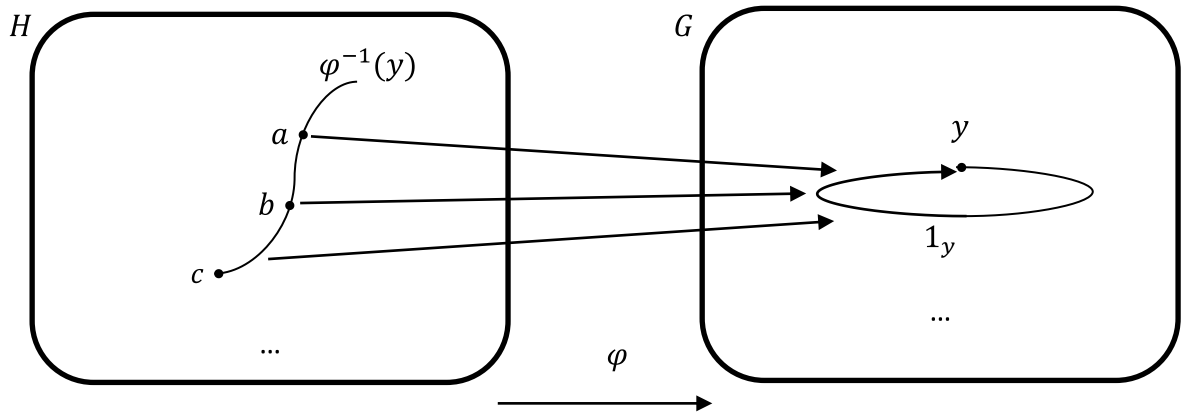

Definition 4.5. Let $\varphi : H \longrightarrow G$ be a soft groupoid homomorphism. The fibre of G in an object y is $\varphi^{-1}(y)$, for $\forall\, y \in Ob(G)$;

$$\mathcal{F} : Ob(G) \longrightarrow P(H)$$
$$y \mapsto \mathcal{F}(y) = \varphi^{-1}(y) \leq H$$

is a soft groupoid.

This soft groupoid is called **soft fibre groupoid** and is denoted by $(H, \mathcal{F}, Ob(G))$.

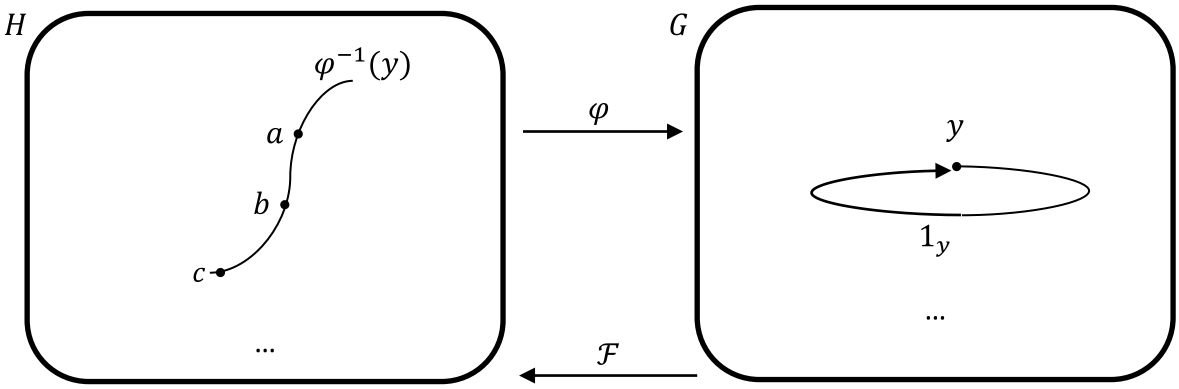

$$Ob(G) \xrightarrow{\mathcal{F}} P(H)$$
$$y \mapsto \mathcal{F}(y) = \varphi^{-1}(y) \leq H$$

Explanation 4.1. Let $\varphi : H \longrightarrow G$ be a soft groupoid homomorphism as given above.

Let us show that $\varphi^{-1}(y) \leq H$ for $\forall\, y \in Ob(G)$:

Since φ is a soft groupoid homomorphism and defined as $\varphi^{-1}(y) = \{a \in H : \varphi(a) = 1_y\}$, we can write the following:

i. For $\forall\, a, b \in \varphi^{-1}(y)$, $\varphi(a * b) = \varphi(a) \circ \varphi(b) = 1_y \circ 1_y = 1_y$.

   Then $a * b \in \varphi^{-1}(y)$.

ii. For $\forall\, a \in \varphi^{-1}(y)$, $\varphi(a^{-1}) = (\varphi(a))^{-1} = (1_y)^{-1} = 1_y$.

   Then $a^{-1} \in \varphi^{-1}(y)$.

As a result, $\varphi^{-1}(y) \leq H$.

Proposition 4.1. Let $\varphi: H \longrightarrow G$ be a soft groupoid homomorphism, where $(G, F', Ob(G))$ is a wide soft subgroupoid of the soft groupoid $(H, F, Ob(H))$. In this case, $(H, \mathcal{F}, Ob(G))$ soft fibre groupoid is a normal soft subgroupoid of $(H, F, Ob(H))$.

Proof. First, let's show that $(H, \mathcal{F}, Ob(G)) \leq (H, F, Ob(H))$:

- **i.** Since G is a wide soft subgroupoid of H, $Ob(G) \subseteq Ob(H)$.
- **ii.** For the soft groupoid $(H, F, Ob(H))$, let the F transformation be defined as follows:

$$\begin{aligned} F : Ob(H) &\longrightarrow P(H) \\ y &\mapsto F(y) = ker\varphi \leq H \end{aligned}$$

In this case, $\mathcal{F}(y) = \varphi^{-1}(y) = \{a \in H : \varphi(a) = 1_y\} \leq ker\varphi = F(y)$, for every $y \in Ob(G)$. We showed that the groupoid $\mathcal{F}(y)$ is an wide subgroupoid of $F(y)$.

Moreover, since there will be $f^{-1} * \varphi^{-1}(y)\{b\} * f = \varphi^{-1}(y)\{a\}$, for every $a, b \in F(y) = ker\varphi$ and $f \in \text{mor}(a, b)$, the groupoid $\mathcal{F}(y)$ is a normal subgroupoid of $F(y)$.

Then $(H, \mathcal{F}, Ob(G))$ soft fibre groupoid is a normal soft subgroupoid of $(H, F, Ob(H))$.

□

We showed above that kerφ is a normal soft subgroupoid of H. Accordingly, we can write the following diagram:

$$\begin{tikzcd} H \arrow[r, "\varphi"] \arrow[dr, "k(\varphi)"'] & G \\ & H/ker\varphi \arrow[u, "q(\varphi)"'] \end{tikzcd}$$

For a general φ soft homomorphism, the kernel of $q(\varphi)$ consists of only identities. In this case, $q(\varphi)$ is said to have a soft discrete kernel.

Definition 4.6. Let (H, F, A) and (G, F', B) be soft groupoids and $\varphi : H \longrightarrow G$ be a soft groupoid homomorphism.

1) If the constraints on the mapping $H(x,y) \longrightarrow G(\varphi(x),\varphi(y))$ for $\forall\ x,y \in H$ are surjective, φ is said to be ***soft full***. Here, since the φ transformation is surjective by definition, it is *soft full* without any other conditions.

2) If the constraints on the mapping $H(x,y) \longrightarrow G(\varphi(x),\varphi(y))$ for $\forall\ x,y \in H$ are injective, φ is said to be ***soft faithfull***.

5.CONCLUSIONS

In this study, the concept of soft set and the concept of fibre, which finds a place in covering spaces, are discussed together and various concepts such as soft quotient map, soft fibre, and soft fibre groupoid, each of which are original concepts, are introduced. In addition, these concepts have been made more understandable with proposition, explanation and figures.

REFERENCES

1. D.A. Molodtsov, *Soft set theory-First results,* Comput. Math. Appl., 37 (4-5), 19-31, 1999.

2. P. K. Maji, R. Biswas and R. Roy, *Soft set theory,* Comput. Math. Appl., 45(4-5), 555-562, 2003.

3. M. I. Ali, *A note on soft sets, rough soft sets and fuzzy soft sets,* Appl.Soft Comput., 11, 3329-3332, 2011.

4. H. Aktas and N. Cagman, *Soft sets and soft groups,* Inform.Sci., 77(13), 2726-2735, 2007.

5. A. O. Atagun, A. Sezgin, *Soft substructures of rings, fields and modules,* Comput. Math. Apply., 61, 592-601, 2011.

6. M. Shabir, M. Naz, *On Soft topological spaces,* Comput. Math. Apply., 61(7), 1786-1799, 2011.

7. W. K. Min, *A Note on Soft Topological Spaces,* Comput. Math. Apply., 62, 3524-3528, 2011.

8. N. Cagman, S. Karatas and S. Enginoğlu, *Soft topology,* Comput. Math. Apply., 62(1), 351-358, 2011.

9. A. Aygunoğlu, A. Aygun, *Some notes on soft topological spaces,* Neural Comput. Apply., 22(1), 113-119, 2012.

10. O. Zahiri, *Category of soft sets,* An. Univ. Craiova Ser. Mat. Inform., 40(2), 154-166, 2013.

11. T. Shah, S. Shaheen, *Soft topological groups and rings,* Ann. Fuzzy Math. Inform., 7(5), 725-743, 2014.

12. D. Pie and D. Miao, *From soft sets to information systems*. İn: X. Hu, Q. Liu, A. Skowron, T.Y. Lin, R.R. Yager, B. Zhang (Eds.), Proceedings of Granular Computing, Vol.2, IEEE., pp. 617-621, 2005.

13. S. K. Sardar, S. Gupta, *Soft category theory-an introduction,* J. Hyperstructures, 2, 118-135, 2013.

14. G. Oguz, M. H. Gursoy and I. Icen, *On Soft Topological Categories,* Hacet. J. Math. Stat., 2018.

15. G. Oguz, I. Icen, and M. H. Gursoy, *Actions of Soft Groups,* Commun. Fac. Sci. Univ. Ank. Ser. A1 Math. Stat. Volume 68, number 1, Pages 1163-1174, 2019.

16. S. Gecen, Reflections of global action on soft set theory, master's thesis İnönü University, Malatya, Türkiye, 2021.

17. P. J. Higgins, *Categories and groupoids*, Van Nostrand, New York, 1971.

18. R. Brown, *Topology: A geometric account of general topology, homotopy types and the fundamental groupoid,* Ellis Horwood, Chichester, 1988.

19. R. Brown, G. Danesh-Naruie and J. P. L. Hardy, Topological groupoids II: Covering morphism and G-spaces, Math. Nachr., 74, 143-145, 1976.

20. O. Mucuk, *Covering groups of non-connected topological groups and the monodromy groupoid of a topological groupoid,* Ph. D. Thesis, University of Whales, England, 1993.

21. O. Mucuk and I. Icen, *Covering of Groupoids,* Hadronic J. Suppl., 16, no.2, 183-196, 2001.

22. J. P. Hardy, *Topological groupoids: Coverings and Univeral Constructions,* Ph. D. Thesis, University College of North Wales, 1974.

23. G. Oguz, *Soft approach to some algebraic structures*, İnönü University, Ph.D. Thesis, Malatya, Türkiye, 2018.

24. R. Brown, *Fibrations of Groupoids*, Journal of Algebra, 15, 103-132, 1970.

9TH INTERNATIONAL CONFERENCE ON COMPUTATIONAL MATHEMATICS AND ENGINEERING SCIENCES

17 – 19 May 2025,
Diyarbakır – Türkiye

cmescongress.org